GEORGIA INSTITUTE OF TECHNOLOGY
OFFICE OF RESEARCH ADMINISTRATION

RESEARCH PROJECT INITIATION

Date: July 19, 1973

Project Title: Determination of the Acoustic Responses of Solid Propellants by the Impendance Tube Method

Project No: E-16-633

Principal Investigator: Dr. Ben T. Zinn

Sponsor: Air Force Office of Scientific Research; Arlington, Virginia

Agreement Period: From June 30, 1973* Until June 29, 1974

Type Agreement: Grant No. AFOSR-73-2571

Amount: $49,593 AFOSR Funds (E-16-633)
2,610 GIT contrib. (E-16-330)*
$52,203 TOTAL

Reports Required:
Final Scientific Report; Interim (Annual) Report if project extended beyond one year.

Sponsor Contact Person (s): Technical Matters

Capt. Lloyd R. Lawrence, Jr.
Program Manager
AFOSR (NAE)
1400 Wilson Boulevard
Arlington, Virginia 22209

Contractual Matters

(Thru ORA)
Ms. Joan O. Marshall
Buyer
AFOSR (PMD)
(same address)

*Cost Sharing consists of funding for June 1-30, 1973.

Assigned to: School of Aerospace Engineering

COPIES TO:

- Principal Investigator
- School Director
- Dean of the College
- Director, Research Administration
- Director, Financial Affairs (2)
- Security-Reports-Property Office
- Patent Coordinator
- Library
- Rich Electronic Computer Center
- Photographic Laboratory
- Project File
- Other

RA-3 (6-71)

GEORGIA INSTITUTE OF TECHNOLOGY
OFFICE OF CONTRACT ADMINISTRATION

SPONSORED PROJECT TERMINATION

Date: 3 May 78

Project Title: Determination of the Acoustic Response of Solid Propellents by the Impedance Tube Method.

Project No: E-16-633

Project Director: B. T. Zinn

Sponsor: Air Force Office of Scientific Research

Effective Termination Date: 9/30/77

Clearance of Accounting Charges: 9/30/77

Grant/Contract Closeout Actions Remaining:

- x Final Invoice and Closing Document
- x Final Fiscal Report
- _ Final Report of Inventions
- _ Govt. Property Inventory & Related Certificate
- _ Classified Material Certificate
- _ Other _____

Assigned to: Aerospace Engineering (School/Laboratory)

COPIES TO:

- Project Director
- Division Chief (EES)
- School/Laboratory Director
- Dean/Director—EES
- Accounting Office
- Procurement Office
- Security Coordinator (OCA)
- Reports Coordinator (OCA)
- Library, Technical Reports Section
- Office of Computing Services
- Director, Physical Plant
- EES Information Office
- Project File (OCA)
- Project Code (GTRI)
- Other _____

CA—4 (3/76)

AFOSR INTERIM SCIENTIFIC REPORT

AFOSR-TR

SOLID PROPELLANT ADMITTANCE MEASUREMENTS BY THE DRIVEN TUBE METHOD

Prepared for

Air Force Office of Scientific Research
Aerospace Sciences Directorate
Arlington, Virginia

by

B. T. Zinn
B. R. Daniel
W. A. Bell
M. Salikuddin

School of Aerospace Engineering
Georgia Institute of Technology
Atlanta, Georgia 30332

Approved for public release; distribution unlimited

Grant No. AFOSR-73-2571 August 1974

Conditions of Reproduction

Reproduction, translation, publication, use and disposal in whole or in part by or for the United States Government is permitted.

ABSTRACT

Results obtained during the first year of a research program concerned with the development of a driven tube burner for the measurement of the admittances of burning solid propellants are presented. In the experimental phase of the program, a driven tube burner has been developed and tested under both cold and hot flow conditions. The cold flow tests provided a check on the proper operation of the facility and the data reduction scheme. Temperature measurements of the gas inside the burner tube, taken during the burning of a solid propellant sample, indicate the presence of axial and radial temperature gradients in the burner. The effect of these gradients upon the quality of the measured admittance data is under investigation. Preliminary hot tests conducted to date confirmed the proper operation of the facility and its ability to provide good pressure amplitude and phase data. These data are now being used to compute the desired solid propellant admittances. In the analytical phase of this program, a most promising analytical technique for the determination of both the admittance and entropy perturbation at the propellant burning surface, from dynamic pressure and steady temperature measurements, has been developed. The accuracy of this technique is currently under investigation. Also, the effect of the steady state temperature gradients upon the wave structure inside the burner tube has been investigated analytically.

TABLE OF CONTENTS

NOMENCLATURE

Symbols

a	proportionality constant appearing in the burning rate law; see Eq. (5-2); or the parameter $k\bar{M}/(1-\bar{M}^2)$ which arises from the Doppler shift; Eq. (4-24)
C	velocity of sound
c_p	specific heat at constant pressure; Btu/lbm.$^{\circ}$R
c_v	specific heat at constant volume; Btu/lbm.$^{\circ}$R
A_+, A_-, A	complex integration constants; see Eqs. (4 18) - (4-20)
D	diameter of the burner tube; ft.
h	heat transfer coefficient, Btu/sec. ft.^{2}$^{\circ}$R
i	imaginary unit, $\sqrt{-1}$
L	length, ft.
m	mass flow rate per unit cross sectional area , lbm/ft^2
n	exponent appearing in the steady state burning rate law
P	pressure; Lbf/ft.^{2}
Q	volumetric heat source
r	burning rate; ft/sec.
R	specific gas constant; ft.-lbf/slug$^{\circ}$R, also, solid propellent response function
S	entropy
T	temperature, $^{\circ}$R, Btu/lbm.$^{\circ}$R
t	time; sec.
u	axial velocity; ft./sec.
x	axial distance along the tube; ft.

Y specific admittance

γ ratio of specific heats

ρ density; slugs/ft.^{3}

ω frequency, rad/sec.

Superscripts

$(\bar{\ })$ variable describing steady state conditions

$(\ )'$ a perturbation

Subscripts

$(\ )_b$ variable evaluated at the burning surface

$(\ )_c$ quantity evaluated at the propellant surface

$(\ )_r$ real part of a complex quantity

$(\ )_i$ imaginary part of a complex quantity

$(\ )_s$ quantity describing conditions inside the solid phase

$(\ )_w$ quantity evaluated at the wall

LIST OF FIGURES

CHAPTER I

INTRODUCTION

This report summarizes the results obtained during the first year of support under Air Force Grant No. AFOSR-73-2571. This grant was initiated on July 1, 1973 and it is concerned with the "Determination of the Acoustic Responses of Solid Propellants by the Impedance Tube Method."

Combustion instability has been recognized as one of the most serious problems encountered in the development of solid-propellant rockets. Combustion instability is the result of an interaction between the combustion process and disturbances within the rocket motor; an interaction which often leads to the amplification of these disturbances into finite amplitude oscillations. The appearance of combustion instability frequently produces dramatic and even catastropic changes in the motor's performance. Combustion instability may also result in mechanical failure of engine components, extremely high heat transfer rates to the combustor's walls and interference with the control and guidance systems. Any one of these effects can result in engine or mission failure.

To determine the susceptibility of a given propulsion system to combustion instability, it is necessary to determine the energy balance that exists between the various gains and losses of wave energy present within the combustor. Wave energy loss mechanisms tend to damp the amplitude of a disturbance in the combustor and thus exert a stabilizing influence upon the engine. Examples of wave energy loss mechanisms are

convective energy losses caused by the mean flow, energy dissipation processes associated with viscosity and heat transfer, energy dissipation due to wave interaction with particulate matter, and energy losses resulting from the interaction of the disturbance with various mechanical components of the engine such as the exhaust nozzle. On the other hand, wave energy gains tend to amplify the engine disturbances and thus exert a destabilizing influence upon the combustor. The primary source of wave energy gain is the unsteady combustion process. If the energy gains out weigh the wave energy losses, an initial disturbance will amplify and lead to undesirable self-sustained oscillations inside the combustor. To evaluate the stability of a solid-propellant rocket motor, it is necessary to quantitatively describe the various gain and loss mechanisms that are present in the system.

The wave energy gain in a solid rocket may be determined from either a theoretical or an experimental investigation of the interaction between a burning solid propellant and an oscillating gas phase. This interaction can be described by specifying the response function* of the burning solid propellant surface which can also be used to compute the wave energy gain resulting from the above-mentioned interaction. Since instability is often caused by small differences between wave energy gains and losses, it is imperative that the contributions from all processes affecting the stability of rocket engines be known as accurately as possible. Hence, it is of utmost importance that experimental

---

* See later discussion for definition of the response function.

techniques capable of accurate determination of the responses of burning solid-propellants be available. The development of such an experimental technique is one of the main objectives of the present study which is concerned with the adaptation of the impedance tube method in the determination of the responses of burning solid propellants. The impedance tube technique has its origin in acoustics where it has been successfully utilized to measure the responses of sound absorbing materials under no flow conditions.[1] This technique was later modified to determine the responses of choked rocket nozzles[2] and acoustic liners[3] under cold flow conditions. This report describes the efforts undertaken to further modify the impedance tube technique for the measurement of the responses of burning solid propellants.

CHAPTER II

BACKGROUND

Because of the complexity of the combustion process, no satisfactory theoretical analysis currently exists for accurately determining the response (or admittance) of a burning solid propellant. Therefore, the responses, or "driving" capabilities, of solid propellants must be determined experimentally. To date, the T-burner has been the most widely used device for the experimental determination of the responses of solid propellants[4]. Several variations of this device have been developed; and, although considerable data have been obtained, the accuracy of the results is open to question. To explain the operation and limitations of the T-burner, it is important that one be familiar with the definitions of the various quantities measured by this device (e.g., response functions and admittances) as well as with different available variations of the T-burner.

Response Function and Admittances

The admittance is a measure of the propellant's ability to drive the gas phase pressure oscillations; it also represents the boundary condition that must be satisfied at the combustors boundary in a rocket motor stability analysis. The admittance is defined as the complex ratio of the gas velocity perturbation normal to the surface and the local pressure perturbation. The nondimensional form of the admittance of a burning propellant is often expressed in the following form:

$$Y_b = \frac{\gamma \bar{P}}{\bar{c}_b} \cdot \frac{u'}{P'} \tag{2-1}$$

where the various quantities are defined in the nomenclature.

As mentioned earlier, the interaction between the combustion process and the gas phase oscillations can also be described by means of the "response function" of the propellant. The latter is defined as the complex ratio of the propellant burning rate perturbation to the pressure perturbation, evaluated at the burning surface. The non-dimensional form of the response function is:

$$R_b = \frac{\bar{P}}{\bar{r}} \cdot \frac{r'}{P'} = \frac{\bar{P}}{\bar{m}} \cdot \frac{m'}{P'} \tag{2-2}$$

The relationship between the propellant response function and its admittance is often of interest. The mass flux m at the burning surface is given by

$$m = \rho u = \rho_s r \tag{2-3}$$

It follows from Eq. (2-3) that

$$\frac{m'}{\bar{m}} = \frac{\rho'}{\bar{\rho}} + \frac{u'}{\bar{u}} \tag{2-4}$$

and using Eqs. (2-1), (2-3) and (2-4) one can easily show that:

$$R_b = \frac{Y_b}{\gamma \bar{M}_b} + \frac{\rho'/\bar{\rho}}{P'/\bar{P}} \tag{2-5}$$

If the oscillations are isentropic, then

$$\frac{\rho'}{\bar{\rho}} = \frac{1}{\gamma}\frac{P'}{\bar{P}} \tag{2-6}$$

and Eq. (2-5) reduces to the following expression:

$$R_b = \frac{1}{\gamma \bar{M}_b}\left[Y_b + \bar{M}_b\right] \tag{2-7}$$

Self-Excited T-Burners

The self-excited T-burner, shown in Figure (1), consists of a cylindrical tube with disc-shaped propellant samples located at both ends[5]. An exhaust vent is located at the center of the tube. The propellant samples are ignited; and if the propellant is sufficiently unstable, the interaction between the combustion process and gas phase disturbances results in the development of a pressure oscillation in the tube, the amplitude of which increases exponentially with time until a maximum amplitude is reached. The oscillation decays once the propellant samples are completely burned. The experimental procedure consists of measuring the exponential growth and decay rates of the oscillation immediately after ignition and upon the completion of burning. Using this data, the real part of the propellant admittance can be calculated.

When no losses are present in the system, the interaction of a disturbance with the combustion process would result in its amplification and the corresponding pressure perturbation would exhibit the following time dependence:

$$p' \sim e^{\alpha t} \tag{2-8}$$

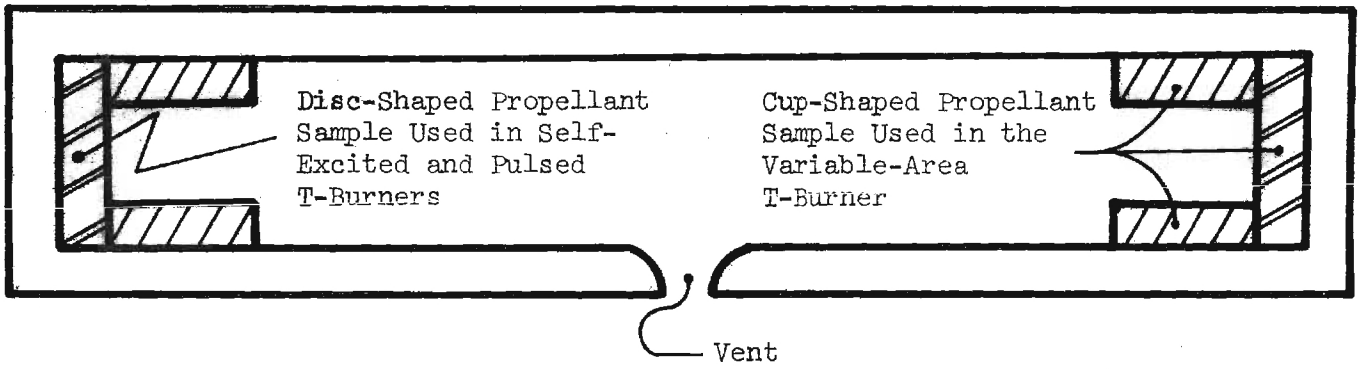

Figure 1. T-Burner

For such a situation, the measured growth rate α can be related to the real part of the propellant admittance by the following relationship[5]:

$$\alpha = \frac{2\bar{C}_b}{L}\left(Y_{br} + \bar{M}_b\right) \tag{2-9}$$

When the burning of the propellant samples is completed, the acoustic losses present in the system will result in the exponential decay of the oscillation which will now exhibit the following time dependence:

$$p' \sim e^{-\alpha_d t} \tag{2-10}$$

where the positive constant α_d is the system's "decay constant."

In the T-burner experiment, the observed growth rate constant α_g, presumably represents the difference between the amplification provided by the burning propellant and the losses present in the system; hence α_g can be heuristically expressed as follows:

$$\alpha_g = \frac{2\bar{C}_b}{L}\left(Y_{br} + \bar{M}_b\right) - \alpha_d \tag{2-11}$$

Equation (2-11) can be rewritten in the following form which directly relates the real part of the admittance to the measured experimental data:

$$Y_{br} = \frac{L}{2\bar{C}_b}\left(\alpha_g + \alpha_d\right) - \bar{M}_b \tag{2-12}$$

Similarly, the real part of the response function can be obtained from the following expression which holds when the oscillation is isentropic:

$$R_{b_r} = \frac{\bar{P}}{4\rho_s \bar{r} \bar{C}_b} \cdot \frac{2L}{\bar{C}_b}\left(\alpha_g + \alpha_d\right) \tag{2-13}$$

In deriving Eq. (2-13) the perfect gas law and the steady state continuity equation $\bar{u}\,\bar{\rho} = \rho_s \bar{r}$ was used to express the Mach number in the following from:

$$\bar{M}_b = \frac{\rho_s \bar{r} \bar{C}_b}{\gamma \bar{P}} \qquad (2\text{-}14)$$

The determination of the admittances of solid propellants in T-burners is based upon the critical assumption that the wave-energy losses in the T-burner are the same during both the growth and decay phases of the oscillation. However, since the flowfield temperatures and frequencies are not the same during the growth and decay periods, the validity of this assumption is open to question. Another limitation of this technique is that since the frequency of the oscillation is determined by the length of the burner, (i.e., $f = \bar{C}/2L$), then several T-burners of different lengths must be available for the determination of the dependence of the propellant admittance upon the frequency.

Since the admittance of a burning solid propellant depends on both the frequency and growth rate of the gas oscillation, in comparing the driving capabilities of different solid propellants it is important that their responses be determined under identical conditions. This practice has not been followed to date. Instead, the relative driving capabilities of different propellants have been determined by comparing their responses at the same frequency and completely ignoring the different growth rates of the oscillations for which these responses were measured. Finally, in reducing the T-burner data, it is customarily assumed that the mean gas temperature in the T-burner is uniform and

that the spatial wave structure is the same as in the acoustic case; it is a matter of fact that the mean gas temperature in the T-burner is not uniform and hence the wave structure is not the same as in the acoustic case.

Variable-Area T-Burner

The variable-area T-burner is an alternate approach for determining the admittances of burning solid propellants[6]. Whereas the self-excited T-burner usually employs propellant discs with the same cross-sectional area as the tube, with the variable-area T-burner cup-shaped propellant samples, whose burning surface area may be varied, are used (see Figure 1). The desired propellant admittance is obtained by running a series of experiments and varying the area of the burning propellant surface between experiments. The critical assumption with this technique is that the admittance of the burning solid propellant and the system damping remain constant from test to test for all values of the area ratio S_b/S_c where S_b is the area of the burning surface and S_c is the cross-sectional area of the tube. If this assumption is valid, then one can write[6]:

$$\alpha_g + \alpha_d = \frac{2\bar{C}_b}{L} (Y_{br} + \bar{M}_b) \cdot \frac{S_b}{S_c} \qquad (2\text{-}15)$$

And using Equation (2-15) a plot of measured growth rate constants α_g versus S_b/S_c should yield a straight line. Extrapolation of this line to $S_b/S_c = 0$ should give the value of α_d. The slope of this line is $(Y_{br} + \bar{M}_b)$ and this value can be used to determine the desired solid propellant admittance. However, data have been obtained which indicate

that a plot of α_g versus S_b/S_c does not produce a straight line. In addition, data scatter limits the accurate determination of α_g and the slope of the line from which the admittance is determined. Also, a number of experiments is required to produce a single point on the propellant admittance versus frequency curve.

To date, the variable-area method has been used to determine the admittances of aluminized and weakly unstable propellants. This method requires the use of large burning surface areas to derive sufficient energy from the combustion process to overcome the wave energy losses in the T-burner so that pressure oscillations can be excited. This necessitates the use of the cup-shaped grains which extend over different lengths of the tube. However, the characteristics of the combustion and damping processes vary along the length of the tube, and the use of cup-shaped samples also introduces two-dimensional effects. These phenomena are not accounted for in the derivation of Equation (2-15) and their omission causes inaccuracies and uncertainties in data interpretation.

Pulsed T-Burner

In addition to the variable-area T-burner, the pulsed T-burner[4], [7], [8] is also used to determine the admittances and system losses for aluminized propellants. With this method it is not necessary for the combustion process to generate and sustain oscillations in the burner. Instead, a charge is fired into the T-burner during and immediately after completion of the propellant combustion. The difference in the decay rates of the resulting pressure oscillations is used to determine

the admittance of the burning propellant surface. The principal disadvantages of this technique are the introduction of foreign particles by the charge into the burner, the inability to control the frequency of the oscillations, the uncertainty whether the system damping is the same after the firing of both the first and second charges and the marginal difference between the observed decay rates of both pulses that leads to considerable scatter in the measured admittance data. Because of these difficulties, the accuracy of the admittance results obtained from pulsed T-burners is limited.

Forced Oscillation Methods

Because of the limitations of the various T-burner techniques, investigators[9], [10], [11] have resorted to the use of forced oscillation experiments to measure the admittances of burning solid propellants. In a recent study[9] the experimental setup (see Figure 2) consisted of a short tube whose walls were lined with a solid propellant. An exhaust nozzle at the end of the tube controlled the combustor pressure and a rotating valve produced periodic blocking and opening of a small orifice which, in turn, produced a small amplitude pressure oscillation of desired frequency in the chamber. Assuming that the combustor length is short compared with the acoustic wave length, the oscillating pressure is taken to be spatially uniform in the chamber. Under these conditions the admittance of the burning propellant can be determined from measurement of the amplitude ratio and phase difference between the area oscillation at the rotating valve and the pressure oscillation in the chamber.

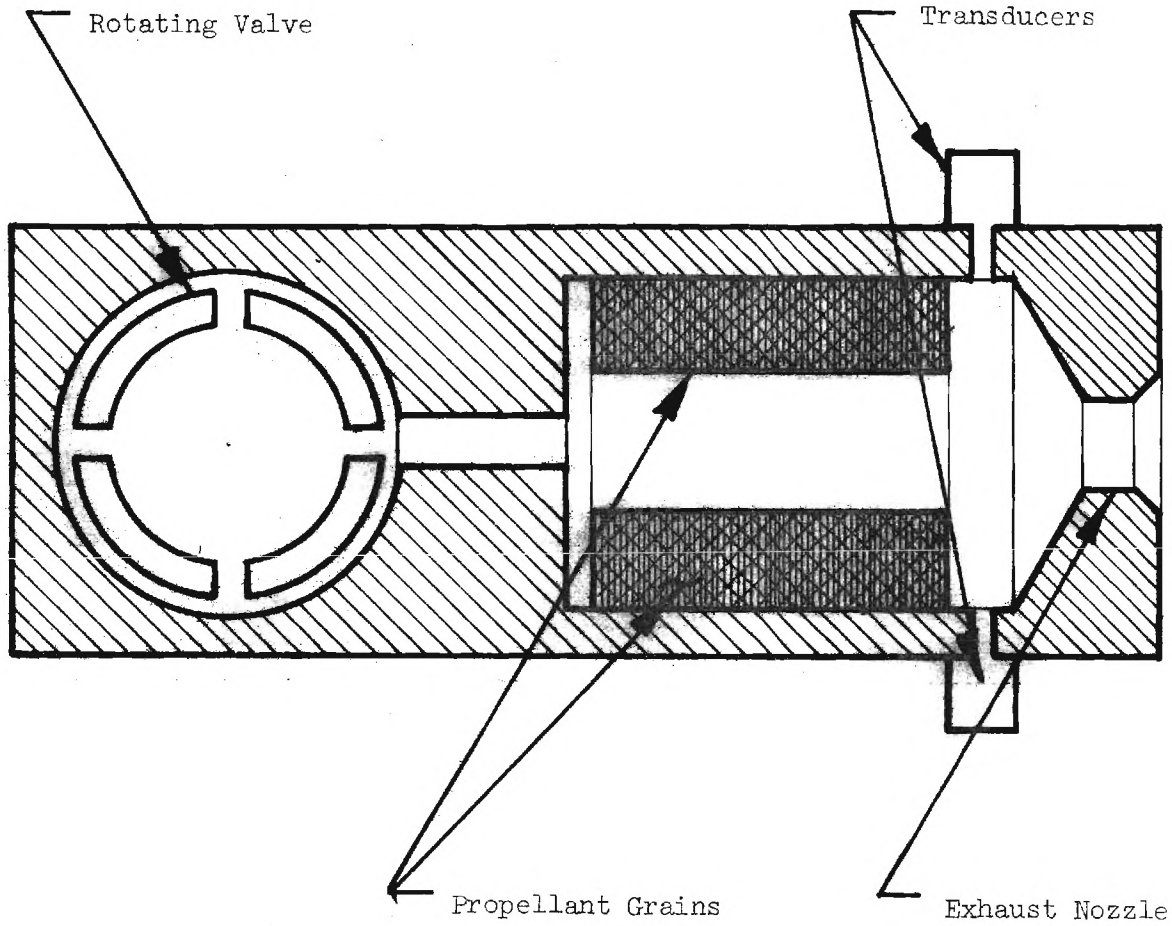

Figure 2. Forced Oscillation Method

The principal disadvantage of the above-mentioned experiment is that due to the short motor assumption employed in the development of its theory this experimental setup can only be used for admittance measurements at low frequencies. This setup is basically a driven L-burner. Other disadvantages are particle damping associated with aluminized propellants cannot be determined and in its present configuration both velocity and pressure oscillations affect the measured combustion response function and it is impossible with this method to evaluate the contribution of each one of these effects.

Forced oscillations experiments have also been conducted by investigators in France[10] and investigators at the Applied Physics Labs in the U. S.[11]. In the French study, oscillations were generated in a cylindrical rocket motor having a tubular propellant by periodically and partially blocking the exhaust nozzle throat area. However, due to the lack of an appropriate theory to guide the experimental efforts, it became impossible in this study to deduce the needed propellant admittance from the measured data. Similar shortcomings have also plagued an earlier forced oscillation study in the U. S.[11]. In this case, the choice of an awkward experimental setup and measurement technique caused considerable difficulties in the conduct of the experiment and in the data reduction.

When properly planned and executed, the forced oscillation experiment can offer many advantages; these include the possibility for accounting for the influence of aluminum particles in both the combustion zone and the gaseous phase; the possibility of carefully controlling the

frequency and growth rate of the oscillation; and, contrary to T-burner type experiments, the same setup may be used to study the response of a given solid propellant over a whole frequency range and fewer tests are needed than with any of the T-burner-type experiments.

The Impedance Tube

To overcome the limitations of T-burners and previously developed forced oscillations experiments, a driven burner, based on the classical impedance tube technique,[2],[12] is under development in the present program. Traditionally, the impedance tube has been used to measure the admittances of various sound absorbing materials. In such studies, the experimental setup (see Figure 3) consists of a tube with an acoustic driver at one end and the sample whose admittance is to be measured at the other end. During an experiment, the driver generates an incident wave P_i of a given frequency ω that propagates along the tube until it impinges upon the tested sample. Because of the interaction between the incident wave and the sample material, the incident wave reflects off the tested sample with modified amplitude and phase. The reflected wave P_r then combines with the incident wave to form a standing wave pattern in the tube whose structure depends, among other things, upon the admittance of the tested sample. It can be shown,[2],[12] that the sample admittance Y depends upon two parameters, α and β, which respectively describe the changes in amplitude and phase between the incident and reflected waves at the sample surface, that is

$$Y = \frac{u'}{p'} = f(\alpha,\beta,\omega, \ldots) \qquad (2\text{-}16)$$

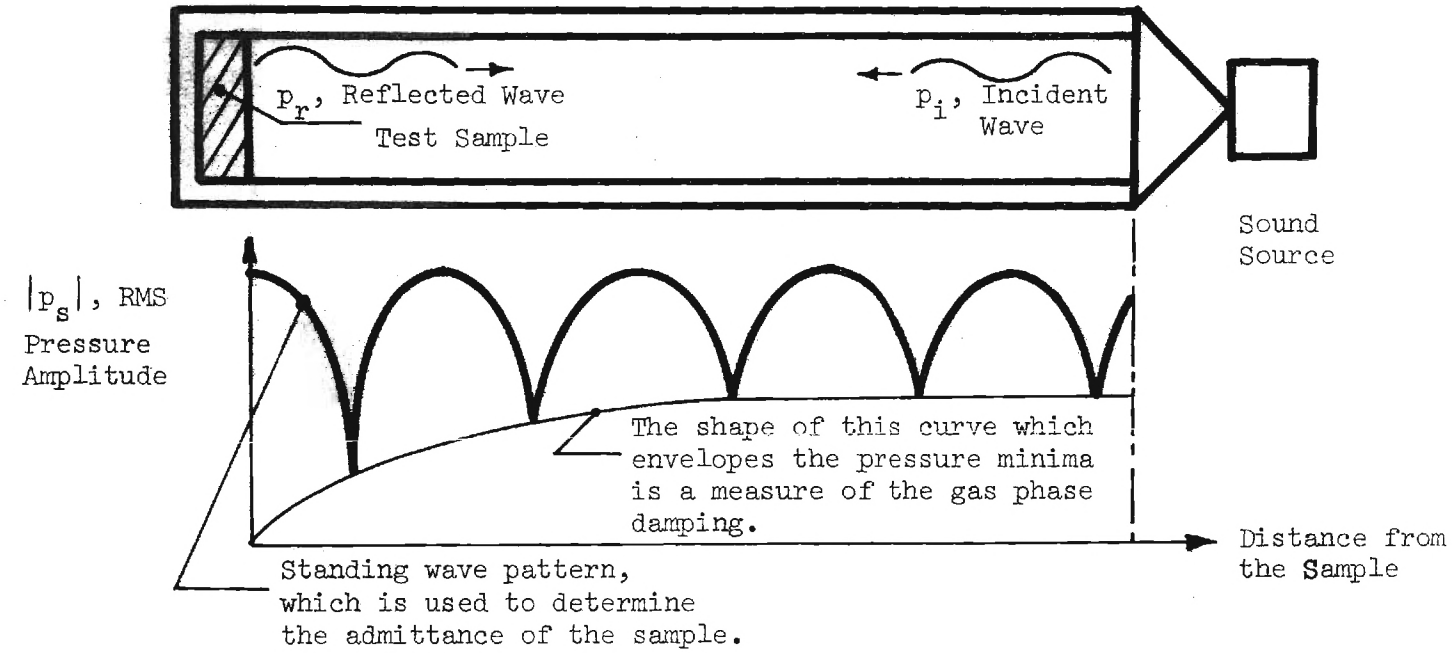

Figure 3. An Impedance Tube and a Typical Standing Wave Pattern

where f is a known functional form. The admittance Y can be determined once the parameters α and β are known. It can also be shown[2],[12] that the structure of the amplitude $|P(x)|$ of the standing wave in the tube can be described by an expression having the following functional form:

$$|P(x)| = g(\alpha,\beta, y,\lambda,x \ldots) \qquad (2\text{-}17)$$

Where y is a measure of attenuation of the waves due to acoustic energy losses in the gas phase, λ is the wave length of the oscillation and x describes the axial location in the tube. In impedance tube experiments a microphone is traversed along the tube to measure $|P(x)|$. Once this data is available, it can be used together with the above equation to determine the unknowns α, β and y. The quantities α and β are then used to determine Y. This technique has recently been successfully applied to measure the admittances of choked nozzles in the presence of a mean flow[2],[3]. This data provides a measure of the attenuation provided[29] by choked nozzles during axial and three-dimensional instabilities.

CHAPTER III

EXPERIMENTAL MEASUREMENTS

In applying the impedance tube technique to the measurement of the admittances of burning solid propellants, existing measurement techniques had to be modified due to the high temperature of the gases inside the burner tube. Also, existing data reduction schemes had to be extended to account for the axial gradients in mean flow properties caused by heat transfer to the burner tube walls.

The experimental setup is shown in Figures 4 and 5 and consists of a circular tube, the propellant sample and its holder, the acoustic drivers, and a pressure regulating exhaust valve. Three burner tubes have been fabricated to date, two of the tubes are made of acrylic material while the other is made of stainless steel. The acrylic tubes have been chosen in order to determine whether its low heat conductivity will reduce the heat transfer to the walls, which causes severe axial temperature gradients in the steady state temperature profiles. Each of the burner tubes has an inside diameter of 1.5 inches and it is approximately 4.5 ft. long. These tubes have provisions for the attachment of pressure transducers and thermocouples at numerous locations along their walls. The distribution of the pressure transducers and thermocouples along the burner wall, during each experiment, is determined by the experimental conditions (e.g., the frequency of the wave).

Two Ling EPT-94B electropneumatic drivers, each capable of developing 4,000 watts of acoustic power, are close-coupled to the tube

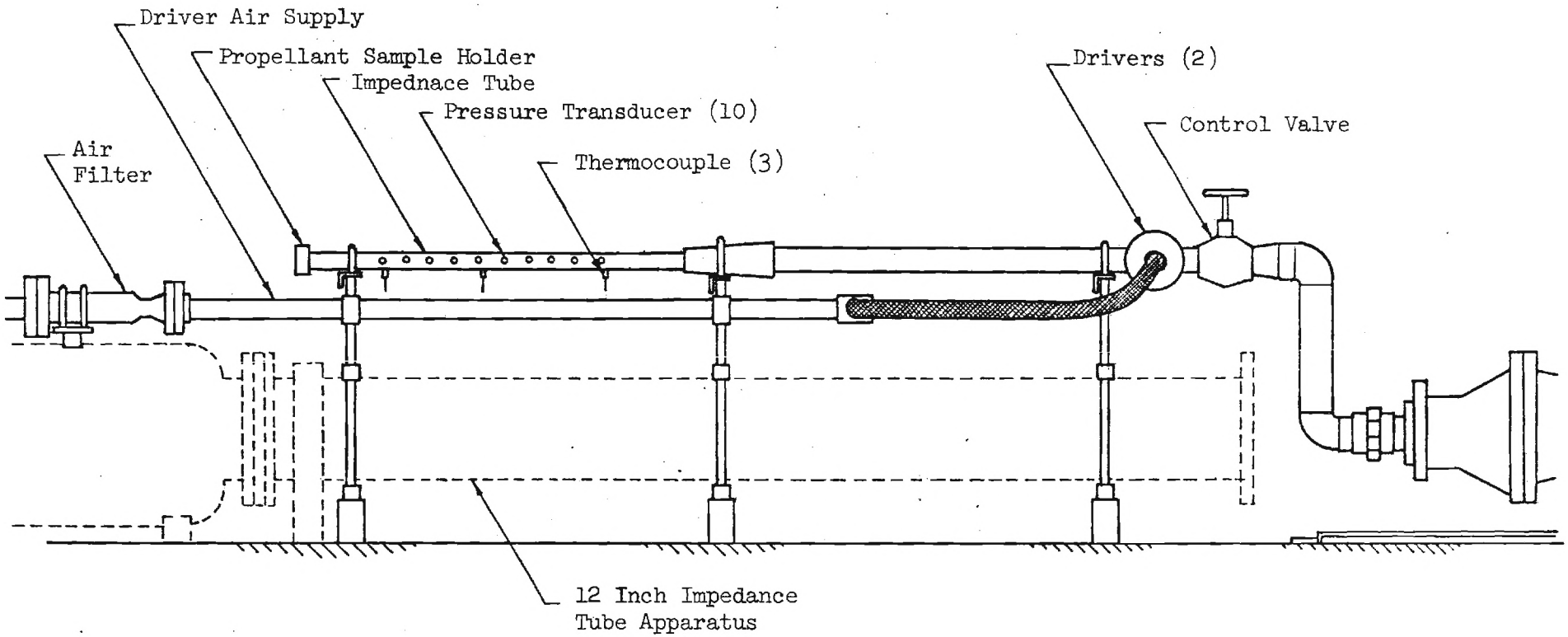

Figure 4. Sketch of the General Arrangement of the Unpressurized Driven Burner Experiment

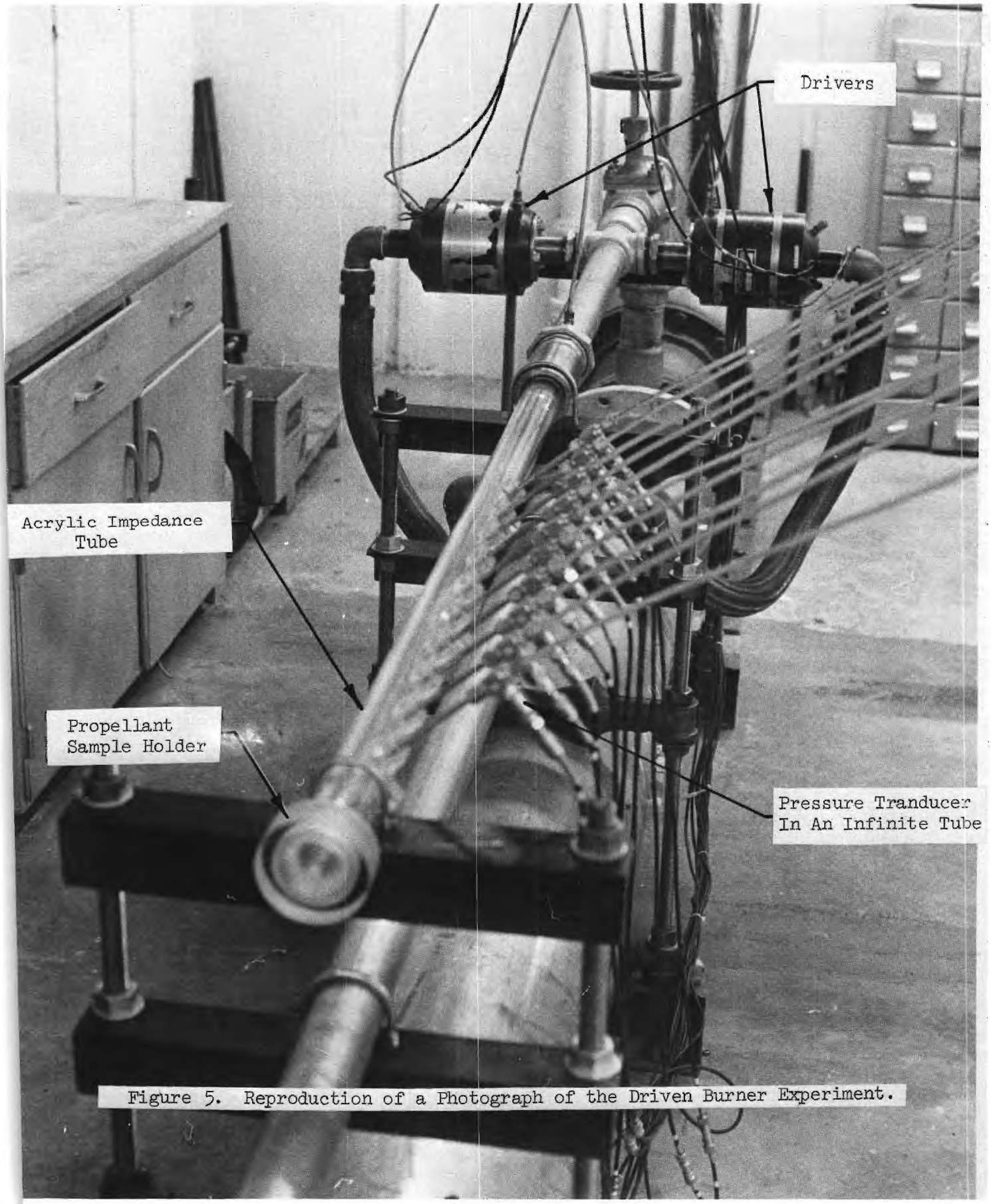

Figure 5. Reproduction of a Photograph of the Driven Burner Experiment.

wall a short distance upstream of the exhaust valve. The frequency and waveform output of the acoustic drivers are controlled by a Spectral Dynamics Oscillator, Model SD104A-5. For this investigation, the waveforms of the oscillations are sinusoidal and the frequency of the oscillation is maintained constant during a given test. These drivers are capable of developing sound pressure levels greater than 180 decibels (referenced to 2.2×10^{-4}, dynes per cm^2) in the tube. To minimize acoustic feedback from outside the tube, a supercritical pressure ratio is maintained across the exhaust valve (nozzle) during a test.

Measuring the admittance of a burning solid propellant using the impedance tube technique imposes stringent requirements on the instrumentation. The pressure measurement at high temperatures poses the problem of protecting the highly sensitive transducers from direct exposure to the hot gases in the tube. Various ways for protecting the transducers were tested. Satisfactory results were obtained using the semi-infinite tube technique. In this technique the infinite tube is attached to the tube's wall while the pressure transducer is attached to the side of the infinite tube several inches away from the hot tube wall. Good results were also obtained by coating the face of the transducer with a thin film of plastic cement and locating the transducer flush with the inside of the tube wall. In tests conducted to date the semi-infinite tube arrangements shown in Figure 6 have been sued with no apparent adverse effects on the transducers. The need to measure the high temperature of the hot gas in the tube called for the use of special thermocouples. In the present study platinum/platinum 13% rhodium thermocouples were used. These thermocouples are capable of

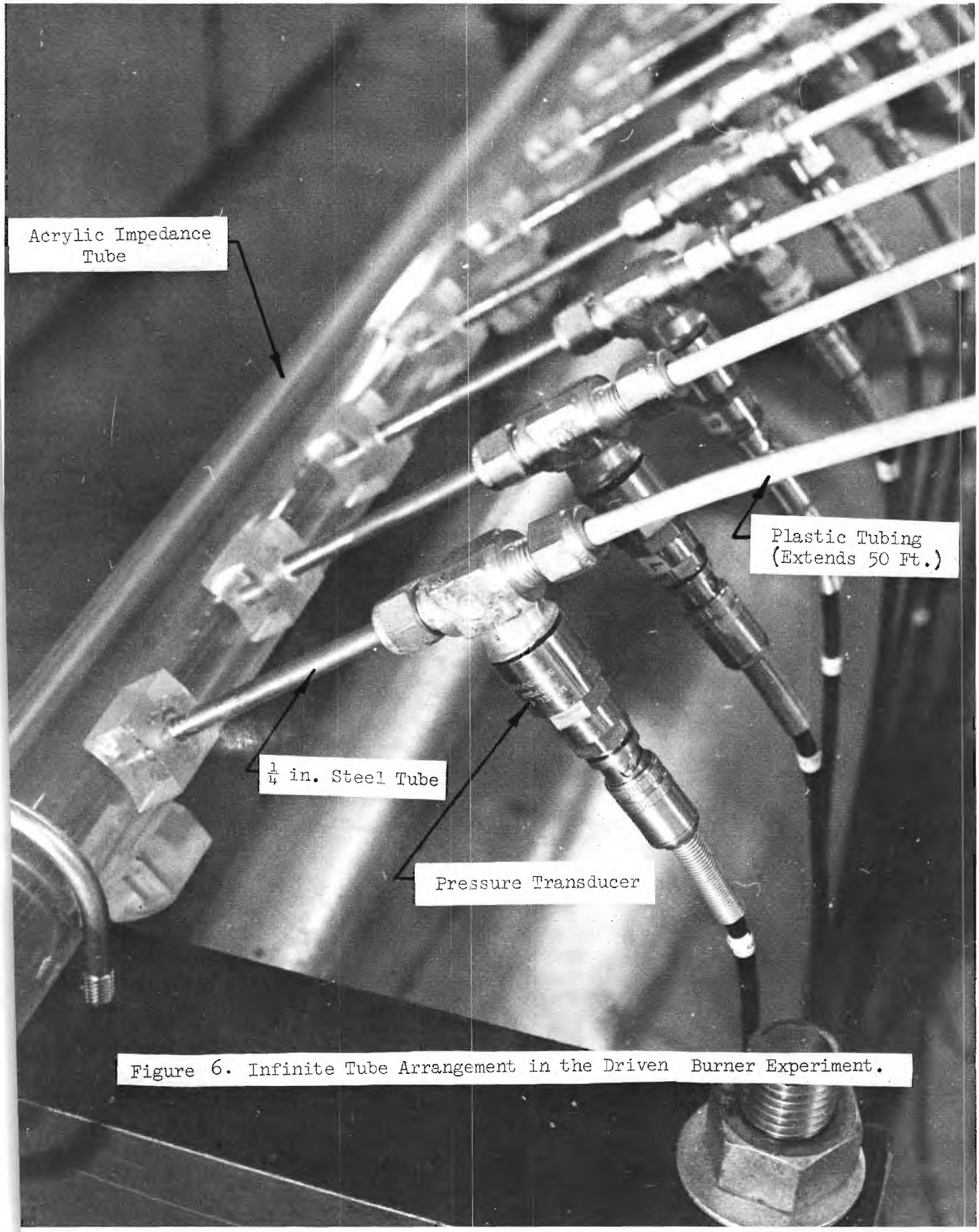

Figure 6. Infinite Tube Arrangement in the Driven Burner Experiment.

measuring temperatures up to 3090°F (3550°R).

In order to achieve a uniform combustion of the tested samples, it is of utmost importance that all parts of the sample surface be ignited simultaneously. After considerable experimentation, best results were obtained with a nichrome wire glued to the sample surface in a "Z" shape. The surface of the sample was then coated with an X-225 pyrotechnic mixture (potassium percholate (72.4%); titanium (14,8%); boron powder (6.9%); and polyisobutylene binder (6.0%) dissolved in toulene). The nichrome wires were attached to copper wire leads which were connected to a power supply. Uniform ignition was obtained when the power supply was turned on.

Experimental Procedures

A test run includes three phases; a brief pre-ignition test period during which only the acoustic drivers are turned on, the ignition, and the propellant burning period. For each test run the dynamic pressure and temperature data are recorded on a 14 channel analog magnetic tape recorder. These data are then played back at reduced speed and automatically plotted providing a time history of the sound pressure levels, phase relationship of the pressures, and the temperatures of the hot gases at several locations inside the tube. An analysis of the time history plots indicates when or if "steady-state" conditions are established in the burner tube during the run. The pressure, phase, and temperature recorded during the selected "steady-state" period can be used to calculate the admittance of the burning solid propellant. This computation will be discussed in the next section.

CHAPTER IV

ANALYTICAL CONSIDERATIONS

This section is concerned with the development of analytical means that would enable the use of mean temperature and dynamic pressure data measured at discrete points along the wall of the driven burner tube, in the determination of the admittance of the tested propellant surface. During an experiment, heat transfer to the tube's walls results in axial and radial mean temperature gradients in the burner tube. These temperature gradients affect the wave structure inside the burner tube and they must be taken into consideration in the data reduction.

To develop the needed data reduction scheme, the standing wave structure inside the burner tube needs to be investigated. To derive the needed conservation equations, the following assumptions are introduced: (1) the combustion process is concentrated at the propellant surface; (2) the gas in the burner is perfect and consists of a single species; (3) the fluctuating part of the heat transfer to the wall is negligible; (4) both the steady state flow quantities and the waves are one dimensional: and (5) the ratios of the various perturbation quantities and the corresponding steady state quantities are sufficiently small so that all nonlinear terms involving products of these quantities may be neglected in the conservation equations. Under these assumptions, the flow in the burner tube can be described by the following system of conservation equations:

continuity: $$\frac{\partial \rho}{\partial t} + \frac{\partial}{\partial x}(\rho u) = 0 \tag{4-1}$$

momentum: $$\frac{\partial u}{\partial t} + u\frac{\partial u}{\partial x} = -\frac{1}{\rho}\frac{\partial P}{\partial x} \tag{4-2}$$

entropy: $$\frac{\partial s}{\partial t} + u\frac{\partial s}{\partial x} = C_v \frac{Q}{P} \tag{4-3}$$

state: $$P = \rho RT$$

$$ds = C_p \frac{dT}{T} - R\frac{dP}{P} \tag{4-4}$$

For the problem under consideration, the various dependent variables can be expressed in the following form:

$$\begin{aligned} u &= \bar{u}(x) + u'(x,t) \\ P &= \bar{P}(x) + P'(x,t) \\ \rho &= \bar{\rho}(x) + \rho'(x,t) \\ T &= \bar{T}(x) + T'(x,t) \\ S &= \bar{S}(x) + S'(x,t) \end{aligned} \tag{4-5}$$

where the barred quantities describe steady state variables while the primed quantities describe the perturbations. Substituting the expressions given in Eq. (4-5) into Eqs. (4-1) through (4-4), linearizing the resulting equations accounting for the periodicity of the waves (e.g., $P' \alpha e^{i\omega t}$), and using the equation of state to eliminate the entropy yields the following system of wave equations:

$$\text{continuity:} \qquad i\omega\rho' + \frac{d}{dx}\left(\bar{\rho}u' + \bar{u}\rho'\right) = 0 \tag{4-6}$$

$$\text{momentum:} \quad \left\{i\omega u' + \frac{d}{dx}\left(\bar{u}u'\right)\right\}\bar{\rho} + \bar{u}\frac{d\bar{u}}{dx}\rho' = -\frac{dP'}{dx} \tag{4-7}$$

$$\text{Entropy:} \qquad i\omega p' + \frac{d\bar{P}}{dx}u' + \bar{u}\frac{dP'}{dx} = \bar{C}^2\left\{i\omega\rho'\right.$$

$$\left. + \frac{d\bar{\rho}}{dx}u' + \bar{u}\frac{d\rho'}{dx} + \bar{u}\frac{d\bar{\rho}}{dx}\frac{P'}{\bar{P}} - \bar{u}\frac{d\bar{\rho}}{dx}\frac{\rho'}{\bar{\rho}}\right\} \tag{4-8}$$

where $$\bar{C}^2 = \gamma\bar{P}/\bar{\rho}$$

The corresponding steady state conservation equations are:

$$\text{continuity:} \qquad \frac{d}{dx}\left(\bar{\rho}\bar{u}\right) = 0 \tag{4-9}$$

$$\text{momentum:} \qquad \bar{u}\frac{d\bar{u}}{dx} = -\frac{1}{\rho}\frac{d\bar{P}}{dx} \tag{4-10}$$

$$\text{entropy:} \qquad \bar{u}\frac{d\bar{S}}{dx} = C_v\frac{\bar{Q}}{\bar{P}} \tag{4-11}$$

Before proceeding with the solution of the wave equations, the solutions of the steady state equations will be briefly discussed. In the present problem the mean flow gradients are caused by the heat transfer from the hot combustion products to the cool burner walls. The quantity $\bar{Q}$ appearing in Eq. (4-11) describes this phenomenon. This relatively simple heat transfer problem has been analyzed by Perry[5] who has shown that for convective heat transfer to the tube's walls the

steady state temperature profile is given by an expression having the following form:

$$\bar{T} = T_w + (T_c - T_w)\, e^{-x/\lambda};\ \lambda = \frac{\rho_s D C_p \bar{r}}{4\bar{h}} \qquad (4\text{-}12)$$

where T_w is a known constant wall temperature. When the mean flow velocity or Mach number is small, it can be shown that the mean pressure $\bar{P}$ is approximately constant. Under these conditions, one can use the equation of state to determine the steady state density profile from the known (i.e., Eq. (4-12)) temperature profile as follows:

$$\bar{\rho} = \frac{\bar{P}}{RT} \quad \text{or} \quad \frac{1}{\bar{\rho}} \frac{d\bar{\rho}}{dx} = -\frac{1}{\bar{T}} \frac{d\bar{T}}{dx} \qquad (4\text{-}13)$$

Once $\bar{\rho}$ is known, $\bar{u}$ can be determined from Eq. (4-9) and the appropriate initial conditions. When the assumption $\bar{P}$ = constant is not used, then by proper manipulations of the steady state equations the distributions of $\bar{u}$, $\bar{\rho}$ and $\bar{P}$ can be determined from the known distribution of $\bar{T}(x)$.

With the steady state quantities known, one can proceed with the solution of the wave equations (i.e., Eqs. (4-6) - (4-8)). In what follows the solution of these equations will be considered for a number of situations encountered under different experimental conditions. When the flow moving through the tube is at the same temperature as the tube's walls, the quantity $\bar{Q}$ in Eq. (4-11) is identically zero and all the mean flow quantities are constant. Under these conditions, the flow may be assumed to be isentropic and the behavior of the waves is described by the following equations:

$$\text{continuity:} \qquad i\omega\rho' + \bar{\rho} \frac{du'}{dx} + \bar{u} \frac{d\rho'}{dx} = 0 \qquad (4\text{-}14)$$

momentum: $$i\omega u' + \bar{u}\frac{du'}{dx} = -\frac{1}{\bar{\rho}}\frac{dP'}{dx} \tag{4-15}$$

entropy: $$\rho' = \frac{P'}{\bar{C}^2} \tag{4-16}$$

Eliminating variables between the above equations yields the following equation for P':

$$(1 - \bar{M}^2)\frac{d^2P'}{dx^2} - 2ik\bar{M}\frac{dP'}{dx} + k^2P' = 0 \tag{4-17}$$

where $\bar{M}$ and $k = \omega/\bar{C}$ respectively respresent the constant mean flow Mach number and the wave number. The solution of Eq. (4-17) can be expressed in the following form:

$$P' = A_+ \; e^{-\frac{ikx}{1+\bar{M}}} + A_- \; e^{\frac{ikx}{1-\bar{M}}} \tag{4-18}$$

and by use of the momentum equation it can be shown that:

$$\bar{\rho}\bar{u}u' = A_+ \; e^{-\frac{ikx}{1+\bar{M}}} - A_- \; e^{\frac{ikx}{1-\bar{M}}} \tag{4-19}$$

Rewriting the complex constants A_+ and A_- in the following form:

$$\begin{aligned} A_+ &= \tfrac{1}{2}Ae^{\pi\alpha - i\pi(\beta + \frac{1}{2})} \\ A_- &= \tfrac{1}{2}Ae^{-\pi\alpha + i\pi(\beta + \frac{1}{2})} \end{aligned} \tag{4-20}$$

It can be shown[2] that the constants α and β have the following physical interpretation:

$$\left[\frac{\text{Amplitude of Reflected Pressure Wave}}{\text{Amplitude of Incident Pressure Wave}}\right]_{x=0} = e^{-2\pi\alpha} \qquad (4\text{-}21)$$

$$(\text{The Phase difference between the incident and reflected pressure waves})_{x=0}$$

$$= \pi(2\beta + 1)$$

Where x = 0 represents the location where the admittance is measured. Substituting Eqs. (4-20) into Eqs. (4-18) and (4-19) reduces the latter into the following forms:

$$P' = - iAe^{iax} \sinh[\pi\alpha - i(\pi\beta + k_1 x)] \qquad (4\text{-}22)$$

$$u' = \frac{-iAe^{iax}}{\bar{\rho}\,\bar{c}} \{\cosh[\pi\alpha - i(\pi\beta + k_1 x)]\} \qquad (4\text{-}23)$$

where

$$a = \frac{k\bar{M}}{1-\bar{M}^2} \; ; \; k_1 = \frac{k}{1-\bar{M}^2} \qquad (4\text{-}24)$$

Using the above expressions for P' and u' it can be shown the nondimensional admittance Y at x = 0 is given by the following expression:

$$Y = \bar{\rho}\,\bar{c}\,\frac{u'}{P'}\Big|_{x=0} = \text{Coth}\,\pi(\alpha - i\beta) \qquad (4\text{-}25)$$

Equation (4-25) can be used to determine the unknown admittance Y once the values of α and β are known for given test conditions. Since according to Eq. (4-22) the pressure wave P' depends upon α and β, then these quantities could in principle be determined from measurements of pressure amplitudes and phases and the "fitting" of the experimental data with the corresponding theoretical expressions given by Eq. (4-22). This procedure was followed with great success in studies aimed at the

determination of choked nozzle admittances[2,3].

Since in the studies conducted under this program the mean velocity and flow Mach number are expected to be small, it is quite possible that reasonalbe solutions might be obtained by setting these quantities equal to zero in Eqs. (4-6)- (4-8). The resulting system of equations describes the wave structure in a tube in which the medium is stationary but it exhibits property gradients due to heat transfer to the tube's walls. The conservation equation describing this flow situation are:

continuity: $$i\omega\rho' + \frac{d}{dx}(\bar{\rho}\, u') = 0 \qquad (4\text{-}26)$$

momentum: $$i\omega u' = -\frac{1}{\bar{\rho}}\frac{dP'}{dx} \qquad (4\text{-}27)$$

entropy: $$i\omega P' = \bar{C}^2 \{u'\frac{d\bar{\rho}}{dx} - \frac{d}{dx}(\bar{\rho}u')\} \qquad (4\text{-}28)$$

Examination of the above system of equations indicates that Eqs. (4-27) and (4-28) contain P' and u' only and they can be solved numerically once the values of u' and P' at some "initial" location and the distribution of the mean flow variables are known. Once u' and P' are determined, ρ' can in principle be determined from Eqs. (4-26) and (4-28).

When $\bar{u}$ or $\bar{M}$ are not identically zero, then solutions can be obtained by solving the originally derived systems of wave equations; that is Eqs. (4-6) through (4-8). To be amenable to numerical integration, these equations are rearranged into the following form:

$$\frac{du'}{dx} = -\frac{\rho'}{\bar{\rho}}\frac{d\bar{u}}{dx} + \{(-\frac{\bar{\rho}\bar{u}}{\bar{P}}\frac{d\bar{\rho}}{dx})\rho' + u'[\bar{u}\,\bar{\rho}\frac{d\bar{u}}{dx} - \frac{d\bar{P}}{dx}] + P'(\frac{\bar{u}\bar{c}^2}{\bar{P}}\cdot\frac{d\bar{\rho}}{dx})$$

$$+ i\omega(\bar{u}\,\bar{\rho}\,u' - P')\}/\,\bar{\rho}(\bar{c}^2 - \bar{u}^2) \qquad (4\text{-}29)$$

$$\frac{d\rho'}{dx} = -\,(i\omega\rho' + \bar{\rho}\,\frac{du'}{dx} + u'\,\frac{d\bar{\rho}}{dx} + \rho'\,\frac{d\bar{u}}{dx}\,)/\bar{u} \qquad (4\text{-}30)$$

$$\frac{dP'}{dx} = -\,\{(i\omega u' + \bar{u}\,\frac{du'}{dx} + u'\,\frac{d\bar{u}}{dx}\,)\,\bar{\rho} + \rho'\bar{u}\,\frac{d\bar{u}}{dx}\,\} \qquad (4\text{-}31)$$

The above are a system of three linear, homogeneous coupled ordinary differential equations. To obtain their solutions, the steady state variables and three initial or boundary conditions must be known.

Since the solutions of the wave equations for the cases $\bar{u} = 0$ and $\bar{u} = \bar{u}(x) \neq 0$ are similar, the method of solution for these two cases can be illustrated by discussing the $\bar{u} \neq 0$ case. As stated earlier, Eqs. (4-29) - (4-31) could be integrated numerically if the values of u', ρ' and P' were known at some x location. Since in the experimental arrangement under consideration it would be extremely difficult, if not impossible, to accurately measure u' and ρ', then the question arises whether the measurements of these quantities could be replaced by pressure perturbation measurements. Stated differently, the question is whether solutions of Eqs. (4-29) - (4-31) can be obtained from pressure amplitude and phase measurement at three locations along the burner tube. The answer to this question is yes because of the linearity of the system of the wave equations. The mathematical technique that enables one to convert the solution of this boundary value problem into the solution of an initial value problem is discussed in Appendix A.

CHAPTER V

RESULTS

The efforts during the first year of investigation were divided into analytical and experimental studies. The experimental efforts concentrated on the development of the experimental setup, experimental procedures and measurement techniques, while the analytical studies concentrated on the development of a reliable data reduction scheme. These two efforts will be briefly discussed in the following subsections.

Analytical Studies

The main objectives of the analytical studies are (1) the development of analytical technique for the determination of the admittances of burning solid propellants from measured pressure amplitudes and phases and (2) investigation of the accuracy of the developed solution technique.

To obtain the steady state solutions the following experimentally determined* steady state temperature distribution and steady state burning rate law

$$\bar{T}(x) = T_w + (T_c - T_w)\, e^{-x/\lambda} \quad ; \; T_w = 530; \; T_c = 3780; \; \lambda = 4.4 \qquad (5\text{-}1)$$

$$\bar{r} = a\bar{P}^n \quad ; \; a = .05 \quad n = .35 \qquad (5\text{-}2)$$

were used to determine the distrubutions of $\bar{u}$, $\bar{\rho}$, $\bar{c}$ and $\bar{s}$ in the burner tube; and the results were shown in Figure 7.

---

* See discussion of experimental results.

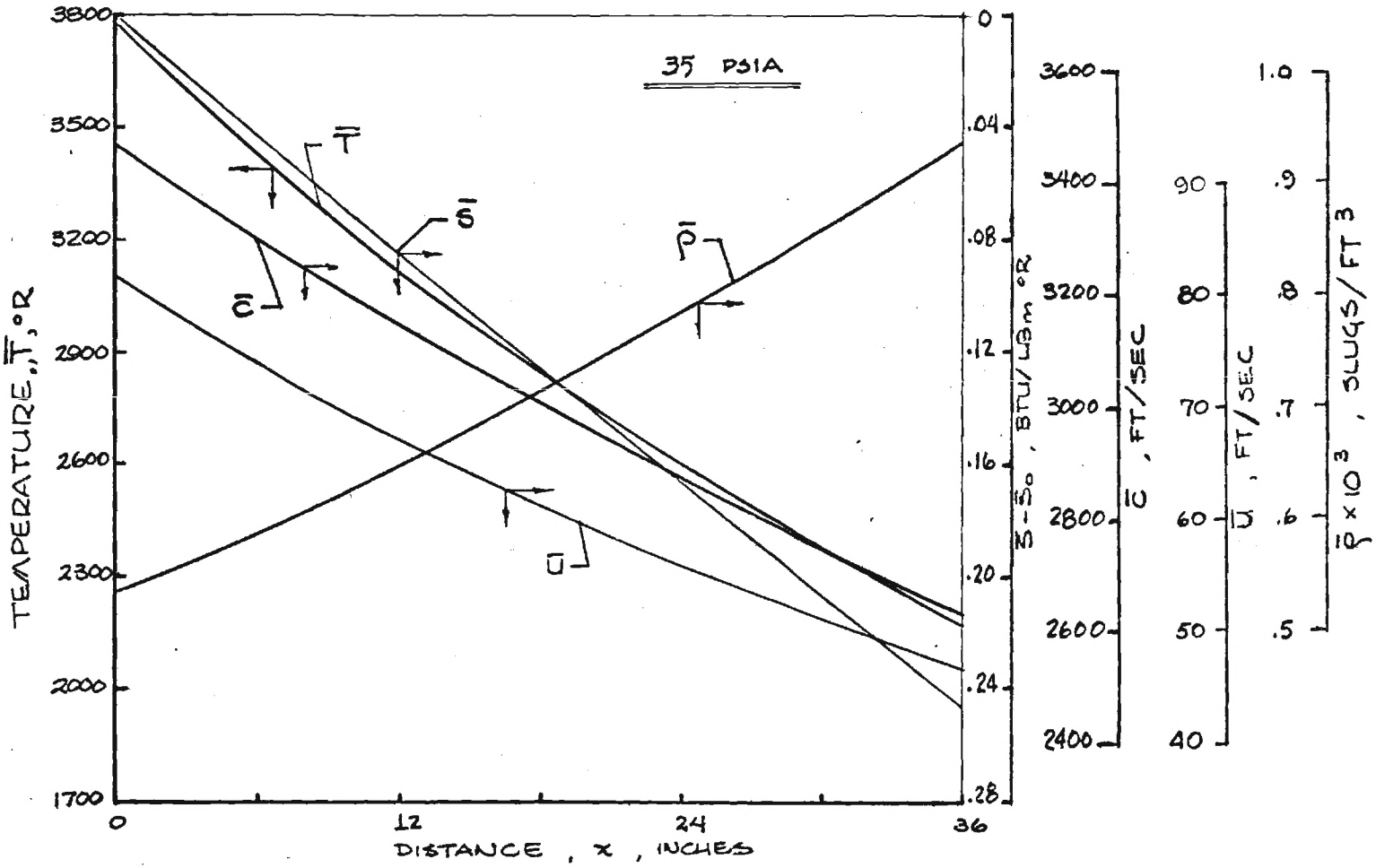

Figure 7. Axial Variation of Mean Parameters

To gain an insight into the properties of the wave structure inside a burner with a mean temperature and velocity gradients, the admittance pressure and density perturbations at the burning propellant surface have been assumed to be known (i.e., $Y_i = .00015$, $Y_r = .005$, $P'_r = -5.0$, $P'_i = -6.0$, $\rho'_r = -.458 \times 10^{-6}$, $\rho_i = -.550 \times 10^{-6}$) and the desired wave structure was obtained by integrating Eqs. (4-29) - (4-31) numerically starting at x = 0. In this computation the steady state profiles shown in Fig. 7 were used. The results of those computations are shown in Figures (8) through (11). The most interesting result obtained from these computations is that successive pressure amplitude maxima and minima increase with x. The same wave structure is known to occur when an acoustic wave is excited in a tube containing an attenuating medium but no mean flow. Hence, it appears that the presence of a negative temperature gradient (i.e., $d\bar{T}/dx < 0$) exerts the same effect upon the wave structure as the presence of wave-energy attenuation in the medium. This interesting observation will have to be born in mind when the attenuation provided by aluminum particles in the flow will be investigated later on in this program.

Next, the accuracy of the data reduction scheme was investigated. In this study the admittance at the propellant surface was assumed to be known, and Eqs. (4-26) - (4-28), for the case $\bar{u} = 0$, were integrated to determine the wave structure in the tube. Once the wave structure was known, the admittance was recomputed using hypothetical pressure measurements and the mathematical technique discussed in Appendix A. The hypothetical pressure measurements were obtained by adding errors to the computed exact solutions. Using this procedure, the error in

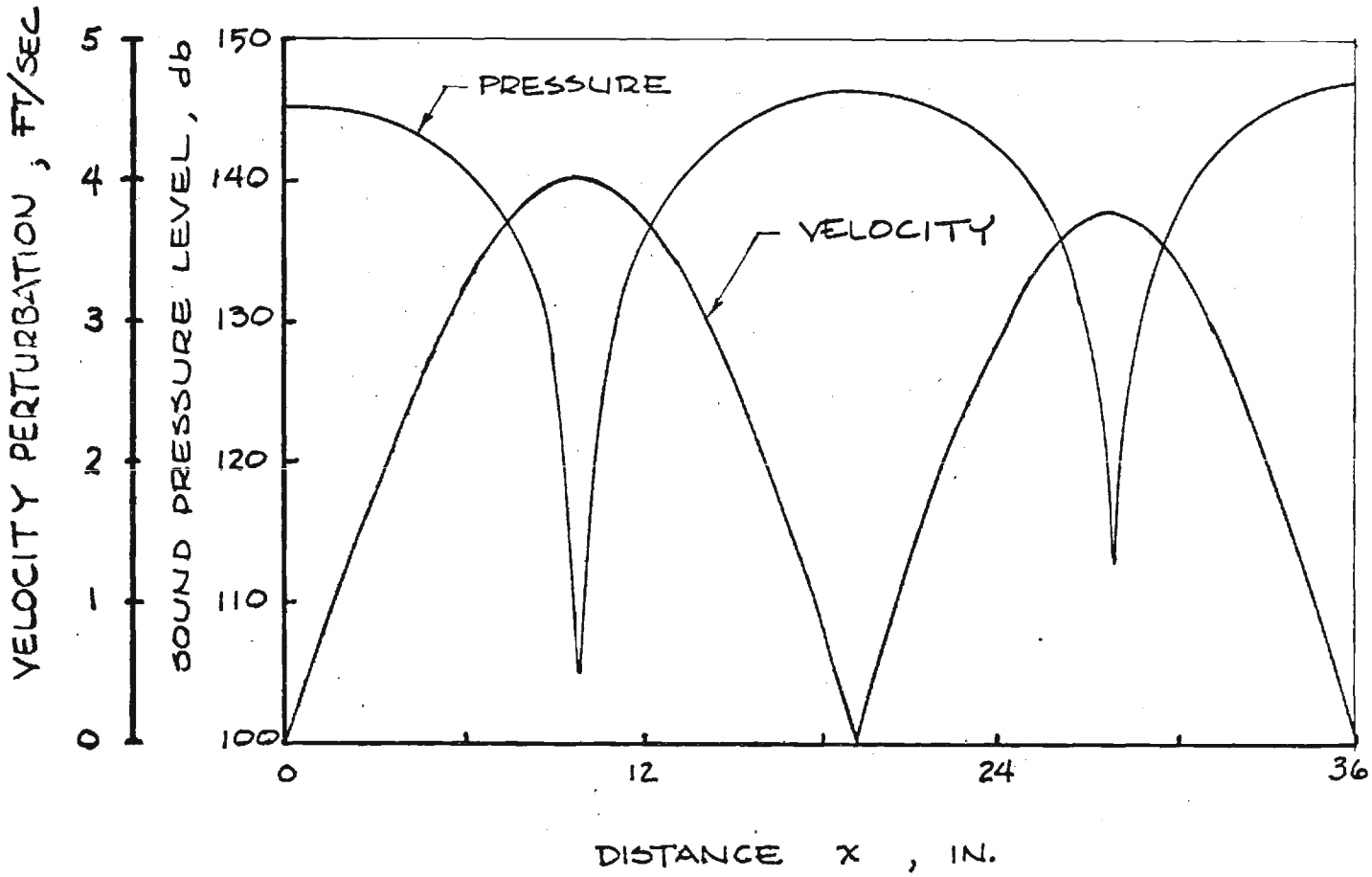

Figure 8. Axial Variation of Pressure and Velocity Amplitudes, ω = 1000 Hz

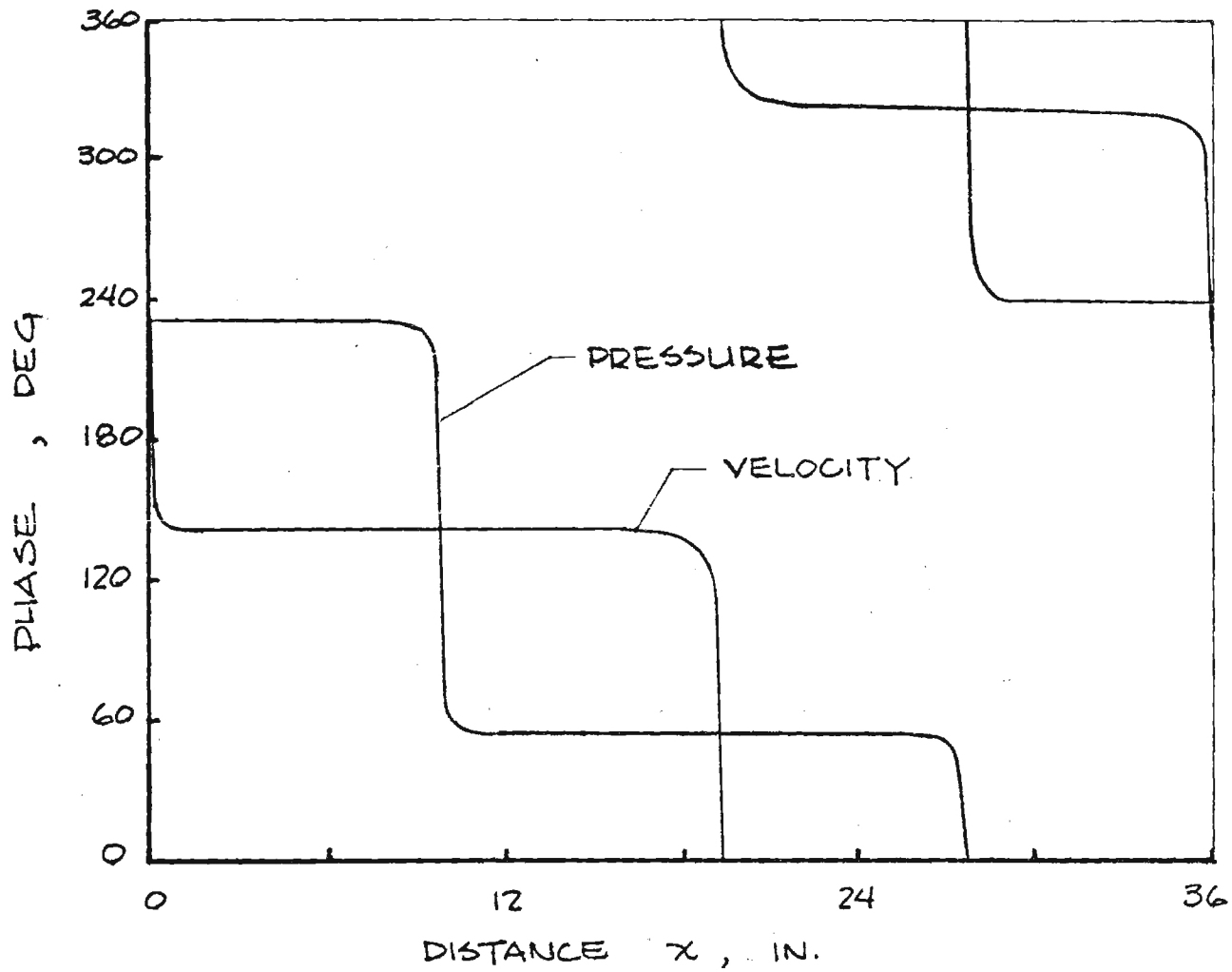

Figure 9. Axial Variation of Pressure and Velocity Phases for W = 1000 Hz

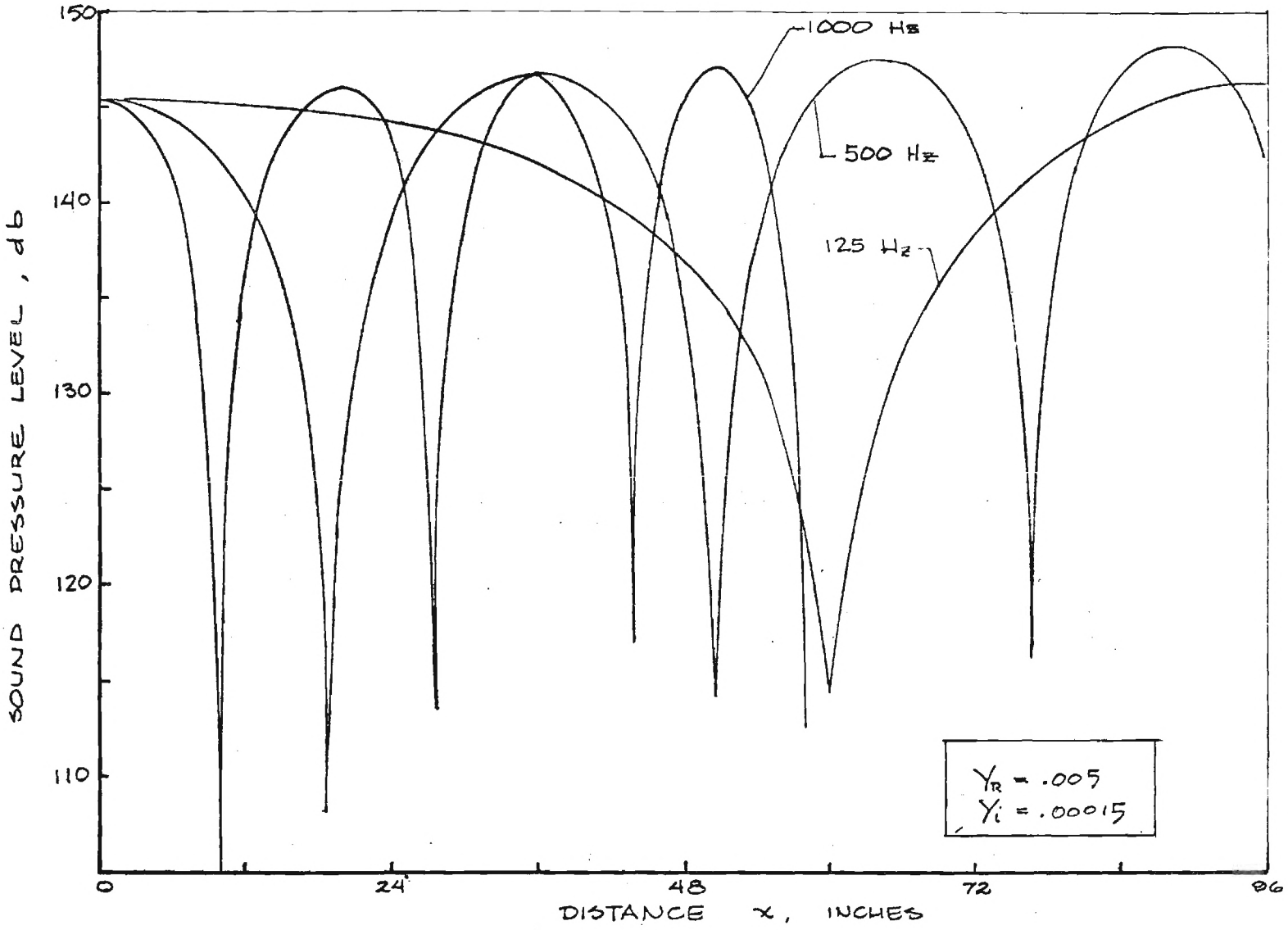

Figure 10. Axial Variation of Pressure Amplitudes for Various Frequencies

$\bar{U} = 0$
$Y_R = -6.822$
$Y_i = -1.281$
$\omega = 1000$ Hz
LOCATION OF MEASUREMENTS . $X = 0$, $X = 1$

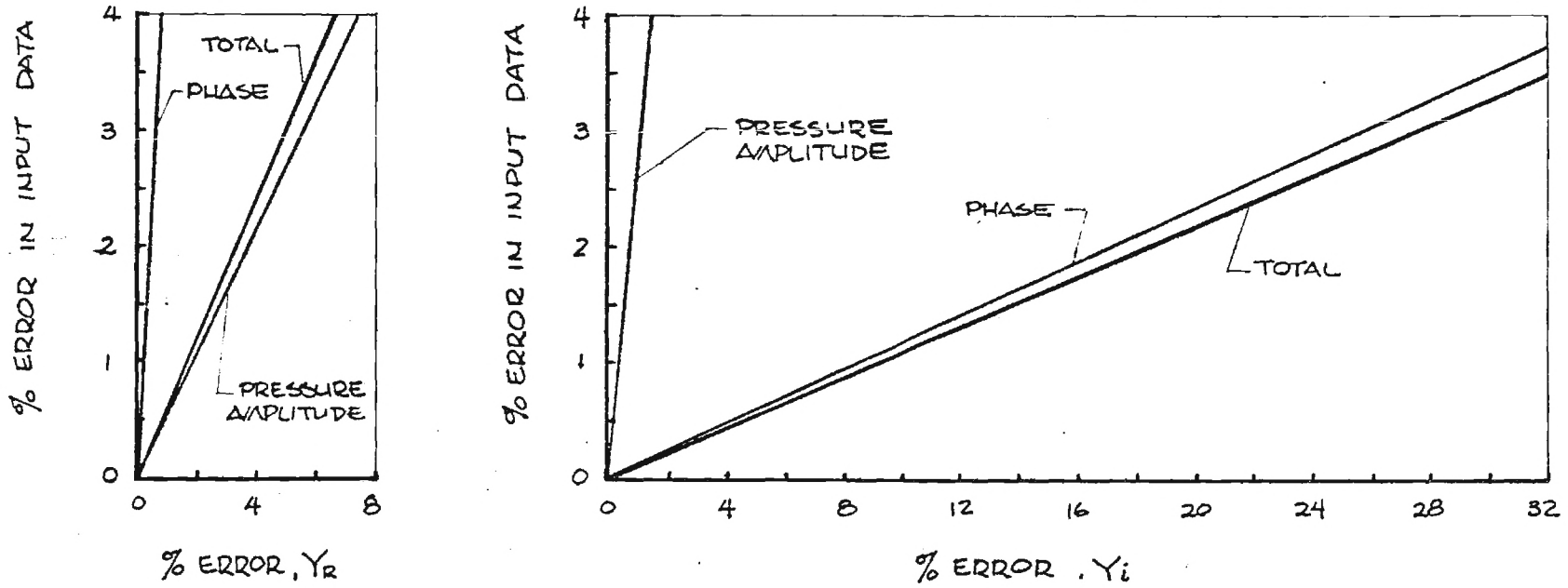

Figure 11. Error in Admittance, Due to the Error in Input Data

the computed admittances were determined. The results of such a computation, for a specific case, are presented in Fig. (11) where the resulting percent errors in the real and imaginary parts of the propellant admittances are plotted versus the percent errors in the input data. For this computation a 1% error in input data produced 2% and 8% in the real and imaginary parts of the admittances, respectively. Figure 11 suggests that some cancellation of errors occurs. This became evident when the plot for the error in Y_r is examined. The total error in Y_r produced when intentional errors were introduced in both the amplitude and phase data was smaller than the error produced in Y_r when only intentional errors in pressure amplitude were introduced. It is also interesting to note that linear relationships exist between the errors in input data and the resulting errors in Y_r and Y_i.

Studies currently underway are concerned with the development of a similar data reduction computational scheme for the case where $\bar{u} \neq 0$. Some computational difficulties arise in this case as it involves the solution of three coupled equations and the coupling between u' and P', and ρ' is weak. Various methods for overcoming these difficulties are currently under study. In addition, studies are underway to determine the optimum distribution of transducers, along the burner tube walls, that will minimize the resulting errors in Y_i and Y_R. The results of this study will be used as a guide in the optimization of the distribution of transducers along the tube in the experimental phase of this program.

Experimental Results

As a first step toward checking the proper operation of the experimental setup developed in this program, a series of cold-flow tests have been conducted. In these tests the solid propellant were placed with two material samples of widely different admittance values; one of the tested materials was a hard acrylic plate whose theoretical admittance is known to be zero, and the other material was a one-inch thick sound absorbing insulating material. The admittances of these materials were measured in the burner tube by use of the perviously discussed methods, and the data are plotted in Fig. (12). As shown in this figure, the experimental technique was indeed sensitive enough to detect the differences between the admittances of the tested samples. Also, the measured data indicates that within the anticipated experimental accuracy, the real and imaginary parts of the admittance of the tested acrylic material are identically zero throughout most of the tested frequency range. This results is in agreement with the theoretically known admittances of a hard surface.

The next series of tests was conducted to determine the flow conditions inside the burner tube during the combustion of solid propellant samples. Specifically, the steady state temperature gradients inside the tube were determined, in several tests, by use of the previously mentioned thermocouples several tests were run with the thermocouples inserted different distances into the tube. All the tests were conducted with a T-13 propellant kindly provided by Dr. Dave Flanigan from Thiohol. The results are presented in Figs. (13) through (18); Figs. (13) through (16) show the temperature-time histories

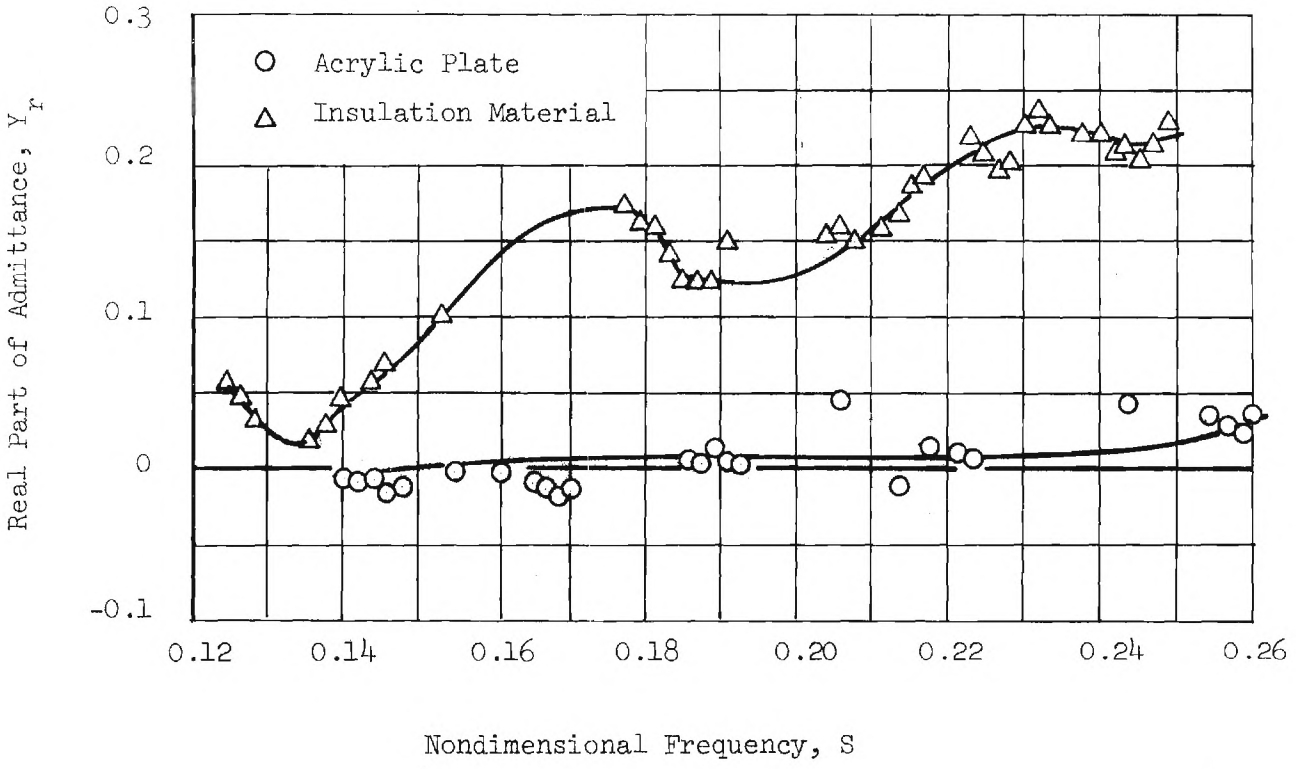

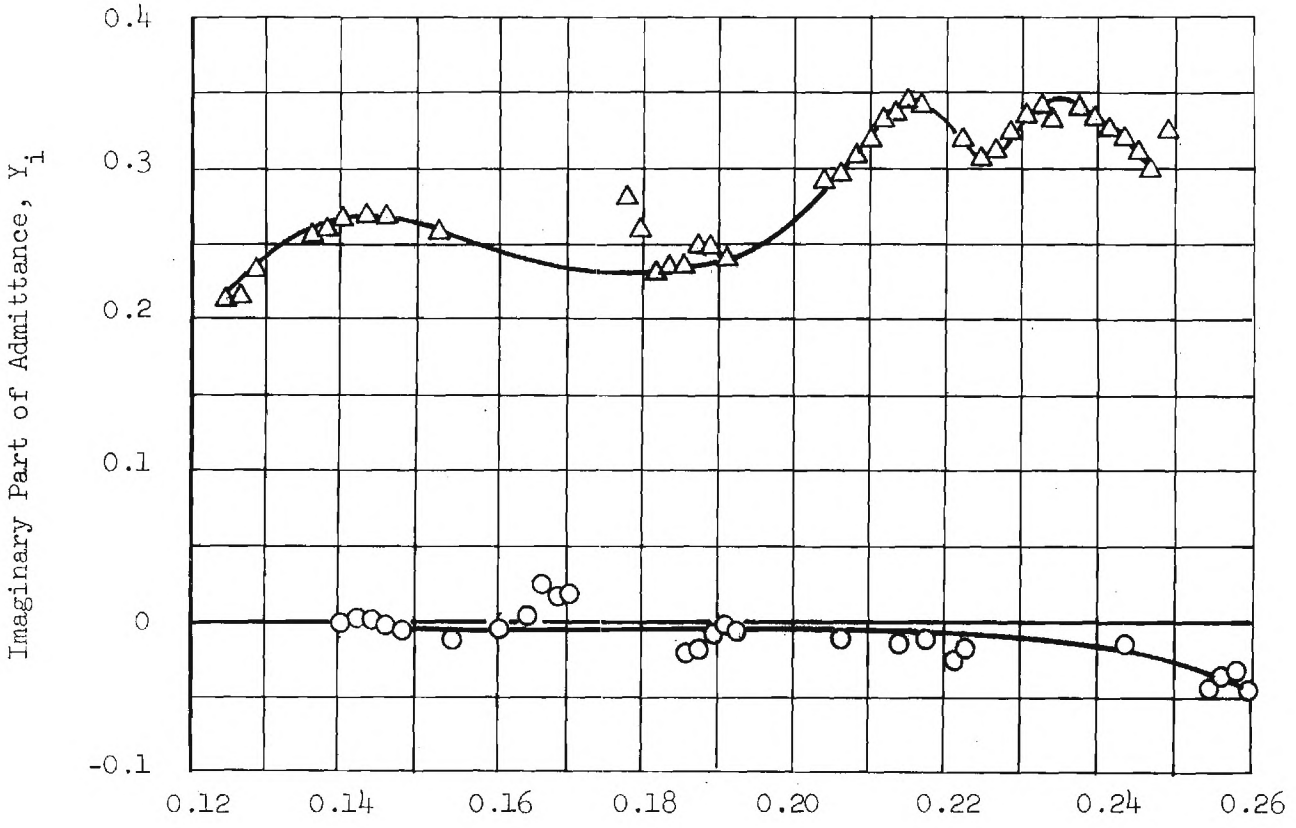

Figure 12. Admittance Values from Cold Flow Tests.

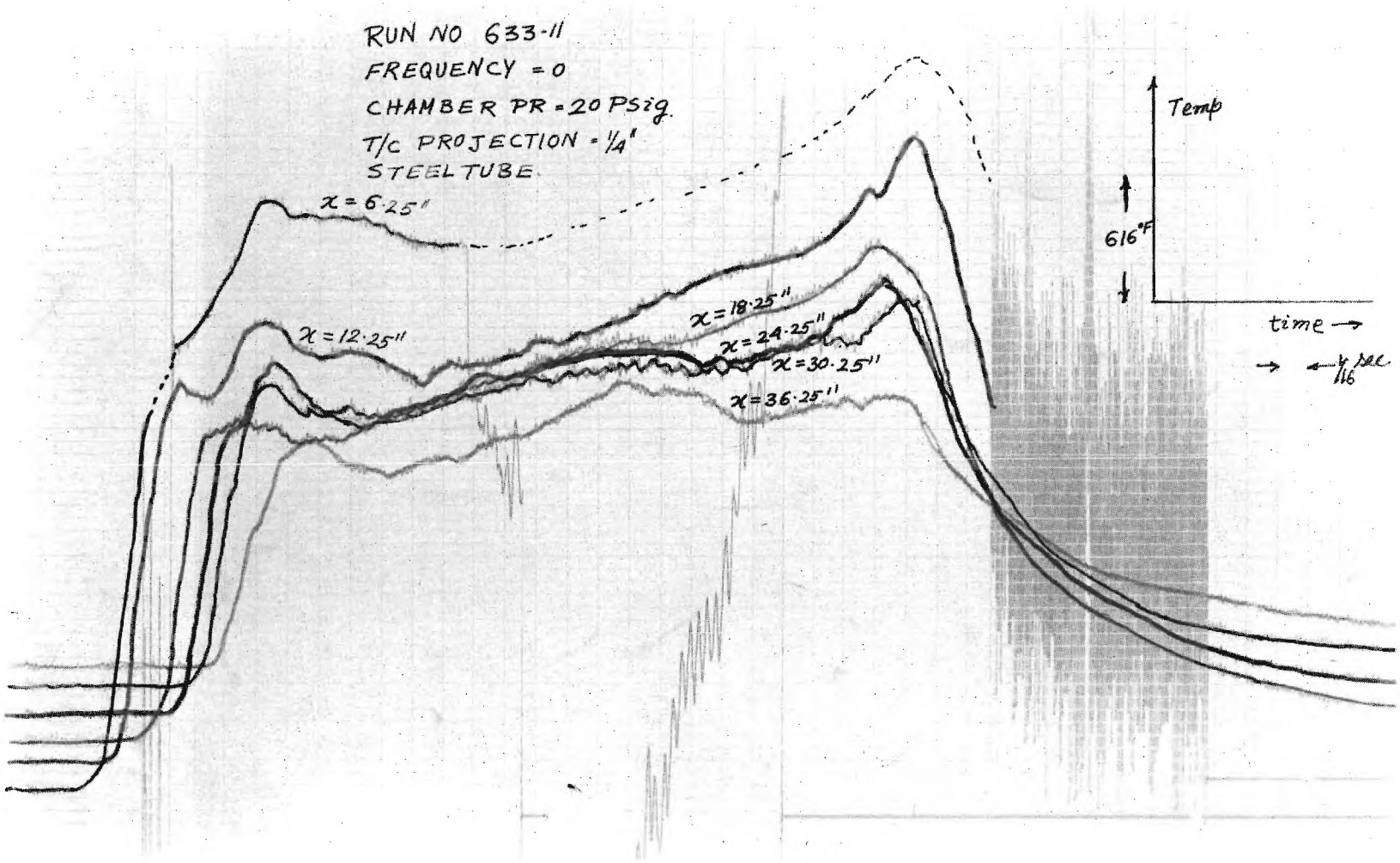

Figure 13. Mean Temperature Variation with Respect to Time

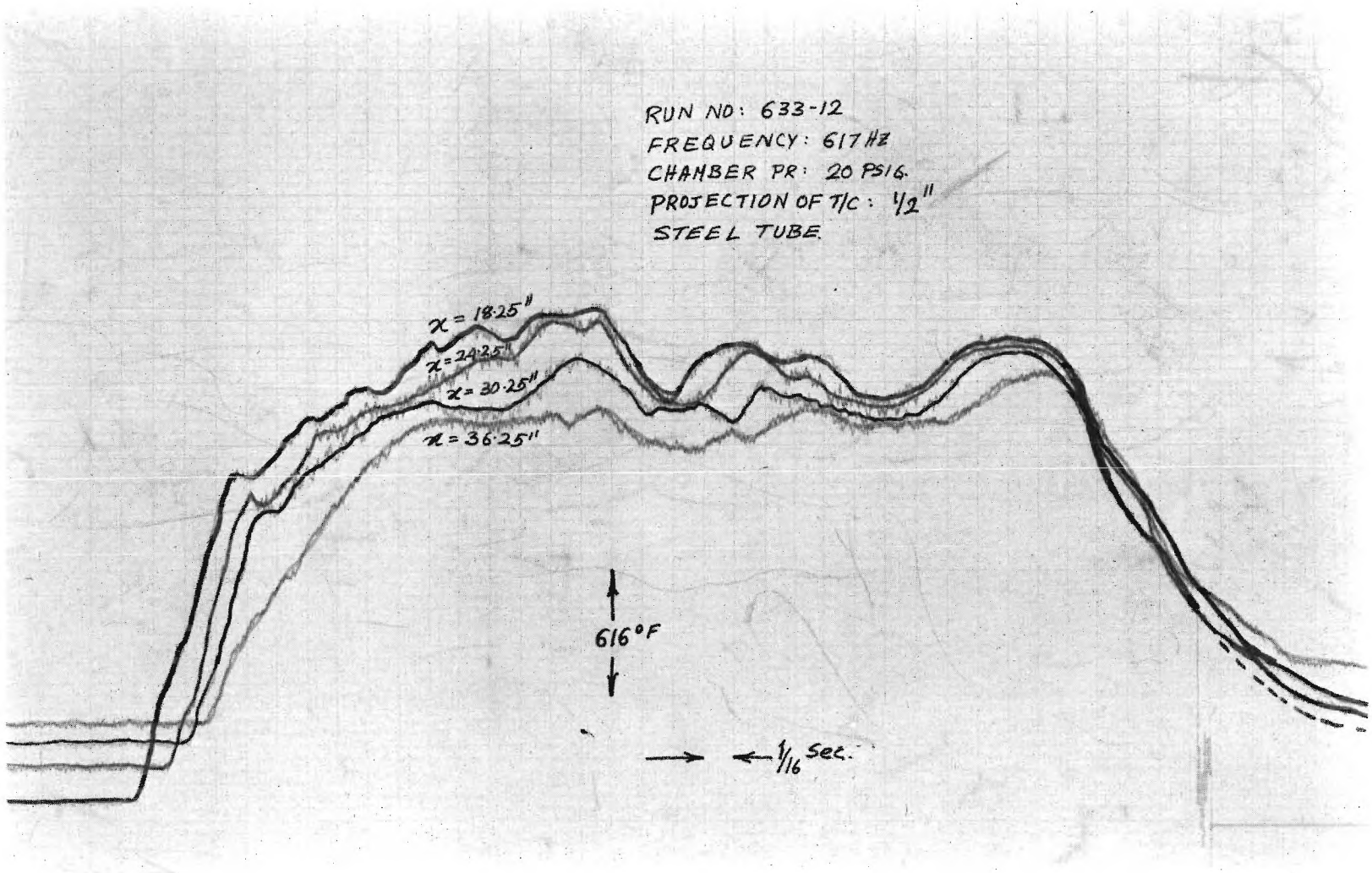

Figure 14. Mean Temperature Variation with Respect to Time

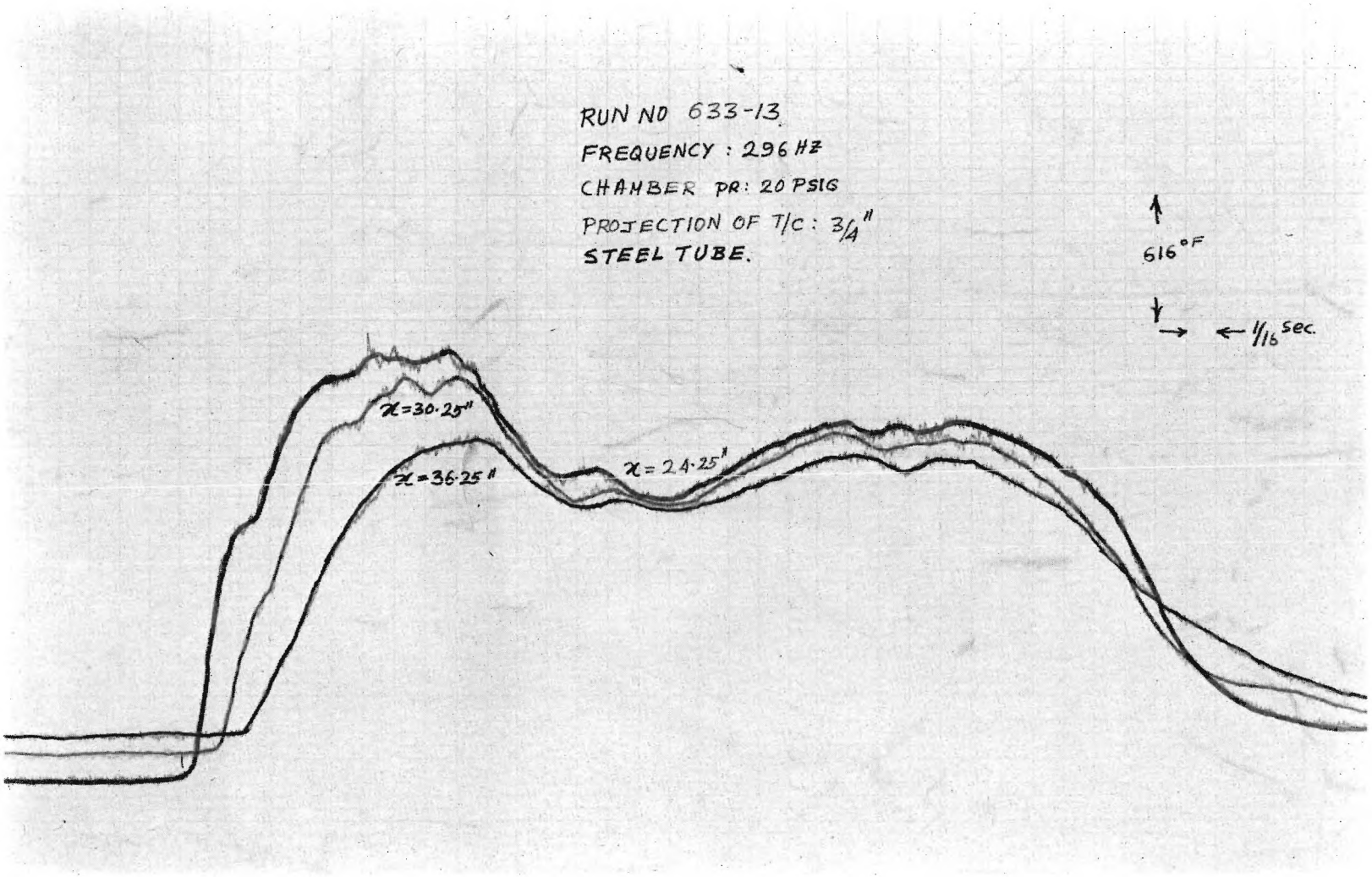

Figure 15. Mean Temperature Variation with Respect to Time

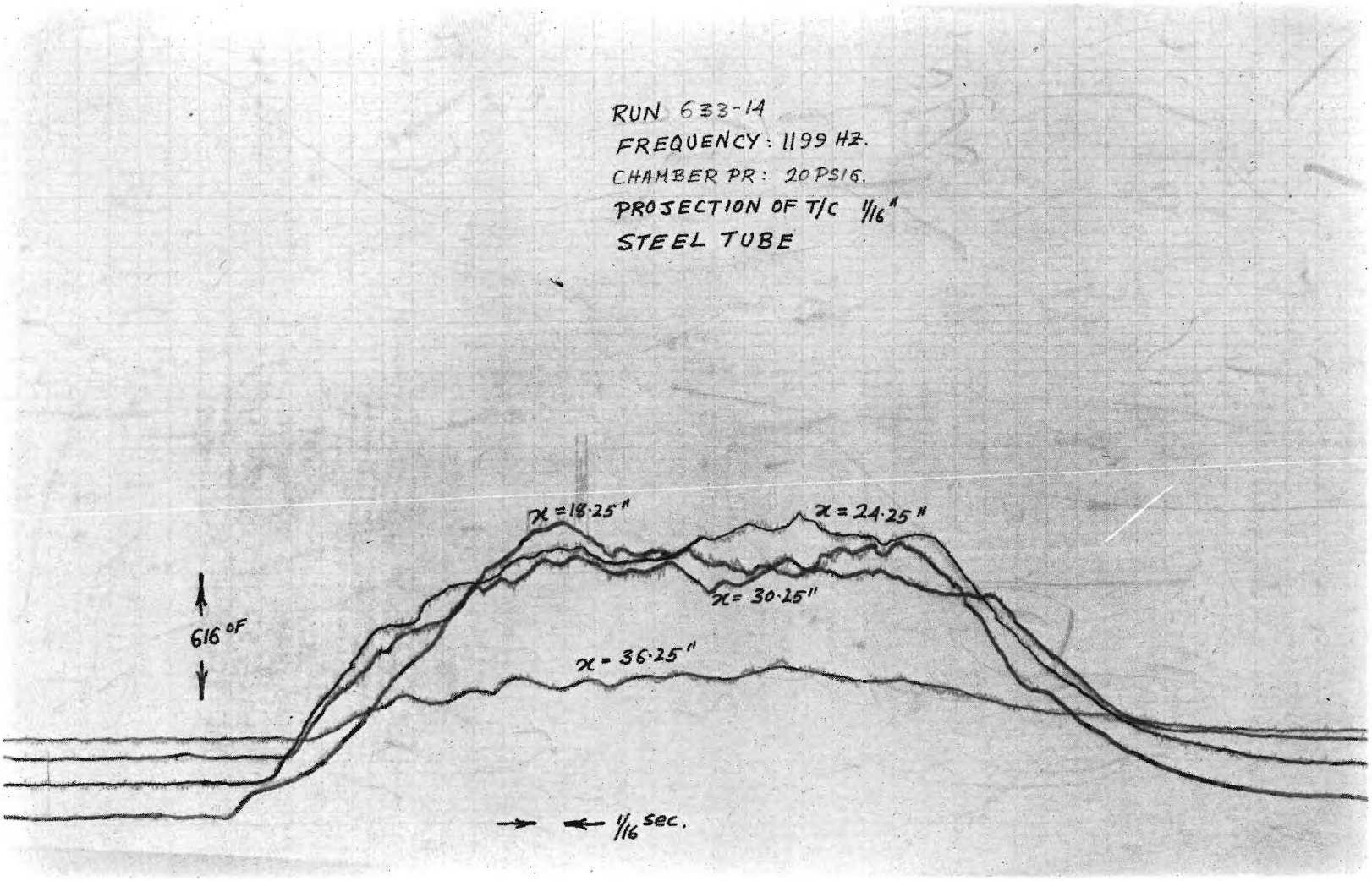

Figure 16. Mean Temperature Variation with Respect to Time

of the various thermocouples at different tests while Fig. (17) shows instantaneous axial temperature profiles constructed by use of the above-mentioned temperature-time curves; the data presented in Fig. (17) was cross plotted to deduce radial temperature profiles at various axial locations and the results were presented in Fig. 18. It should also be pointed out that although some of the temperature tests were conducted without any wave oscillations in the tube and others were conducted with wave oscillations, there is no apparent difference in the measured data. This print will be further investigated in the future. The inescapable conclusion reached from this temperature data is that both axial and radial temperature gradients exist in forced oscillations burner as well as in T-burners and their effect upon the data reduction procedure and deduced admittances needs to be investigated.

The experimental data describing the variation of the temperature along the tube were fitted with the analytical solution given by Eq. (4-12) and the results are shown as solid lines in Fig. (17). For these computations T_w was taken to equal $70^{\circ}F$ and the corresponding effective values of the constant λ are listed in the accompanying table; the corresponding values of T_c can be obtained from the curves.

The next set of experiments was conducted with the objective of determining the wave structure inside the tube during forced oscillation experiments. Tests at a number of frequencies were conducted; however, for the sake of brevity, only the data obtained at the frequency of 467 Hz will be discussed in detail in this report. Presented in Figs. (19) through (26) are the time histories of all the temperatures, pressure

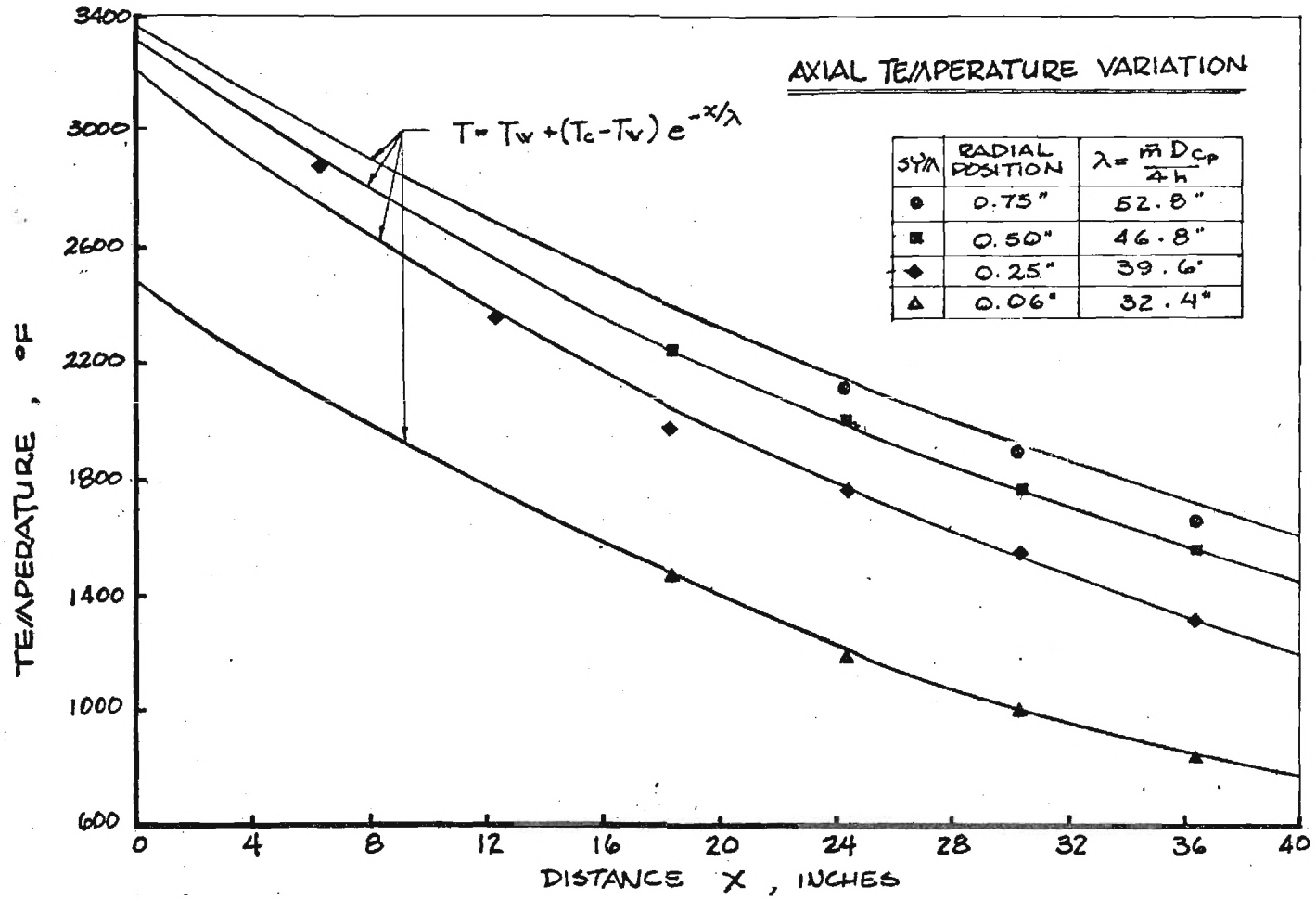

Figure 17. Axial Variation of Mean Temperature

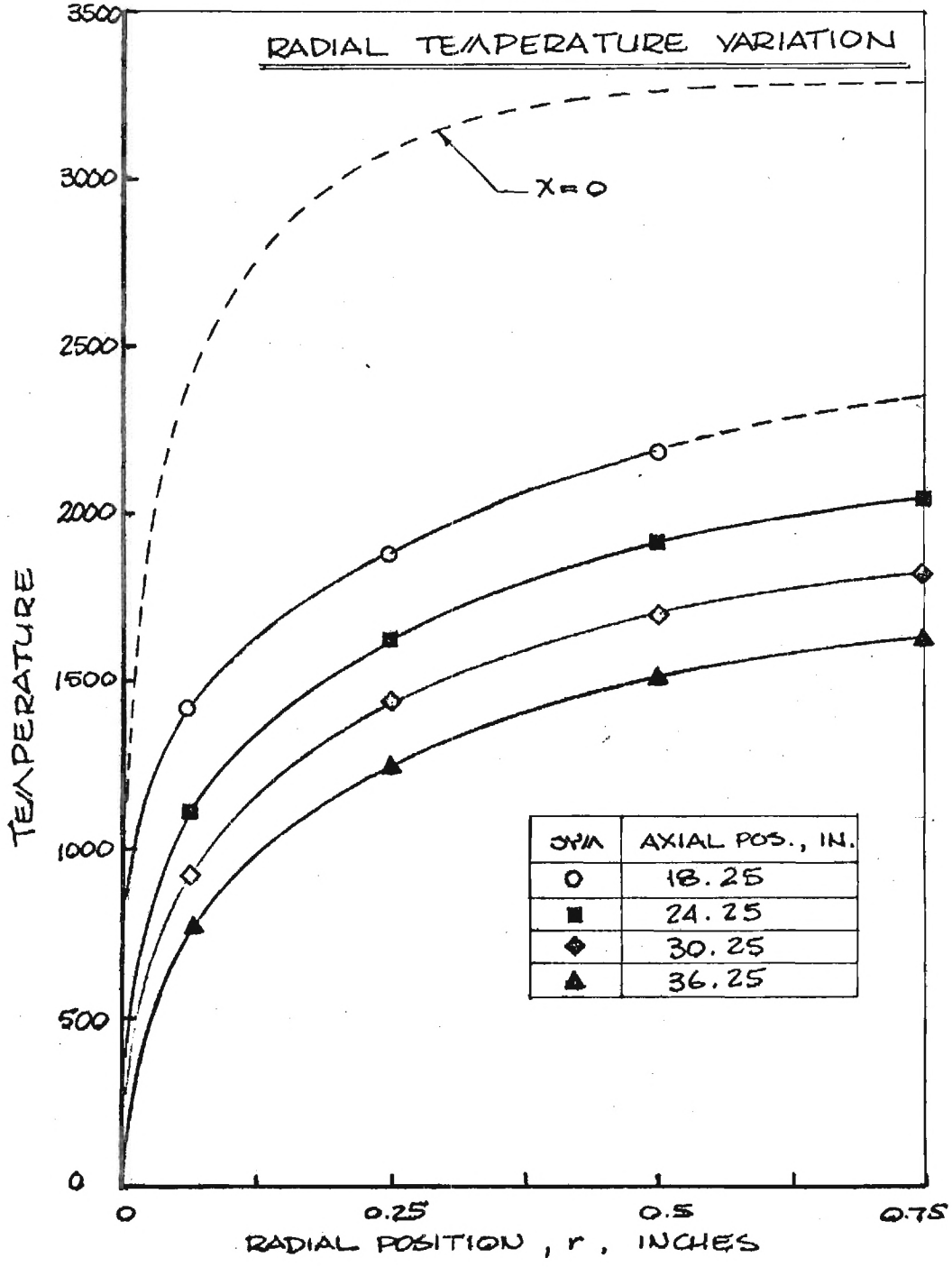

Figure 18. Radial Variation of Mean Temperature

amplitudes and pressure phases measured during this test. Examination of Fig. (19) clearly indicates the transient temperature rise in the tube following the ignition of the T-13 propellant, the quasi-steady period of burning and the temperature drop after completion of burning. Figures (20) through (26) describe the corresponding time-histories of the pressure amplitudes and phases. Careful examination of these figures points out to a very interesting phenomenon; namely, after ignition, conditions in the burner tube are never truly steady. On the other hand, the pressure amplitudes and phases prior and after burning appear to be perfectly stable. Based on observations of high-speed movies taken during two of the tests, it is conjectured herein that the unsteadiness observed during the propellant burning is due to nonuniform burning of the sample or unsteadiness of the flame on the surface of the propellant. This conjecture needs, however, further verification and study.

The next step in the analysis is to use the dynamic pressure data presented in Figs. (20) through (26) in the determination of the instantaneous pressure amplitude and phase distributions in the tube. Cross plotting the amplitude and phase data at $t = t^*$ in Figs. (20) through (26), yields the instantaneous amplitude and phase patterns shown in Fig. (27). Note that Fig. (27) indicates the locations of the pressure transducers along the tube during the experiment; the broken lines indicate extrapolation of the measured data.

Once the development of the computer program for determining the admittances from pressure data is completed, the data of Fig. 27 and similar data obtained at tests conducted with other frequencies will

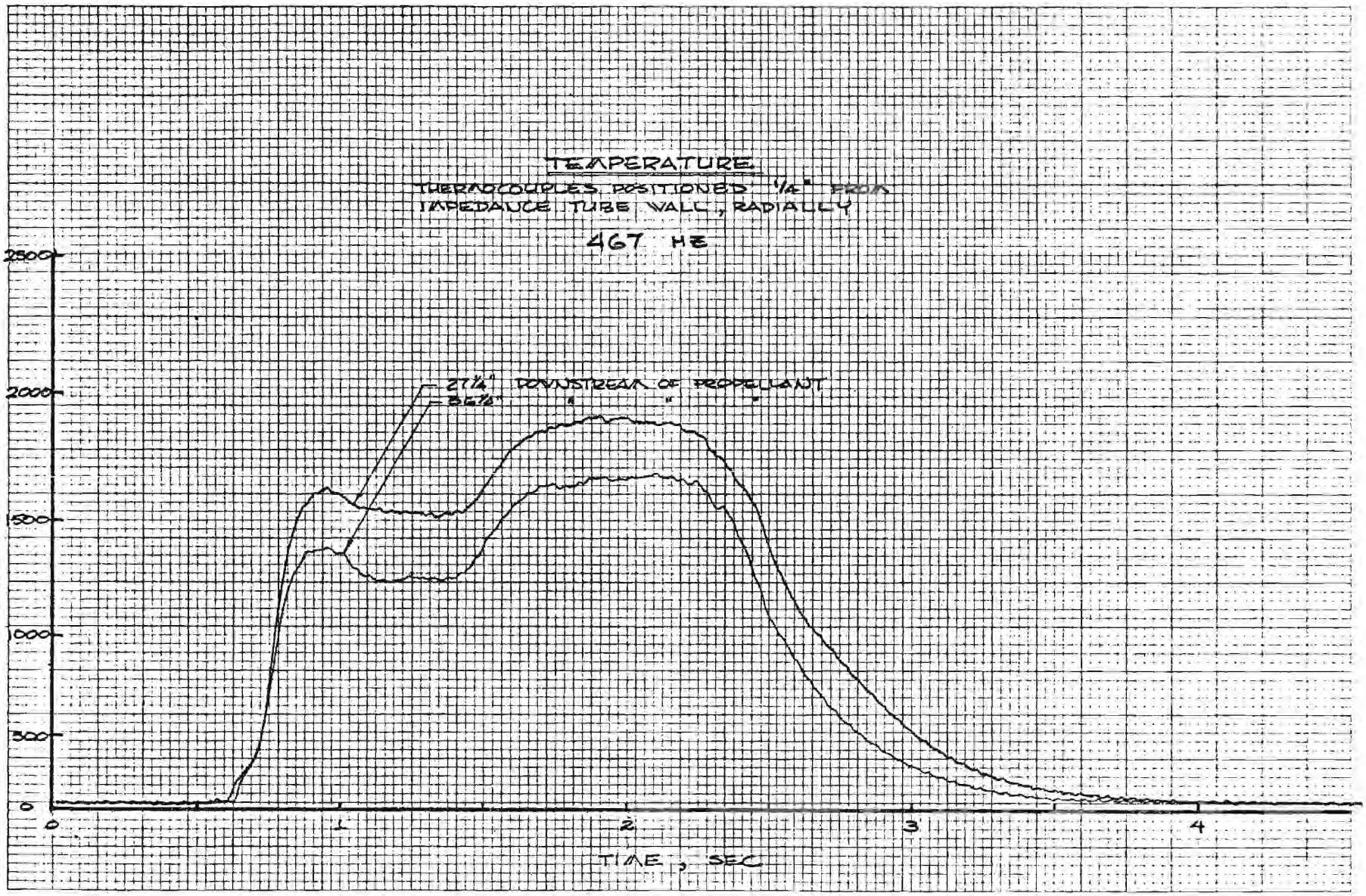

Figure 19. Variation of Mean Temperature with Respect to Time

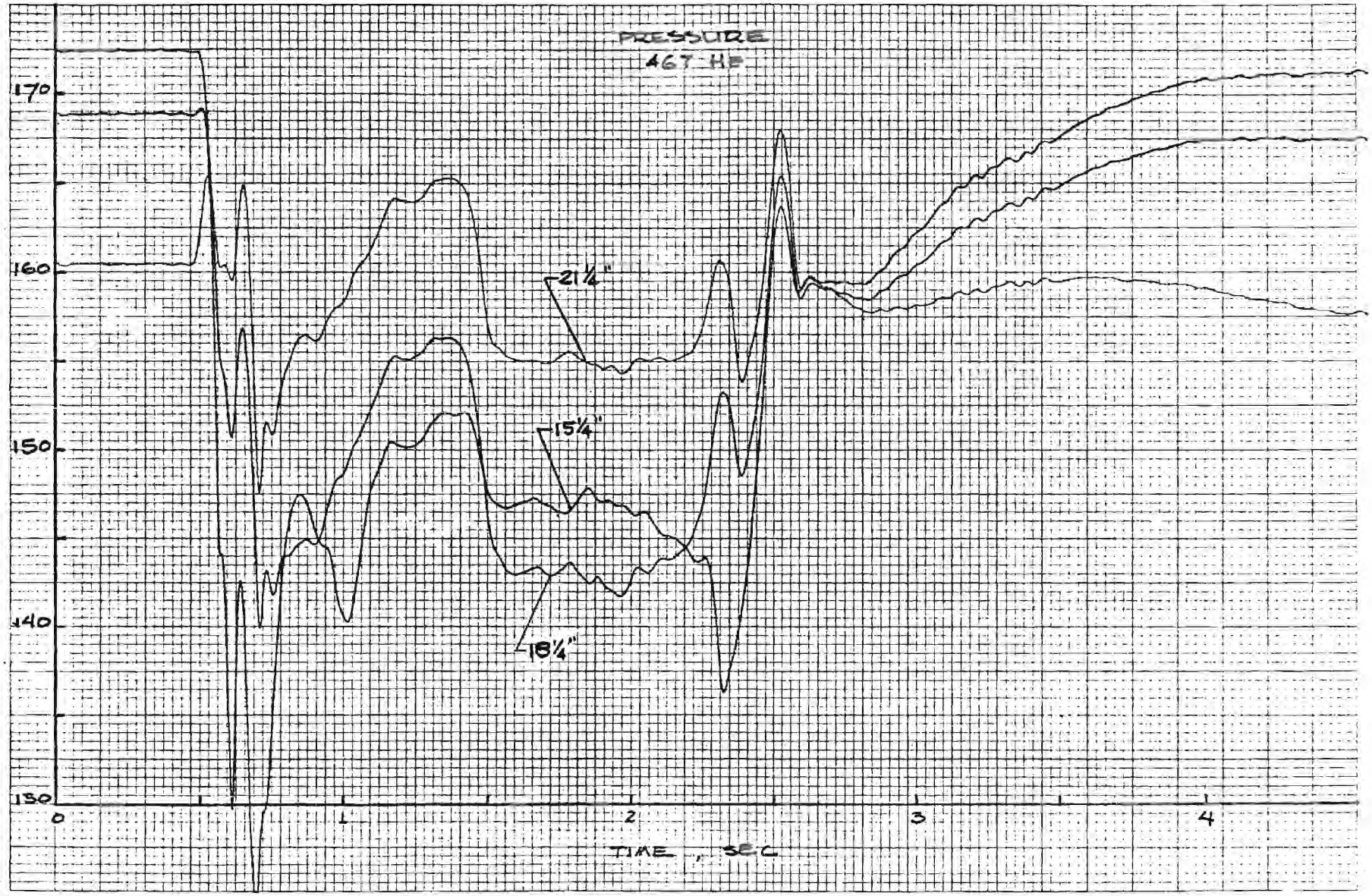

Figure 20. Variation of Pressure Amplitude with Respect to Time

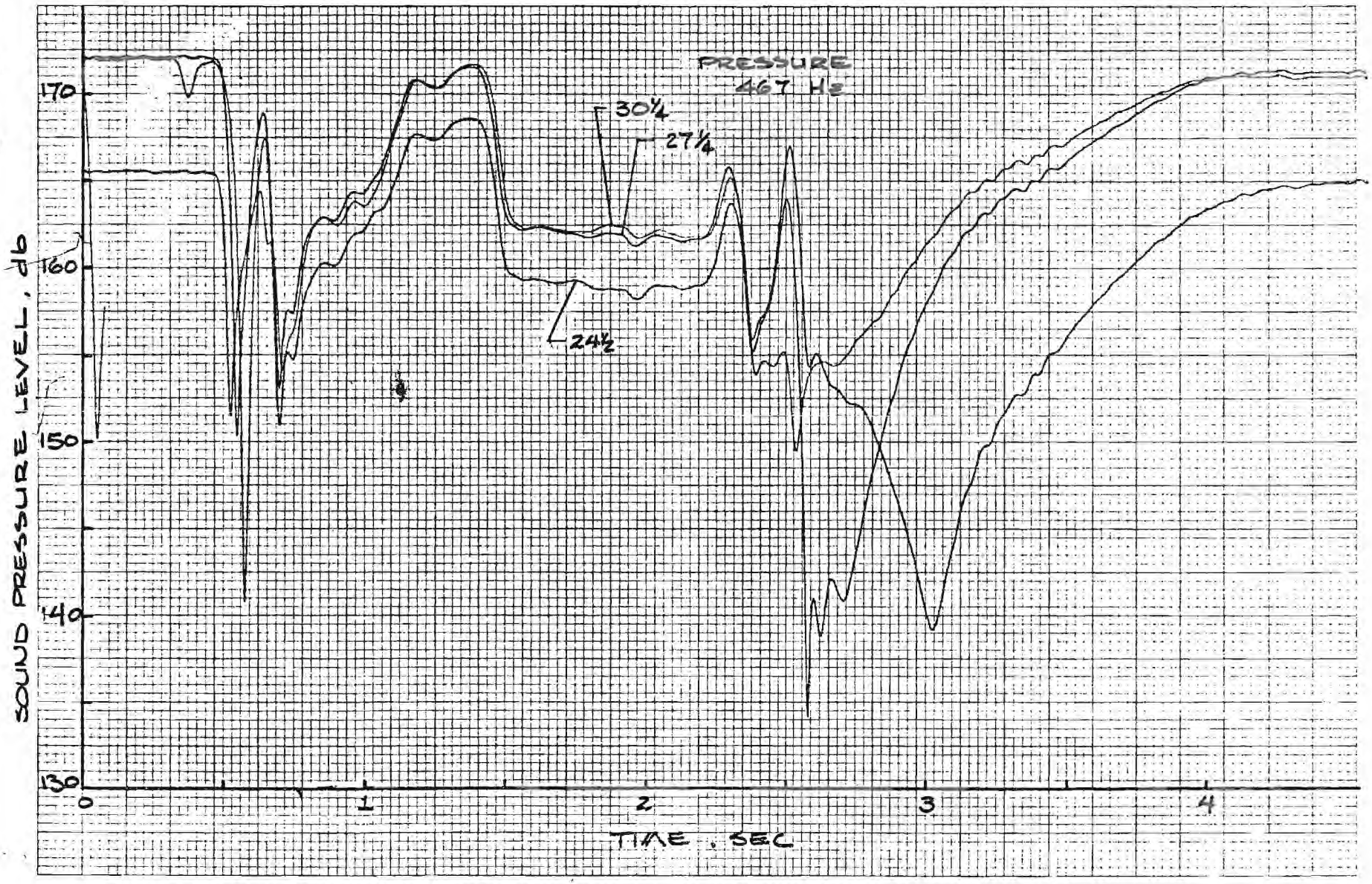

Figure 21. Variation of Pressure Amplitude with Respect to Time

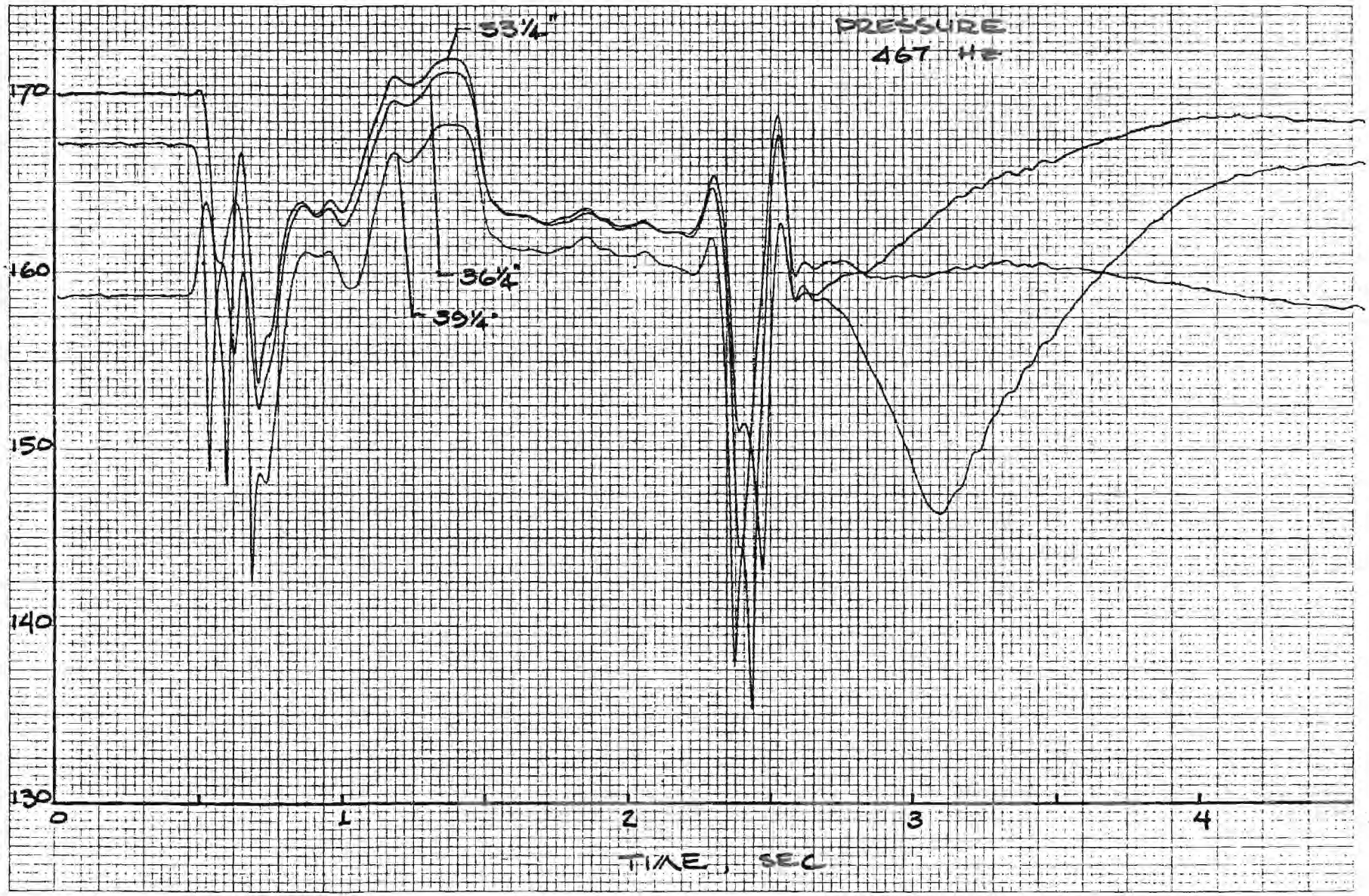

Figure 22. Variation of Pressure Amplitude with Respect to Time

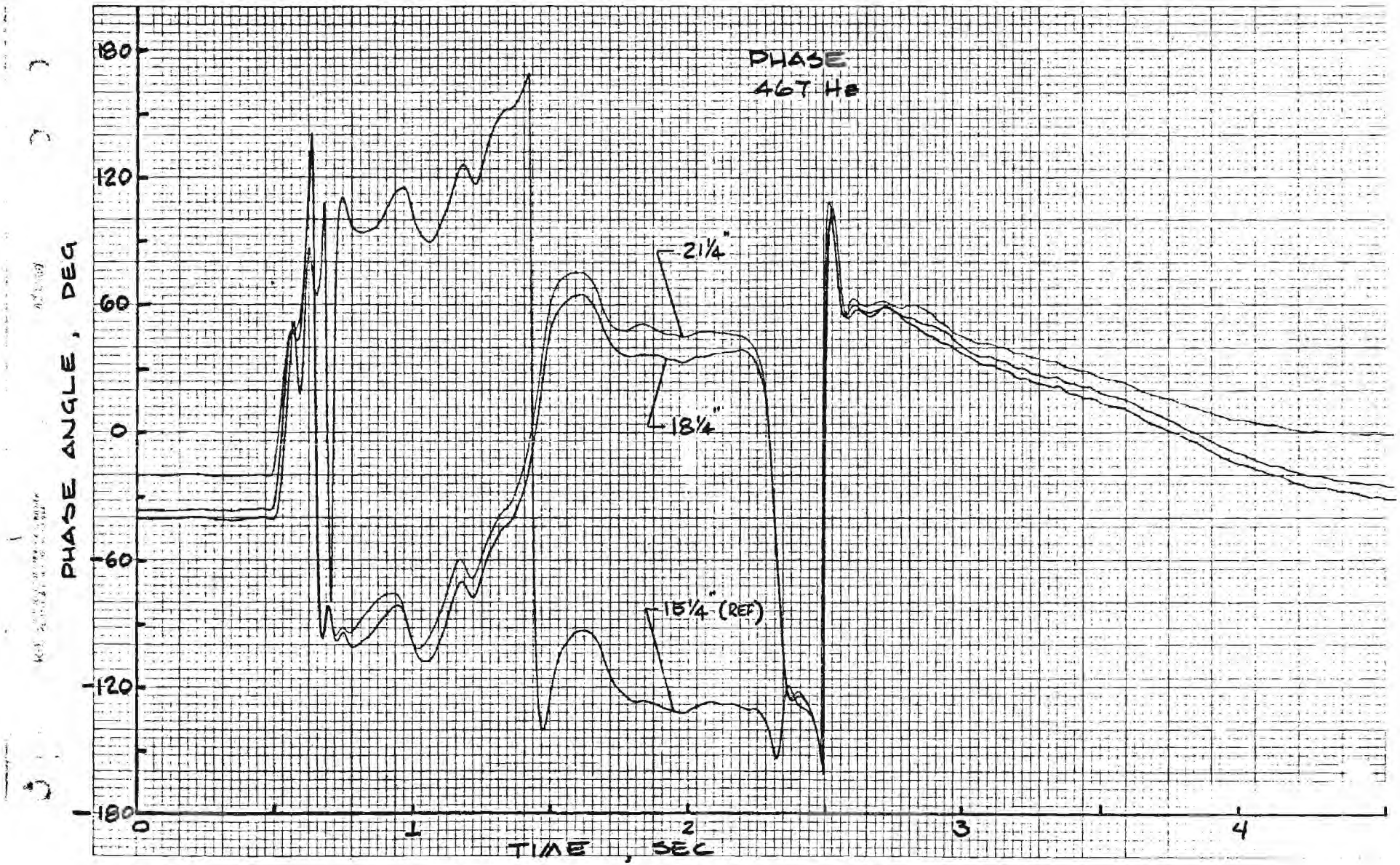

Figure 23. Variation of Pressure Phases with Respect to Time

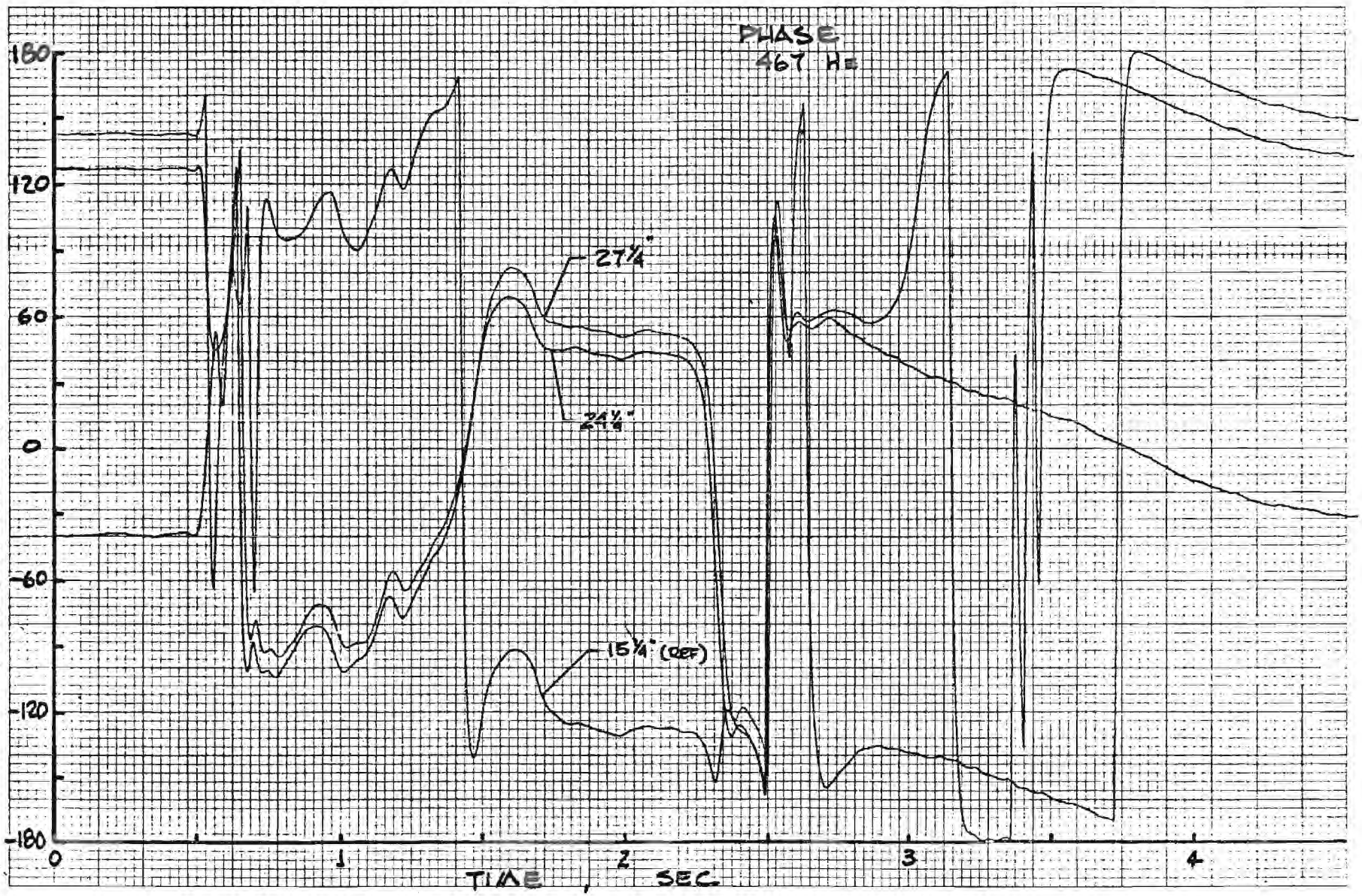

Figure 24. Variation of Pressure Phases with Respect to Time

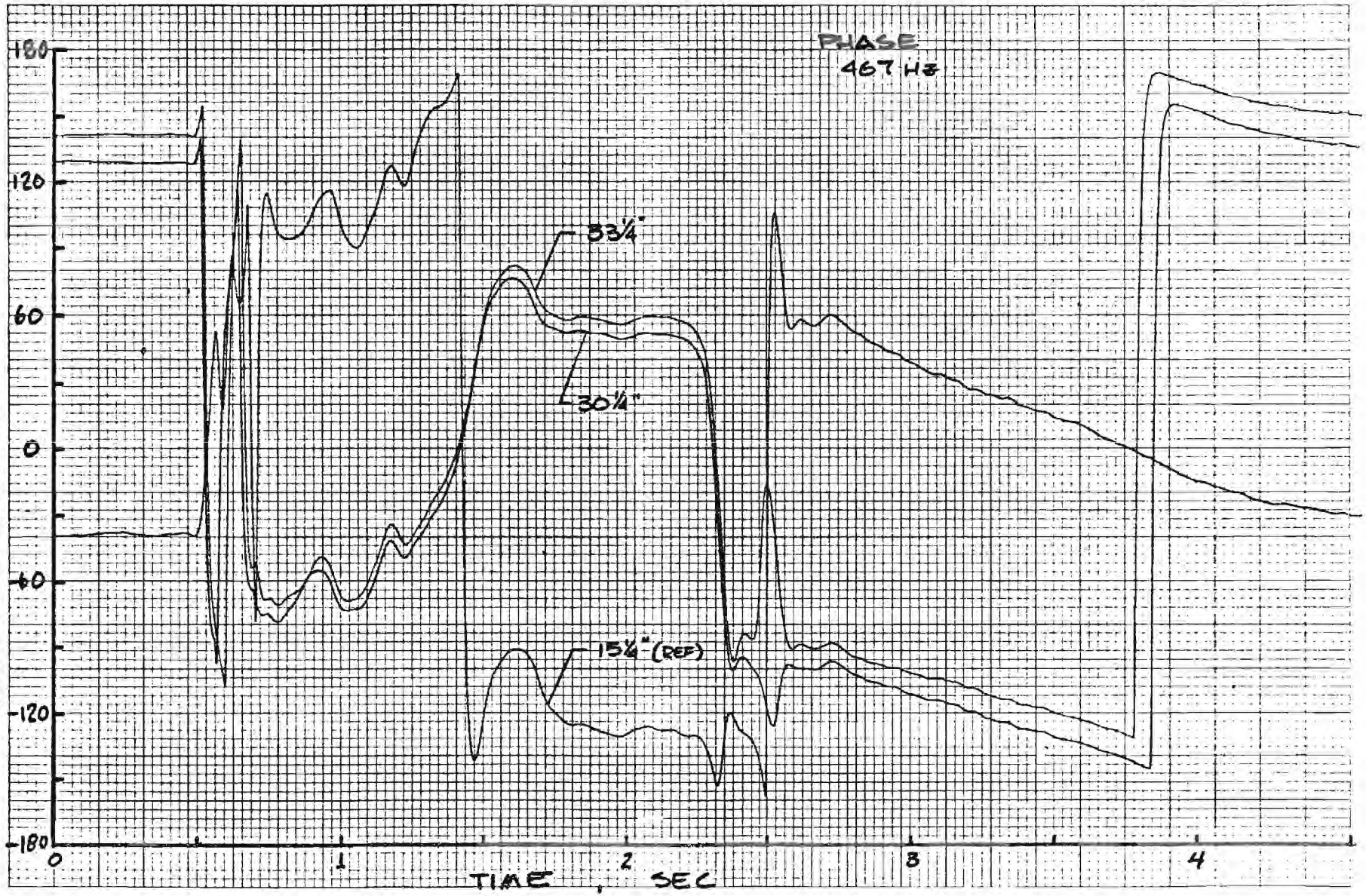

Figure 25. Variation of Pressure Phases with Respect to Time

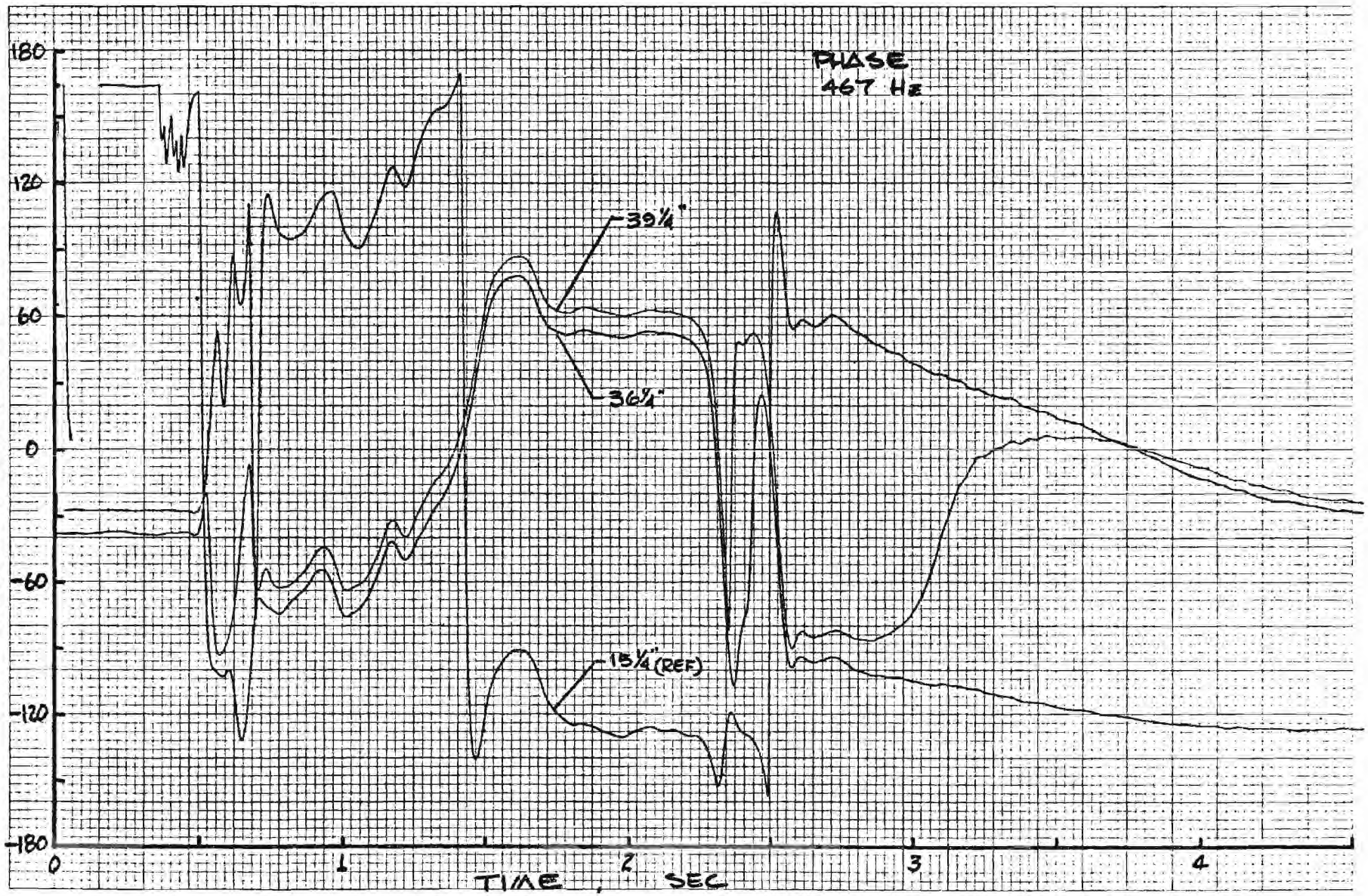

Figure 26. Variation of Pressure Phases with Respect to Time

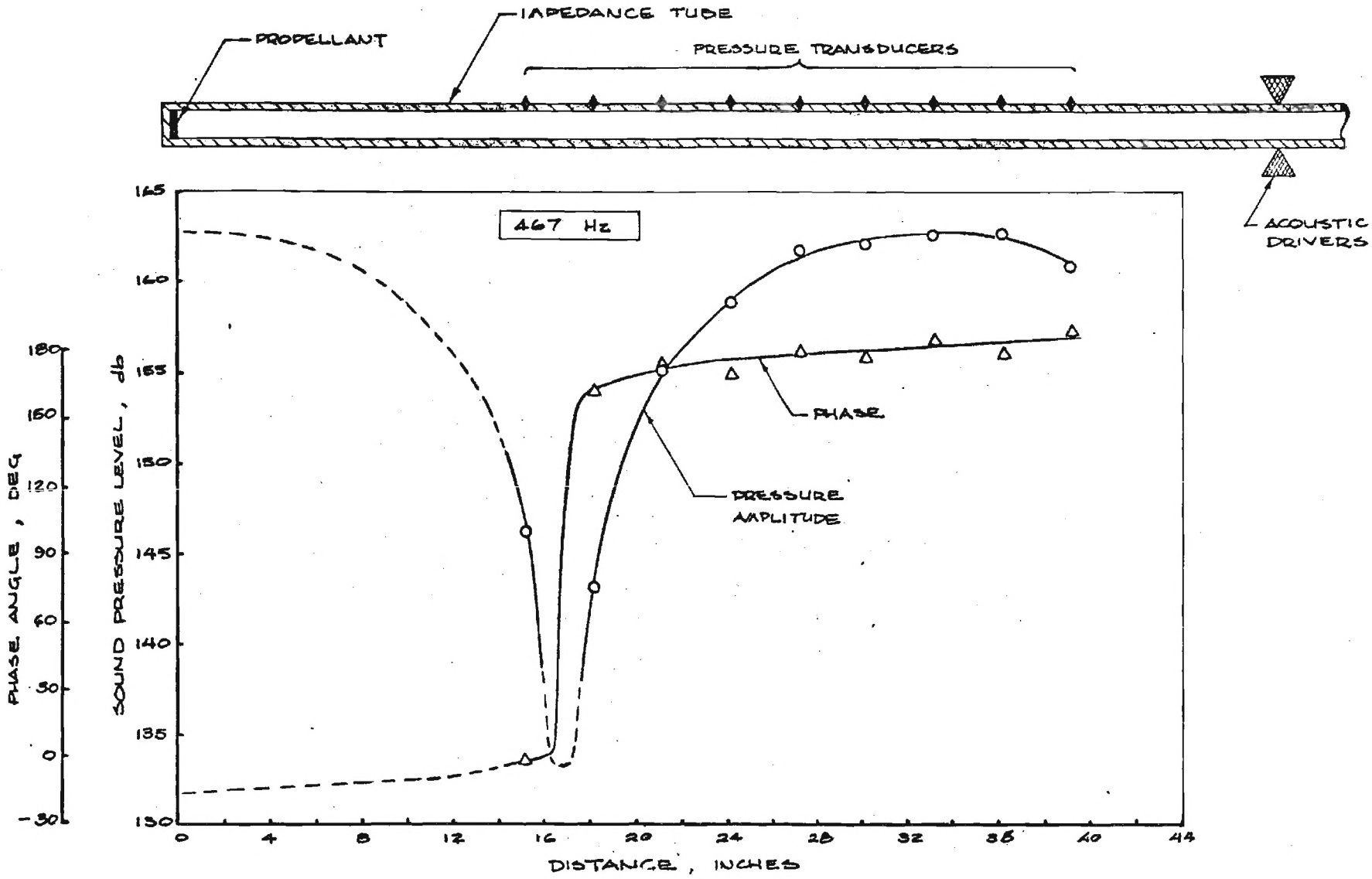

Figure 27. Axial Variation of Pressure Amplitude and Phase in the Burner Tube

be used to determine the frequency dependence of the admittances of burning solid propellants. To assure the accuracy and reliability of the data, the admittances will be determined at several instances during a given run. Also, since only three pressure measurements are needed to calculate the unknown admittance and up to ten pressure measurements will be taken during each test, different combinations of three pressure measurements will be used to compute the instantaneous admittance, and the desired admittance will be obtained by taking a proper average of the computed set of admittances at each instant of time.

SUMMARY

The following are the major accomplishments during the first year of investigation under this program:

(1) A new experimental setup for conducting forced oscillation experiments for the determination of the admittances of burning solid propellants has been developed.

(2) Cold flow tests to check the proper operation of the facility have been conducted successfully.

(3) Tests conducted with burning solid propellant samples clearly indicate the presence of axial and radial temperature gradients in all burners of this type. The effect of these temperature gradients upon the data reduction scheme and the measured admittances needs to be assessed.

(4) The capability of the facility to measure instantaneous amplitude and phases distribution along the tube has been demonstrated.

(5) The wave structure inside a burner tube containing a flow

with an axial temperature gradient has been investigated.

(6) A promising analytical technique for the use of pressure amplitude and phase data, measured at different locations along the tube, in the determination of the admittance and entropy perturbation at the burning propellant surface has been developed.

(7) An error analysis aimed at the determination of the accuracy of the above-mentioned analytical technique has been initiated.

APPENDIX A

This appendix will illustrate how the solution of a "quasi-boundary value" problem can be transformed to the solution of an initial value problem. In this case the known "boundary-values" may be thought of as being the dynamic pressures measured at different locations along the tube while the velocity and density perturbation at the burning surface are missing (or unknown) initial conditions.

Consider the following system of n coupled ordinary differential equations:

$$\begin{aligned}
\frac{dz_1}{dx} &= F_1(z_1, z_2, \ldots z_i, \ldots, z_n, x) \\
\frac{dz_2}{dx} &= F_2(z_1, z_2, \ldots z_i, \ldots, z_n, x) \\
&\vdots \\
\frac{dz_i}{dx} &= F_i(z_1, z_2, \ldots z_n, x) \\
&\vdots \\
\frac{dz_n}{dx} &= F_n(z_1, z_2, \ldots z_i, \ldots, z_n, x) \quad , \quad i=1,2,\ldots,n
\end{aligned} \tag{A-1}$$

Subject to the following restrictions on z_1 only*

$$\begin{aligned}
z_1(x=0) &= z_1^{(0)} = \text{constant} \\
z_1(x=x_j) &= z_1^{(xj)} = \text{constant for } j = 1, 2, \ldots, (n-1).
\end{aligned} \tag{A-2}$$

---

* The quantity z, may be considered as being analogous to the pressure perturbation.

The following transformation of the dependent variables is introduced:

$$z_i = Y_{i,1} + \sum_{j=1}^{n-1} K_j Y_{i,j+1} \quad , \; i = 1, 2, \ldots, n. \qquad \text{(A-3)}$$

Where the K_j are unknown constant coefficients and the Y_{ij} are unknown solutions of Eqs. A-1. Substituting Eq. (A-3) into Eq. (A-1) yields

$$\frac{dY_{i,1}}{dx} + \sum_{j=1}^{n-1} K_j \frac{dY_{i,j+1}}{dx} = F_i(Y_{11}, Y_{21}, \ldots Y_{n,1}, x)$$

$$+ \sum_{j=1}^{n-1} K_j F_i(Y_{j+1,1}, Y_{j+1,2} \ldots, Y_{j+1,n}, x),$$

$$i = 1, 2, \ldots, n \qquad \text{(A-4)}$$

Since the differential equations are linear, then it follows that the coefficients of the K_j's in Eq. (A-4) must be identically zero. Equating these coefficients to zero yields the following n x n system of differential equations:

$$\frac{dY_{i,j}}{dx} = F_i(Y_{1,j}, \ldots Y_{n,j}, x), \quad i = 1, 2, \ldots, n$$
$$j = 1, 2, \ldots, n \qquad \text{(A-5)}$$

To integrate the above system of differential equations, n x n initial conditions must be specified. To obtain a solution the following

initial conditions are specified:

$$Y_{1,1}(0) = z_1(0)$$

$$Y_{1,2}(0) = Y_{1,3}(0) = \ldots = Y_{1,n}(0) = 0 \qquad \text{(A-6)}$$

$$Y_{i,j}(0) = G_{i,j} \quad , \; i = 2, 3, \ldots, n$$
$$j = 1, 2, \ldots, n$$

Where the $G_{i,j}$ are arbitrarily assumed non zero constants that are different from one another. Using these initial conditions, Eqs. (A-5) can be integrated numerically to determine all the unknowns $Y_{i,j}$. Once the values of $Y_{1,j}(x)$ for $j = 1, \ldots n$ are known, then the definition of z_1 together with its known values at $x_j = 1, 2, \ldots n-1$ can be used to obtain a system of (n-1) linear equations for the determination of the unknown constants K_j where $j = 1, 2, \ldots n-1$; that is:

$$z_1(x_j) = Y_{11}(x_j) \; +$$

$$\sum_{i=1}^{n-1} K_i \, Y_{1,i+1}^{(x_T)} \quad , \; j = 1, 2, n-1 \qquad \text{(A-7)}$$

REFERENCES

1. Scott, R. A., "An Apparatus for Accurate Measurement of the Acoustic Impedance of Sound Absorbing Materials," Proceedings of the Physical Society, Vol. 58, 1946, pp. 253-264.

2. Bell, W. A., Experimental Determination of Three-Dimensional Liquid Rocket Nozzle Admittances, Ph.D. Thesis, School of Aerospace Engineering, Georgia Institute of Technology, Atlanta, Georgia, July 1972.

3. Zinn, B. T., Daniel, B. R., Janardan, B. A., and Smith, A. J., Jr., "Damping of Axial Instabilities by Minuteman II, Stage III, Minuteman III, Stage III, Exhaust Nozzles," Air Force Rocket Propulsion Laboratory Interim Report, AFRPL-TR-72-71, August 1972.

4. Chemical Propulsion Information Agency, T-Burner Manual, CPIA Publication No. 191, Silver Spring, Maryland, November 1969.

5. Perry, E. H., Investigations of the T-Burner and its Role in Combustion Instability Studies, Ph.D. Thesis, Daniel and Florence Guggenheim Jet Propulsion Center, California Institute of Technology. Pasadena, California, May 1970.

6. Derr, R. L., "Evaluation of a Variable Area T-Burner for Metalyzed Propellants," Lockheed Propulsion Company Technical Report AFRPL-TR-72-97, February 1973.

7. Price, E. W., Mathes, H. B., and Crump, J. E., "Evolution of Laboratory T-Burners for Study of Solid Propellant Combustion Instability," Naval Weapons Center Technical Note 608-109 (Revision 1), China Lake, Calif., August 1972.

8. Oberg, C. L., Ryan, N. W., and Baer, A. D., "A Pulsed T-Burner Technique," AIAA Journal, Vol. 6, No. 5, May 1968, pp. 920-921.

9. Brown, R. S., and Erickson, J. E., "Measuring Combustion Response by a Forced Oscillation Method," AIAA Paper No. 72-1054, presented at the AIAA/SAE 8th Joint Propulsion Specialist Conference, New Orleans, La., November 29 - December 1, 1972.

10. Barrére, M., Nadaud, L., and Thuillier, J. N., "Survey of ONERA and SNPE Work on Combustion Instability in Solid Propellant Rockets," AIAA Paper No. 72-1052, presented at the AIAA/SAE 8th Joint Propulsion Specialist Conference, New Orleans, La. November 29 - December 1, 1972.

11. Fonner, S. N., Hudson, R. L., and Nall, B. H., "Admittance Measurements of Solid Propellants by an Acoustic Oscillator Technique," AIAA Journal, Vol. 2, No. 6, June 1964, pp. 1123-1129.

12. Morse, P. M., and Ingard, K. U., Theoretical Acoustics, McGraw-Hill, Inc., New York, N. Y., 1968, p. 467 ff.

REPORT DOCUMENTATION PAGE

READ INSTRUCTIONS BEFORE COMPLETING FORM

1. REPORT NUMBER
2. GOVT ACCESSION NO.
3. RECIPIENT'S CATALOG NUMBER

4. TITLE *(and Subtitle)*
SOLID PROPELLANT ADMITTANCE MEASUREMENTS
BY THE DRIVEN TUBE METHOD

5. TYPE OF REPORT & PERIOD COVERED
INTERIM
JUNE 1973 - JULY 1974

6. PERFORMING ORG. REPORT NUMBER

7. AUTHOR(s)
B. T. ZINN M. SALIKUDDIN
B. R. DANIEL
W. A. BELL

8. CONTRACT OR GRANT NUMBER(s)
AFOSR - 73 - 2571

9. PERFORMING ORGANIZATION NAME AND ADDRESS
GEORGIA INSTITUTE OF TECHNOLOGY
SCHOOL OF AEROSPACE ENGINEERING
ATLANTA, GEORGIA 30332

10. PROGRAM ELEMENT, PROJECT, TASK AREA & WORK UNIT NUMBERS
681308
9711-01
61102F

11. CONTROLLING OFFICE NAME AND ADDRESS
AIR FORCE OFFICE OF SCIENTIFIC RESEARCH
1400 WILSON BOULEVARD
ARLINGTON, VIRGINIA 22209

12. REPORT DATE
AUGUST 1974

13. NUMBER OF PAGES
65

14. MONITORING AGENCY NAME & ADDRESS *(if different from Controlling Office)*

15. SECURITY CLASS. *(of this report)*
UNCLASSIFIED

15a. DECLASSIFICATION/DOWNGRADING SCHEDULE

16. DISTRIBUTION STATEMENT *(of this Report)*
APPROVED FOR PUBLIC RELEASE
DISTRIBUTION UNLIMITED

17. DISTRIBUTION STATEMENT *(of the abstract entered in Block 20, if different from Report)*

18. SUPPLEMENTARY NOTES

19. KEY WORDS *(Continue on reverse side if necessary and identify by block number)*
COMBUSTION INSTABILITY
SOLID PROPELLANT RESPONSE FUNCTIONS
SOLID PROPELLANT ROCKETS
IMPEDANCE TUBE MEASUREMENTS

20. ABSTRACT *(Continue on reverse side if necessary and identify by block number)*

Results obtained during the first year of a research program concerned with the development of a driven tube burner for the measurement of the admittances of burning solid propellants are presented. In the experimental phase of the program, a driven tube burner has been developed and tested under both cold and hot flow conditions. The cold flow tests provided a check on the proper operation of the facility and the data reduction scheme. Temperature measurements of the gas inside the burner tube, taken during the burning of a

solid propellant sample, indicate the presence of axial and radial temperature gradients in the burner. The effect of these gradients upon the quality of the measured admittance data is under investigation. Preliminary hot tests conducted to date confirmed the proper operation of the facility and its ability to provide good pressure amplitude and phase data. These data are now being used to compute the desired solid propellant admittances. In the analytical phase of this program, a most promising analytical technique for the determination of both the admittance and entropy perturbation at the propellant burning surface, from dynamic pressure and steady temperature measurements, has been developed. The accuracy of this technique is currently under investigation. Also, the effect of the steady state temperature gradients upon the wave structure inside the burner tube has been investigated analytically.

E-16-633

AFOSR INTERIM SCIENTIFIC REPORT

AFOSR-TR

SOLID PROPELLANT ADMITTANCE MEASUREMENTS BY THE DRIVEN TUBE METHOD

Prepared for

Air Force Office of Scientific Research
Aerospace Sciences Directorate
Arlington, Virginia

by

B. T. Zinn
M. Salikuddin
B. R. Daniel
W. A. Bell

School of Aerospace Engineering
Georgia Institute of Technology
Atlanta, Georgia 30332

Approved for public release; distribution unlimited

Grant No. AFOSR-73-2571 August 1975

Conditions of Reproduction

Reproduction, translation, publication, use and disposal in whole or in part by or for the United States Government is permitted.

UNCLASSIFIED

SECURITY CLASSIFICATION OF THIS PAGE *(When Data Entered)*

REPORT DOCUMENTATION PAGE

READ INSTRUCTIONS BEFORE COMPLETING FORM

1. REPORT NUMBER

2. GOVT ACCESSION NO.

3. RECIPIENT'S CATALOG NUMBER

4. TITLE *(and Subtitle)*
SOLID PROPELLANT ADMITTANCE MEASUREMENTS
BY THE DRIVEN TUBE METHOD

5. TYPE OF REPORT & PERIOD COVERED
INTERIM
JUNE 1974 - JULY 1975

6. PERFORMING ORG. REPORT NUMBER

7. AUTHOR(s)
B. T. ZINN M. SALIKUDDIN
B. R. DANIEL
W. A. BELL

8. CONTRACT OR GRANT NUMBER(s)
AFOSR - 73 - 2571

9. PERFORMING ORGANIZATION NAME AND ADDRESS
GEORGIA INSTITUTE OF TECHNOLOGY
SCHOOL OF AEROSPACE ENGINEERING
ATLANTA, GEORGIA 30332

10. PROGRAM ELEMENT, PROJECT, TASK AREA & WORK UNIT NUMBERS
681308
9711-01
61102F

11. CONTROLLING OFFICE NAME AND ADDRESS
AIR FORCE OFFICE OF SCIENTIFIC RESEARCH
1400 WILSON BOULEVARD
ARLINGTON, VIRGINIA 22209

12. REPORT DATE
AUGUST 1975

13. NUMBER OF PAGES
60

14. MONITORING AGENCY NAME & ADDRESS *(if different from Controlling Office)*

15. SECURITY CLASS. *(of this report)*
UNCLASSIFIED

15a. DECLASSIFICATION/DOWNGRADING SCHEDULE

16. DISTRIBUTION STATEMENT *(of this Report)*
APPROVED FOR PUBLIC RELEASE

DISTRIBUTION UNLIMITED

17. DISTRIBUTION STATEMENT *(of the abstract entered in Block 20, if different from Report)*

18. SUPPLEMENTARY NOTES

19. KEY WORDS *(Continue on reverse side if necessary and identify by block number)*
COMBUSTION INSTABILITY
SOLID PROPELLANT RESPONSE FUNCTIONS
SOLID PROPELLANT ROCKETS
IMPEDANCE TUBE MEASUREMENTS

20. ABSTRACT *(Continue on reverse side if necessary and identify by block number)*

Progress made during the second year of an investigation on the application of the impedance tube technique in the measurement of the response function of a burning solid propellant, subjected to oscillating flow conditions, is described in this report. Modifications to the originally proposed measurement technique are outlined and the admittances of a number of different solid propellants measured at low pressures and over frequency ranges of interest in solid propellant instability are presented. Also discussed in

DD FORM 1 JAN 73 1473 EDITION OF 1 NOV 65 IS OBSOLETE

UNCLASSIFIED

SECURITY CLASSIFICATION OF THIS PAGE *(When Data Entered)*

this report are the results of analytical studies concerned with (1) determination of the behavior of a standing wave in a tube containing a steady flow and a steady temperature gradient; (2) the dependence of the standing wave structure upon the boundary condition at the propellant surface and the characteristics of the steady axial temperature profile in the burner tube; (3) the use of acoustic pressure data in the determination of the propellant response factor; and (4) the development of a non-linear regression technique for the improvement of the accuracy of the measured propellant response factor. Finally, the measured low pressure propellant response factor data is analyzed and its possible dependence upon particle gas phase attenuation and the propellant "self-driving" is discussed.

AFOSR INTERIM SCIENTIFIC REPORT

AFOSR-TR

SOLID PROPELLANT ADMITTANCE MEASUREMENTS BY THE DRIVEN TUBE METHOD

Prepared for

Air Force Office of Scientific Research
Aerospace Sciences Directorate
Arlington, Virginia

by

B. T. Zinn
M. Salikuddin
B. R. Daniel
W. A. Bell

School of Aerospace Engineering
Georgia Institute of Technology
Atlanta, Georgia 30332

Approved for public release; distribution unlimited

Grant No. AFOSR-73-2571 August 1975

Conditions of Reproduction

Reproduction, translation, publication, use and disposal in whole or in part by or for the United States Government is permitted.

ABSTRACT

Progress made during the second year of an investigation on the application of the impedance tube technique in the measurement of the response function of a burning solid propellant, subjected to oscillating flow conditions, is described in this report. Modifications to the originally proposed measurement technique are outlined and the admittances of a number of different solid propellants measured at low pressures and over frequency ranges of interest in solid propellant instability are presented. Also discussed in this report are the results of analytical studies concerned with (1) determination of the behavior of a standing wave in a tube containing a steady flow and a steady temperature gradient; (2) the dependence of the standing wave structure upon the boundary condition at the propellant surface and the characteristics of the steady axial temperature profile in the burner tube; (3) the use of acoustic pressure data in the determination of the propellant response factor; and (4) the development of a nonlinear regression technique for the improvement of the accuracy of the measured propellant response factor. Finally, the measured low pressure propellant response factor data is analyzed and its possible dependence upon particle gas phase attenuation and the propellant "self-driving" is discussed.

TABLE OF CONTENTS

NOMENCLATURE

Symbols

A_{ij}	coefficients defined in Eqs. (2-11) through (2-19); i, j = 1, 2, 3
c	velocity of sound, ft./sec.
C_p	specific heat at constant pressure, Btu/lbm.$^{\circ}$R
C'_p	specific heat of solid particles, Btu/lbm.$^{\circ}$R
C_v	specific heat at constant volume, Btu/lbm.$^{\circ}$R
D	diameter of the burner tube, ft.
F_p	drag force per particle, lbf./particle
f	frequency, Hz.
h	heat transfer coefficient, Btu/sec. ft.^{2} $^{\circ}$R
I	unit or identity matrix
i	imaginary unit, $\sqrt{-1}$
k	coefficient of Thermal Conductivity, Btu/sec. ft. $^{\circ}$R; also wave number, $\omega/\bar{c}$, rad./ft.
L	length, ft.
m′	particle mass, lbm./particle
M	Mach number
n	temperature exponent of viscosity law, see Eq. (2-24); also number of particles per unit volume
p	pressure, lbf./ft.^{2}
P_r	Prandtl Number
Q	volumetric heat source

Q_p	heat transferred per particle
r	burning rate, ft./sec.; also particle radius, ft.
R	specific gas constant, ft.-lbf./slug $^{\circ}R$
T	temperature; $^{\circ}R$; also transmission matrix
t	time, sec.
u	axial velocity, ft./sec.
V_p	particle volume, $ft.^3$
x	axial distance, ft.
Y	specific admittance
γ	ratio of specific heats
λ	wave length, ft.
μ	viscosity coefficient, lbm./ft. sec.
ν	particle loading
Λ	heat transfer parameter, see Eq. (2-27)
ρ	density, $slug/ft.^3$
ω	angular frequency, rad./sec.
τ_d	dynamic relaxation time, sec.
τ_t	thermal relaxation time, sec.

Superscripts

$(\bar{\ })$	variable describing steady state conditions
$(\ )'$	a perturbation quantity

Subscripts

$(\ )_c$	quantity evaluated at the propellant surface
$(\ )_r$	real part of a complex quantity
$(\ )_i$	imaginary part of a complex quantity

$( )_p$	quantity related to a particle
$( )_w$	quantity evaluated at the wall

LIST OF FIGURES

Figure Page

CHAPTER I

INTRODUCTION

This report summarizes the work done during the second year of research supported by Air Force Grant No. AFOSR-73-2571. This grant was initiated on July 1, 1973 and it is concerned with the determination of the acoustic responses of solid propellants by the impedance tube method.

Combustion instability has seriously hindered the development and operation of many solid and liquid propellant rocket motors and air breathing propulsion systems for many years. This phenomenon is characterized by large amplitude pressure oscillations which are sustained by an unsteady combustion process. Combustion instability may lead to mechanical failure of engine components, high heat transfer rates to the combustor walls and interference with the control and guidance systems.

To determine the susceptibility of a given propulsion system to combustion instability, it is necessary to determine the energy balance that exists between the various sources of wave energy gains and losses that are present within the combustor. Wave energy loss mechanisms tend to attenuate the disturbance in the combustor and thus exert a stabilizing influence upon the engine. Examples of wave energy loss mechanisms are convective energy losses caused by the mean flow, energy dissipation processes associated with viscosity and heat transfer and

losses resulting from the interaction of the disturbance with various mechanical components of the engine such as the exhaust nozzle. On the other hand, wave energy gains tend to amplify the engine disturbances and thus exert a destabilizing influence upon the combustor. The primary source of wave energy gain is the unsteady combustion process. If the energy gains outweigh the energy losses, an initial disturbance will amplify and lead to undesirable self-sustained oscillations inside the combustor.

To evaluate the stability of a given solid propellant rocket motor it is necessary to quantitatively determine the characteristics of the various gain and loss mechanisms that are present in the system. The wave energy gain in a solid rocket motor may be determined from either theoretical or experimental investigations of the interaction between a burning solid propellant and an oscillatory gas phase. This interaction can be described by means of the admittance of the burning surface which, in turn, can be used[1] to compute the wave energy gain resulting from the above-mentioned interaction. Defined as the ratio of the normal velocity perturbation to the pressure perturbation at the burning propellant surface, the propellant admittance also describes the boundary condition that the combustor oscillation must satisfy at the propellant surface in combustion instability analysis.

Since instability is often caused by small differences between wave energy gains and losses, it is imperative that the contributions from all processes affecting the stability of a rocket motor be known as accurately as possible. Hence, it is of utmost importance that experimental techniques capable of accurate determination of the re-

sponses of burning solid propellants be available. The development of such an experimental technique is one of the main objectives of the present study which is concerned with the adaptation of the impedance tube method in the determination of the responses of burning solid propellants. The impedance tube technique has its origin in acoustics where it has been successfully utilized to measure the responses of sound absorbing materials under no flow conditions[2]. This technique was later modified to determine the responses of choked rocket nozzles[3,4] under cold flow conditions.

In an earlier publication[5], published in August 1974, the progress made under this program during the first year of study, as well as the basic concepts underlying the application of the impedance tube technique were described. Included in that report are definitions of the admittance and response factor and discussions of the various experimental techniques used in their measurement. Notable among these techniques are the self excited T-burner, the variable area T-burner and the pulsed T-burner. Reference 5 also contains descriptions of the experimental facility, the measurement technique and the mathematical background of the data reduction procedure used in this program. Finally, the first-year report[5] contains experimental data describing the behavior of the steady state axial and radial temperature distributions and the behavior of the standing acoustic wave in the driven burner tube.

In this report, the progress made in analytical and experimental efforts during the second year of investigation of this program are described. The analytical investigations presented herein describe

the mathematical treatment of the behavior of a standing wave in a tube containing a steady flow and a steady temperature gradient; the investigation of the dependence of the standing wave structure in the burner tube upon the boundary conditions at the propellant surface; the determination of the steady state axial temperature distribution in the burner tube; the use of acoustic pressure data (i.e., amplitude and phase), measured at various locations along the burner tube, in the determination of the propellant response factor; the development of a non-linear regression technique that improves the accuracy of the measured propellant response factor; the dependence of the standing acoustic wave in the driven burner tube upon particle attenuation in the gas phase; and, the dependence of the wave structure inside the burner tube upon the propellant "self-noise".

The experimental aspects of the program discussed herein include descriptions of improved measurement techniques for the determination of the characteristics of the steady state flow and the wave structure inside the burner tube, and experimental data which show the frequency dependence of the response factors of a number of different solid propellants tested under low pressure conditions.

CHAPTER II

ANALYTICAL INVESTIGATIONS

1. The Driven Tube Wave Structure

In this section, the mathematical formulation of the equations describing the behavior of the wave structure inside the driven burner tube is presented. These equations will be used later in this report to investigate the characteristics of the standing acoustic wave inside the driven burner tube and to demonstrate the manner in which measured acoustic pressure data can be used in the determination of the admittance at the surface of a burning solid propellant sample.

To develop the needed equations, the following assumptions are introduced: (1) the combustion process is concentrated at the propellant surface; (2) the gas in the burner tube is perfect and it consists of a single species; (3) the fluctuating part of the heat transfer to the wall is negligible; (4) both the steady and unsteady flows are one dimensional; (5) the ratios of the various perturbation quantities and the corresponding steady state quantities are sufficiently small so that all non-linear terms involving products of these quantities may be neglected in the conservation equations; and (6) gas phase damping is negligible. Under these assumptions, the flow in the burner tube can be described by the following system of conservation equations:[5,6]

Continuity: $$\frac{\partial \rho}{\partial t} + \frac{\partial}{\partial x}(\rho u) = 0 \tag{2-1}$$

Momentum: $$\frac{\partial u}{\partial t} + u\frac{\partial u}{\partial x} = -\frac{1}{\rho}\frac{\partial p}{\partial x} \tag{2-2}$$

Energy: $$\frac{\partial s}{\partial t} + u\frac{\partial s}{\partial x} = C_v \frac{Q}{p} \tag{2-3}$$

State: $$p = \rho RT$$

$$ds = C_p \frac{dT}{T} - R\frac{dp}{p} \tag{2-4}$$

Linearizing the above equations and accounting for the periodicity of the oscillation in time, yield the following system of wave equations:[5]

Continuity: $$i\omega\rho' + \frac{d}{dx}(\bar{\rho}u' + \bar{u}\rho') = 0 \tag{2-5}$$

Momentum: $$\left\{i\omega u' + \frac{d}{dx}(\bar{u}\,u')\right\}\bar{\rho} + \bar{u}\frac{d\bar{u}}{dx}\rho' = -\frac{dp'}{dx} \tag{2-6}$$

Energy: $$i\omega p' + \frac{d\bar{p}}{dx}u' + \bar{u}\frac{dp'}{dx} = \bar{c}^{-2}\left\{i\omega p' + \frac{d\bar{\rho}}{dx}u' + \bar{u}\frac{d\rho'}{dx} + \bar{u}\frac{d\bar{\rho}}{dx}\frac{p'}{\bar{p}} - \bar{u}\frac{d\bar{\rho}}{dx}\frac{\rho'}{\bar{\rho}}\right\} \tag{2-7}$$

where

$$\bar{c}^{-2} = \gamma\bar{p}/\bar{\rho}$$

To be amenable to numerical integration, the above system of equations are rewritten in the following form

$$\frac{dZ_1}{dx} = A_{11}Z_1 + A_{12}Z_2 + A_{13}Z_3 \tag{2-8}$$

$$\frac{dZ_2}{dx} = A_{21} Z_1 + A_{22} Z_2 + A_{23} Z_3 \tag{2-9}$$

$$\frac{dZ_3}{dx} = A_{31} Z_1 + A_{32} Z_2 + A_{33} Z_3 \tag{2-10}$$

where Z_1, Z_2 and Z_3 respectively represent u', p', and ρ' and the coefficient A_{ij}, i, j = 1, 2, 3 are defined as follows:

$$A_{11} = \left\{ \bar{u}\,\bar{\rho}\,\frac{d\bar{u}}{dx} - \frac{d\bar{p}}{dx} + i\,\omega\,\bar{u}\,\bar{\rho} \right\} \Big/ \bar{\rho}\,(\bar{c}^2 - \bar{u}^2) \tag{2-11}$$

$$A_{12} = \left\{ \frac{\bar{u}\bar{c}^2}{\bar{p}} \frac{d\bar{\rho}}{dx} - i\omega \right\} \Big/ \bar{\rho}\,(\bar{c}^2 - \bar{u}^2) \tag{2-12}$$

$$A_{13} = -\frac{1}{\bar{\rho}} \frac{d\bar{u}}{dx} - \left\{ \frac{\bar{c}^2\,\bar{u}}{\bar{p}} \frac{d\bar{\rho}}{dx} \right\} \Big/ \bar{\rho}\,(\bar{c}^2 - \bar{u}^2) \tag{2-13}$$

$$A_{21} = -\left\{ i\omega\bar{\rho} + \bar{\rho} \frac{d\bar{u}}{dx} + (\bar{u}^2 \frac{d\bar{u}}{dx} - \bar{u} \frac{d\bar{p}}{dx} + i\omega\bar{u}^2\bar{\rho}) \right\} \Big/ (\bar{c}^2 - \bar{u}^2) \tag{2-14}$$

$$A_{22} = -\,\bar{u} \left\{ \frac{\bar{u}\bar{c}^2}{\bar{p}} \frac{d\bar{\rho}}{dx} - i\omega \right\} \Big/ (\bar{c}^2 - \bar{u}^2) \tag{2-15}$$

$$A_{23} = \bar{u} \left\{ \frac{\bar{c}^2\,\bar{u}}{\bar{p}} \frac{d\bar{\rho}}{dx} \right\} \Big/ (\bar{c}^2 - \bar{u}^2) \tag{2-16}$$

$$A_{31} = -\,\frac{1}{\bar{u}} \left\{ \frac{d\bar{\rho}}{dx} + \left[\bar{u}\bar{\rho} \frac{d\bar{u}}{dx} - \frac{d\bar{p}}{dx} + i\,\omega\,\bar{u}\,\bar{\rho} \right] \Big/ (\bar{c}^2 - \bar{u}^2) \right\} \tag{2-17}$$

$$A_{32} = -\,\frac{1}{\bar{u}} \left\{ \frac{\bar{u}\,\bar{c}^2}{\bar{p}} \frac{d\bar{\rho}}{dx} - i\omega \right\} \Big/ (\bar{c}^2 - \bar{u}^2) \tag{2-18}$$

$$A_{33} = \frac{1}{\bar{u}} \left[-\,i\omega + \left\{ \frac{\bar{c}^2\,\bar{u}}{\bar{p}} \frac{d\bar{\rho}}{dx} \right\} \Big/ (\bar{c}^2 - \bar{u}^2) \right] \tag{2-19}$$

To solve Eqs. (2-8) through (2-10), the coefficients A_{ij} must be evaluated. Inspection of Eqs. (2-11) through (2-19) reveals that the A_{ij}'s depend upon the properties of the mean flow whose behavior must be determined from experimental data. It has been shown elsewhere[5] that the distribution of $\bar{p}(x)$, $\bar{\rho}(x)$ and $\bar{u}(x)$ can be determined from knowledge of $\bar{T}(x)$; however, in view of the high temperatures in the burner tube, the accurate determination of $\bar{T}(x)$ required the development of a special experimental-analytical approach whose description is provided in a later section of this report.

2. Determination of the Steady Temperature Profile

In this section the determination of the steady state temperature distribution in the driven burner tube, which is needed for the solution of the burner tube equations, will be considered. During an experiment, the burning propellant sample produces a stream of hot gases that flows along the tube towards the exhaust nozzle. Heat transfer from the hot combustion products to the cooler burner walls results in a steady temperature gradient along the burner axis. Performing a differential analysis, it has been shown[7] that the heat transfer $\dot{dq}$ to a section of the burner wall of width dx is given by the following expression

$$\dot{dq} = h(\bar{T} - \bar{T}_w)\, \pi\, D\, dx \qquad (2\text{-}20)$$

where the various quantities are defined in the nomenclature. Application of the conservation of energy principle to the flow within the differential tube section of width dx gives

$$d\dot{q} = - \bar{\rho}\, \bar{u} C_p \frac{\pi}{4} D^2 \, d\bar{T} \tag{2-21}$$

Combining Eqs. (2-20) and (2-21) yields the following expression for the steady temperature gradient

$$\frac{d\bar{T}}{dx} = - \frac{4h}{\bar{\rho}\, \bar{u} D C_p} (\bar{T} - T_w) \tag{2-22}$$

Since the flow in the burner tube is turbulent, the heat transfer coefficient for turbulent boundary layer (i.e., see Ref. 8) is used in Eq. (2-22); that is

$$h = \frac{C_o}{D^{0.2}} \left(\frac{\mu^{0.2} C_p}{P_r^{0.6}} \right)_o (\bar{\rho}\, \bar{u})^{0.8} \sigma \tag{2-23}$$

where

$$\sigma = - \frac{1}{\left[\frac{1}{2} \frac{T_w}{T} \left(1 + \frac{\gamma - 1}{2} M^2 \right) + \frac{1}{2} \right]^{(0.8 - n/5)} \left[1 + \frac{\gamma - 1}{2} M^2 \right]^{n/5}} \tag{2-24}$$

and the subscript o, C_o and n, respectively represent a quantity evaluated at stagnation conditions, a constant coefficient and the temperature exponent of the viscosity law; n will be taken equal to 0.6 in this study. When the Mach number M is small, $\frac{\gamma - 1}{2} M^2 \ll 1$ and the expression for σ simplifies to:

$$\sigma \approx \frac{1}{\left[\frac{1}{2} (T_w/T + 1) \right]^{.68}} \tag{2-25}$$

Using the steady state result that $\bar{\rho}\, \bar{u}$ = constant and assuming that C_p and P_r are constants, it can be shown that $h = C_1 \sigma$, where C_1 is a con-

stant. Using this relationship, Eq. (2-22) can be rewritten in the following form:

$$\frac{d\bar{T}}{dx} = - \frac{(\bar{T} - T_w)}{\Lambda} ; \qquad \bar{T}_o = T_c \tag{2-26}$$

where

$$\Lambda = C[1 + T_w/\bar{T}]^{0.68} \tag{2-27}$$

and C is a heat transfer parameter which depends upon the steady flow properties (e.g., μ, C_p, P_r, etc.) associated with the convective heat transfer coefficient h and the radial temperature variation in the tube.

Since the radial temperature variation and the various properties of the gas flowing in the tube are not known, the value of C is evaluated by a special analytical approach that will be discussed in a later section of this report. Once the values of C and the wall temperature T_w are known, the axial distribution of the temperature in the burner tube can be readily obtained by integrating Eq. (2-26).

Contrary to the assumption that the wall temperature T_w is a constant, the experimental studies conducted under this program clearly indicate that T_w varies with x, as shown by the data presented in Fig. 1. Using the experimental temperature data of Fig. 1, an analytical expression for T_w is obtained using a least square technique. The resulting expression for T_w is

$$T_w = A + Be^{Gx} \tag{2-28}$$

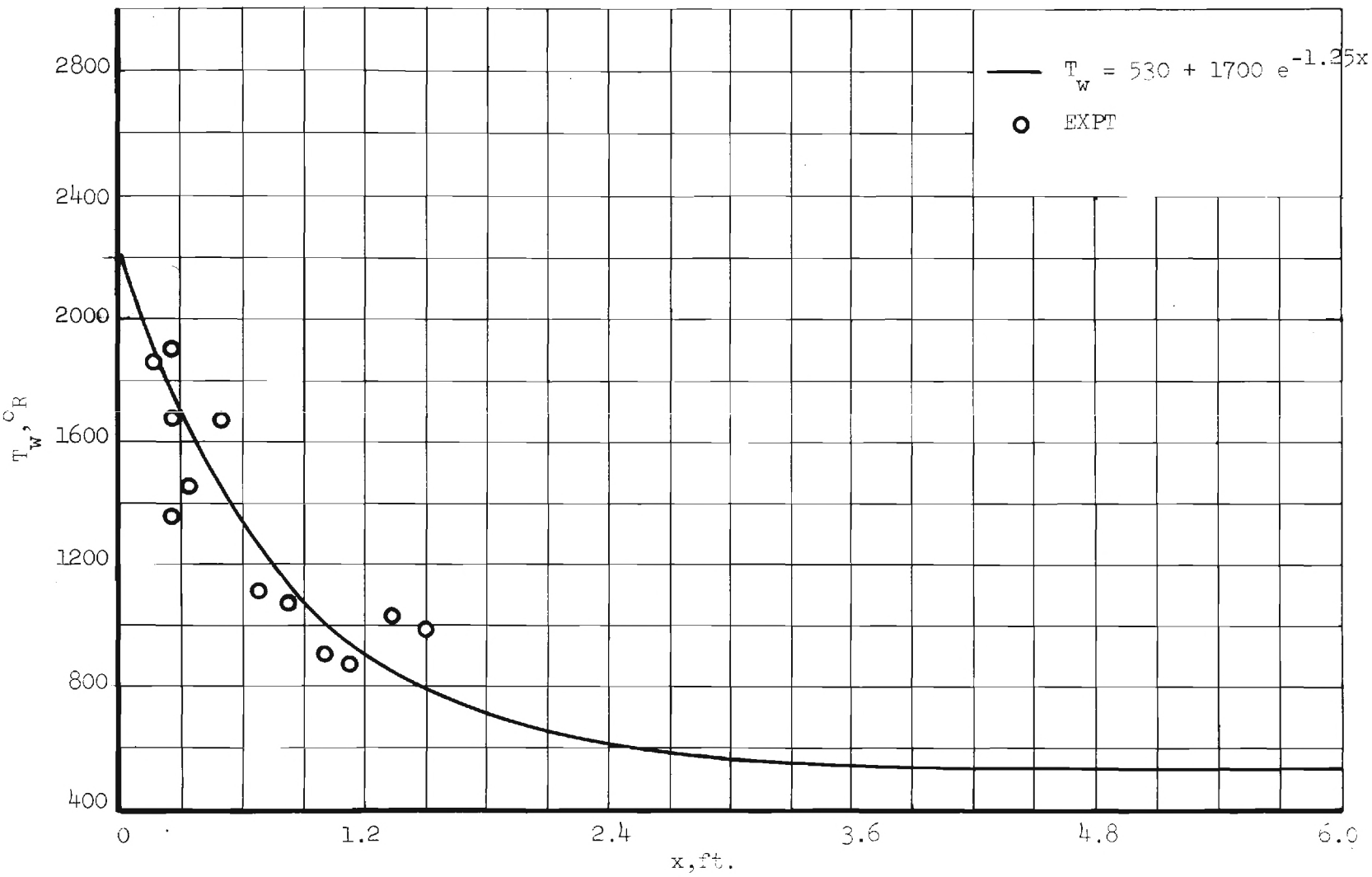

Figure 1. Wall Temperature Distribution Along the Burner Tube Axis

where

$$A = 530 \qquad B = 1700 \qquad \text{and } G = -1.25$$

If on the other hand T_w and Λ are assumed to be constant, then Eq. (2-25) can be integrated and the axial temperature variation can be expressed as follows[7]:

$$\bar{T} = T_w + (T_c - T_w)e^{\frac{-x}{\Lambda}} \tag{2-29}$$

Temperature profiles calculated using different combinations of the above equations are presented in Figs. 2 through 4. Figure 2 presents three temperature profiles which are obtained using a constant value of T_w. One of these profiles is obtained by numerically integrating Eq. (2-26) while the other two are evaluated using Eq. (2-29), taking a constant value for Λ in one of them and using Eq. (2-27) in the other. Figure 3 shows three steady temperature profiles which were obtained using Eq. (2-28) for T_w, keeping the rest of the parameters the same as in Fig. 2. Figure 4 presents a comparison of two of the temperature profiles presented in Figs. 2 and 3. It is observed from the Fig. 4 that the temperature profile obtained using a constant wall temperature differs considerably from the one obtained using Eq. (2-28) for the computation of the wall temperature. Since there is no basis for assuming a constant wall temperature, the temperature profile obtained by using Eq. (2-28) for T_w is probably a better representation of the steady state temperature distribution in the burner. However, in the present analysis of the burner wave structure, the wall temperature has been assumed to be constant. The validity of this assumption

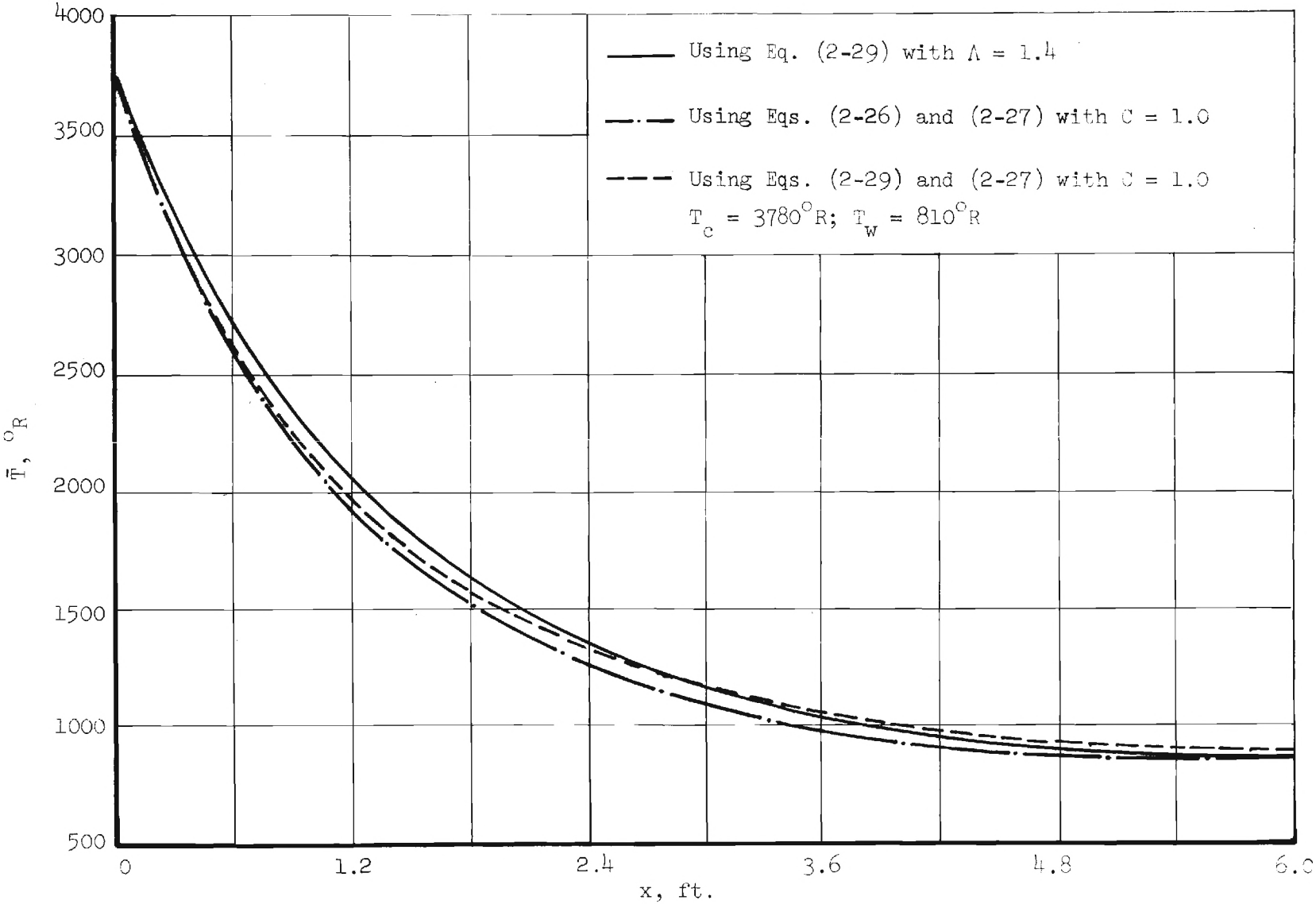

Figure 2. Mean Temperature Distribution Along the Burner Tube Axis, for a Constant T_w

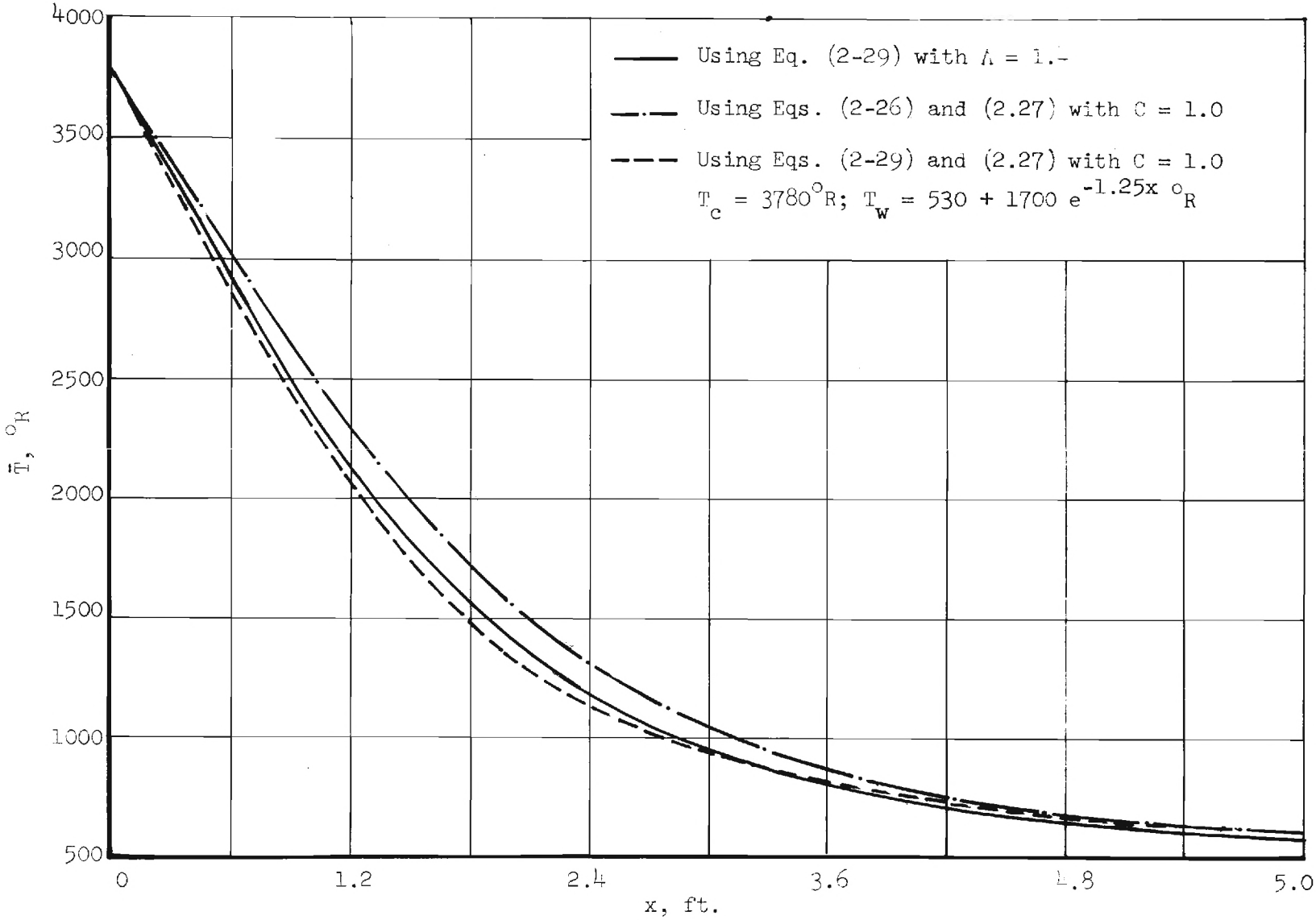

Figure 3. Mean Temperature Distribution Along the Burner Tube Axis, with Variable T_w

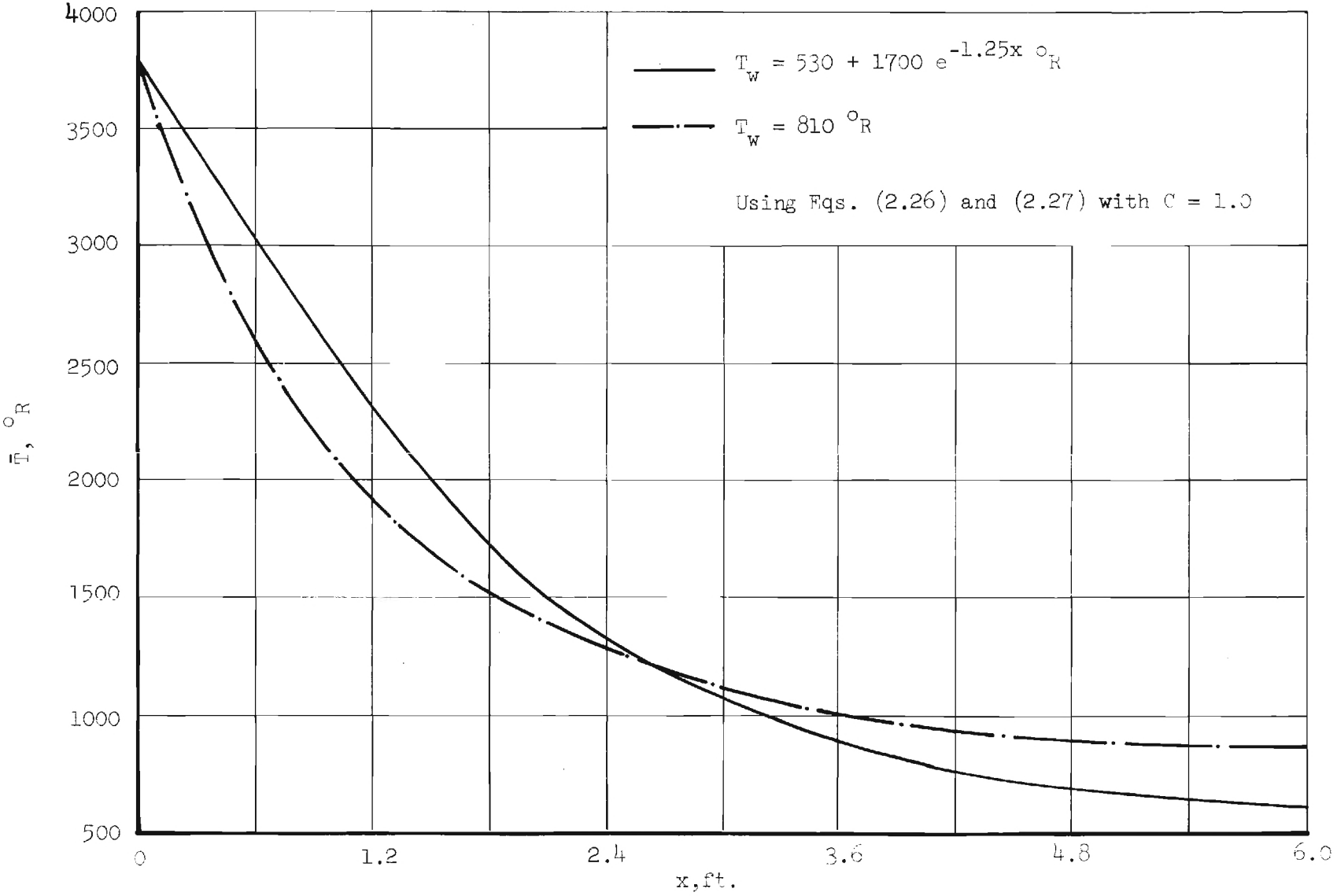

Figure 4. Comparison of Mean Temperature Distributions Along Burner Tube Axis

and the sensitivity of the computed wave structure to the behavior of T_w will be investigated at a later date.

3. Dependence of the Burner Tube Wave Structure Upon the Propellant Surface Boundary Conditions

An extensive study of the dependence of the burner tube wave structure upon the boundary conditions at the propellant surface has been conducted to obtain a better understanding of the acoustic characteristics of the burner tube. The boundary conditions at the propellant surface may be described by the admittance Y, the oscillatory pressure p' and the oscillatory density ρ'. The oscillatory velocity u' at the propellant surface is then obtained from the known values of Y and p'. Equations (2-8) through (2-10) can then be solved, using the specified values of u', p' and ρ' at the propellant surface, to obtain the wave structure in the burner tube. During the present investigation, the wave structure in the burner tube has been determined for both positive and negative values of the admittance Y. A positive real admittance at the propellant surface implies a condition which results in wave energy addition from the burning propellant to the gas phase (i.e., an unstable situation). On the other hand, the oscillation in the burner tube is attenuated (or damped) by the boundary if the real part of the admittance at the propellant surface is negative. In this section the relationship between the sign of the propellant admittance and the characteristics of the pressure phase-distance curve will be investigated and the results will be used in the experimental phase of this program to determine the propellant's characteristics from experimental phase data.

The axial variation of the acoustic pressure amplitude and phase obtained during the present study are presented in Figs. 5 and 6. An examination of these figures indicated that for a positive real admittance at the propellant surface the slope of the pressure phase-distance curve is negative, and vice-versa. Also, a near zero slope is observed when the real part of the surface admittance is a very small number.

The above results are applicable when the mean flow velocity $\bar{u}$ is neglected in the computations. When the mean flow velocity $\bar{u}$ is incorporated in the computations, the above-mentioned symmetry is lost, as shown in Fig. 5. These results show that the presence of a mean flow velocity tends to make the slope of the phase-distance curve more negative, with the result that for zero and small negative values of the real part of the propellant admittance the slope of the phase-distance curve still remains negative. An examination of the pressure amplitude data shown in Fig. 6 indicates that the amplitudes of the acoustic pressure at successive nodes and antinodes increase with increasing distance from the propellant boundary (i.e., the left-hand boundary). Also, the pressure amplitude at a given antinode increases with increasing magnitude of the real part of admittance at the propellant surface.

4. Determination of Propellant Response Factors Using Acoustic Pressure Data

It will be shown in this section that Eqs. (2-8) through (2-10) can be used together with appropriate acoustic pressure data to determine the response factor at the propellant surface. Mathematically, Eqs. (2-8) through (2-10), which are a system of three linear, homo-

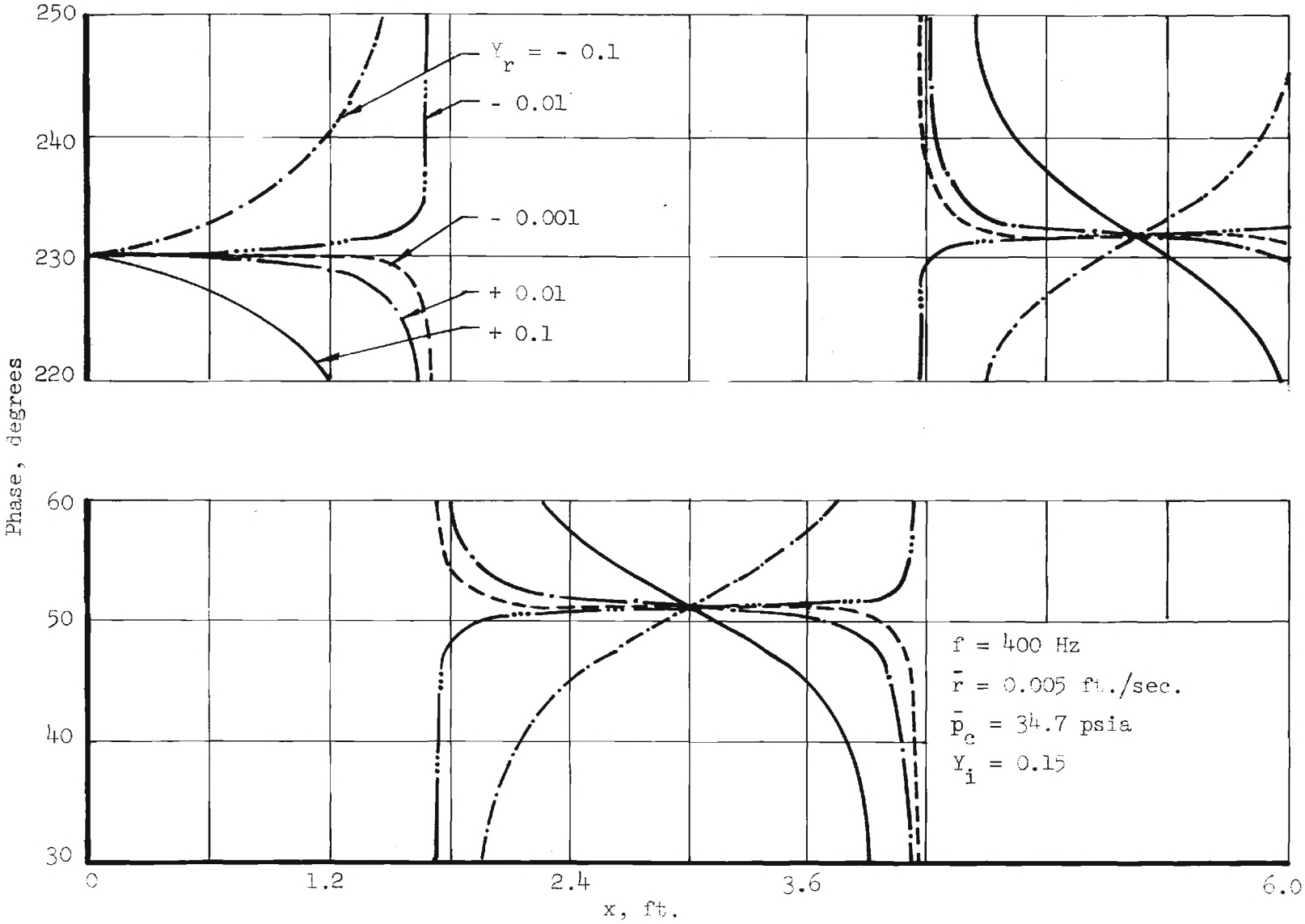

Figure 5. Dependence of Axial Pressure Phase Distribution Upon Y_r

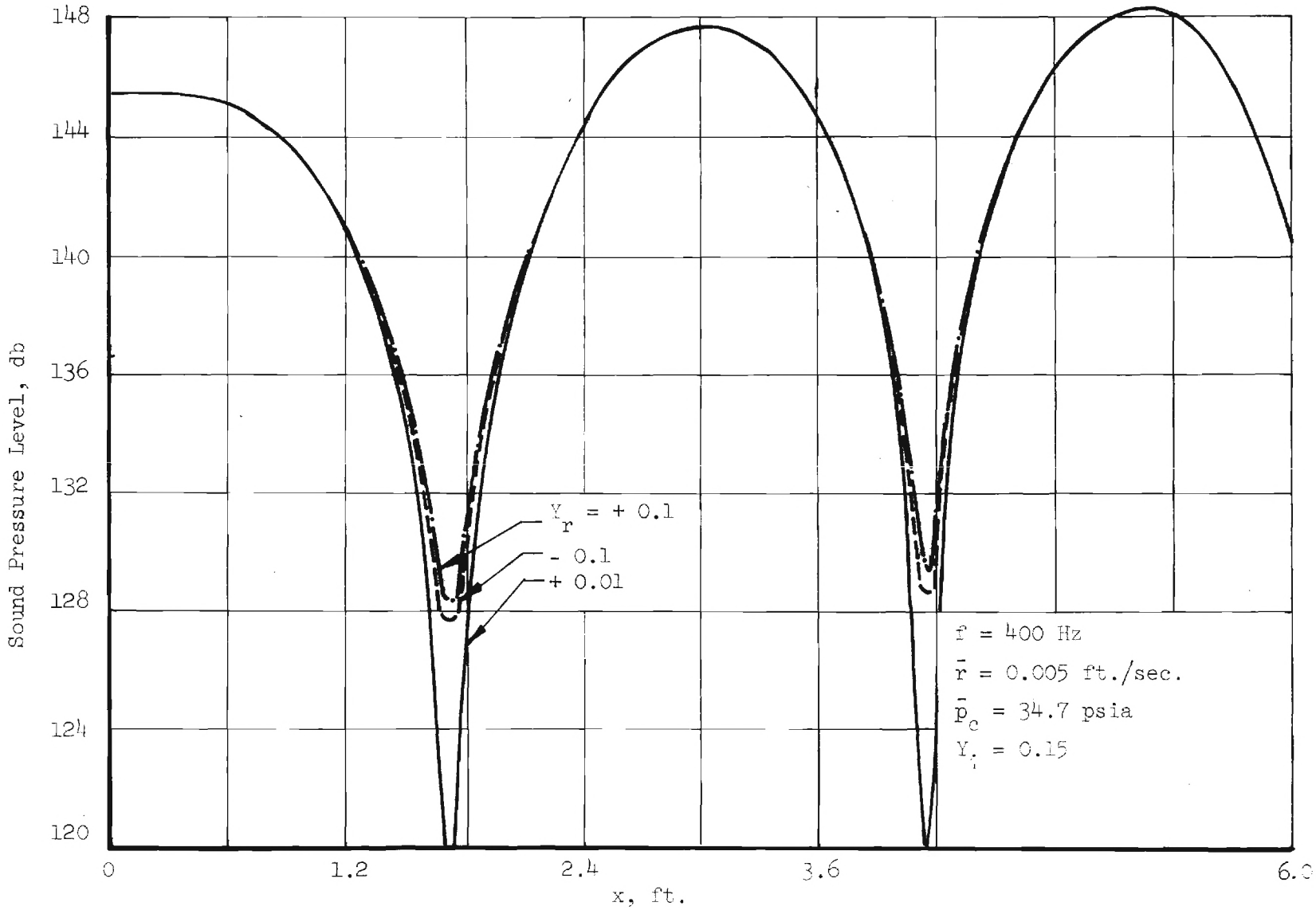

Figure 6. Dependence of Axial Pressure Amplitude Upon Y_r

geneous, coupled, ordinary differential equations, can be solved if three values of the dependent variable Z, at a given location, and all the coefficients A_{ij} are known.

As shown in Ref. 5, the response factor of a solid propellant is expressible in terms of the oscillatory pressure, velocity and density at the surface of the propellant, which are represented by components of the vector Z in the present analysis. Thus, the propellant response factor can be evaluated once these variables are obtained by solving Eqs. (2-8) through (2-10). Equations (2-8) through (2-10) could be treated as an initial value problem if Z_1, Z_2 and Z_3 (i.e., u', p' and ρ') can be measured at some location x. Unfortunately, accurate measurements of Z_1 and Z_3 (i.e., u' and ρ') are, with present day technology, extremely difficult if not impossible. Hence, one must resort to the use of a different analytical technique for the solution of the above-mentioned system of equations. The development of such a technique is discussed in this section. It will be shown that the needed data on Z_1 and Z_3 can be replaced by measurements of Z_2 (i.e., p') at two additional axial locations. The mathematical technique that allows the use of measured Z_2 data to solve the system of equations is based on the "transmission matrix" concept[9], and it is discussed below.

Equations (2-8) through (2-10) can be rewritten in the following matrix form:

$$\{Z'\}_x = [A]_x\{Z\}_x \qquad (2\text{-}30)$$

where the subscript x represents the location at which the elements of the matrix are evaluated. Introducing the backward transmission matrix

$[T]^9$, $\{Z\}$ can be written as follows

$$\{Z\}_x = [T]_x \{Z\}_{x_o} \tag{2-31}$$

Equation (2-31) indicates that once the transmission matrix $[T]_x$ and $\{Z\}_{x_o}$ are known, $\{Z\}_x$ can be evaluated. To determine $[T]_x$ and $\{Z\}_{x_o}$, one can use Eq. (2-31) to get the following expression for $\{Z\}_{x_o}$

$$\{Z\}_{x_o} = [T]_x^{-1} \{Z\}_x \tag{2-32}$$

Now, differentiating Eq. (2-31) with respect to x and using Eq. (2-32) yield the following expression for $\{Z'\}_x$:

$$\{Z'\}_x = [T']_x [T]_x^{-1} \{Z\}_x \tag{2-33}$$

Comparing Eqs. (2-30) and (2-33), one gets

$$[A]_x \{Z\}_x = [T']_x [T]_x^{-1} \{Z\}_x \tag{2-34}$$

Since $\{Z\}_x$ is an arbitrary matrix, it can be eliminated from both sides of Eq. (2-34) to give

$$[T']_x = [A]_x [T]_x \tag{2-35}$$

The matrix $[T]_x$ can be determined from integration of Eq. (2-35) once $[T]_{x_o}$ is known. By letting x go to x_o in Eq. (2-31) one obtains $[T]_{x_o}$ = I, the identity matrix. From eq. (2-31) it follows that

$$\{Z\}_{x_1} = [T]_{x_1} \{Z\}_{x_o} \tag{2-36}$$

$$\{Z\}_{x_2} = [T]_{x_2} \{Z\}_{x_o} \tag{2-37}$$

Using Eqs. (2-36) and (2-37) to obtain expressions for the elements $(Z_2)_{x_1}$, $(Z_2)_{x_2}$ leads to the derivation of two algebraic equations involving $(Z_1)_{x_o}$ and $(Z_3)_{x_o}$. These algebraic equations can then be solved for $(Z_1)_{x_o}$ and $(Z_3)_{x_o}$, since Z_2 at x_o, x_1 and x_2 are known (from experimental data). Thus, making use of $\{Z\}_{x_o}$ and $[T]_x$, $\{Z\}_x$ can be evaluated from Eq. (2-31).

The coefficients A_{ij} in Eqs. (2-11) through (2-19) can be evaluated once the steady state temperature profile $\bar{T}(x)$, the mean pressure $\bar{p}$ at any one location in the tube, the mean burning rate of the propellant $\bar{r}$, the thermodynamic properties of the gaseous products (i.e., C_p, R, etc.) and the propellant density ρ_s are known. Temperature measurements along the burner tube could, in principle, be used to provide an axial temperature profile; however, in view of the presence of radial temperature gradients in the tube, the question comes up regarding the "best" radial location to be used for the measurement of a bulk axial temperature distribution that is "consistent" with a one-dimensional flow model. Since it is difficult to locate such a radial position in the burner tube, an entirely different approach for the determination of the effective axial temperature distribution has been developed under this program and it is discussed below.

One of the temperature profiles discussed in this chapter (i.e., see Eq. (2-29)) is described by the following expression:

$$\bar{T} = T_w + (T_c - T_w)e^{-x/\Lambda} \tag{2-38}$$

where

$$\Lambda = C[1 + T_w/\bar{T}]^n; \qquad n = 0.68 \tag{2-39}$$

The evaluation of the constant C using the experimentally-determined locations of two successive pressure nodes x_o and x_1 of the standing wave will now be discussed. The locations x_o and x_1 are related to one another by the following expression

$$x_1 = x_o + \frac{\lambda(x)}{2} \tag{2-40}$$

An average speed of sound for the flow between positions x_o and x_1 can be obtained from the relation

$$\bar{c}_{ave} = \frac{1}{(\lambda/2)} \int_{x_o}^{x_1} \sqrt{\gamma R \bar{T}}\, dx \tag{2-41}$$

Using the relationship $\bar{c}_{ave} = \lambda f$, where f is the frequency, Eq. (2-41) can be rewritten as

$$K\lambda^2 = \int_{x_o}^{x_1} \bar{T}^{\frac{1}{2}}\, dx, \qquad K = \frac{f}{2\sqrt{\gamma R}} = \text{Const.} \tag{2-42}$$

Substituting the expression for $\bar{T}$ into Eq. (2-42) and using Eq. (2-39), a transcendental equation for C is obtained. Once this equation is solved for C, the temperature profile can be determined using Eq. (2-38).

With the temperature distribution $\bar{T}(x)$ known, the mean pressure $\bar{p}$ (which is almost constant with x) can be measured directly and the burning rate $\bar{r}$ can be determined from the known propellant sample thickness and the total burning time. The specific heat γ, the gas constant R, the flame temperature T_c and the propellant density ρ_s are generally

known before hand. With these quantities known, the coefficients A_{ij} can be determined and used in the data reduction program.

5. Error Minimization by Application of a Regression Technique

As discussed in Section 4, any three pressure measurements together with a known axial temperature profile can be used to determine the unknown propellant admittance. However, errors in the experimental measurements result in errors in the computed admittance values. As will be shown in this section, these errors can be minimized by increasing the number of acoustic pressure measurements and utilizing a nonlinear regression technique in the data reduction.

Let E_i be a quantity measured at x_i, $i = 1, 2, \cdots, n$ and T_i the corresponding theoretically calculated quantity evaluated at the same location x_i. In the present problem, the experimentally-measured quantity is the acoustic pressure Z_2 which is measured at various x_i locations. Nonlinear regression consists of finding values of u', p' and ρ' at $x = 0$, (i.e., values of Z_{o_1}, Z_{o_2} and Z_{o_3}) which give the best fit between the theoretically predicted acoustic pressure distribution, obtained from the solution of Eqs. (2-8) through (2-10), and the experimentally measured acoustic pressures. This is accomplished by computing the values of u', p' and ρ' at $x = o$ which minimize the root-mean-square deviation between the theoretically predicted acoustic distribution and and experimental data. The calculated optimum values of u', p' and ρ' at $x = 0$ can then be used to obtain optimum values of the propellant admittance and response factor. To find the minimum root-mean-square deviation, the following function F is minimized:

$$F = \sum_{i=1}^{n} (E_i - T_i)^2 \tag{2-43}$$

If a minimum of F exists, then the gradient of F vanishes at the minimum; that is

$$\frac{\partial F}{\partial Z_{o_1}} = \frac{\partial F}{\partial Z_{o_2}} = \frac{\partial F}{\partial Z_{o_3}} = 0$$

or

$$\frac{\partial F}{\partial Z_{o_k}} = -2 \sum_{i=1}^{n} \left[(E_i - T_i) \frac{\partial T_i}{\partial Z_{o_k}} \right] = 0,; \qquad k = 1, 2, 3 \tag{2-44}$$

Equation (2-44) represents a set of three nonlinear equations for the unknowns Z_{o_1}, Z_{o_2}, Z_{o_3} as T_i and $\partial T_i/\partial Z_{o_k}$ are both functions of Z_{o_k}. A Newton-Raphson iterative scheme is used to obtain a solution of Eq. (2-44) utilizing a linearized version of this equation which involves the expansion of T_i in a first order Taylor series with respect to the parameters Z_{o_1}, Z_{o_2} and Z_{o_3}. The resulting system of linear algebraic equations can be expressed in the following for m:

$$\sum_{i=1}^{n} \left(E_i - T_i^m\right) \partial T/\partial Z_{o_k}\Big|_{(i,m)} = \sum_{j=1}^{3} \left[\left(Z_{o_j}^{m+1} - Z_{o_j}^{m}\right) \sum_{i=1}^{n} \frac{\partial T}{\partial Z_{o_j}}\Big|_{(i,m)} \frac{\partial T}{\partial Z_{o_k}}\Big|_{(i,m)} \right]$$

$$k = 1, 2, 3 \tag{2-45}$$

where m represents the m^{th} iteration.

For compactness, Eq. (2-45) will now be rewritten in matrix form; letting

$$b_k^m = \sum_{i=1}^{n} \left(E_i - T_i^m\right) \left.\frac{\partial T}{\partial Z_{o_k}}\right|_{(i,m)}$$

$$a_{kj}^m = a_{ik}^m = \sum_{i=1}^{n} \left.\frac{\partial T}{\partial Z_{o_j}}\right|_{(i,m)} \left.\frac{\partial T}{\partial Z_{o_k}}\right|_{(i,m)}$$

$$B^m \equiv \begin{Bmatrix} b_1^m \\ b_2^m \\ b_3^m \end{Bmatrix}; \qquad A_m = \begin{bmatrix} a_{11}^m & a_{12}^m & a_{13}^m \\ a_{21}^m & a_{22}^m & a_{23}^m \\ a_{31}^m & a_{32}^m & a_{33}^m \end{bmatrix} \; ; \qquad Z_o^m = \begin{Bmatrix} Z_{o_1}^m \\ Z_{o_2}^m \\ Z_{o_3}^m \end{Bmatrix}$$

Equation (2-45) can be expressed as follows

$$A^m \left(Z_o^{m+1} - Z_o^m\right) = B^m$$

or equivalently

$$Z_o^{m+1} = Z_o^m + (A^m)^{-1} B^m \tag{2-46}$$

Equation (2-46) is a linear equation for the unknown Z_o^{m+1} and can be readily solved once the elements of A^m and B^m have been computed. The computation of these elements requires the determination of the derivatives $\left.(\partial T/\partial Z_{o_k})\right|_{(i,m)}$. Since these derivatives cannot be determined analytically, numerical values for these derivatives are obtained using the following finite difference formula

$$\left.\frac{\partial T_i}{\partial Z_{o_k}}\right|_{(i,m)} \approx \frac{T_i(Z_{o_1}^m, \ldots, Z_{o_k}^m (1+\epsilon), \ldots) - T_i^m}{\epsilon Z_{o_k}^m}$$

where ϵ is a small number. Thus, to solve for the elements of the matrices A^m and B^m of Eq. (2-46), it is necessary to compute T_i four times for each iteration by solving Eqs. (2-8) through (2-10). The first solution is obtained at Z_o^m and the remaining solutions of T_i are obtained by varying each of three parameters by a small amount $\epsilon Z_{o_k}^m$ in succession.

6. Particulate Matter - Acoustic Wave Interaction

This section presents the results of an investigation carried out to determine the influence of particulate matter upon acoustic behavior of the burner tube. This analysis has been performed in an effort to understand some of the trends exhibited by the experimental data, which will be discussed in the next chapter of this report. The theory of particulate attenuation and dispersion of sound is formulated in a manner that explicitly shows the relaxation character of the problem[12,13]. The analysis presented herein is based on the following assumptions: (1) the gas is thermally and calorically perfect; (2) the density of the particles is much greater than the density of the surrounding gas; (3) mass transfer between particles and gas is absent (i.e., evaporation, condensation and chemical reaction are excluded); (4) the total heat-transfer and drag force between the particulate and gas phases is the sum of the effects due to each particle. This assumption implies that the particle diameter is much smaller than the distance between the particles and it restricts the theory to low particle-volume concentrations; (5) the fluctuations of pressure, density, and temperature produced by the acoustic wave are assumed to be sufficient-

ly small as compared with their mean values so that their products can be neglected. Similarly, the fluid velocity is assumed to be much smaller than the speed of sound.

Using the above assumptions, one-dimensional wave motion through a stationary gas phase containing spherical particles in suspension is investigated by solving the following system of linearized conservation equations:

Gas Phase Continuity: $$\frac{\partial \rho'}{\partial t} + u' \frac{d\bar{\rho}}{dx} + \bar{\rho} \frac{\partial u'}{\partial x} = 0 \qquad (2\text{-}47)$$

Gas Phase Momentum: $$\bar{\rho} \frac{\partial u'}{\partial t} + \frac{\partial p'}{\partial x} = \bar{n} F_p \qquad (2\text{-}48)$$

Gas Phase Energy: $$\frac{C_v}{R}\left\{\frac{\partial p'}{\partial t} - c^{-2}\left(\frac{\partial \rho'}{\partial t} + u' \frac{d\bar{\rho}}{dx}\right)\right\} = \bar{n} Q_p + \bar{n} F_p (u_p' - u') \qquad (2\text{-}49)$$

Particulate Continuity: $$\frac{\partial \rho_p'}{\partial t} + \bar{n} m' \frac{\partial u_p'}{\partial x} = 0 \qquad (2\text{-}50)$$

Particulate Momentum: $$m' \frac{\partial u_p'}{\partial t} = - F_p \qquad (2\text{-}51)$$

Particulate Energy: $$m' C_p' \left[\frac{\partial T_p'}{\partial t} + u_p' \frac{d\bar{T}}{dx}\right] = - Q_p \qquad (2\text{-}52)$$

Eq. of State: $$p' = \bar{R}(\rho' \bar{T} + \bar{\rho} T') \qquad (2\text{-}53)$$

Assuming a low Reynolds number flow, the drag of the particles can be expressed by Stoke's law for the motion of a sphere in a viscous fluid and the heat transfer coefficient h can be taken to equal k/r, where k is the coefficient of thermal conductivity of the gas and r

is the particle radius. Thus[13],

$$F_p = \frac{6\pi\mu r}{g} (u_p' - u') \tag{2-54}$$

and

$$Q_p = 4\pi rk (T_p' - T') \tag{2-55}$$

The dynamic relaxation time of the particle can be expressed as

$$\tau_d = 2r^2 \bar{\rho}_p/9 \mu \tag{2-56}$$

while the thermal relaxation time of the particle is given by[13]

$$\tau_t = P_r C_p' r^2 \bar{\rho}_p/3 \mu C_p$$

or

$$\tau_t = \frac{3}{2} \left(\frac{C_p'}{C_p}\right) P_r \tau_d \tag{2-57}$$

Using the above expressions, the momentum and energy equations for the particles can be rewritten as:

$$\frac{\partial u_p'}{\partial t} = - (u_p' - u')/\tau_d \tag{2-58}$$

and

$$\frac{\partial T_p'}{\partial t} + u_p' \frac{d\bar{T}}{dx} = - (T_p' - T')\tau_t \tag{2-59}$$

Assuming periodic time behavior of u_p' and T_ρ' (e.g., $u' \propto e^{i\omega t}$), Eqs. (2-58) and (2-59) can be used to obtain the following results.

$$u_p' = u'/(1 + i\omega\tau_d) \tag{2-60}$$

$$T_p' = (T' - \tau_t u_p' \frac{d\bar{T}}{dx})/(1 + i\,\omega\,\tau_t) \tag{2-61}$$

Rewriting Eq. (2-55) in the form

$$T' = \frac{1}{R\bar{\rho}}\left[p' - \frac{\bar{p}}{\bar{\rho}}\rho'\right] \tag{2-62}$$

and using Eqs. (2-60) through (2-62), F_p and Q_p can be expressed as

$$F_p = -\frac{6\pi\mu r}{g}\left\{i\,\omega\,\tau_d/(1 + i\omega\tau_d)\right\} u' \tag{2-63}$$

$$Q_p = -4\pi rk\left\{\frac{\tau_t}{(1+i\omega\tau_t)}\left[\frac{i\omega}{R\bar{\rho}}\left(p' - \frac{\bar{p}}{\bar{\rho}}\rho'\right) + \frac{u'}{(1+i\omega\tau_d)}\frac{d\bar{T}}{dx}\right]\right\} \tag{2-64}$$

Neglecting $\bar{n}\,F_p(u_p' - u')$ in Eq. (2-49) and assuming periodic time behavior of u', p' and ρ', Eqs. (2-47) through (2-49) can be rewritten as follows:

Continuity:
$$i\omega\rho' + \frac{d\bar{\rho}}{dx}u' + \bar{\rho}\frac{du'}{dx} = 0 \tag{2-65}$$

Momentum:
$$i\omega\bar{\rho}u' + \frac{dp'}{dx} = \bar{n}F_p \tag{2-66}$$

Energy:
$$i\omega p' - \bar{c}^2(i\omega\rho' + \frac{d\bar{\rho}}{dx}u') = \frac{R\bar{n}}{C_v}Q_p \tag{2-67}$$

Solving Eqs. (2-65) through (2-67) for $\frac{dp'}{dx}$ and $\frac{du'}{dx}$ yields

$$\frac{dp'}{dx} = A_{11}\,p' + A_{12}\,u' \tag{2-68}$$

$$\frac{du'}{dx} = A_{21}\,p' + A_{22}\,u' \tag{2-69}$$

where

$$A_{11} = 0$$

$$A_{12} = -\frac{6\pi\mu r\bar{n}}{g}\left\{\frac{i\omega\tau_d}{1 + i\omega\tau_d}\right\} - i\omega\bar{\rho} \qquad (2\text{-}70)$$

$$A_{21} = -\frac{i\omega}{\bar{\rho}\bar{c}^2}\left[\frac{1 + C_o}{1 + C_o/\nu}\right]$$

$$A_{22} = \frac{RC_o}{\bar{c}^2}\frac{d\bar{T}}{dx}\frac{i\omega\tau_d}{(1+i\omega\tau_d)(1+\frac{o}{\nu})}$$

and

$$C_o = \frac{4\pi rk\bar{n}}{C_v\bar{\rho}}\left(\frac{\tau_t}{1 + i\omega\tau_t}\right)$$

To investigate the effect of the particulate matter upon the wave structure in the burner tube, Eqs. (2-68) and (2-69) are solved for different boundary conditions at x = 0 and different particle loadings in the gas phase. In the present investigation the particle diameter is taken as 1 micron and the particle properties are chosen to be close to those of carbon particles; the chosen particle and gas phase are listed in Appendix A.

The computed wave structures are plotted in Figs. 7 through 10. In Fig. 7 the dependence of the acoustic pressure phases are plotted for an assumed admittance value of .0002 + i 0.15 at the burning propellant surface (i.e., x = 0) for various particle loadings. For zero particle loading, the phase plot indicates wave energy addition (i.e., driving) at the propellant surface as discussed earlier in this report when the real part of propellant surface admittance is positive. With

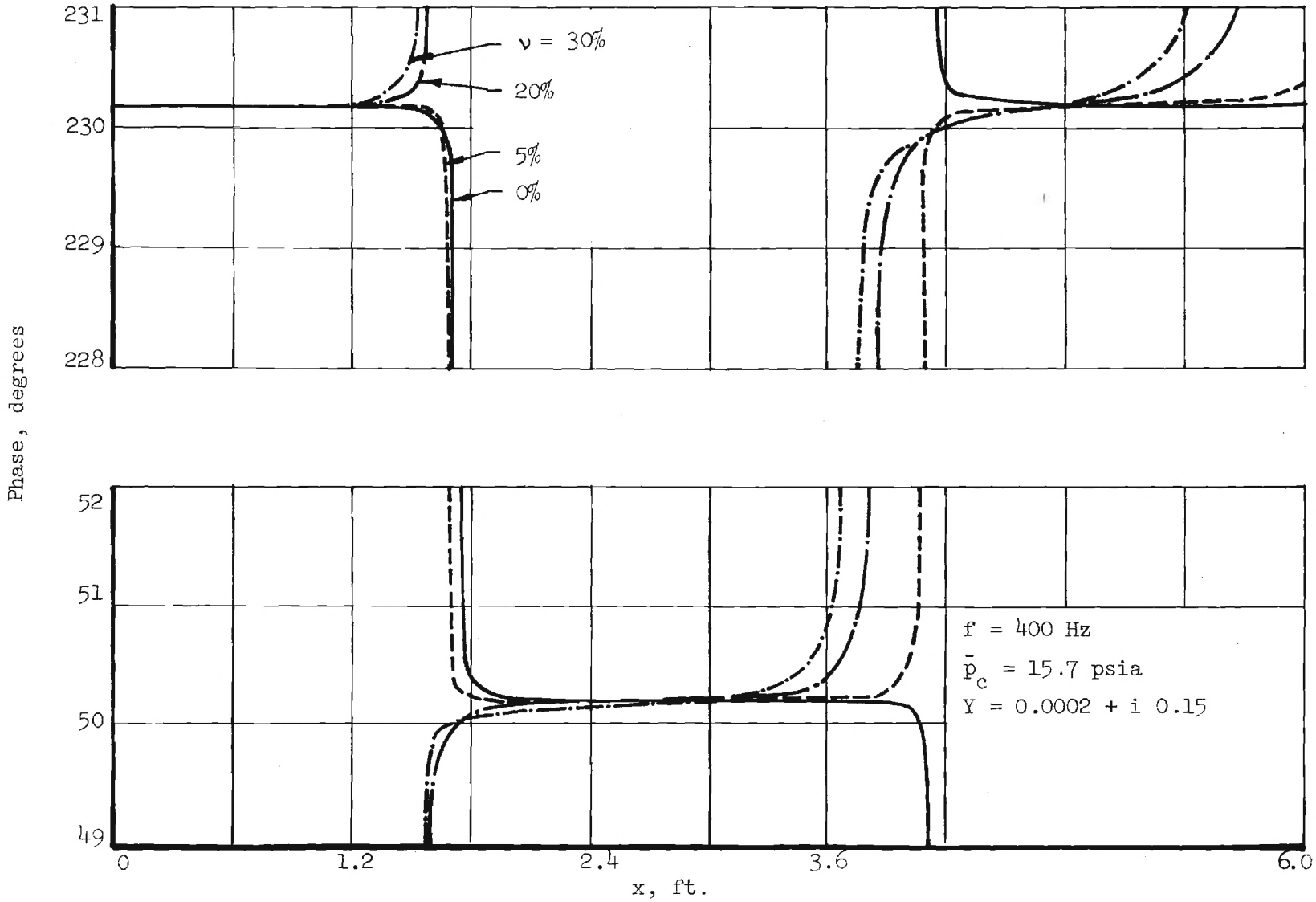

Figure 7. Dependence of Pressure Phase Distribution Upon Particulate Attenuation For a Given Y

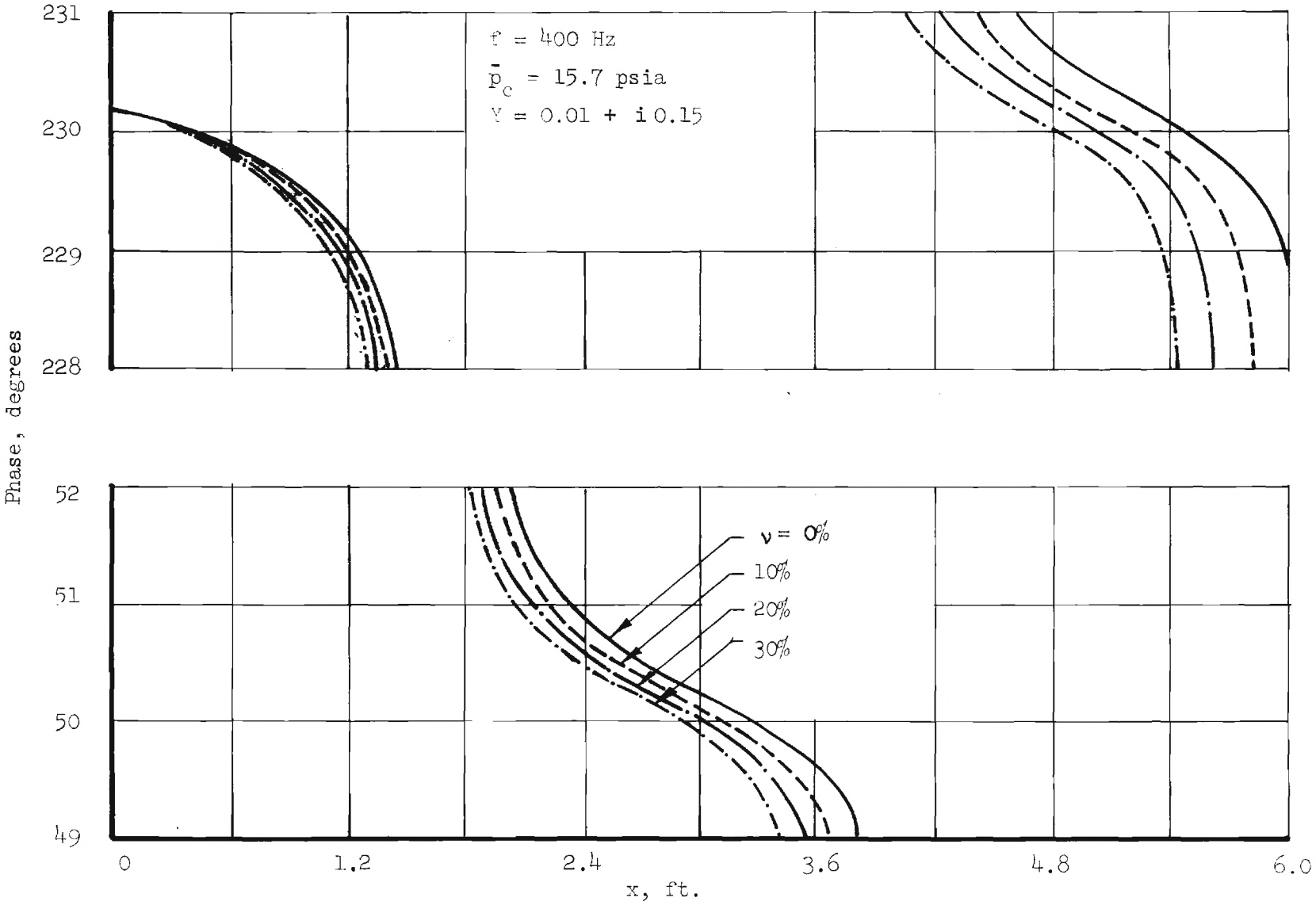

Figure 8. Dependence of Pressure Phase Distribution Upon Particle Attenuation for a Given Y

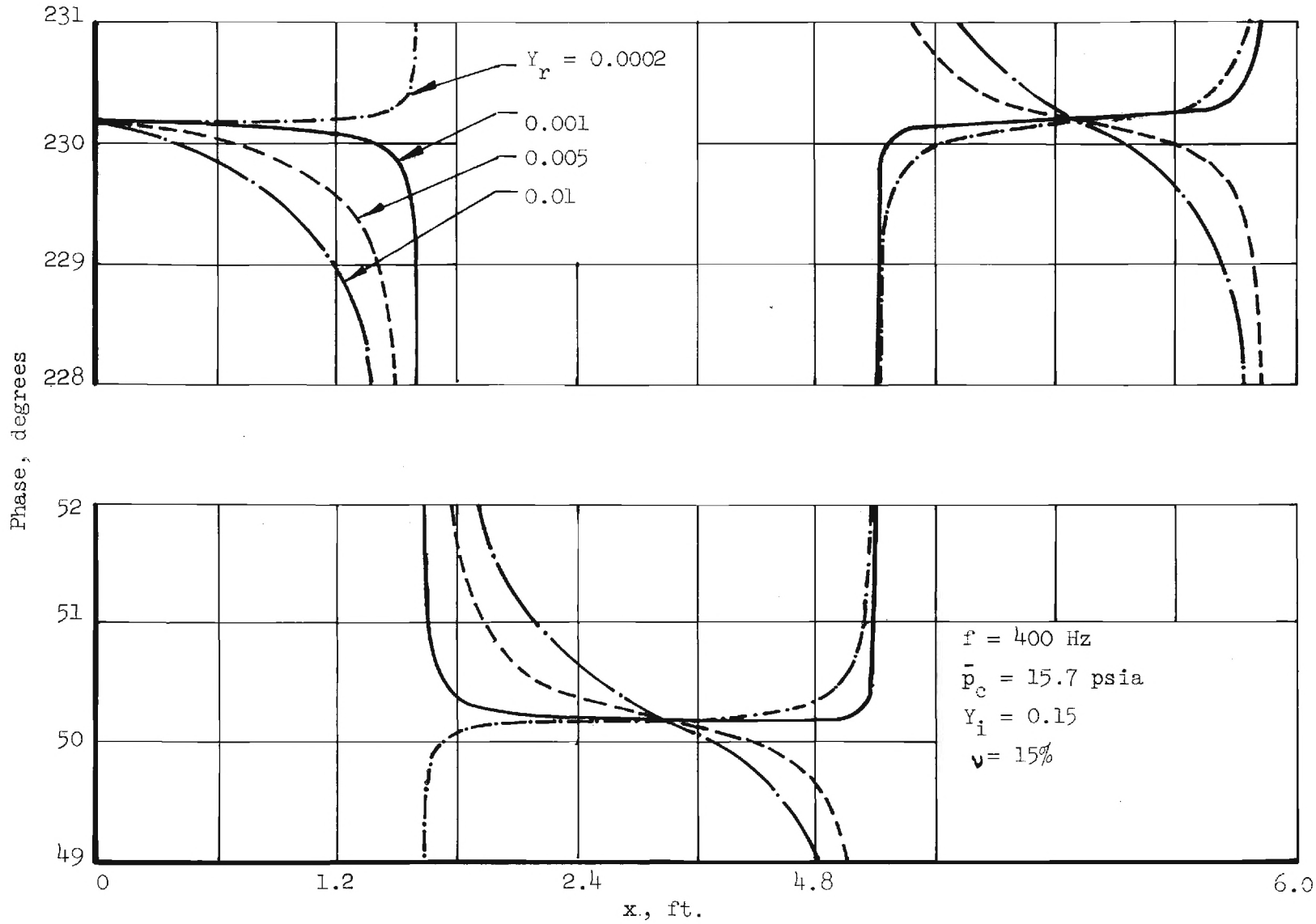

Figure 9. Dependence of Axial Pressure Phase Distribution Upon Y_r, for A Given ν

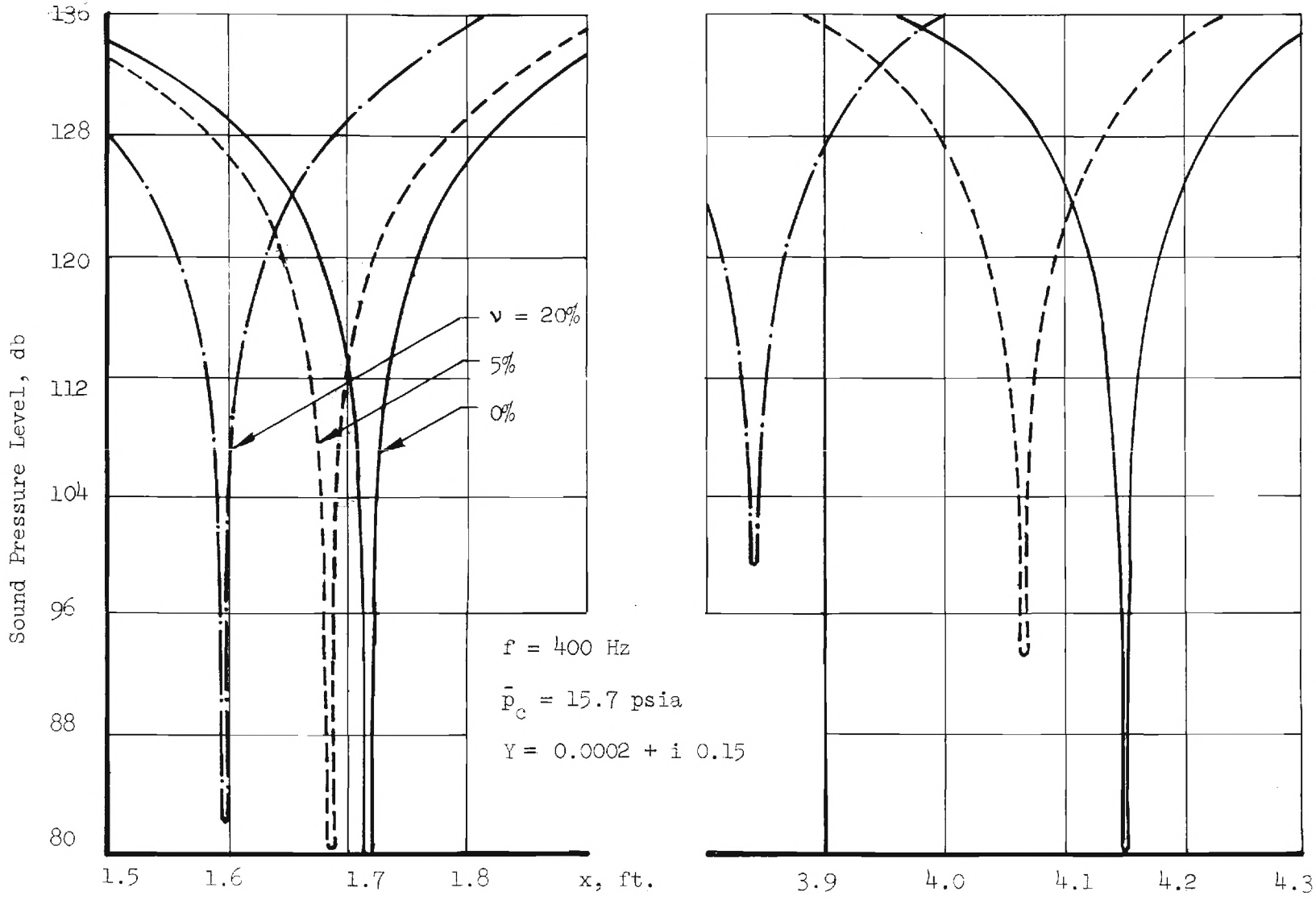

Figure 10. Dependence of Pressure Amplitude Distribution Upon ν

a small particle loading, the slope of the phase-distance curve starts changing beginning at the propellant surface where the slope remains the same as long as the propellant surface remains unchanged. The change in slope as one moves away from the propellant is due to the wave energy dissipation by the particle-wave motion interaction. Further increase in the particle loading results in a complete reversal of the slope of the phase-distance curve from partially negative values to completely positive values. It should be emphasized, however, that in all of these cases, the slope of phase-distance curves does not change at the propellant surface, indicating the same wave energy addition. Figure 8 shows a plot similar to the one presented in Fig. 7 but for higher positive values of the real part of the surface admittance. A comparison of the two indicates that with an increase in the value of the real part of the propellant admittance, wave energy is transmitted from left to right for all the investigated particle loadings. Figure 9 describes the dependence of the phase-distance curve upon the real part of the propellant surface admittance. Trends similar to those observed in the previous figures may also be noted in this figure. Figure 10 presents a plot of the standing wave amplitude for different particle loadings. Examination of this figure shows that a higher value of the particle loading reduces the wave length and increases the pressure amplitude at the nodal points.

7. Dependence of the Burner Wave Structure Upon the Propellant Self-Noise

The study described in this section has been conducted in an effort to explain some of the unexpected results which were obtained

during the experimental phase of this program. Briefly, experiments conducted with two different exhaust conditions downstream of the acoustic drivers produced entirely different wave structures in front of the propellant surface. This result was completely unexpected and it could not be explained by the commonly used propellant surface boundary condition; that is

$$\frac{dp'}{dx} + ikYp' = 0 \tag{2-71}$$

where Y is the propellant surface admittance.

It has been shown[14], that when the propellant responds to the pressure oscillation at its surface and, in addition, produces its own velocity oscillation which is independent of the local pressure oscillation, the boundary condition at the propellant surface can be expressed in the following form

$$\frac{dp'}{dx} + ikYp' = -i\omega\bar{\rho}u' \tag{2-72}$$

where the second term describes the propellant (or boundary) response to the local pressure oscillation and the inhomogeneous part describes the pressure independent velocity perturbation, which will be referred to as the propellant self-noise.

To investigate the effect of the inhomogeneous part of the propellant boundary condition upon the burner tube wave structure, the wave structure in a simple tube whose acoustic behavior is described by the one-dimensional Helmholtz equation

$$\frac{d^2p'}{dx^2} + k^2 p' = 0 \tag{2-73}$$

and whose solutions must satisfy the following inhomogeneous boundary conditions:

$$\frac{dp'}{dx} + ikY_1p' = - i\omega\bar{\rho}u_1 \text{ at } x = 0 \qquad (2\text{-}74)$$

and

$$\frac{dp'}{dx} - ikY_2p' = i\omega\bar{\rho}u_2 \text{ at } x = L \qquad (2\text{-}75)$$

is analyzed in this section. The change in signs between these boundary conditions is due to changes in the direction of the inward unit normal vector at the two boundaries. The solution of Eq. (2-73) is

$$p' = C \sin kx + D \cos kx \qquad (2\text{-}76)$$

where

$$C = \frac{i}{k}\left\{\omega\bar{\rho}u_1 + kY_1D\right\} \qquad (2\text{-}77)$$

and

$$D = - \frac{i\omega\bar{\rho}}{k} \frac{u_2 + u_1 \cos kL + Y_2u_1 \sin kL}{(Y_1Y_2 + 1)\sin kL - i(Y_1 + Y_2)\cos kL} \qquad (2\text{-}78)$$

The above solution was used to investigate the tube's wave structure for four different cases and the results are presented in Figs. 11 through 14. In the cases investigated, all of the parameters of the problem with the exception of $(Y_r)_2$ were kept constant in order to determine the dependence of the phase-distance curve upon $(Y_r)_2$. An examination of Fig. 11 shows that even though the real part of the admittance at the left boundary is positive (i.e., $(Y_r)_1 = .001$), the slope

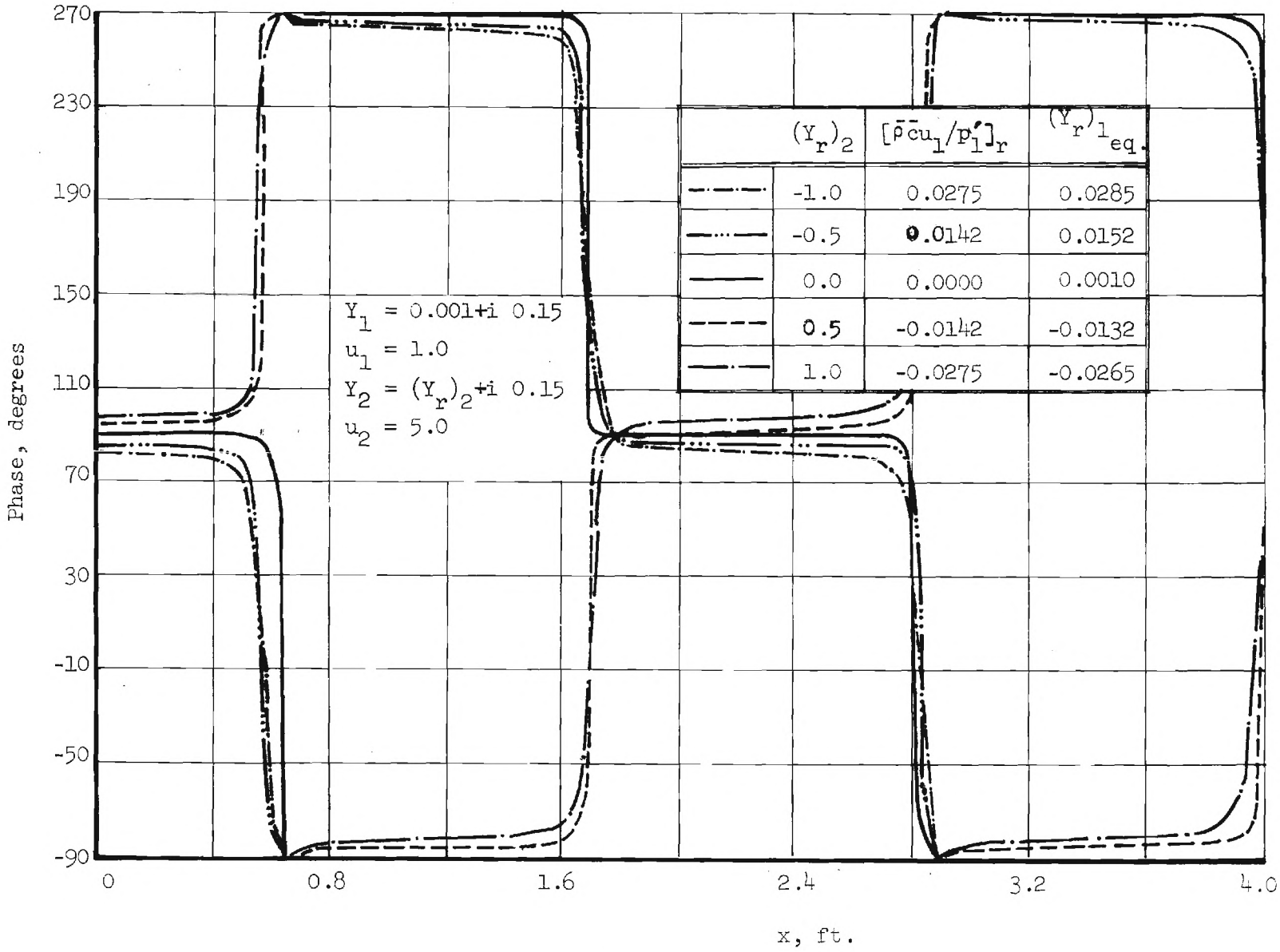

Figure 11. Dependence of Pressure Phase Distribution Upon $(Y_r)_2$.

of the phase-distance curve is positive for positive values of $(Y_r)_2$, indicating wave energy transmission from right to left. This unexpected result may be explained if one recognizes that the direction of movement of acoustic energy at a given point depends upon the sign of the real part of the local effective admittance which can be expressed (using the linearized momentum equation and Eq. (2-74) in the following form at the x = 0 location

$$(Y_r)_{1_{eq.}} = \left\{Y_1 + \bar{\rho}\bar{c}\,\frac{u_1}{p_1'}\right\}_r \qquad (2\text{-}79)$$

Since Y_1 is fixed, the sign of $(Y_r)_{1_{eq.}}$ depends upon $\left\{\bar{\rho}\bar{c}\ u_1/p_1'\right\}_r$ which in turn, depends upon the solution for p'.

Examination of the data in Fig. 11 reveals that the characteristics of the wave structure in front of the left boundary may be changed by merely changing $(Y_r)_2$. This trend is in qualitative agreement with the experimental data of this program. This qualitative agreement suggests that the presence of an inhomegeneous part (i.e., self-noise) in the propellant boundary condition may be the cause of the experimentally observed trends.

Figure 11 also contains a table with the computed values of $(Y_r)_{1_{eq.}}$ for different values of $(Y_r)_2$. Examination of this table shows that as $(Y_r)_2$ increases in value $(Y_r)_{1_{eq.}}$ decreases in value allowing more wave-energy to be absorbed at the left hand boundary. It is of particular interest to note that $(Y_r)_{1_{eq.}}$ approaches $(Y_r)_1$ when $(Y_r)_2 = 0$.

Figure 12 has been prepared to show the effect of changing $(Y_r)_1$

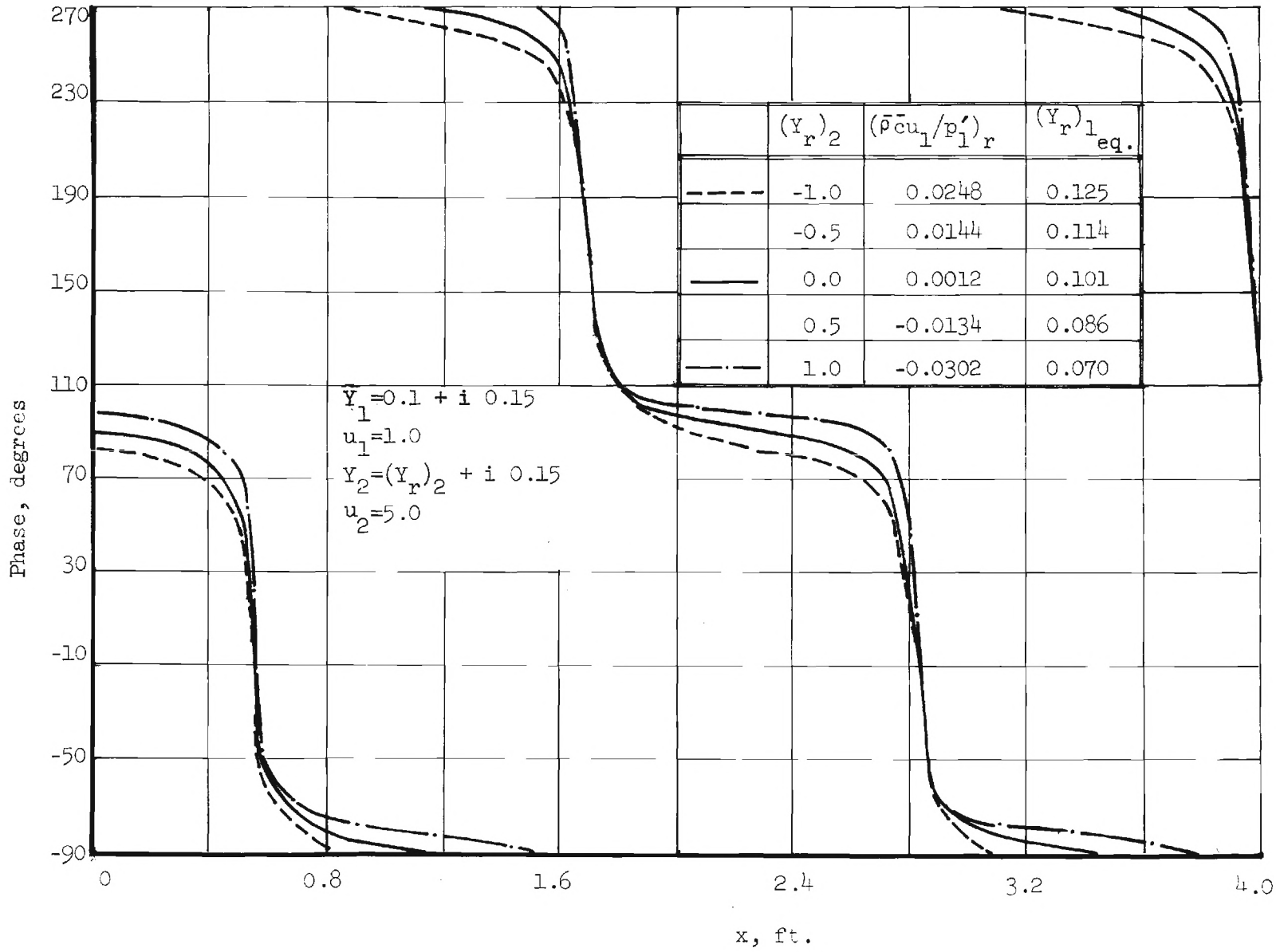

Figure 12. Dependence of Pressure Phase Distribution Upon $(Y_r)_2$.

upon the trends presented in Fig. 11. In going from Fig. 11 to Fig. 12 the value of $(Y_r)_1$ increased from .001 to .1. Examination of Fig. 12 shows that under the new condition the slope of the phase-distance curve is always negative indicating wave energy movement from left to right. Once again, the value of $(Y_r)_{1_{eq.}}$ approaches the value of $(Y_r)_1$ when $(Y_r)_2 = 0$.

In Fig. 13 the value of u_1 was set equal to zero while all the remaining parameters are the same as those used in Fig. 11. Examination of this figure shows that in this case changes in $(Y_r)_2$ do not affect the wave structure in front of the left boundary. A comparison of the data presented in Figs. 11 and 13 provides additional support to the argument that the presence of u_1 in the boundary condition may be responsible for the trends observed in the experimental data. In Fig. 14 data similar to that of Fig. 13 are presented with the exception that now the value of $(Y_r)_1$ is larger than the one used in Fig. 13.

From the above results it becomes evident that if a self driving term (i.e., u_1) is present at x = 0, the observed admittance $(Y_r)_{1_{eq.}}$ will not represent the actual admittance of the surface. However, if the real part of the admittance at x = L is kept zero, the observed real admittance at x = 0 (i.e., $(Y_r)_{1_{eq.}}$) would approach the actual real admittance $(Y_r)_1$. Also, if $(Y_r)_1$ is large, then the effect of $(\bar{\rho}\bar{c}u_1/p_1')_r$ is negligible and the value of $(Y_r)_{1_{eq.}}$ remains close to that of $(Y_r)_1$.

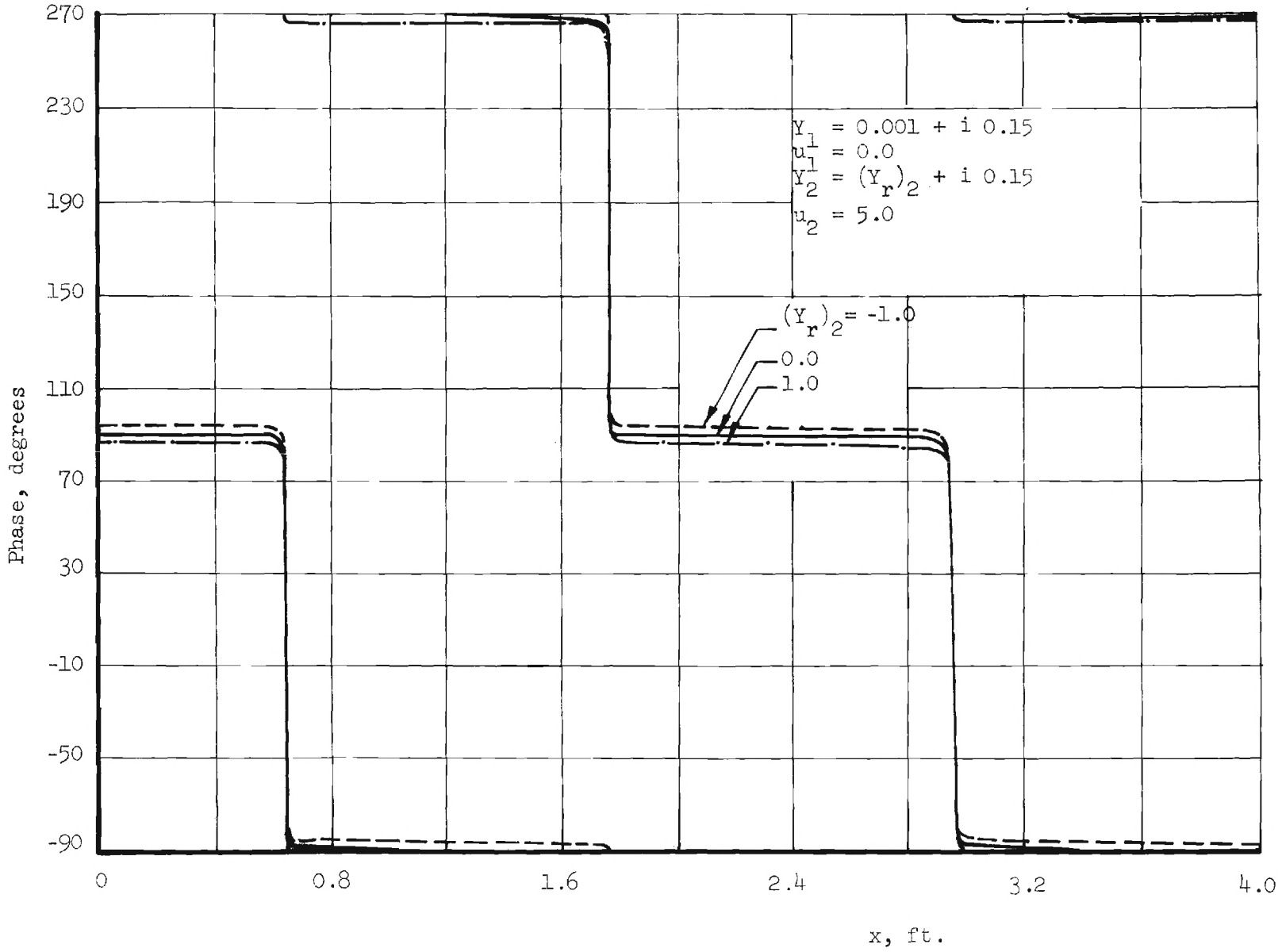

Figure 13. Dependence of Pressure Phase Distribution Upon $(Y_r)_2$.

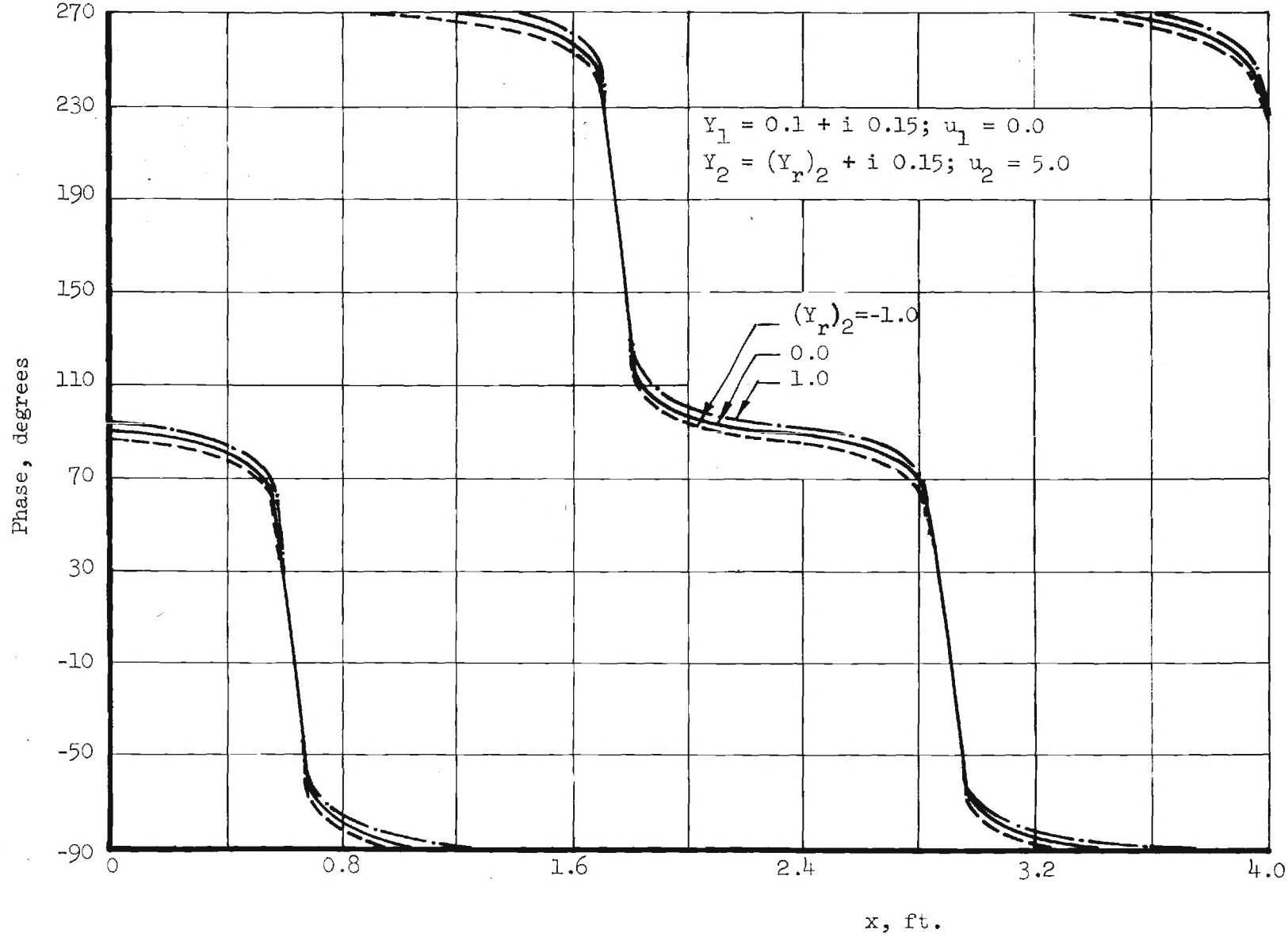

Figure 14. Dependence of Pressure Phase Distribution Upon $(Y_r)_2$.

III. EXPERIMENTAL RESULTS

This chapter describes the data obtained during the experimental phase of this program which is concerned with the application of the driven burner facility in the determination of the response factors and admittances of burning solid propellants. The second year experimental efforts were primarily concerned with the improvement of some of the experimental techniques and the determination of the admittances of a number of propellants under near atmospheric pressure conditions and over a frequency range that is of interest in solid propellant combustion instability. A detailed description of the experimental setup and testing procedure is available in Ref. 5.

Each test typically consists of three phases; the brief pre-ignition period during which the acoustic drivers are the only source of wave excitation, the propellant ignition phase and the steady burning phase. For each test run the dynamic pressure and temperature data are recorded on a 14 channel analog magnetic tape recorder. These data are then played back at reduced speed and plotted to obtain the time histories of the measured dynamic pressures and temperatures of the hot gases at several locations inside the burner tube. Typical time history plots of pressure amplitudes, pressure phases and steady state temperatures are presented in Figs. 15 through 17. By analyzing the data presented in these figures one can determine the period during which "steady state" conditions are established in the burner tube during the run. In addition, these plots are used to obtain the total burning

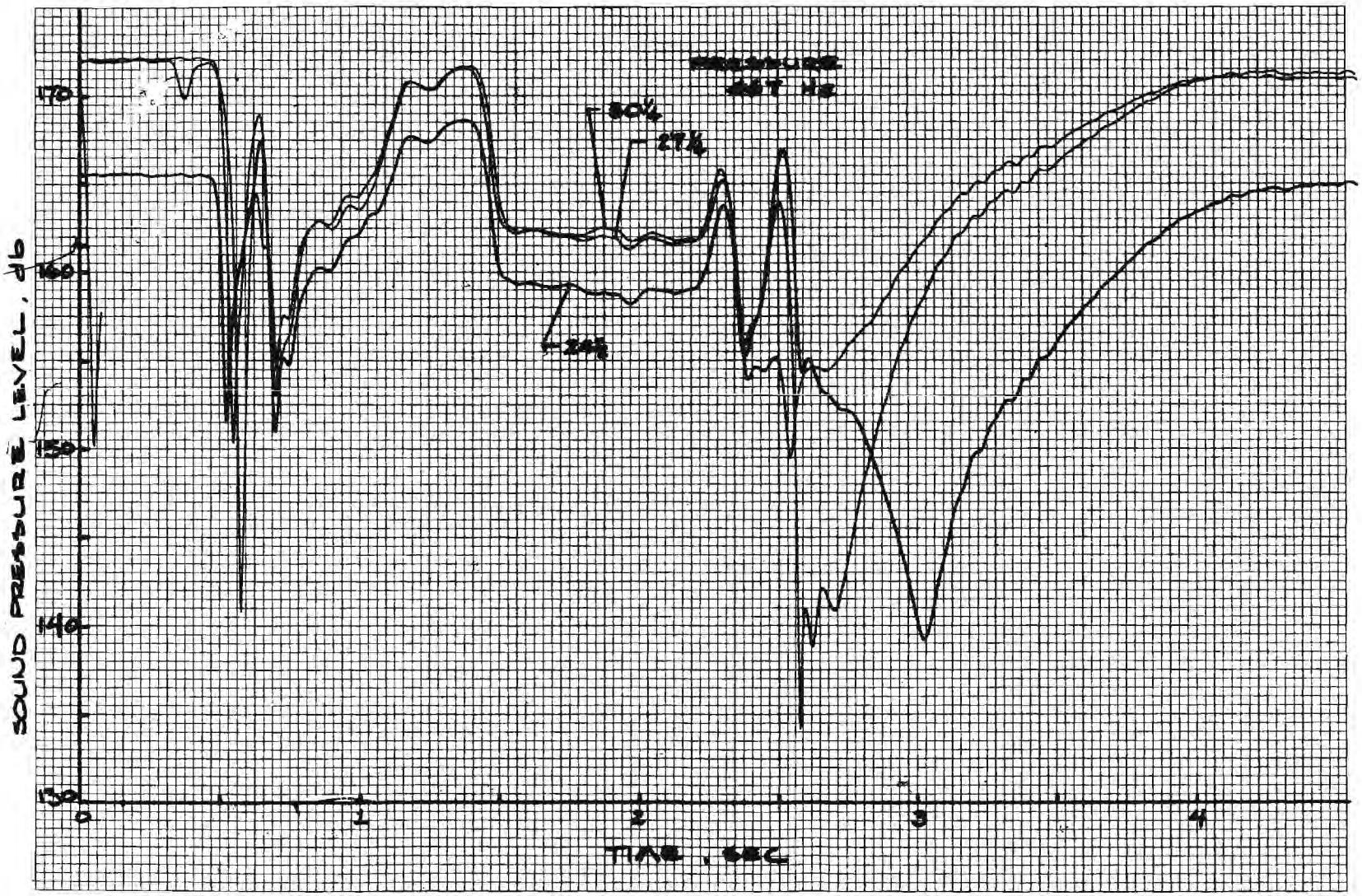

Figure 15. Variation of Pressure Amplitude with Respect to Time at Given Axial Locations.

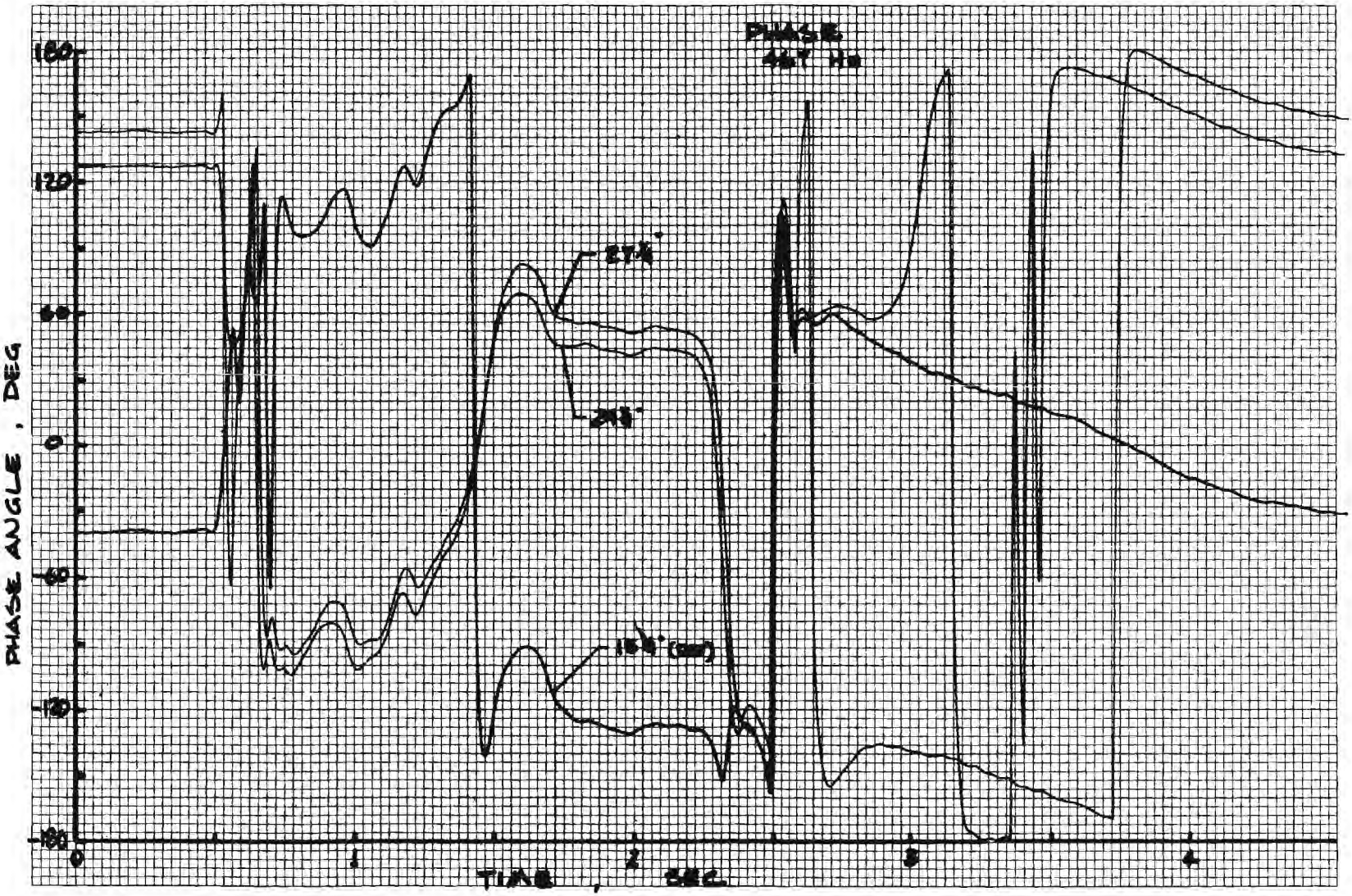

Figure 16. Variation of Pressure Phases with Respect to Time at Given Axial Locations

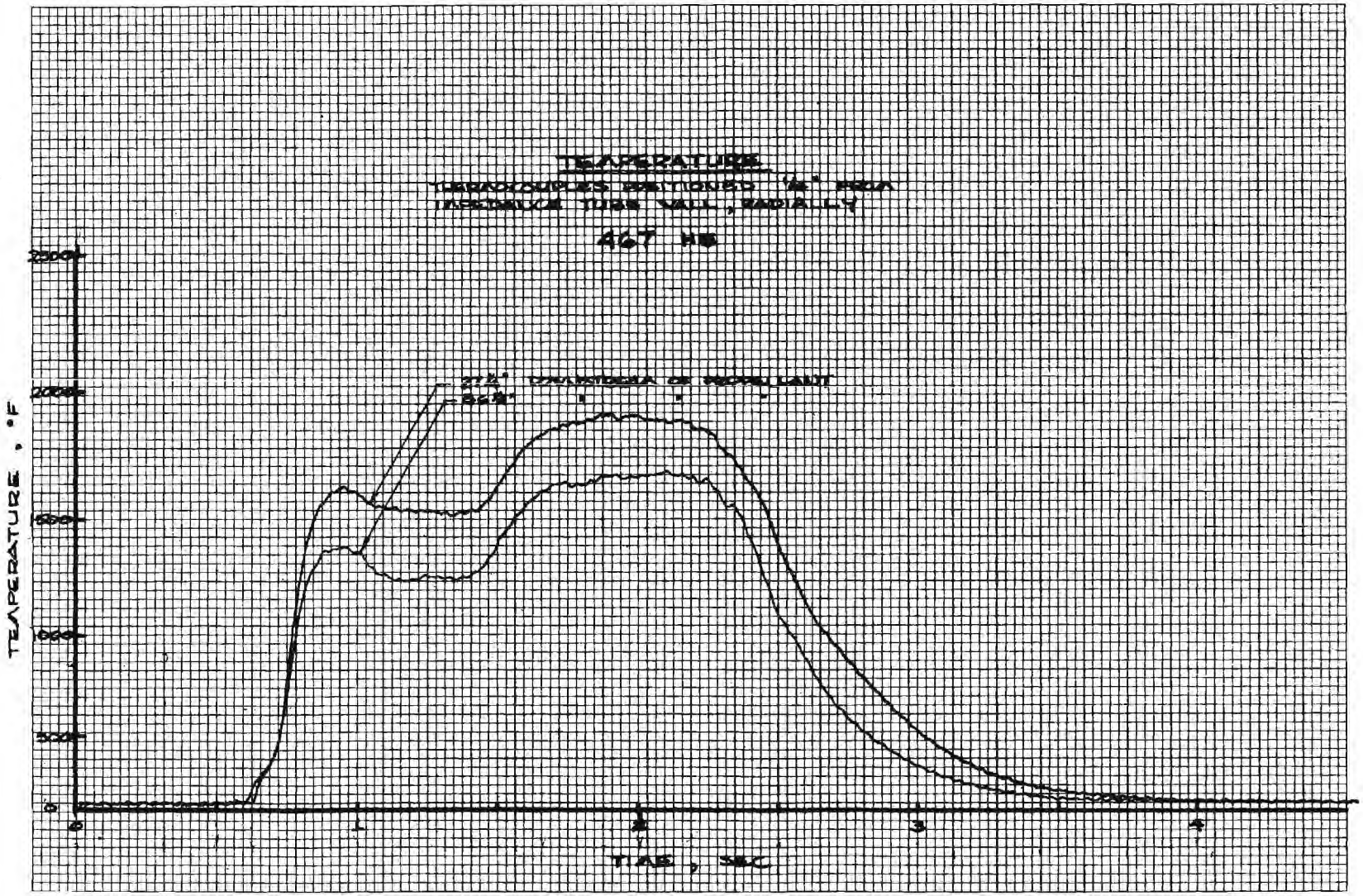

Figure 17. Variation of Mean Temperature with Respect to Time at Given Axial Locations

time of the tested samples, which is used together with the sample thickness to obtain the burning rate of the propellant. To date, the admittances of three different propellants have been investigated in more than one hundred tests. The tested propellants included a T-13 propellant, an undesignated propellant (referred to as propellant B in this report), and an A-13 propellant. To determine the mean temperature profile in the burner tube the heat transfer parameter C, introduced in Eq. (2-39), had to be determined. Using the measured experimental data and following the approach discussed in Chapter II, Section 2, the parameter C has been determined for all of the tested propellants over a wide range of frequencies at a chamber pressure of 15.7 psia. The computed values are plotted in Fig. 18 which shows that the heat transfer parameter is highly frequency dependent.

A summary of the tests run and the characteristics of the measured data are presented in Fig. 19. The table at the top of the page describes the propellants tested, the experimental steady state pressures, the frequency ranges of the various tests, and the location of the exhaust valve. As indicated in the figure, Tasks I, II and III were run with the exhaust valve at position 1, located immediately downstream of the acoustic drivers, while Task IV was run with the exhaust valve at position 2, located forty feet downstream of position 1. The tests of Task IV were conducted after the phase-distance data obtained from tests with the exhaust valve at position 1 failed to indicate wave energy addition at the propellant surface. The characteristics of the measured amplitude and phase data are presented at the bottom of Fig. 19 where it is clearly shown that the phase-distance behavior is

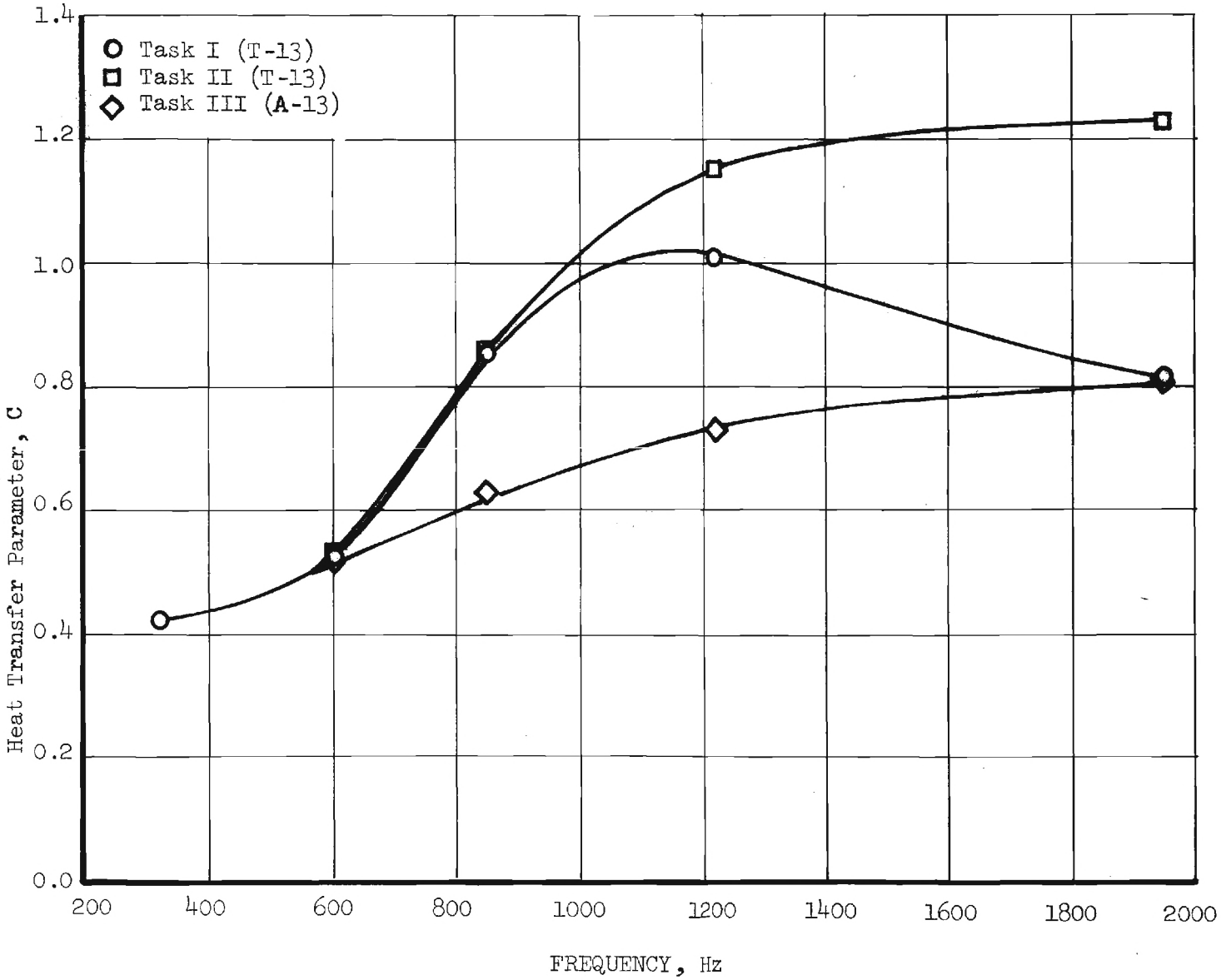

Figure 18. Frequency Dependence of Heat Transfer Parameter C.

TEST SUMMARY

TASKS	I	II	III	IV
PROPELLANT	A-13, T-13, B	T-13	A-13	A-13
PRESSURE, PSIG	1	20	20	20
FREQUENCY, HZ	318 - 1950	318 - 1225	69 - 270	69 - 270
VALVE POSITION	1	1	1	2

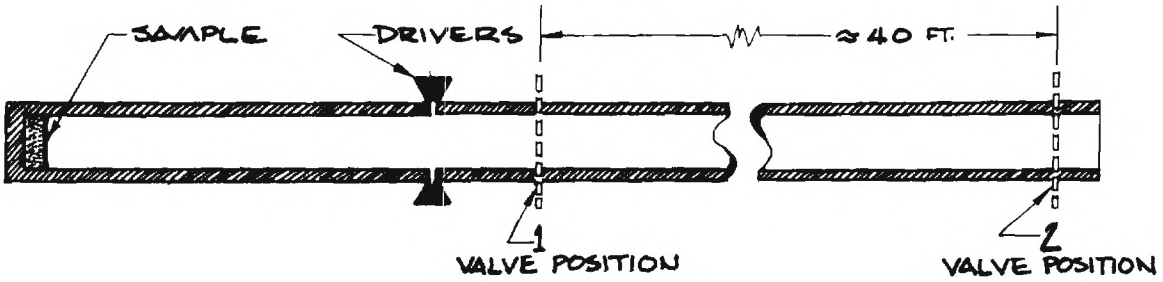

TYPICAL TEST RESULTS

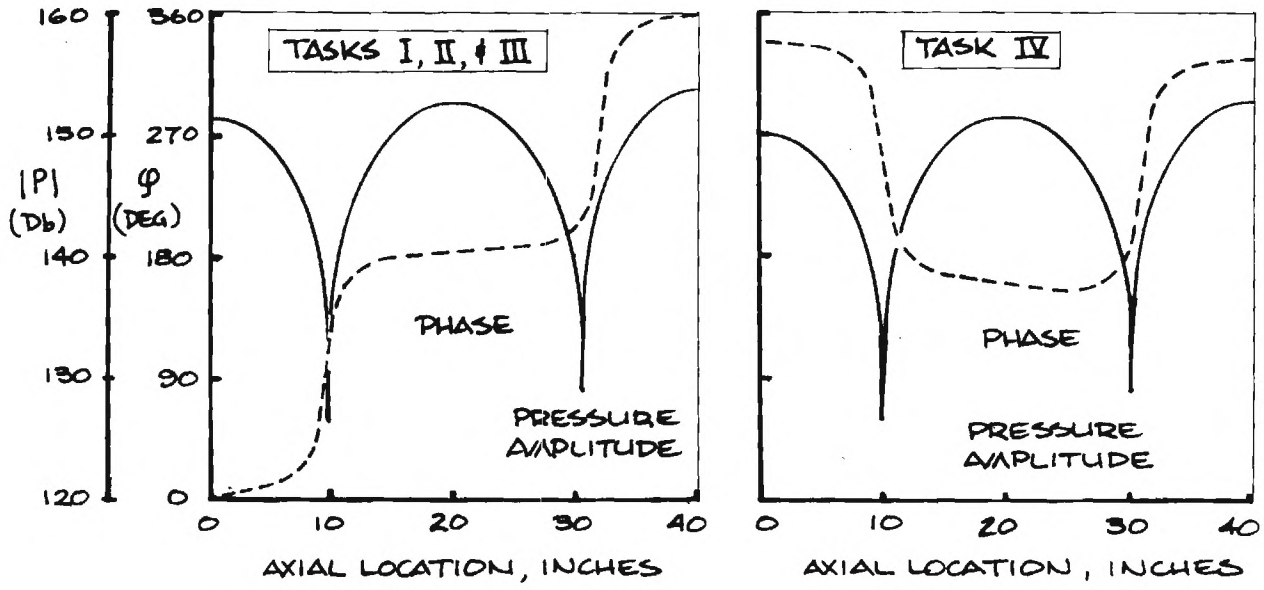

Figure 19. Test Summary and Typical Test Results.

strongly dependent upon the valve position. The phase-distance curves for Tasks I, II and III have a positive slope indicating that acoustic energy is moving from right to left along the burner tube, while the slope of the phase-distance curve for Task IV changes from negative to positive values as one moves away the propellant surface. Figure 20 presents measured amplitude and phase data obtained in experiments conducted with the A-13 propellant with the exhaust valve located in positions 1 and 2.

In the remainder of this chapter an attempt is made to explain the observed experimental trends by correlating them with the predictions of the analytical studies of the previous chapter. First, the change in the sign of the slope of the phase-distance curve is considered. A similar behavior was predicted in Chapter II, Section 6 where particle wave attenuation was considered. It was shown in that section (i.e., see Fig. 7) that for a proper combination of values of the propellant surface admittance and gas phase particle loading the above-mentioned phase-distance behavior is indeed possible. This qualitative agreement between the analytical and experimental trends suggests that the observed experimental behavior may indeed have been caused by wave attenuation in the gas phase.

Next, the change in the slope of the phase-distance curve, at the propellant surface, with change in the exhaust valve position will be considered. It was shown in Section 7 that such a change in slope may be accomplished when the boundary condition describing the propellant surface behavior is inhomogeneous; that is, when there is "self-noise" present at the propellant surface. While the presence of

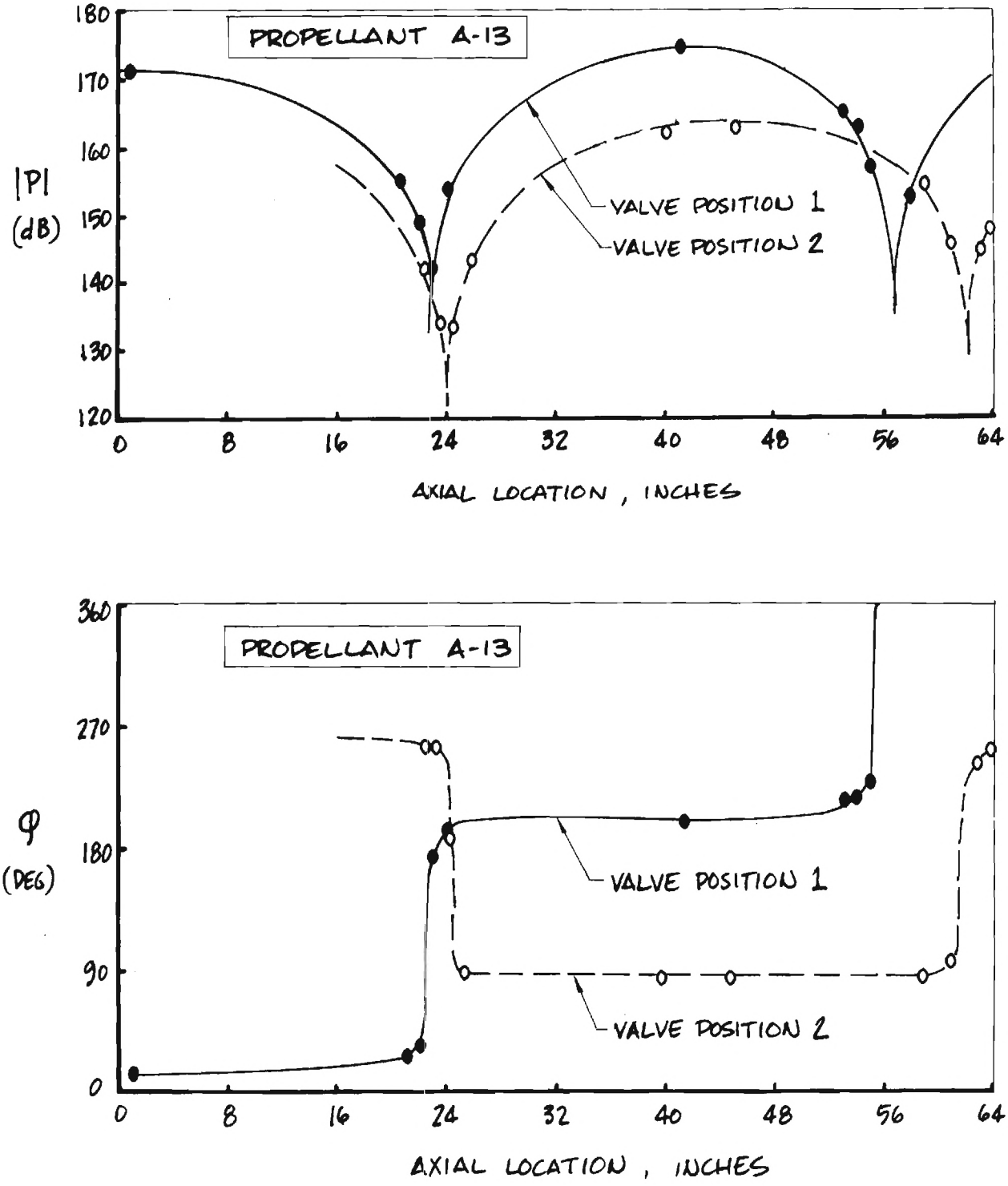

Figure 20. Effects of Valve Position on Pressure Amplitude and Phase

self-noise may offer one possible explanation to the observed experimental behavior, it still remains to be explained why and how wave energy is "absorbed" by the burning propellant when the valve is at position 1, and why and how wave energy is "supplied" by the propellant surface when the valve is at position 2.

The above explanation implies that the self-noise of the propellant may be sufficiently significant as to affect the observed experimental trends. This implication is in contrast with the results obtained in a study currently in progress[15] in which the noise generated by burning solid propellant strands is measured independently. In view of this contridiction and some of the questions raised above, a search for possible other causes for the observed experimental behavior is currently in progress.

The capability of the developed data reduction procedure to determine the admittances of burning solid propellants is demonstrated by the admittance data plotted in Fig. 21 which describes the frequency dependence of the real part of the admittance of A-13 and T-13 propellants tested with different exhaust valve positions. These admittance values were obtained from measured dynamic pressure data using the procedures outlined in Chapter II, Sections 4 and 5. Examination of the A-13 data reveals that a transition from a damping admittance to a driving admittance occurs as one moves toward lower frequencies. A similar trend has recently been observed in an independent set of T-burner tests[16] in which A-13 propellant samples have been tested under near atmospheric conditions.

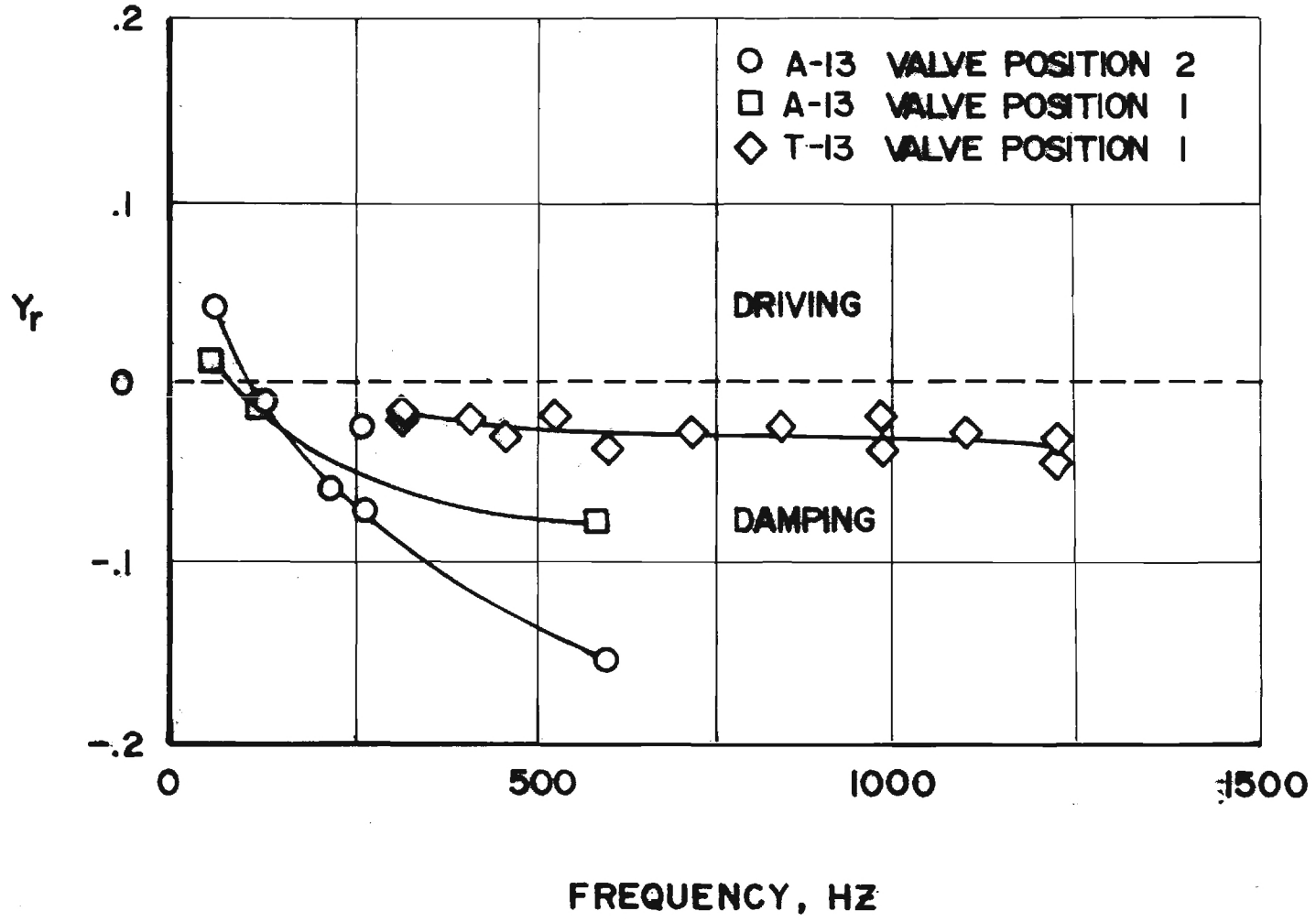

Figure 21. Frequency Dependence of Admittance of A-13 and T-13 Propellants

CHAPTER IV

SUMMARY

Efforts expanded during the second year of investigation under this program were directed toward obtaining low pressure admittance data using the driven burner apparatus. More than one hundred tests have been conducted yielding a number of unexpected results. In a parallel series of theoretical studies plausible explanations of the observed experimental data have been developed. The above-mentioned theoretical studies will continue until satisfactory resolution of all the outstanding questions is achieved.

Current experimental efforts are directed toward the development of an experimental setup in which the admittances of burning solid propellant samples at high pressures (i.e., 0-500 psig) will be measured. A schematic of this facility, which is currently under construction, is shown in Fig. 22. Based on data obtained with T-burners, there is a possibility that some of the difficulties encountered in the low pressure tests will not be repeated during high pressure testing; furthermore, the high pressure facility will enable the determination of propellant admittance data under conditions closer to those observed in actual rocket motors.

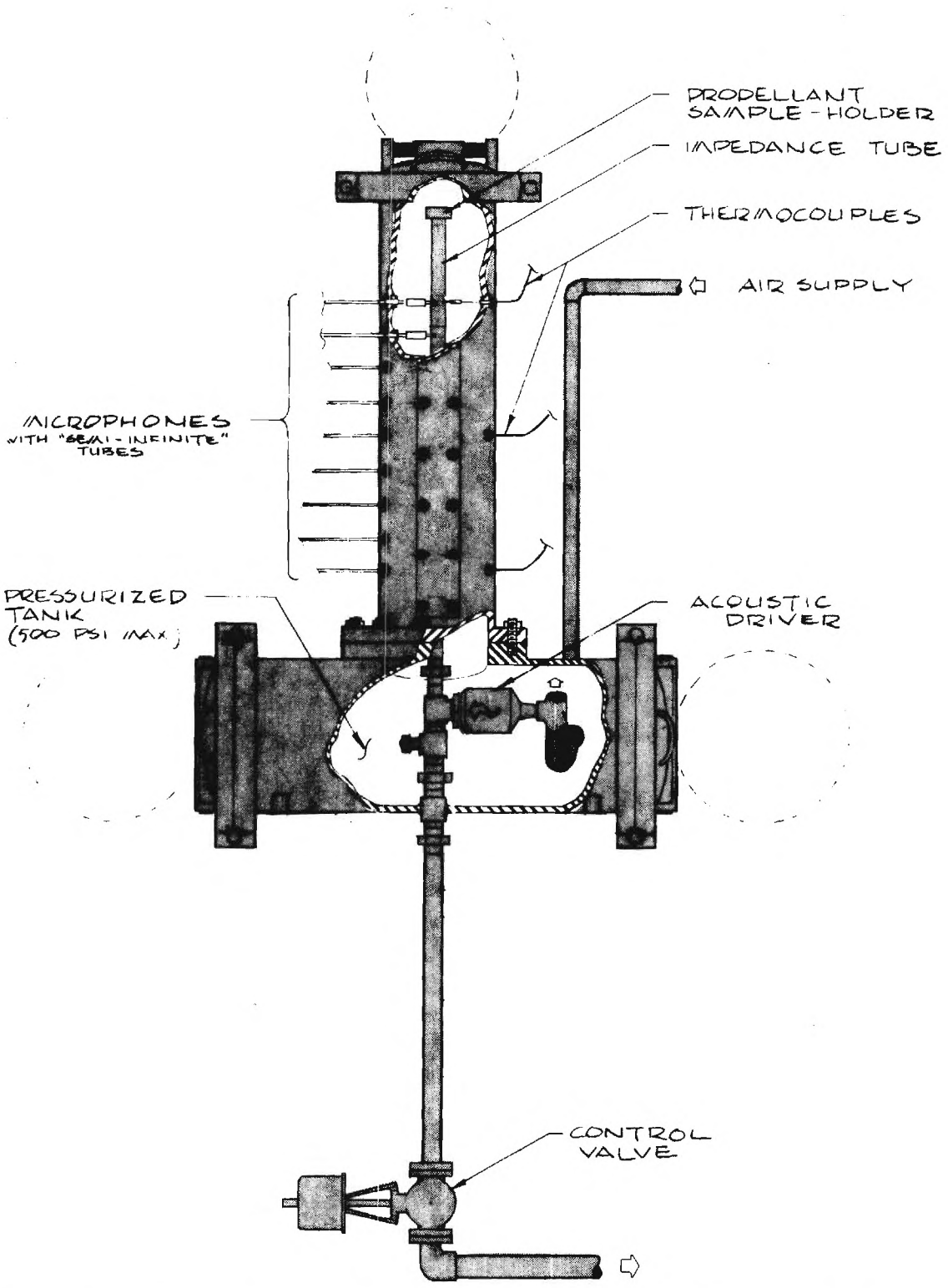

Figure 22. Schematic Diagram of Pressurized Driven Burner Facility

REFERENCES

1. Williams, F. A., Combustion Theory, Addison-Wesley Publishing Co., Inc., Palo Alto, Calif., 1965, pp. 220-226.

2. Scott, R. A., "An Apparatus for Accurate Measurement of the Acoustic Impedance of Sound Absorbing Materials," Proceedings of the Physical Society, Vol. 58, 1946, pp. 253-264.

3. Bell, W. A., Experimental Determination of Three-Dimensional Liquid Rocket Nozzle Admittances, Ph.D. Thesis, School of Aerospace Engineering, Georgia Institute of Technology, Atlanta, Georgia, July 1972.

4. Zinn, B. T., Daniel, B. R., Janardan, B. A., and Smith, A. J., Jr., "Damping of Axial Instabilities by Minuteman II, Stage III, Minuteman III, Stage III, Exhaust Nozzles," Air Force Rocket Propulsion Laboratory Interim Report, AFRPL-TR-72-71, August 1972.

5. Zinn, B. T., Daniel, B. R., Bell, W. A., and Salikuddin, M., "Solid Propellant Admittance Measurements by the Driven Tube Method," AFOSR-73-2571, August 1974.

6. Zinn, B. T., Daniel, B. R., Salikuddin, M., and Bell, W. A., "Determination of the Responses of Burning Solid Propellants by the Impedance Tube Method," AIAA Paper 75-227, presented at the AIAA 13th Aerospace Sciences Meeting, Pasadena, Calif., January 20-22, 1975.

7. Perry, E. H., "Investigations of the T-Burner and its Role in Combustion Instability Studies," Ph.D. Thesis, Daniel and Florence Guggenheim Jet Propulsion Center, California Institute of Technology, Pasadena, California, May 1970.

8. Bartz, D. R., "A Simple Equation for Rapid Estimation of Rocket Nozzle Convective Heat Transfer Coefficients," Jet Propulsion, January 1957.

9. Rubin, S., "Review of Mechanical Impedance and Transmission Matrix Concepts," J. of Acoustical Society of America, Vol. 4, No. 5, May 1967.

10. Zinn, B. T., "Determination of the Acoustic Responses of Solid Propellants by the Impedance Tube Method," A research proposal submitted to AFOSR on March 15, 1975.

11. Pfahl, Robert C., Jr. and Mitchel, Barry J., "Nonlinear Regression Methods for Simultaneous Property Measurement," AIAA Journal, Vol. 8, No. 6, June 1970.

12. Richard A. Dobbins, S. Temkin, "Measurement of Particulate Acoustic Attention," AIAA Journal, Vol. 2, No. 6, 1966.

13. Samuel Temkin, Richard A. Dobbins, "Attenuation and Dispersion of Sound by Particulate Relaxation Process," The Journal of the Acoustical Society of America, Vol. 40, No. 2, 1966.

14. Zinn, B. T., Daniel, B. R., Salikuddin, M., and Bell, W. A., "Determination of the Acoustic Responses of Solid Propellants by the Impedance Tube Method," presented at the Twelfth JANNAF Combustion Meeting, Newport, R. I., August 11-15, 1975.

15. Strahle, W. C., private communication.

16. Derr, R. L., private communications.

APPENDIX A

The analysis is carried out using a particle radius of one micron. The following values for the various properties associated with the two phase flow are used in the computation:

C_p' specific heat of the particle = 0.17 BTU/lb.^{o}F

$\bar{\rho}_p$ density of the particle = 160 lb./ft.^{3}

γ specific heat ratio of the gas = 1.28

C_p specific heat of the gas at constant pressure = 0.45 BTU/lb.^{o}F

P_r Prandtl No. = 0.8

μ coefficient of viscosity of the gas = $5.925 \times 10^{-4}(T^{o}R/6273)^{.66}$ lbm/ft. sec.

k thermal conductivity = $C_p\mu/P_r$ BTU/sec./ft.^{2}(^{o}F/ft.)

$\bar{n}$ particle density = $\nu\bar{\rho}g/\bar{\rho}_p V_p$

R gas constant = 2480 ft. lb_f/slug ^{o}R

AFOSR INTERIM SCIENTIFIC REPORT

AFOSR-TR

SOLID PROPELLANT ADMITTANCE MEASUREMENTS BY THE DRIVEN TUBE METHOD

Prepared for

Air Force Office of Scientific Research
Aerospace Sciences Directorate
Arlington, Virginia

by

B. T. Zinn
M. Salikuddin
B. R. Daniel
W. A. Bell

School of Aerospace Engineering
Georgia Institute of Technology
Atlanta, Georgia 30332

Approved for public release; distribution unlimited

Grant No. AFOSR-73-2571 August 1976

Conditions of Reproduction

Reproduction, translation, publication, use and disposal in whole or in part by or for the United States Government is permitted.

UNCLASSIFIED

SECURITY CLASSIFICATION OF THIS PAGE *(When Data Entered)*

REPORT DOCUMENTATION PAGE		READ INSTRUCTIONS BEFORE COMPLETING FORM
1. REPORT NUMBER	2. GOVT ACCESSION NO.	3. RECIPIENT'S CATALOG NUMBER
4. TITLE *(and Subtitle)* SOLID PROPELLANT ADMITTANCE MEASUREMENTS BY THE DRIVEN TUBE METHOD		5. TYPE OF REPORT & PERIOD COVERED INTERIM JUNE 1975 -JULY 1976 6. PERFORMING ORG. REPORT NUMBER
7. AUTHOR(s) B.T. ZINN M. SALIKUDDIN B. R. DANIEL W. A. BELL		8. CONTRACT OR GRANT NUMBER(s) AFOSR - 73 - 2571
9. PERFORMING ORGANIZATION NAME AND ADDRESS GEORGIA INSTITUTE OF TECHNOLOGY SCHOOL OF AEROSPACE ENGINEERING ATLANTA, GEORGIA 30332		10. PROGRAM ELEMENT, PROJECT, TASK AREA & WORK UNIT NUMBERS 681308 9711-01 61102F
11. CONTROLLING OFFICE NAME AND ADDRESS AIR FORCE OFFICE OF SCIENTIFIC RESEARCH 1400 WILSON BOULEVARD ARLINGTON, VIRGINIA 22209		12. REPORT DATE AUGUST 1976 13. NUMBER OF PAGES
14. MONITORING AGENCY NAME & ADDRESS*(if different from Controlling Office)*		15. SECURITY CLASS. *(of this report)* UNCLASSIFIED 15a. DECLASSIFICATION/DOWNGRADING SCHEDULE

16. DISTRIBUTION STATEMENT *(of this Report)*

APPROVED FOR PUBLIC RELEASE
DISTRIBUTION UNLIMITED

17. DISTRIBUTION STATEMENT *(of the abstract entered in Block 20, if different from Report)*

18. SUPPLEMENTARY NOTES

19. KEY WORDS *(Continue on reverse side if necessary and identify by block number)*

COMBUSTION INSTABILITY
SOLID PROPELLANT RESPONSE FUNCTIONS
SOLID PROPELLANT ROCKETS
IMPEDANCE TUBE MEASUREMENTS

20. ABSTRACT *(Continue on reverse side if necessary and identify by block number)*

The progress made during the third year of an investigation to measure the response of a burning solid propellant to oscillatory flow conditions is presented. In this study a modification of the impedance tube technique is used to measure the response over a wide range of frequencies. Improvements in the data reduction program are discussed. These include a more accurate method of computing the temperature distribution in the burner tube and a technique for determining the response from pressure amplitude measurements only. A high-pressure facility and minicomputer-based data acquisition system are also discussed in the report.

DD FORM 1 JAN 73 1473 EDITION OF 1 NOV 65 IS OBSOLETE

SECURITY CLASSIFICATION OF THIS PAGE *(When Data Entered)*

Data taken at 300 psig indicate that the combustion process of the solid propellant periodically drives and damps acoustic oscillations under most of the test conditions encountered.

ABSTRACT

The progress made during the third year of an investigation to measure the response of a burning solid propellant to oscillatory flow conditions is presented. In this study a modification of the impedance tube technique is used to measure the response over a wide range of frequencies. Improvements in the data reduction program are discussed. These include a more accurate method of computing the temperature distribution in the burner tube and a technique for determining the response from pressure amplitude measurements only. A high-pressure facility and minicomputer-based data acquisition system are also discussed in the report. Data taken at 300 psig indicate that the combustion process of the solid propellant periodically drives and damps acoustic oscillations under most of the test conditions encountered.

TABLE OF CONTENTS

NOMENCLATURE

Symbols

i	imaginary unit, $\sqrt{-1}$
n	temperature exponent of viscosity law, see Eq. (2)
p	pressure, lbf./ft.^{2}
T	temperature, degrees Rankine
u	axial velocity, ft./sec.
x	axial distance, ft.
Λ	heat transfer parameter
ρ	density, slug/ft.^{3}

Superscripts

$(\bar{\ })$	variable describing steady state conditions
$(\ )'$	a perturbation quantity

Subscripts

$(\ )_c$	quantity evaluated at the propellant surface
$(\ )_r$	real part of a complex quantity
$(\ )_i$	imaginary part of a complex quantity
$(\ )_w$	quantity evaluated at the wall

LIST OF FIGURES

LIST OF TABLES

I. INTRODUCTION

This report summarizes the work done during the third year of research supported by Air Force Grant No. AFOSR-73-2571, initiated July 1, 1973. This grant is concerned with the measurement of the acoustic responses of solid propellants by the impedance tube method.

The acoustic response is an important parameter in the study of combustion instability in solid propellant rockets. Combustion instability is characterized by high amplitude pressure oscillations which are driven by the combustion process. These high amplitude pressure oscillations can cause large variations in the thrust with time; can interfere with delicate control and guidance systems; and, in extreme cases, can lead to structural failures. The acoustic response is a measure of the capability of a specific burning solid propellant to initiate and sustain combustion instability in a given solid propellant rocket motor.

To analyze the stability of a particular motor, it is necessary to determine the response (or reaction) of the combustion process to the various disturbances (e.g., pressure fluctuations associated with turbulence or combustion noise) inside the combustion chamber. The amplification or decay of these fluctuations will depend upon the phase relationship between the pressure oscillations and the induced combustion oscillations.[1] If the response time of the combustion process to the combustion pressure oscillation is such that an increase in burn rate occurs during a pressure condensation, then a condition supporting an increase in the amplitude of the pressure oscillation

may result, possibly leading to an unstable engine operation. The question whether instability will occur also depends upon the "losses" in disturbance energy that are present in the combustor. On the other hand, if the burn rate increase occurs during a pressure rarefaction, a condition leading to destructive interference will result and the disturbance will be damped.

The combustion response can be related to the admittance of the burning surface which, in turn, can be used to evaluate the effect of the burning propellant upon the stability of the solid rocket under consideration. Defined as the ratio of the normal velocity perturbation to the pressure perturbation at the burning propellant surface; a positive admittance indicates that the normal velocity and pressure oscillations are in phase and a situation leading to disturbance amplification may result. Negative admittance values indicate that the normal velocity and pressure perturbations are out of phase and damping of the disturbance at the burning propellant occurs. Once determined, the admittance can be used as a boundary condition in combustion instability analysis to predict the stability of a given engine configuration.

The most widely used method for measurement of the admittance is the T-burner. However, several difficulties with this method have been encountered and are discussed in Ref. 2. The present study is concerned with the development of an impedance tube method for measuring the admittances of burning solid propellants.[3] This technique, described in Ref. 2, is known to yield accurate results in studies associated with sound absorbing materials[4] and has been

successfully used in the study of the damping provided by typical solid rocket nozzle configurations.[5]

In this report progress during the past year is discussed and improvements in the supporting theory of the impedance tube technique are presented. These include a more accurate method for determining the steady-state temperature profile in the tube and a method for computing the admittance from pressure amplitude measurements only. In addition, the development of a high pressure facility capable of measuring admittances at pressures up to 500 psig is described. The computerized data acquisition facility which became operational this past year is also discussed and preliminary admittance results at 300 psig are presented.

II. ANALYTICAL INVESTIGATIONS

The equations describing the behavior of the standing wave pattern inside a driven burner tube are discussed in detail in Ref. 3. Also presented are the techniques used to obtain the admittance of a burning solid propellant from experimentally measured pressure amplitude and phase data taken at discrete points along the standing wave. To further improve the accuracy of the computed admittance values, additional refinements have been incorporated in the data reduction methods during the reporting period, and these are described in this section.

A. Determination of the Steady State Temperature Profile

In Ref. 3 a method for determining the steady state temperature distribution in the driven burner tube is presented. From this temperature distribution the variation in wavelength along the axis of the tube can be determined and accounted for in the admittance computations. The equation for the temperature distribution is obtained from the steady state energy equation in the tube[3,6] and is given by the expression

$$\bar{T} = T_w + (T_c - T_w)\, e^{-x/\Lambda} \tag{1}$$

where

$$\Lambda = C \left(1 + \frac{T_w}{\bar{T}}\right)^n ; \quad n = 0.68 \tag{2}$$

T_w = temperature at the wall of the tube

T_c = chamber temperature

Since T_w and T_c are known from experimental measurement, the constant C is the only parameter to be resolved in order to determine the temperature distribution in the tube. As shown in Ref. 3, this

constant can be found by measuring the distance between two successive pressure minima along the standing wave pattern. The accuracy of the value of C depends upon how accurately the positions of the pressure minima can be determined. In the past these positions were determined from pressure amplitude data measured by transducers placed at various locations along the walls of the burner tube. Since the locations of the transducers in general did not coincide with the locations of any of the standing wave minima, these minimum positions were obtained by extrapolation of the measured data - a process which inevitably results in errors in locating these standing wave minima. Hence, a search for a method for the determination of the steady state temperature distribution in the tube was undertaken during this reporting period.

An alternate technique which decreases the inaccuracies involved in locating the pressure minima has recently been developed. This method employs the nonlinear regression technique to determine the constant C from the measured amplitude and phase data. The nonlinear regression technique involves determining the value of C which provides the best fit between the theoretically predicted wave pattern in the burner tube and the experimentally measured pressure amplitude and phase data. The best fit is found by determining the value of C which minimizes the root-mean-square deviation between the theoretically predicted burner tube wave structure and the corresponding experimental data. This technique gives a temperature profile which is consistent with the measured wave structure.

To find the minimum root-mean-square deviation, the following function F, which is a measure of the error, is minimized;

$$F = \sum_{i=1}^{n} (E_i - T_i)^2 \qquad (3)$$

In Eq. (3), E_i represents an experimentally measured quantity (i.e., amplitude or phase) at location i and T_i is the corresponding theoretically predicted quantity which depends among other things, upon the constant C. If a minimum of F exists with respect to C then the gradient of F must vanish at that minimum and the following relationship holds:

$$\frac{dF}{dC} = -2 \sum_{i=1}^{n} \left[(E_i - T_i) \frac{dT_i}{dC} \right] = 0 \tag{4}$$

A Newton-Raphson iterative scheme is used to obtain a solution of Eq. (4) utilizing a linearized version of this equation which involves the expansion of T_i in a first order Taylor series with respect to the parameter C.[3] The resulting linear algebraic equation can be expressed in the following form:

$$\sum_{i=1}^{n} \left(E_i - T_i^m \right) \left. \frac{dT}{dC} \right|_{(i,m)} = \left[\left(C^{m+1} - C^m \right) \sum_{i=1}^{n} \left(\frac{dT}{dC} \right)^2_{(i,m)} \right] \tag{5}$$

where m represents the m^{th} iteration.

Equation 5 can be rewritten as follows:

$$A^m \left[C^{m+1} - C^m \right] = B^m$$

$$C^{m+1} = C^m + B^m / A^m \tag{6}$$

where

$$A^m = \sum_{i=1}^{n} \left(\frac{dT}{dC} \right)^2_{(i,m)} \tag{7}$$

and

$$B^m = \sum_{i=1}^{n} \left(E_i - T_i^m \right) \left. \frac{dT}{dC} \right|_{(i,m)}$$

Equation (7) is a linear algebraic equation for the unknown C^{m+1} and it can be readily solved once A^m and B^m are computed. The computation of these elements requires the determination of the derivative $\frac{dT}{dc}_{(i,m)}$. Since these derivatives cannot be determined analytically, numerical values for these derivatives are obtained using finite difference methods.

B. Computational Scheme to Minimize the Error:

As discussed in Reference 3, the non-linear regression is used to find the values of the velocity wave u_o', pressure wave p_o' and density ρ_o' at the propellant surface which give the best fit between the theoretically predicted acoustic pressure distribution and the corresponding experimentally measured acoustic pressures. These values are then used to determine the propellant admittance and response factor. In the last section it has been shown that a similar non-linear regression technique can be used to obtain the constant C which, in turn, is used to compute the steady state temperature distribution that is consistent with the measured acoustic pressure data. Since these two non-linear regression operations are coupled, they must be solved together to obtain the propellant admittance and response factor data. The manner in which this is being done is briefly explained as follows:

(1) Initially, an arbitrary value of C is chosen, and, using the "Transmission Matrix" scheme[3], a set of "initial" values for u_o', p_o' and ρ_o' at the propellant surface is computed.

(2) The non-linear regression scheme is used to obtain the values of u_o', p_o' and ρ_o' which minimize the root-mean-square deviation between the theoretical equations and the experimental values for the

chosen value of C.

(3) Once these are determined, the value of C is recomputed using the determined "optimum" values of u_o' , p_o' and ρ_o' obtained earlier. Steps (2) and (3) are repeated until the variations in the values of u_o' , p_o' , ρ_o' , and C fall within a specified tolerance.

To check the accuracy of this data reduction scheme, computations were performed for a number of hypothetical cases for which the exact values of C, u_o' , p_o' and ρ_o' were assumed to be known. Using these values as initial conditions, the burner tube equations were solved to determine the "exact" wave structure in the hypothetical burner tube; the latter is plotted (for a specific case) as a solid line in Fig. 1. Next, the points denoted by "x" on Fig. 1 were assumed to be measured pressure data that deviated from the exact data due to experimental errors. This data was then input into the data reduction programs in an effort to determine the error in the admittance computation resulting from experimental inaccuracies. An arbitrary initial value for C was chosen and the computational scheme discussed earlier was used to compute the wave structure and the desired value of C. The computed wave structure is represented by the dashed line in Fig. 1 and the table below provides a comparison between the "exact" and computed values of p_o' , u_o' , ρ_o' and C

TABLE I. The Effect of Assumed Experimental Errors on C

Heat Transfer Parameter C	Pressure p_o'		Velocity u_o'		Density ρ_o'	
	Amplitude in db	Phase in Deg.	Amplitude Ft/Sec	Phase in Deg.	Amplitude Slug/ft^3	Phase in Deg.
0.943	145.4	230.2	1.48	-21.4	$.612 \times 10^{-6}$	229.0
0.972	145.8	229.9	1.30	-18.2	$.647 \times 10^{-6}$	228.7
2.0						

orrect
alues

mputed
alues

essed

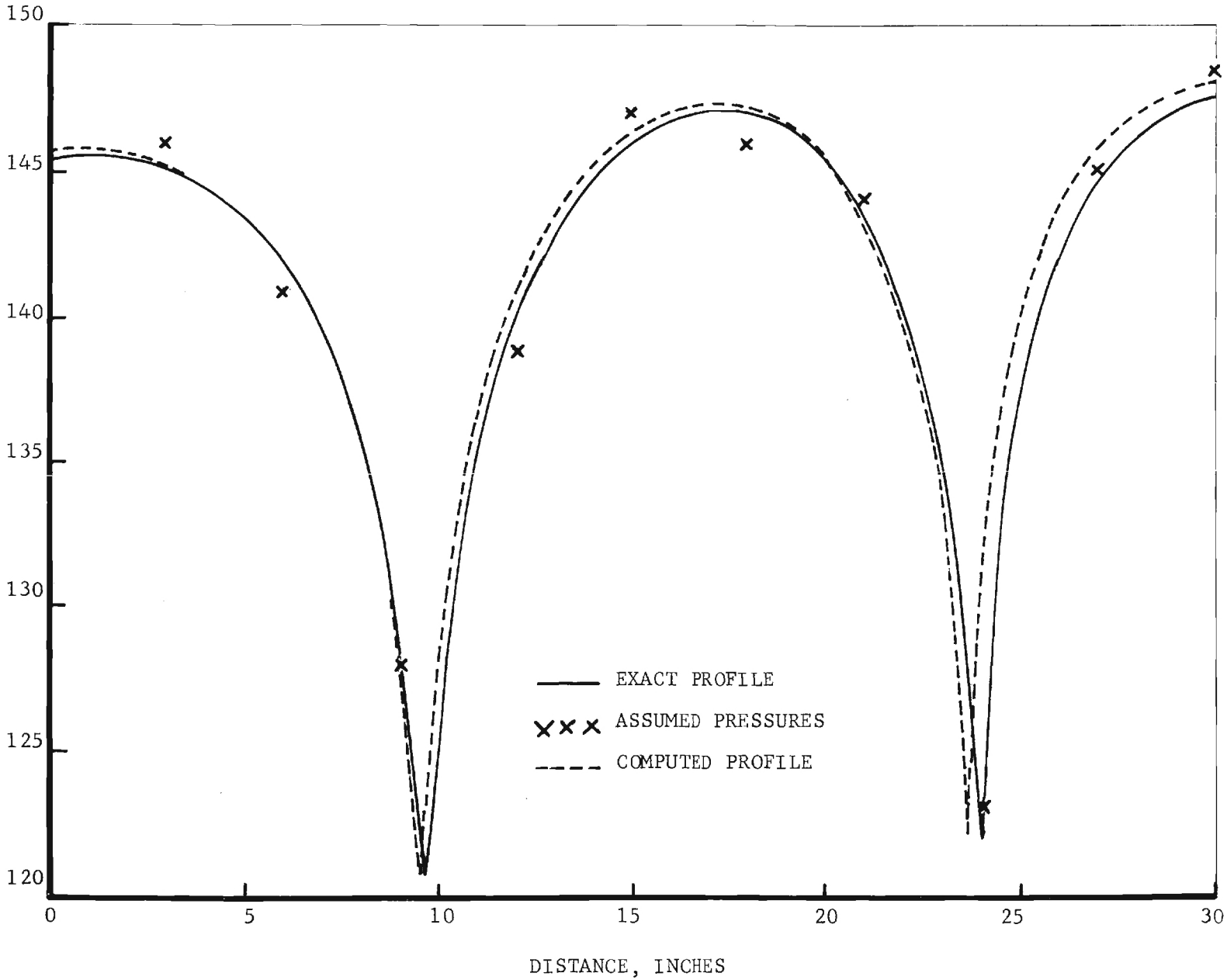

Figure 1. Comparison of an Exact Standing Wave Profile and a Computed Profile with Assumed Experimental Errors.

Examination of the data shown in Table I indicates good agreement between the assumed and computed values of u_o' , p_o' , ρ_o' and C even when small experimental errors are present. This good agreement provides further confirmation that the data reduction program is working satisfactorily.

C. Error Minimization by Application of a Regression Technique Using Pressure Amplitudes Only

Before incorporation of the computerized data acquisition system into the test procedure, it was found that the magnitude of the errors in the measured phases at low amplitudes near the pressure minima were unacceptable. This necessitated the development of a scheme to obtain values of u_o' , p_o' and ρ_o' at the propellant surface using pressure amplitude data, which could be measured within acceptable tolerance near the pressure minima.

In this scheme, the starting values of u_o' , p_o' and ρ_o' are computed as before[3] using the transmission matrix technique. However, in this case, the non-linear regression is performed using only pressure amplitude data. In the earlier scheme[3] the derivatives of both the real part and imaginary parts of the complex pressure are obtained with respect to the real and imaginary values of u_o' , p_o' and ρ_o'. In the modified scheme these derivatives are used to obtain the derivative of pressure amplitude with respect to the real and imaginary values of u_o' , p_o' and ρ_o'. Representing the real and imaginary parts of u_o' , p_o' and ρ_o' by Z_i, i = 1,2, ---,6 the derivatives of pressure amplitude p_a' are given by

$$\frac{\partial p_a'}{\partial Z_i} = \frac{\partial \sqrt{(p_R'^2 + p_I'^2)}}{\partial Z_i} = \frac{1}{p_a'} \left(p_R \frac{\partial p_R'}{\partial Z_i} + p_I \frac{\partial p_I'}{\partial Z_i} \right) \quad (8)$$

where p'_R and p'_I represent the real and imaginary parts of the oscillatory pressure. Once these derivatives are computed the non-linear regression can be used to minimize the error between theoretically computed and the experimentally measured pressure amplitudes. The development of this modified scheme has been completed and it is currently available for data reduction.

III. EXPERIMENTAL APPARATUS

A. High Pressure Experimental Facility

Previous experiments using the driven burner tube to measure the admittance of burning solid propellants have been limited to chamber pressures less than 50 psig because a suitable acoustic driver capable of higher operating pressures was not available. In addition, pressure transducers capable of withstanding pressures of up to 500 psig and having the desired resolution (i.e. 0.01 psi to 3 psi) were not available.

Recently, however, a high pressure facility designed for operating pressures up to 500 psig has been developed. This facility is capable of determining the admittances of burning solid propellant samples under test conditions simulating actual rocket motor operating conditions. A photograph of the high pressure driven burner facility is shown in Fig. 2 and a corresponding schematic is shown in Fig. 3. The driven burner tube with the propellant sample-holder, the pressure transducer, and the acoustic driver are all contained within the 0 to 500 psig pressurization tank which is equipped with high pressure hinged ports to allow easy access for propellant sample changes, burner tube removal, and maintenance.

Air supply for tank pressurization and the flow requirements of the electropneumatic driver is provided by a 3000 psig, 500 cu.ft.

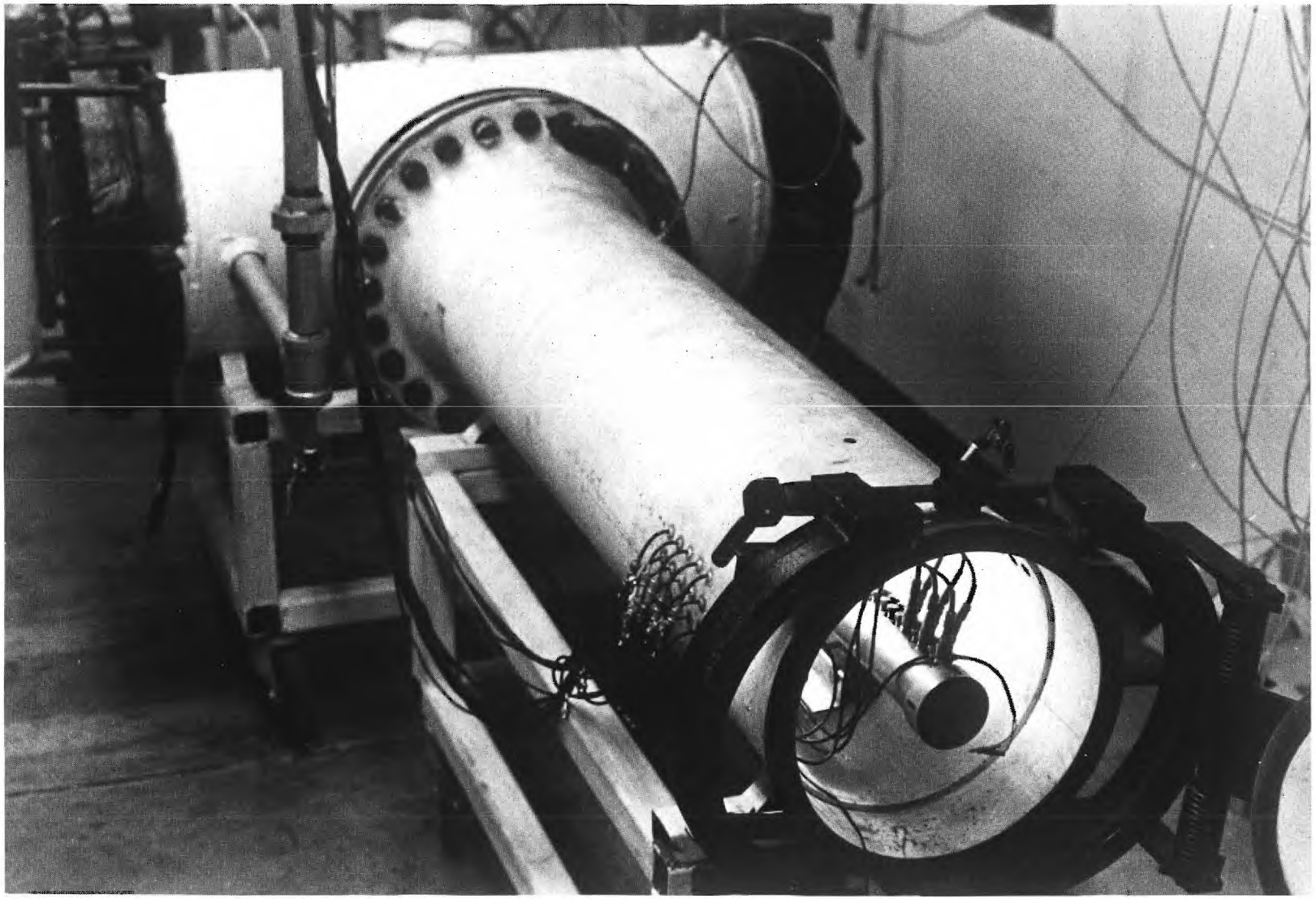

Figure 2. Photograph of Pressurized Driven Burner Facility.

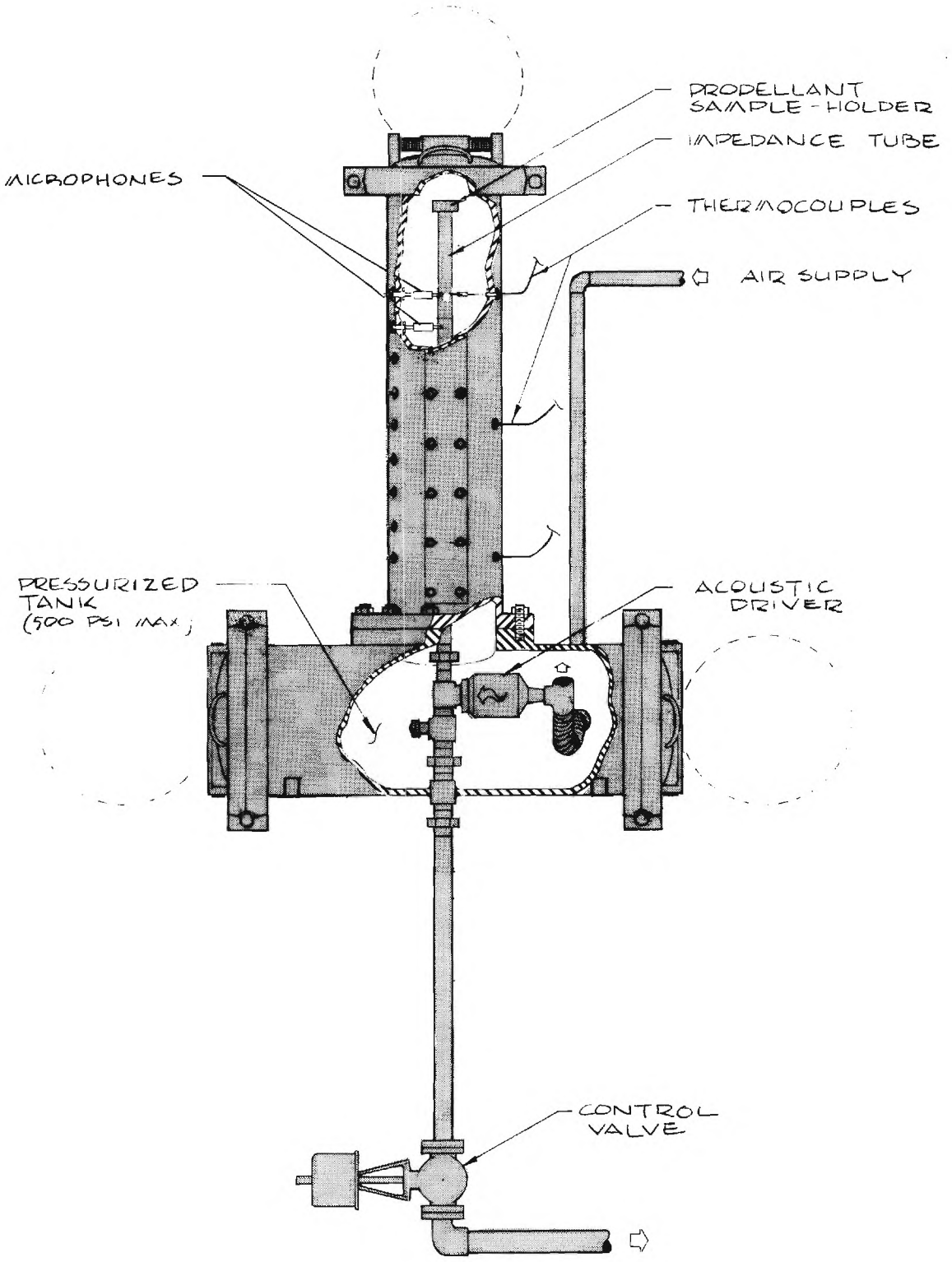

Figure 3. Schematic Diagram of Pressurized Driven Burner Facility.

blow down facility. The tank pressure and driver airflow are maintained by a pressure control valve in the exhaust line of the system as shown in the schematic of the flow system in Fig. 4.

The components of the high pressure driven burner tube facility and the principles of its operation are basically unchanged from the low pressure facility previously in operation. The impedance tube contained in the high pressure tank was fabricated from a stainless steel pipe with a two inch inside diameter. Provisions for a propellant sample holder are included on one end and an acoustic driver capable of developing 4,000 watts of acoustic power is close-coupled to the tube on the other end. Provisions for instrumentation (pressure and/or temperature measurements) have been included along six feet of the tube wall. The instrumentation locations are one-half inch apart measured from the face of the propellant sample. A sketch of the driven burner tube and details of the propellant sample holder are presented in Figs. 5 and 6 respectively. During a test, the propellant sample is ignited by a nichrome wire glued to the sample surface in an "S" shape. A photograph of a propellant sample in a sample holder with the nichrome wire glued in place is shown in Fig. 7. To assure a rapid and uniform ignition of the propellant, the surface of the sample is coated with a thin pyrotechnic mixture comprised of 72.4% potassium perchlorate,14.8% titanium, 6.9% Boron powder, and 6.0% polyisobutylene binder dissolved in toluene. For ignition the nichrome wire is heated by a 40 volt, 15 ampere power supply. Measuring the standing wave pattern in the driven burner tube with a burning solid propellant sample imposes stringent requirements on the instrumentation. The pressure

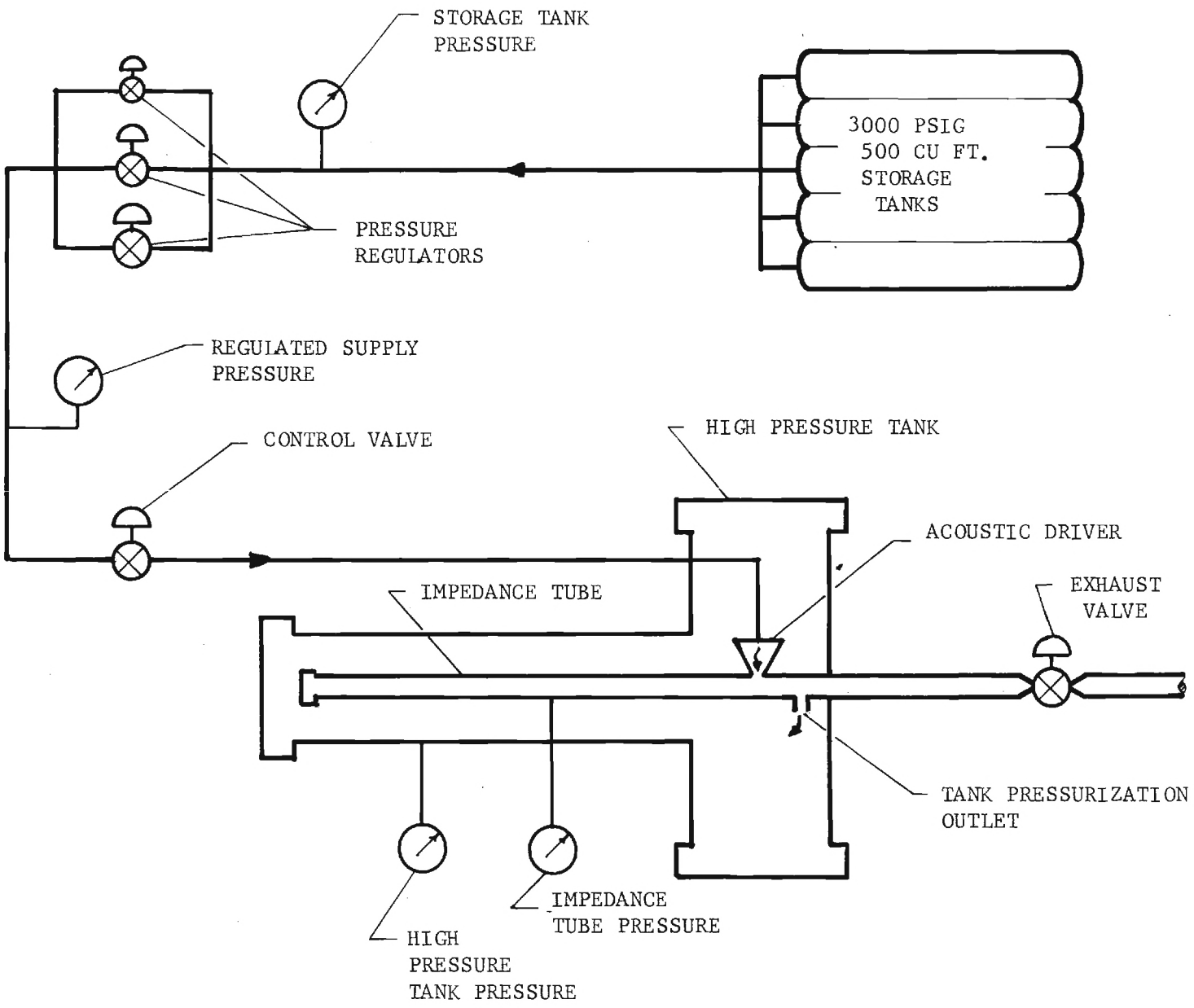

Figure 4. Schematic of Facility Flow System

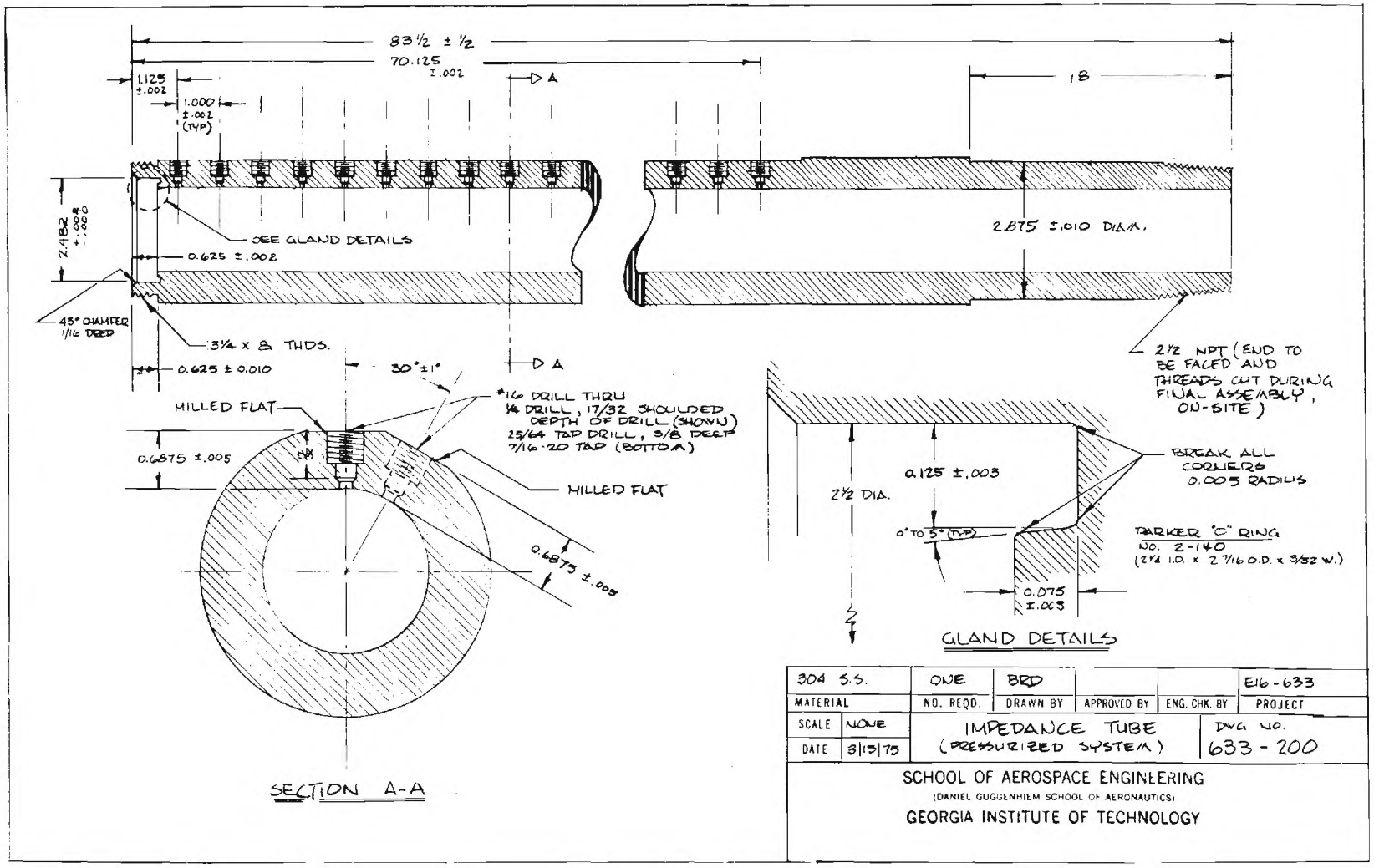

Figure 5. Driven Burner Tube Details

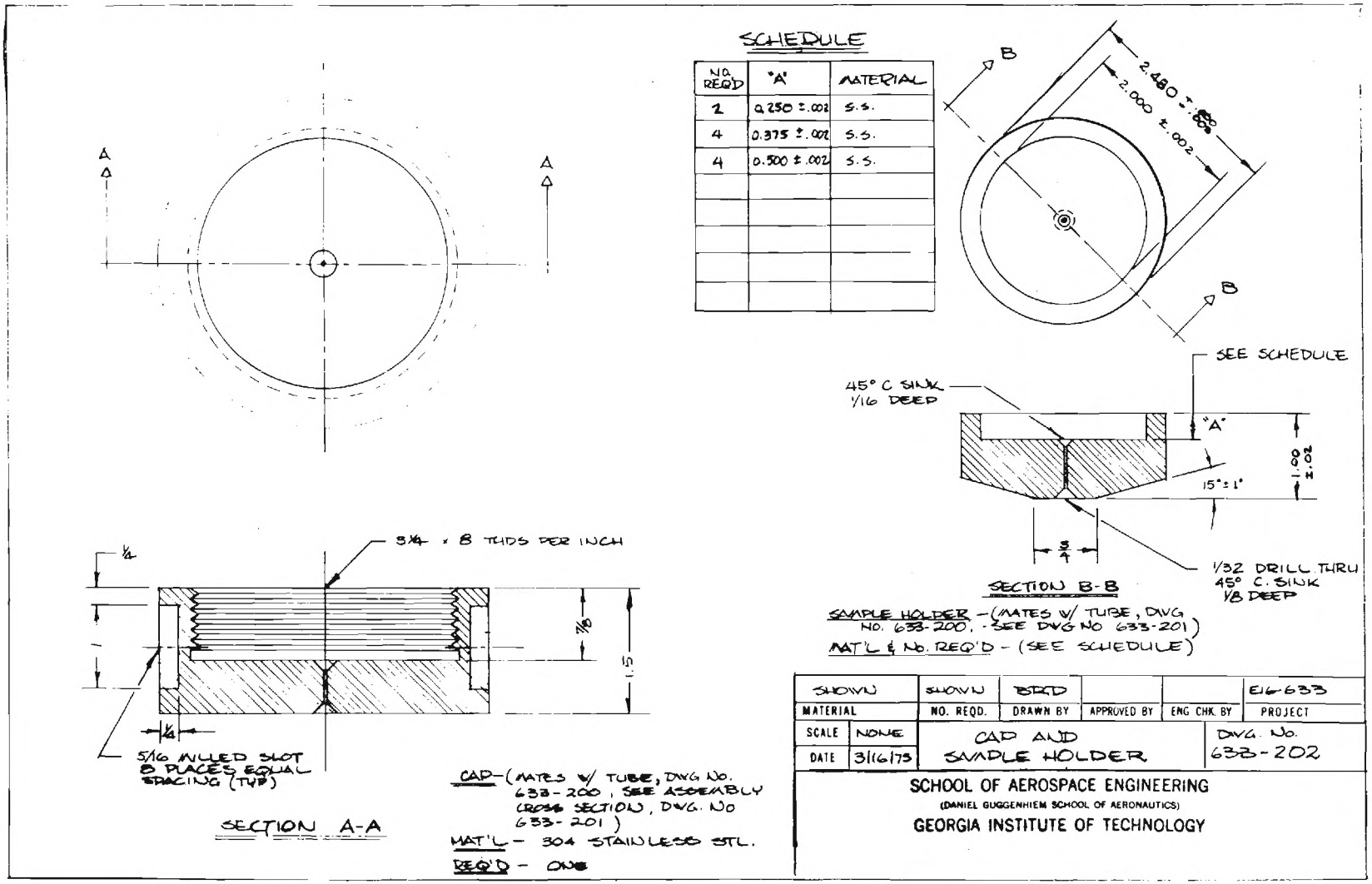

Figure 6. Propellant Sample Holder Details

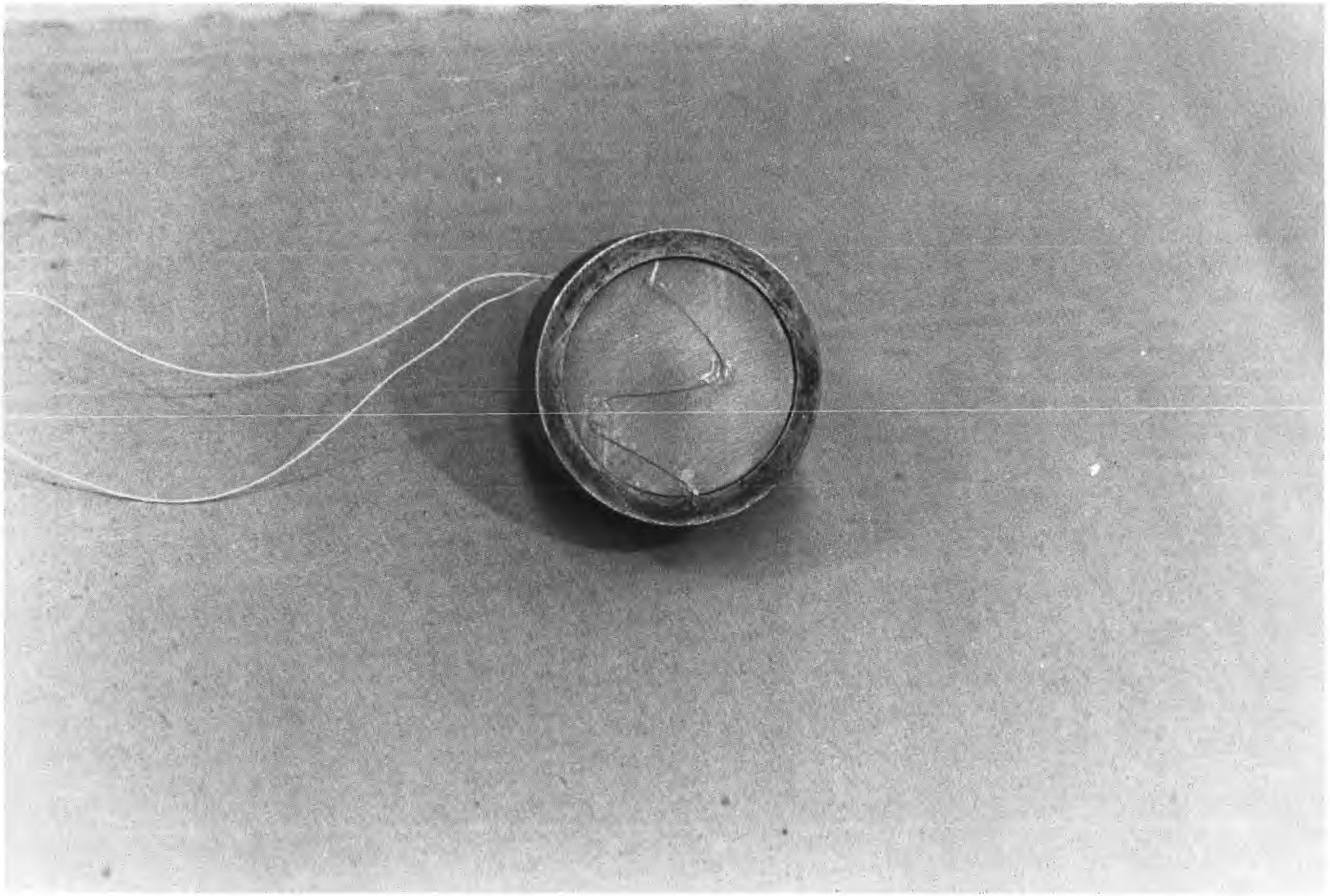

Figure 7. Sample Holder with Ignition Wire.

measurement at high temperatures poses the problem of protecting the highly sensitive transducer diaphragms from the hot gases in the tube. Various methods for the protection of the transducers have been investigated. The semi-infinite tube technique described in Ref. 2 has proven unsatisfactory for high pressure operation because of low frequency resonance in the infinite tube at high pressures. A sketch of an alternate pressure transducer installation utilizing a short adaption is presented in Fig. 8. This adaption has a 3/16-inch inside diameter and it measures 5/8-inch from the transducer face to the inside of the tube wall. Further protection for the transducer is provided by a thin coating of clear silicone grease applied to the transducer diaphragm. Extensive calibration and testing of this short transducer adaptor has been conducted and the results indicate that in the frequency range of interest for this experiment, (i.e., 300 Hz to 1100 Hz), the adapter provides highly satisfactory pressure amplitude and phase measurement characteristics. A detailed discussion with empirical data and design criteria for short probes to be used for dynamic measurements is outlined in Refs. 7 and 8.

The acoustic driver used in the high pressure driven burner tube is a Ling ETP-94 B electropneumatic driver capable of developing 4,000 watts of acoustic power which provides a sound pressure level of 170 decibels in the burner tubes. The driver is close-coupled to the tube wall at the downstream end of the burner tube. The frequency and waveform output of the acoustic driver is controlled by a Spectral Dynamics Oscillator, Model SD104A-5. For this investigation, the waveforms of the pressure oscillations are sinusoidal and the frequency of the oscillations are constant during a given test.

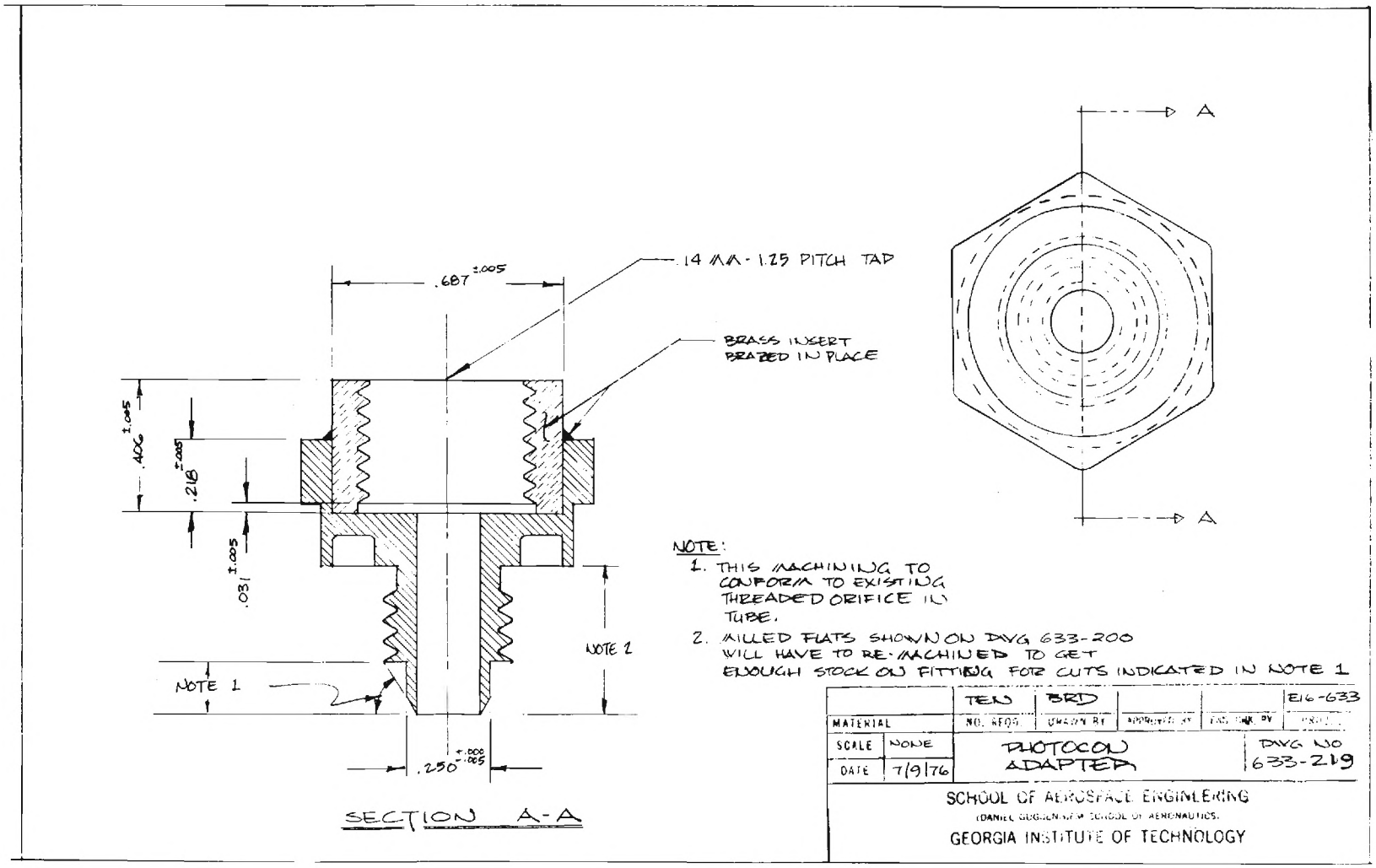

Figure 8. Sketch of Short Probe Pressure Transducer Adapter

B. Test Procedures.

The data acquisition system and the equipment to establish and monitor test conditions are located in a laboratory area adjacent to the room housing the high pressure driven burner tube experiment. A photograph of the control area for the experiment is presented in Fig. 9. Test conditions are established by slowly pressurizing the high pressure tank housing and the burner tube to the desired operating pressure. The pressurization tank pressure and driver airflow requirements are maintained by the tank pressurization control valve in the exhaust line. With tank pressure stabilized and a standing waveform of a desired frequency established a test run is initiated. The data acquisition period of a test run includes four phases; a brief pre-ignition test period with the acoustic drivers on and test conditions established in the burner tube, ignition of the propellant sample, the propellant "quasi-steady" burning period and the propellant extinguishment phase. The data acquisition period is normally about two and one-half seconds. A more detailed discussion of the data acquisition and data reduction procedures are presented in the following section.

C. Minicomputer-Based Data Acquisition System

During the reporting period a minicomputer-based data acquisition system was incorporated in the program to obtain improved pressure and temperature data. This system processes the data in three stages. First, during a test the analog signals from the transducer and thermocouple channels are sampled, digitized, and stored at a controlled rate. Next, the stored readings are processed by the computer. The transducer data

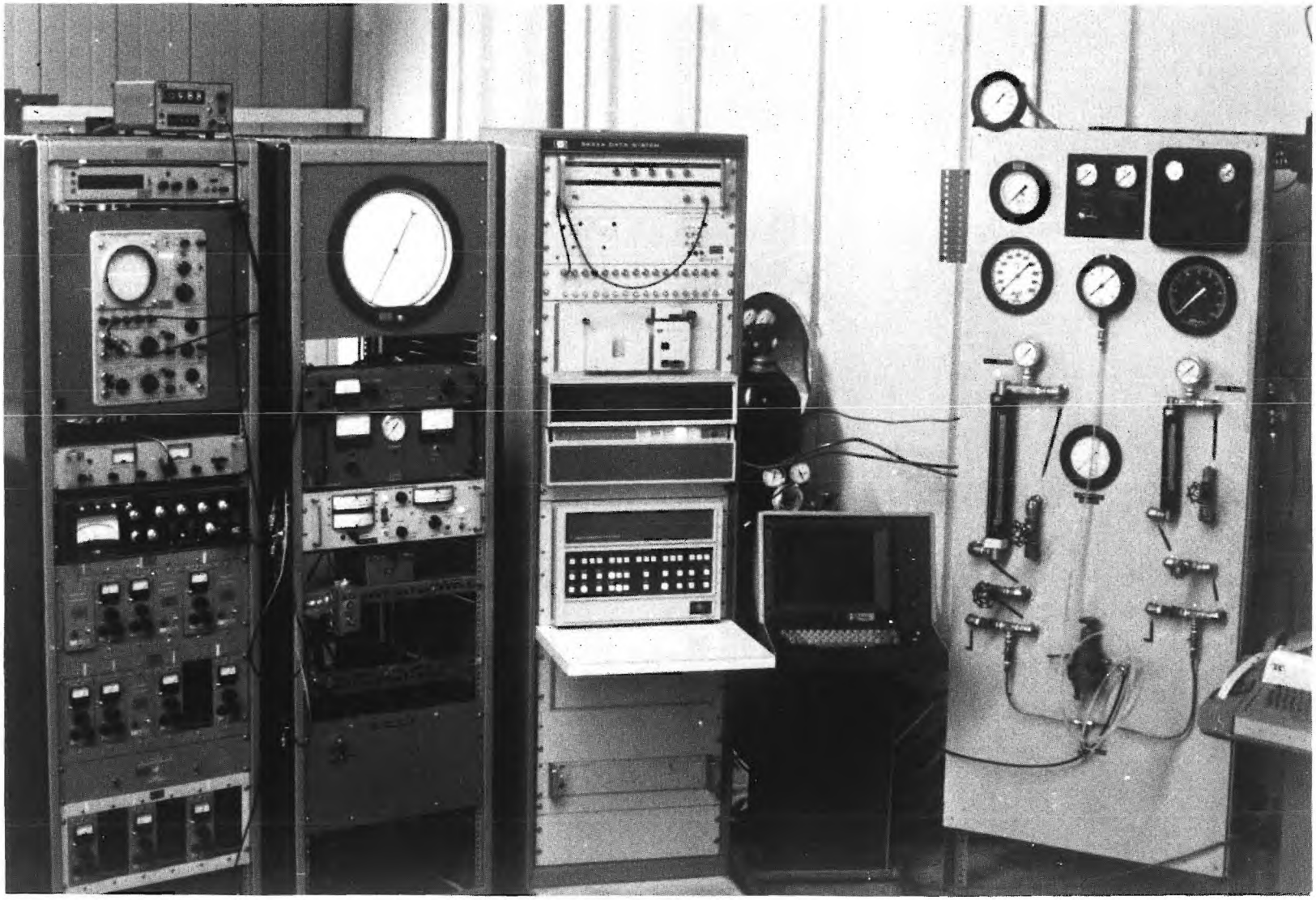

Figure 9. Experiment Control Area.

are digitally filtered and pressure amplitude and phase data are obtained at the frequency of interest. Likewise, thermocouple signals are converted to temperatures. Finally, the pressure and temperature data are printed out and plotted. These values are then used in the data reduction scheme described in Section II to obtain the admittance values. In the remainder of this section, a more detailed description of the data acquisition system is presented.

Phase 1: Data Sampling. As shown in Fig. 10 the data sampling phase involves four major components - a Preston GMAD-11 analog-to-digital converter (ADC), an HP 3220-A frequency synthesizer (pacer), an HP 2100S minicomputer, and a disc storage unit. The ADC is capable of sampling up to 12 channels of input data by use of a multiplexer and has a range of $\pm$ 2.56 volts with a resolution of 20 mv. To obtain maximum signal resolution, the input from the transducer and thermocouple channels are amplified so that the maximum anticipated amplitude for a test is as close to 2.56 volts as possible without exceeding this upper limit.

Upon initiation of a test the following sequence of events occurs as denoted in Fig. 10. (1) The computer initiates a signal to start the analog-to-digital conversion process. (2) The pacer, capable of controlling the sampling rate up to 12 million samples/second, also initiates a signal at the desired sampling rate. In the present experiment up to 12,000 samples per second are taken. When the pacer and computer signals are coincident the sample and hold channels of the ADC go into the "hold" condition so that the input signal voltages at that instant of time are retained. (3) The starting signal from the

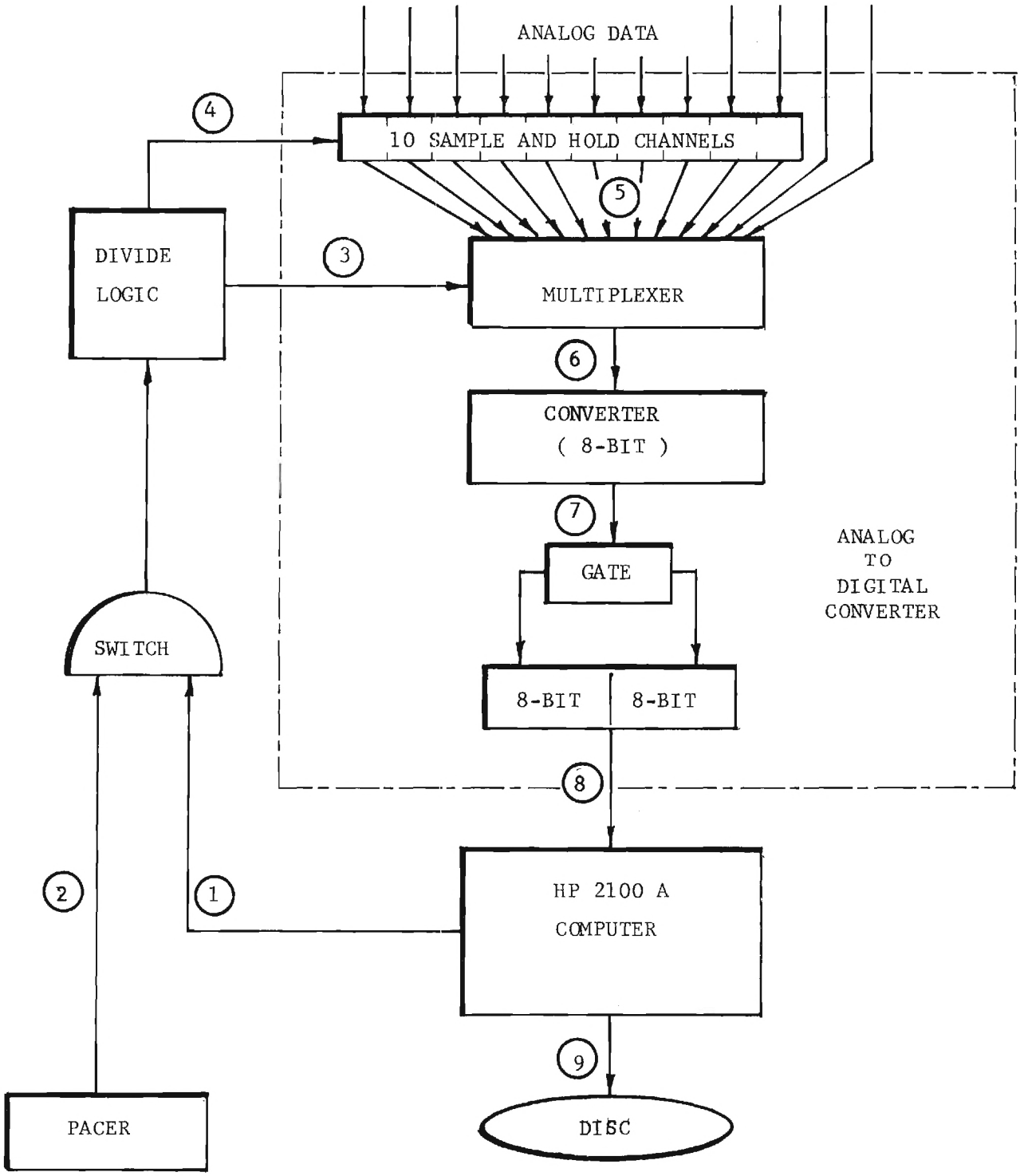

Figure 10. Data Sampling Instrumentation Schematic

switch proceeds to the multiplexer which indexes through the sample-and-hold channels. (4) If the data from all the specified channels have been digitized (determined by the divide logic circuitry), then more data from the input channels are sampled and held. (5) The data from the sample-and-hold device are sequentially transfered two channels at a time by the multiplexer. (6) The voltages from the first of the two channels sampled by the multiplexer enters an 8-bit voltage to binary converter, is digitized, and is stored in a 16-bit output register. (7) The second channel is also digitized and stored in the register. (8) When this process is completed, the computer stores the two 8-bit bytes as a one 16-bit word. By packing the data in this manner the data throughput rate is essentially doubled and increases the upper frequency limit at which reliable data can be acquired. With the present system, reliable pressure data at frequencies of up to 6000 Hz can be obtained. Potentially, the upper frequency limit can be extended to one mega Hz. (9) The packed data word is stored in a buffer in the computer, and the sequence of events is repeated starting with (1).

Before testing, the sampling rate, the size of the data buffer, and the sampling interval are determined. The sampling rate depends upon the frequency of the driven oscillations. The samples are taken rapidly enough to obtain a sufficient number of data points per cycle period for good signal definition. The data buffer and sampling interval are determined by the test conditions. In this study, the ignition and burnout transients produce large variations in pressure amplitude and phase. The sampling interval must be small enough to detect these

variations so that they can be distinguished from the nearly constant amplitudes which occur during the period of quasi-steady burning. On the other hand the sampling interval must be long enough to ensure that the digital filtering interval is sufficient. This last requirement can be relaxed for the tests conducted in the present investigation since the signals thus far encountered have been relatively free of background noise. Once the sampling interval is established the size of the buffer in the computer into which the data is stored is determined.

During a test data are taken at up to 80 sampling intervals of from 10 to 50 milliseconds, and the time between intervals is from 15 to 30 milliseconds. The duration of the run is from two to six seconds for the 3/8" -thick propellant samples used and from 20 to 40 data points are obtained during steady burning. After the digitized data points taken during one sampling interval have been stored, they are then written onto a disc so that room can be made in the buffer to receive the data from the next sampling interval. These steps are depicted in Fig. 11.

Phase 2: Data Processing. During the data processing phase, the disc, computer, and a Tektronix 4012 graphics display terminal are used. The steps involved are shown in Fig. 12. (1) The digitized data taken over one time interval is read from the disc into the computer. (2) The computer software unpacks the data words so that the data from each channel can be processed. From the digitized signals of the transducer channels, the average amplitude and phase over the time interval is obtained. If the time interval is sufficiently short, the time variations

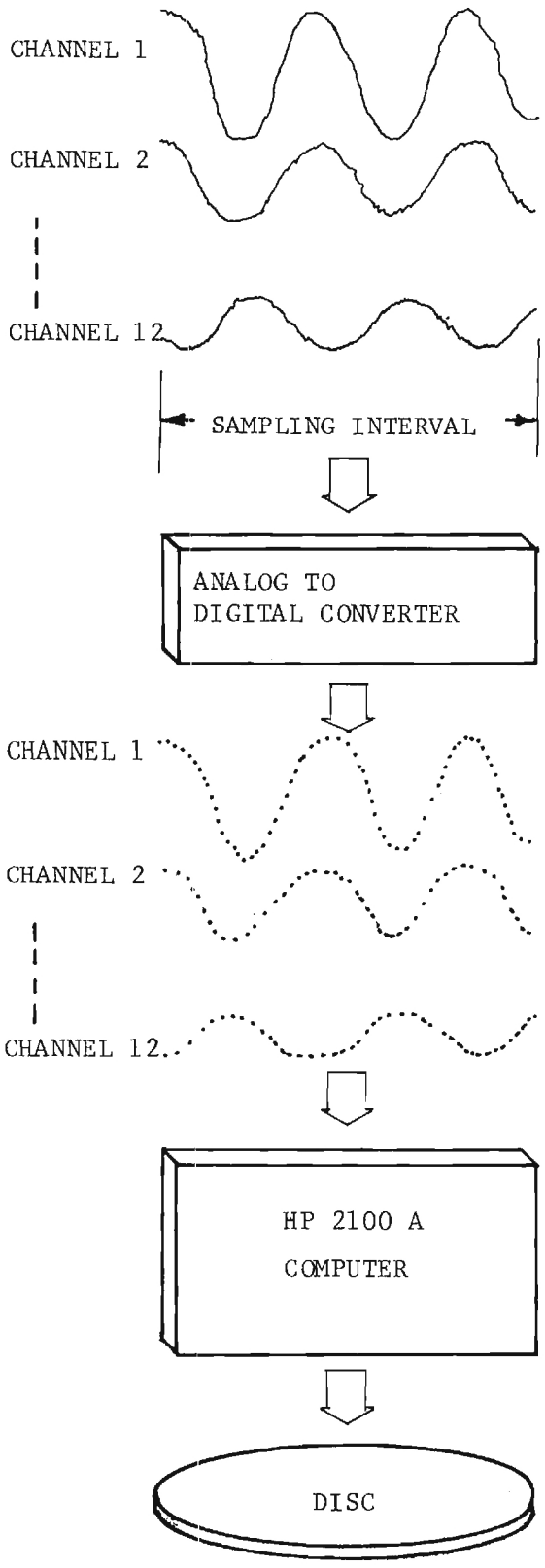

Figure 11. Signal Processing During Data Sampling Phase

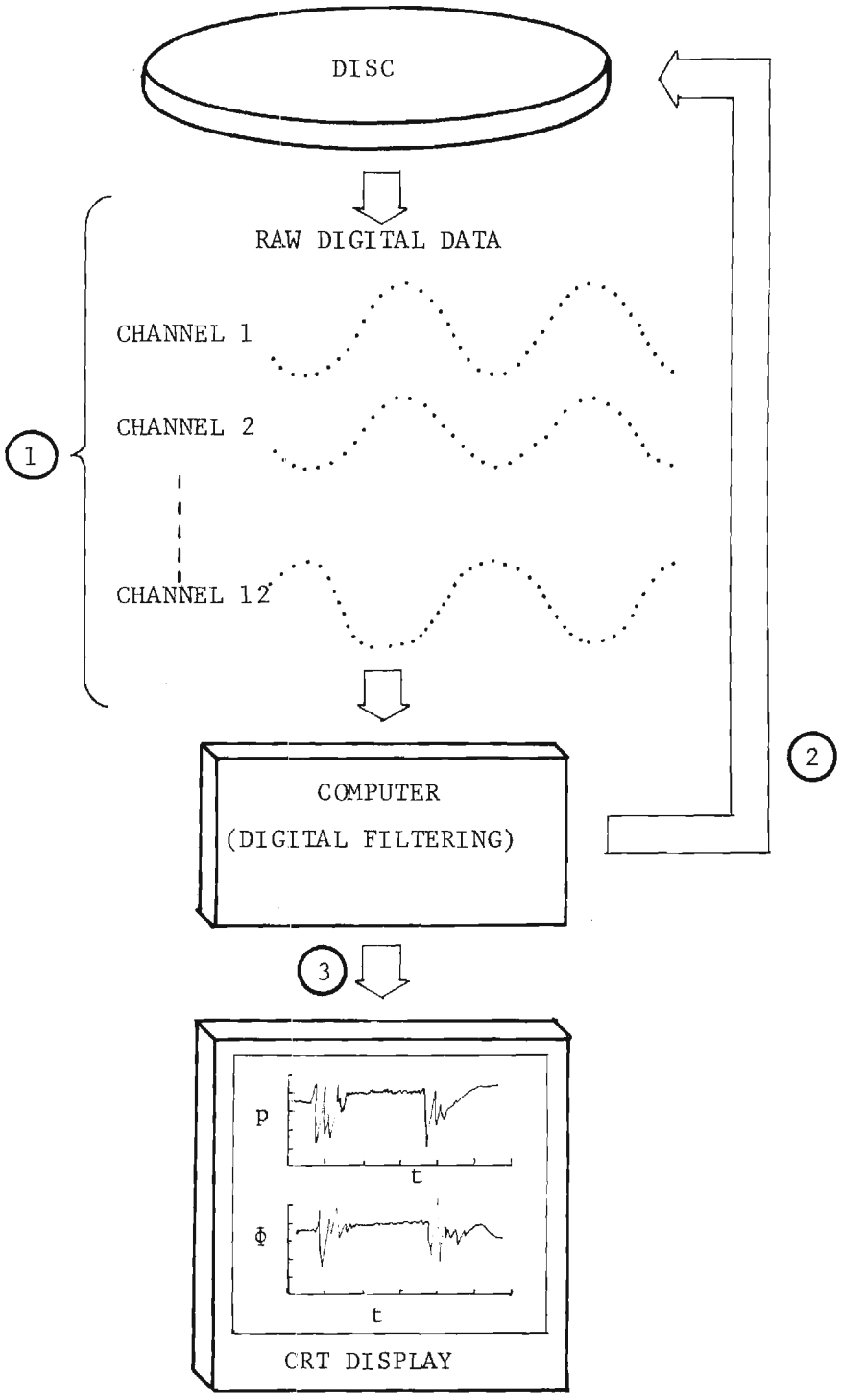

Figure 12. Data Processing Schematic

in amplitude and phase will not be significant and the computed averages will be close to the true value. The average temperature over the time interval is also computed from the digitized thermocouple data by converting the measured voltages to temperature using a Forsyth polynomial expansion obtained from the thermocouple calibration charts. Steps one and two are repeated for each successive time interval. Step (3) consists of taking the resulting amplitude and phase data and plotting them against nondimensional time on the terminal. This provides a check to ensure that proper test conditions were established during the run. The data processing phase generally requires less than five minutes of execution time so that if desired test conditions were not achieved, minimal time is lost between the preliminary data check and retesting. In addition to being displayed on the terminal, the amplitude, phase, and temperature data are also stored on one disc track preassigned to the test which is protected by software. These data can then be displayed at a later date so that minimal time between runs is lost.

Phase 3: Data Presentation. The data presentation phase simply consists of reading the data stored during a run off the disc track assigned to that test and printing or plotting the results. The first step is to plot the amplitude and phase against nondimensional time. From these plots the time intervals at which steady state burning was achieved can be ascertained. At these selected points the amplitude, phase, and temperature data can then be plotted or printed out versus distance. These data are then used in the analyses described in Section II to compute the admittance. This final admittance computation is carried out on a CYBER-70 computer instead of the minicomputer because of the time and storage requirements involved.

IV. EXPERIMENTAL RESULTS AND SUMMARY

The experimental efforts during this reporting period were directed toward improving the experimental techniques and determining the admittances of a number of solid propellants at high pressure test conditions. To date, twenty nine tests have been conducted using three different propellants: (1) a T-13 propellant, (2) an undesignated white propellant supplied by Thiokol (referred to as propellant B in this report), and (3) an A-15 propellant. A summary of the tests conducted thus far is presented in Tables II through IV.

TABLE II. Tests Conducted with Propellant B

Expt. No. E-16-633	Propellant Type	Driving Frequency in Hz	Chamber Mean Pressure in psig	Exhaust End Configuration
550	(White),B	625	300	Closed I
559	"	278	300	Open II
561	"	502	300	Open II
563	"	742	300	Open II
565	"	967	300	Open II
573	"	742	300	Closed I
574	"	967	300	Closed I
577	"	742	300	Muffler End IV
578	"	985	300	Muffler End IV

TABLE III. Tests Conducted with T-13

Expt. No. E-16-633	Propellant Type	Driving Frequency in Hz	Chamber Mean Pressure in psig	Exhaust End Configuration
551	T-13	625	300	Closed I
560	"	278	300	Open II
562	"	502	300	Open II
564	"	742	300	Open II
566	"	967	300	Open II

TABLE IV. Tests Conducted with A-15

Expt. No. E-16-633	Propellant Type	Driving Frequency in Hz	Chamber Mean Pressure in psig	Exhaust End Configuration
552	A-15	625	300	Closed I
553	"	967	300	Closed I
554	"	967	300	Closed I
555	"	1128	300	Closed I
556	"	967	300	Open II
557	"		300	Open II
558	"	1128	300	Open II
569	"	980	300	Extended Open III
570	"	912	300	Extended Open III
575	"	181	300	Closed I
576	"	181	300	Muffler End IV
567	"	967	0	Open II
568	"	181	0	Open II
571	"	181	0	Closed II
572	"	967	0	Closed II

A schematic of the exhaust end configurations used during the tests are presented in Fig. 13. Different configurations were employed to ensure that the conditions at the exhaust end did not affect the relative pressure amplitudes and phases measured along the standing wave, from which the admittance of the propellant is obtained. The data obtained to date indicate that, to within experimental error, no significant change in the admittance values occurs with changing exhaust end conditions.

In Figs. 14 through 17, typical data is presented for a test conducted at 742 Hz with propellant B with an open-ended exhaust condition. Figure 14 is a plot of the pressure amplitude in decibels (re. 2×10^{-4} μ bar) versus record number for four pressure channels located at different axial stations along the tube. Each record represents a short time interval during which data was recorded by the analog-to-digital converter. Consecutive records correspond to consecutive time instances; hence the abscissa can be considered as representing time.

The data in Fig. 14 can be divided into four phases: (1) the pre-ignition period during which the Ling acoustic drivers are the only source of wave excitation (records 1 to 14); (2) the propellant ignition phase (records 15 to 18); (3) the quasi-steady burning phase during which reliable pressure data can be taken to obtain the burning solid propellant admittance values (records 19 to 40); and the burnout phase (records 41 to 80). During the ignition and burnout phases, the temperature in the tube is changing rapidly with time which produces large variations in the wavelength of the standing wave. Therefore,

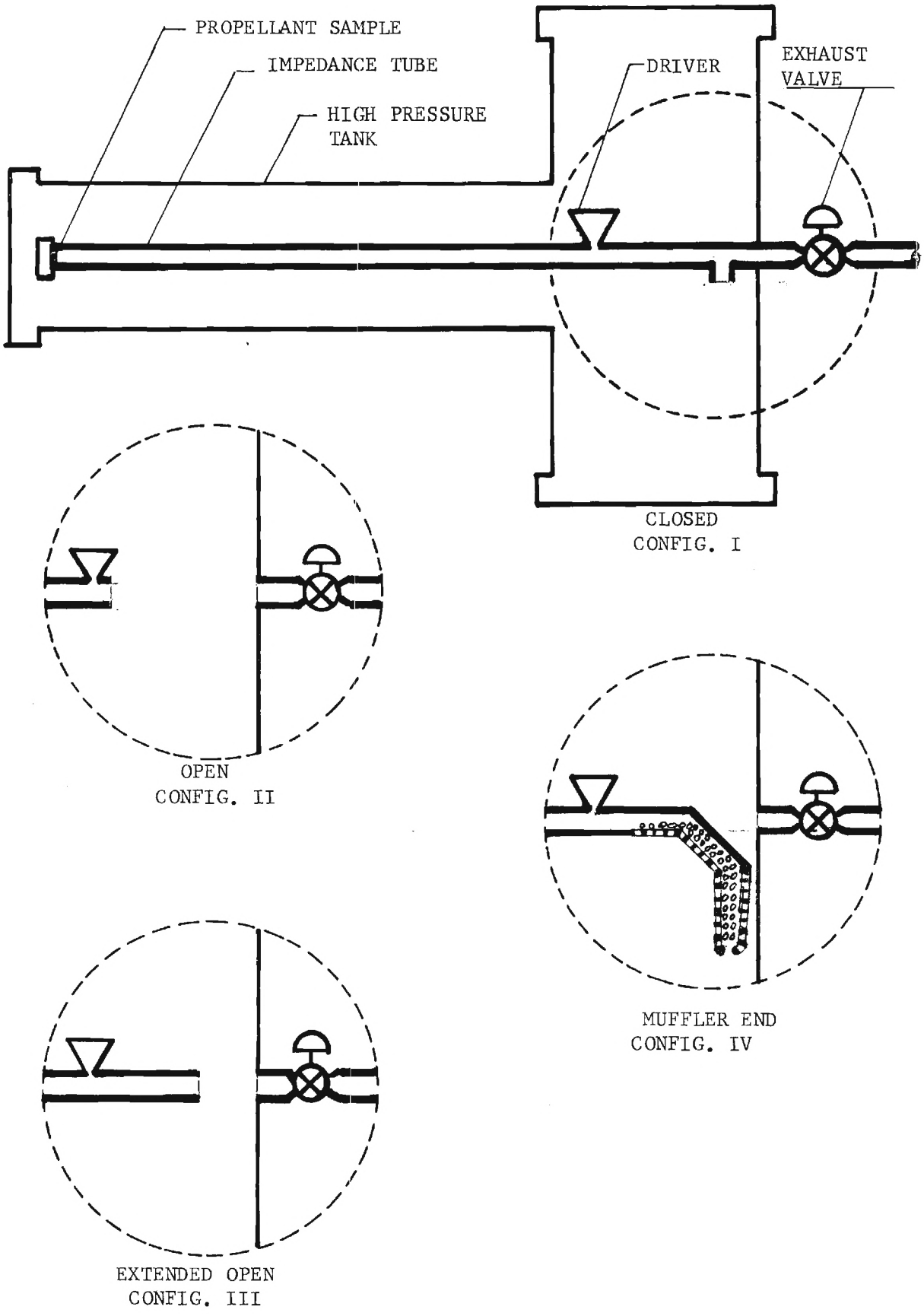

Figure 13. Schematic of Exhaust End Configurations.

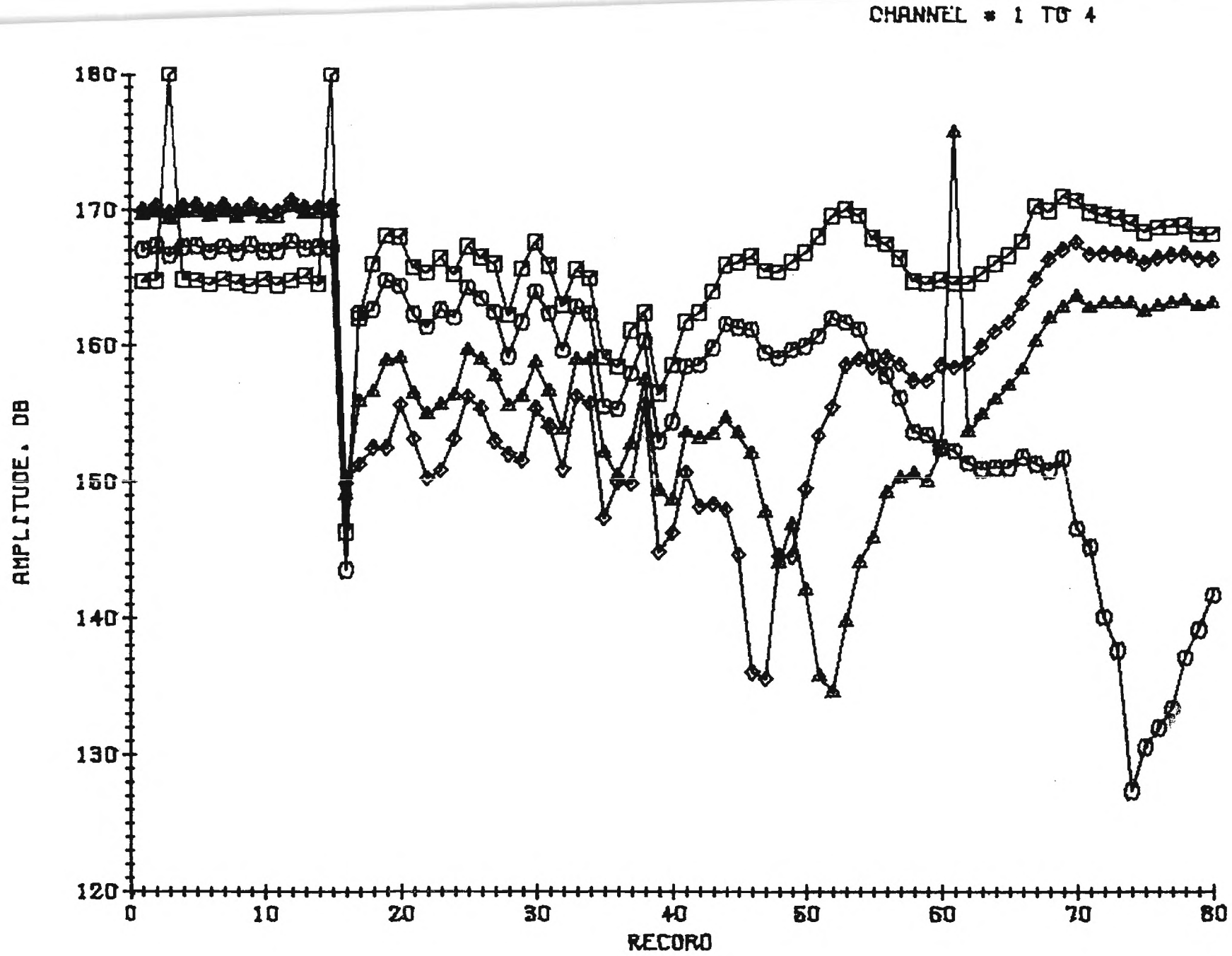

Figure 14. E-16-633-663 WHITE PROPELLANT.742 HI. 300PSIG. OPEN END.

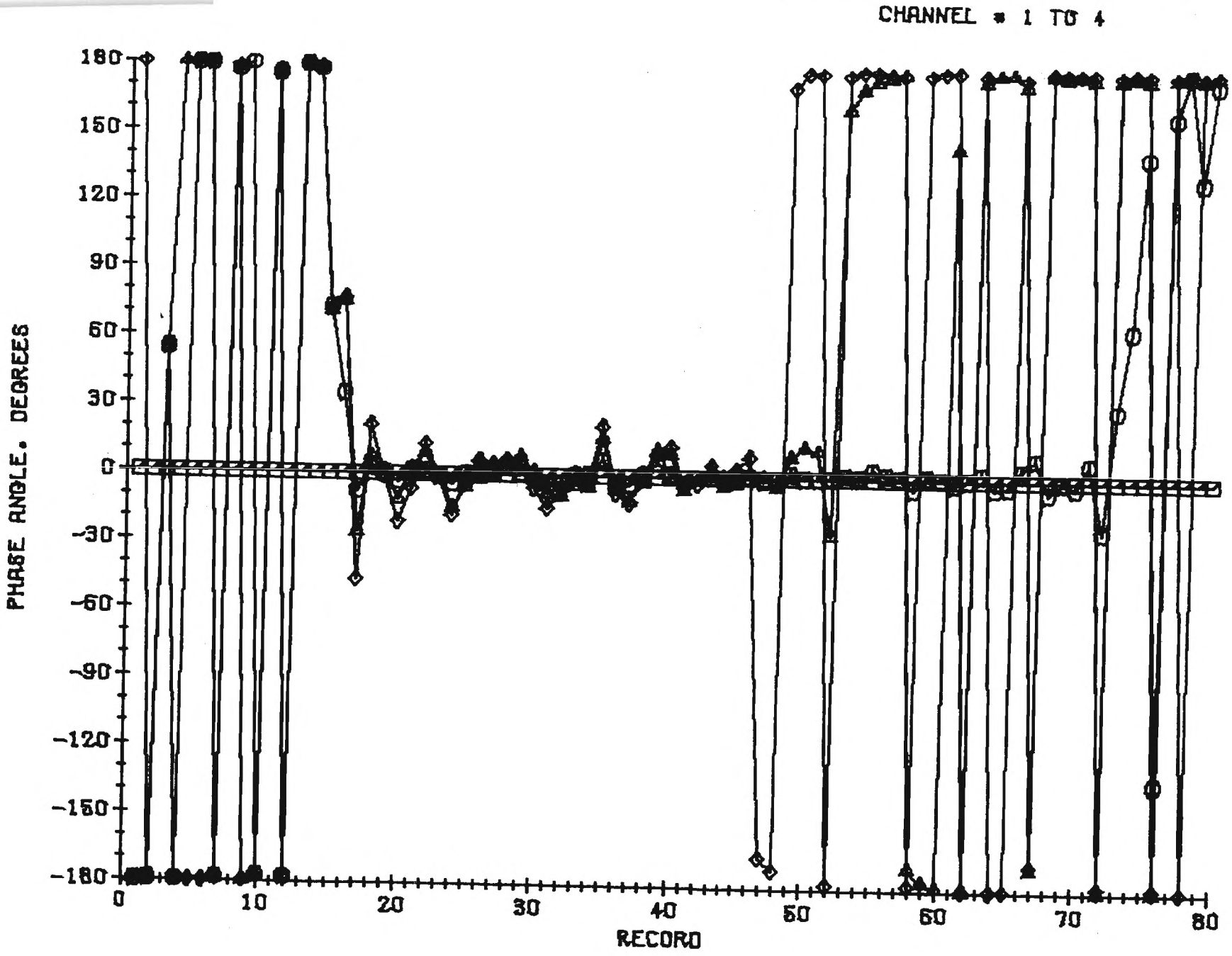

Figure 15. E-16-633-563 WHITE PROPELLANT.742 HZ. 300PSIG. OPEN END.

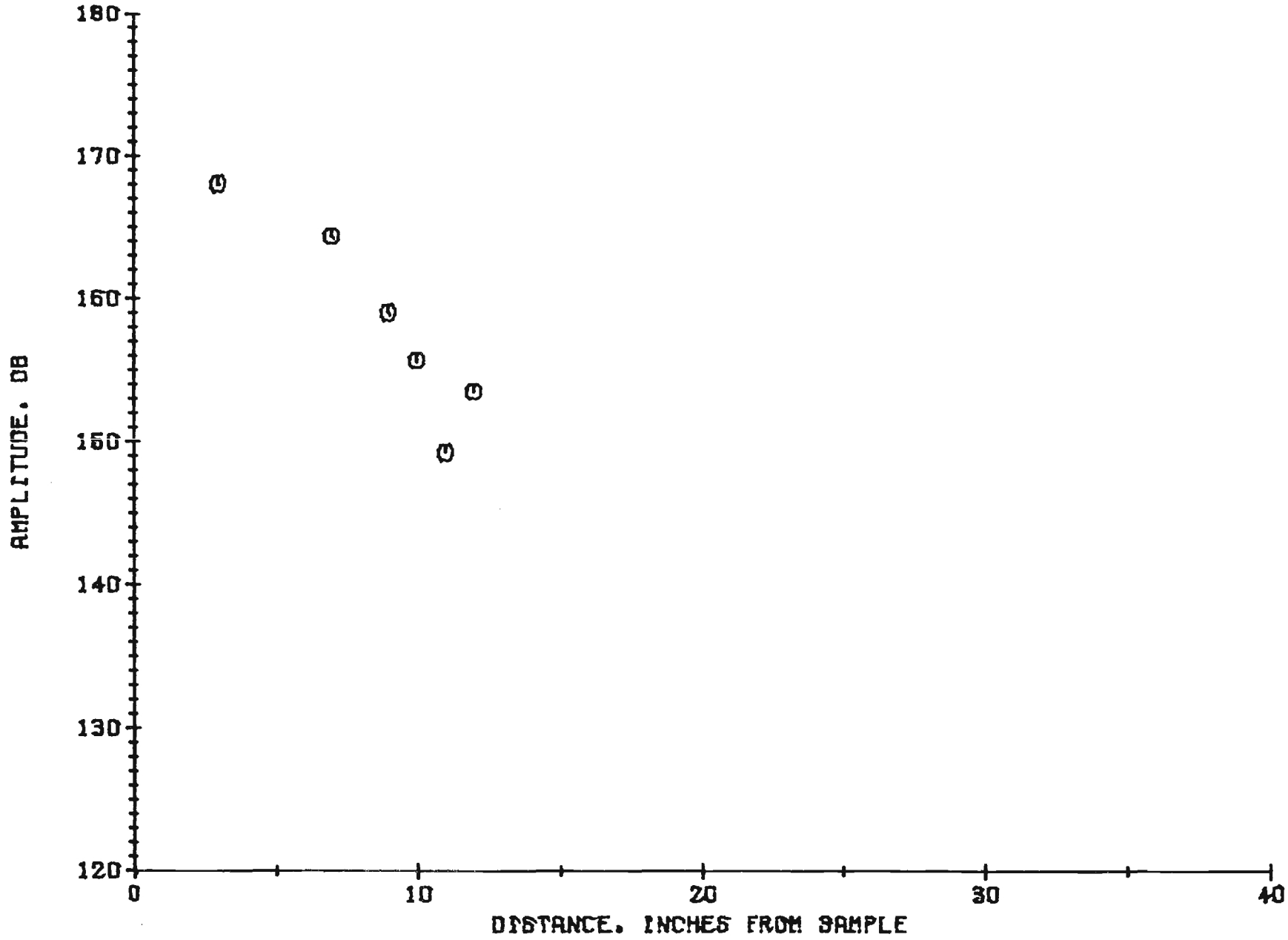

Figure 16. E-16-633-563 WHITE PROPELLANT/742 HZ. 300PSIG. OPEN END.

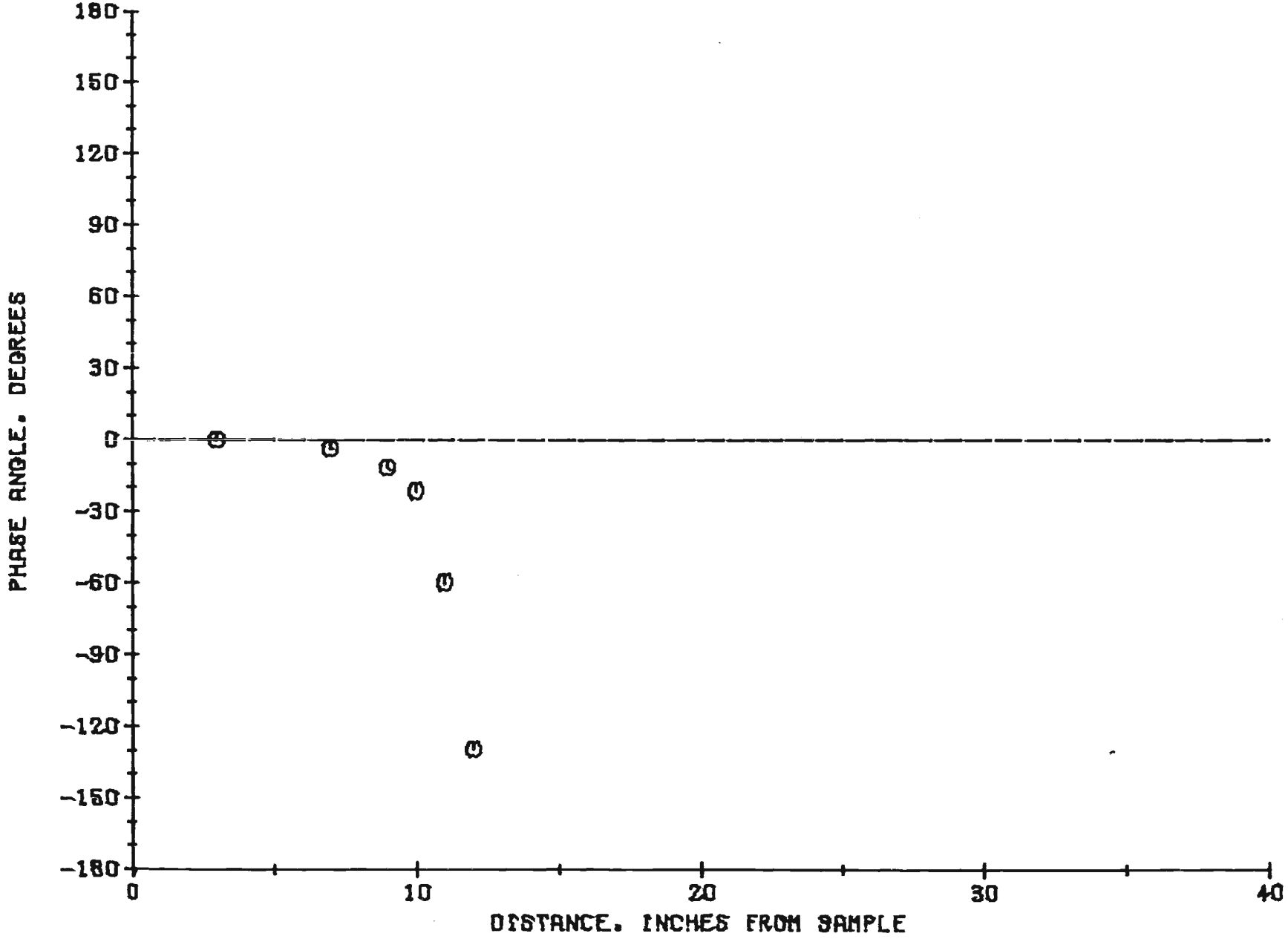

Figure 17. E-16-633-563 WHITE PROPELLANT.742 HZ. 300PSIG. OPEN END.

reliable data cannot be obtained during these periods. On the other hand, no significant rapid temperature variations are expected during the quasi-steady phase of the test. Hence, data measured during this period should produce reliable admittance values for the burning solid propellant.

The behavior of the phase with respect to time is shown in Fig. 15. All phases shown in this plot are referenced to the phase measured three inches from the propellant surface. If the phase differences are positive, then the pressure oscillations seven, nine and ten inches from the sample lead the referenced pressure. This type of condition indicates that the incident wave initiated by the acoustic driver is greater in amplitude than the wave reflected from the burning propellant surface; therefore, the combustion process is damping. On the other hand, if the pressure oscillations further from the burning propellant lag the oscillations closest to the sample, then the phase difference is negative and the wave reflected from the propellant is greater in amplitude than the wave incident from the acoustic driver. This condition indicates that the combustion process is driving.

From the phase data in Fig. 15 it appears that the combustion process is randomly damping and driving the acoustic oscillations during the run. This result is unexpected and behavior of this type has not been reported in other studies of burning solid propellants surveyed under this contract. The pressure amplitude and phase variation with distance, taken at record 20, are presented in Figs. 16 and 17. The increasing phase lag with increasing distance from the sample shown in Fig. 17 indicates driving by the combustion process. Based on these

data, an admittance value of 0.1 was computed which means that the combustion process increased the incident wave amplitude by approximately twenty per cent which indicates a strong driving condition at the propellant surface. However, large damping conditions are observed at other times during the burn (e.g. see Record 35). An investigation of the phenomenon is currently underway.

In Figs. 18 through 21 the behavior of the amplitude and phase of the pressure oscillations with respect to time and distance are presented for the T-13 propellant at a frequency of 742 Hz with an open-end exhaust condition. The two "spikes" in the data in Figs. 18 and 21 at records 38 and 58 are erroneous data caused by the ADC digitization process when a significant bit is either erroneously included or excluded. As seen from Fig. 18, the pressure amplitude rises and falls periodically with time during the burn. Since this behavior occurs only after ignition, it is apparently associated with the combustion process. From the phase data presented in Fig. 19, no large driving or damping characteristics are exhibited by the combustion of the T-13 propellant. Instead, it behaves essentially like a hard termination and does not increase or decrease the amplitude of the incident wave significantly. The axial variation of the pressure amplitude and phase at record 45 is shown in Figs. 20 and 21. From the phase plot, Fig. 21, a weak damping by the combustion process is exhibited. However, at other times (i.e. record 50) a weak driving condition is shown.

In almost all tests conducted thus far, at 300 psig, the tested propellants randomly exhibited driving at some times and damping at others. The propellants which are the most unstable (i.e., the A-15 and propellant B) seem to exhibit the largest variation from driving

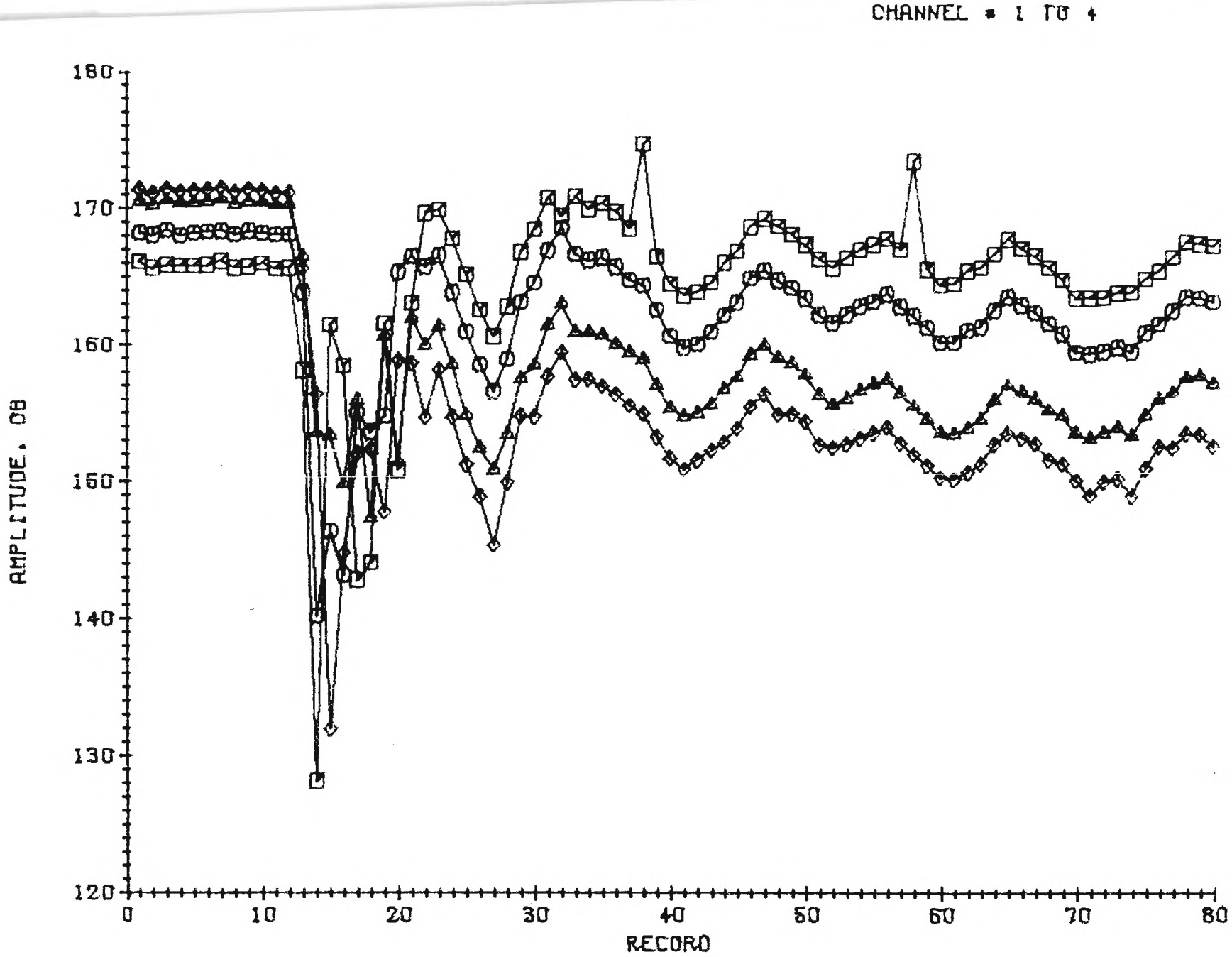

Figure 18. E-16-633-564.T-13.742 HZ..300 PSIG..OPEN END.

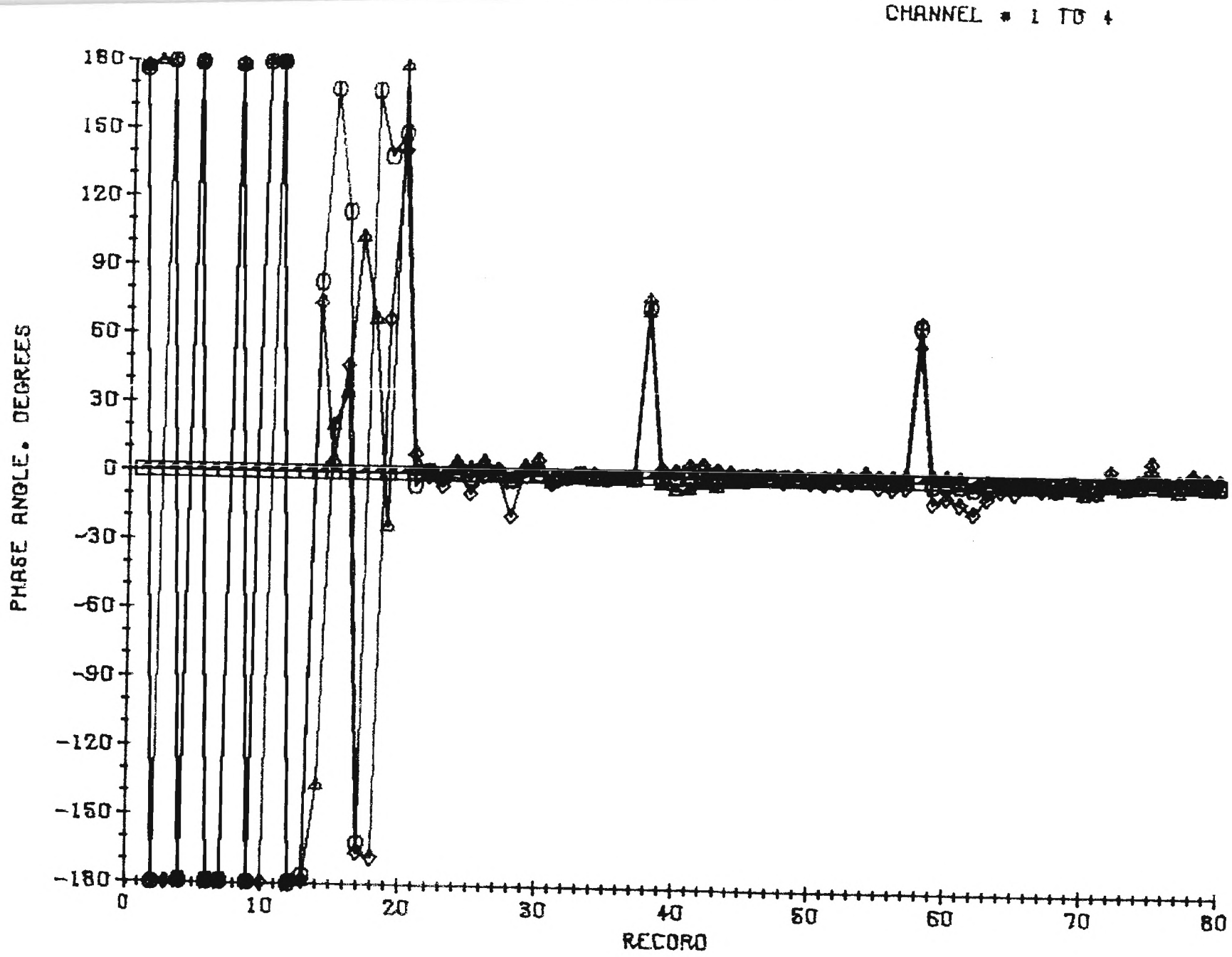

Figure 19. E-16-633-564.T-13.742 HZ-.300 PSIG-.OPEN END.

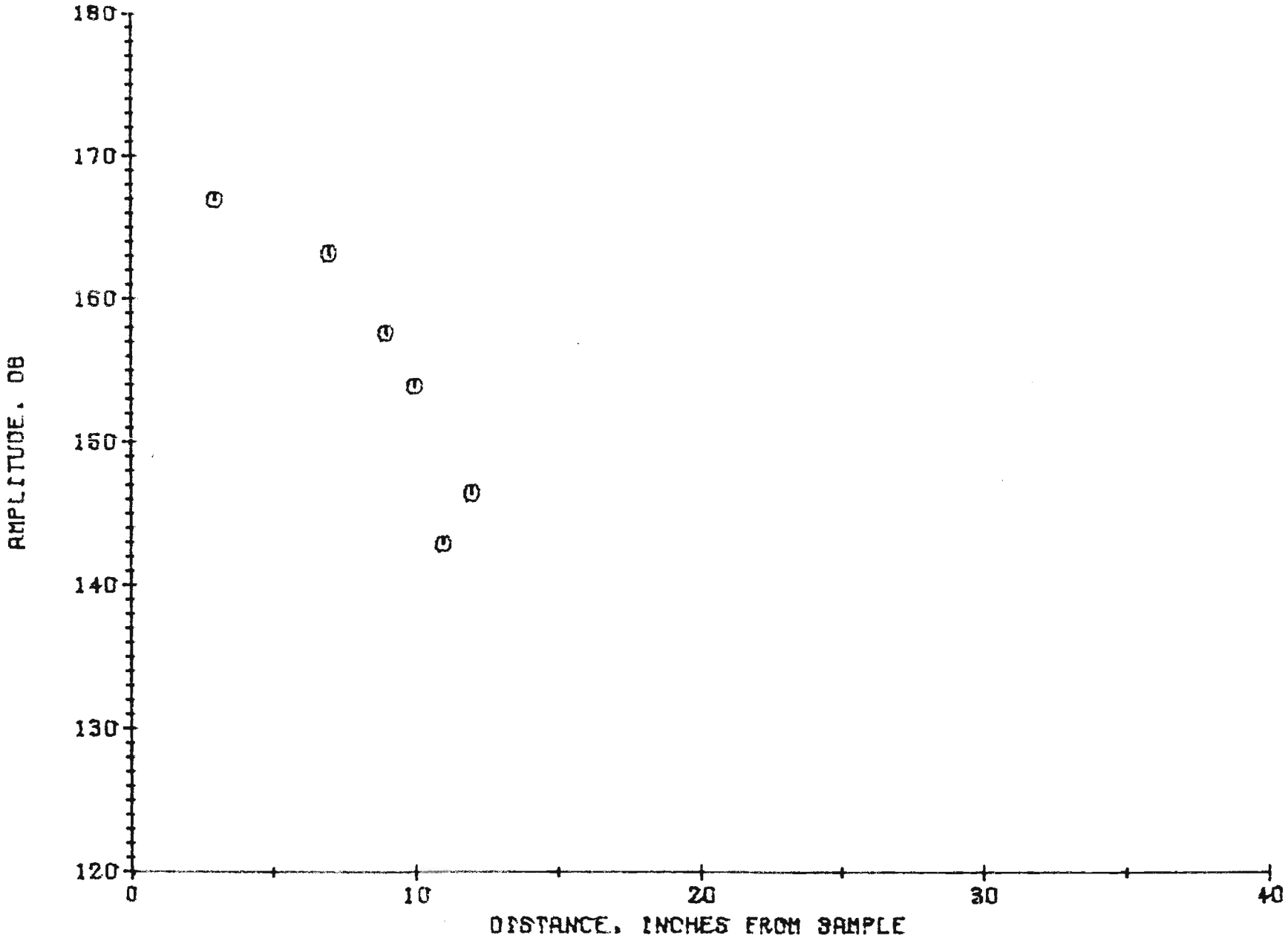

Figure 20. E-16-633-564.T-13.742 HZ-.300 PSIG-.OPEN END.

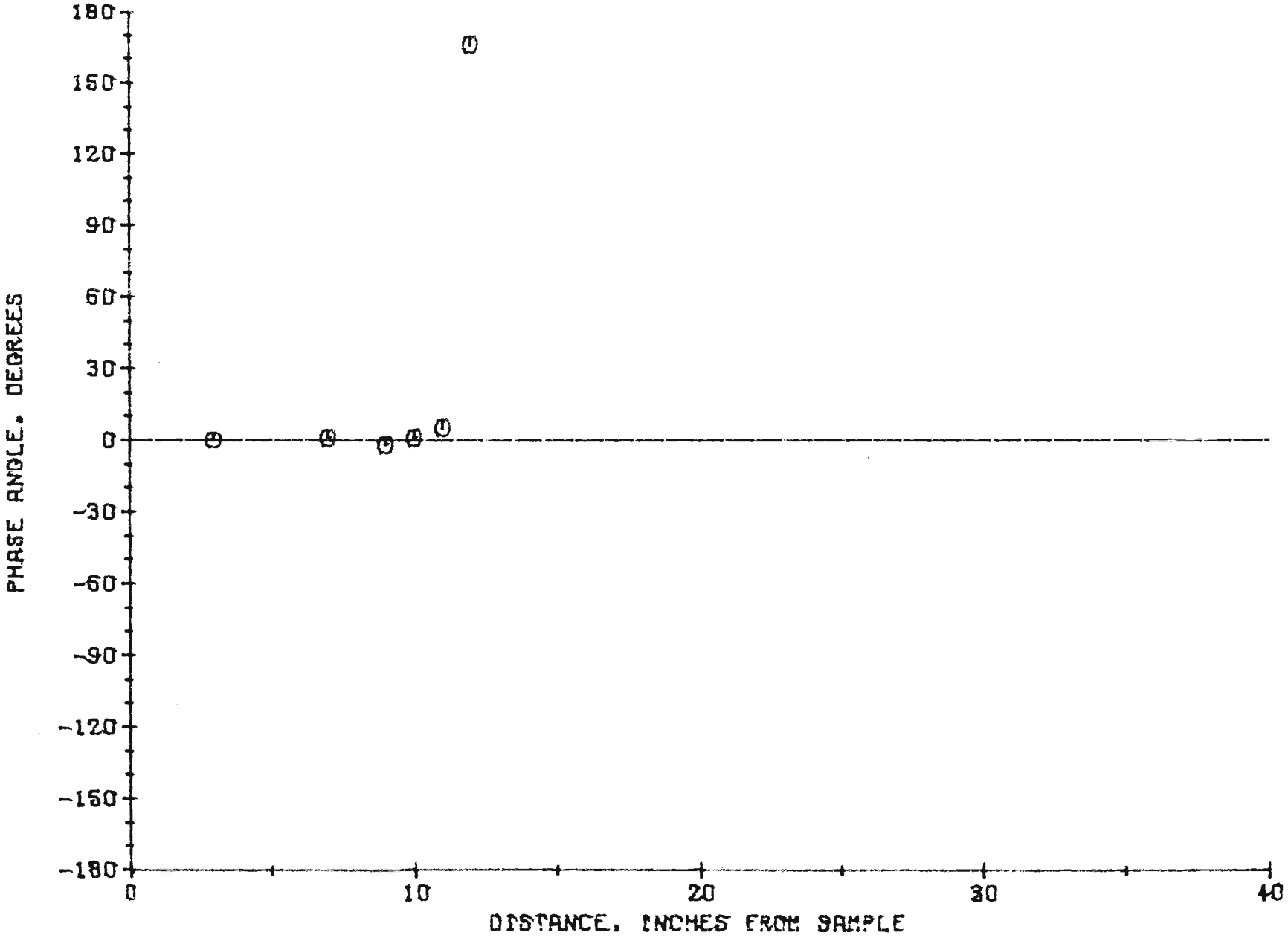

Figure 21. E-16-833-564.T-13.742 MX..300 PSIG..OPEN END.

to damping whereas the most stable propellant (i.e. the T-13) seems to show the least variation. Current research efforts are concerned with the development of an appropriate explanation for the measured experimental data.

REFERENCES

1. Lord Rayleigh, The Theory of Sound, Dover Publications, New York, 1945, Vol. II, Section 322g.

2. Zinn, B. T., Daniel, B. R., Bell, W. A., and Salikuddin, M., "Solid Propellant Admittance Measurements by the Driven Tube Method," Interim Report, AFOSR-73-2571, August 1974.

3. Zinn, B. T., Salikuddin, M., Daniel, B. R., and Bell, W. A., "Solid Propellant Admittance Measurements by the Driven Tube Method," AFOSR-TR-75-1531, August, 1975.

4. Scott, R. A., "An Apparatus for Accurate Measurements of the Acoustic Impedance of Sound Absorbing Materials," Proceedings of the Physical Society, Vol. 58, 1946, pp. 253-264.

5. Zinn, B. T., Daniel, B. R., Janardan, B. A., and Smith, A. J., "Damping of Axial Instabilities by Minuteman II, Stage III, Minuteman III, Stage III Exhaust Nozzles," AFRPL Interim Report, AFRPL-TR-72-71, August 1972.

6. Perry, E. H., "Investigation of the T-Burner and its Role in Combustion Instability Studies," Ph.D. Thesis, Daniel and Florence Guggenheim Jet Propulsion Center, California Institute of Technology, Pasadena, California, May 1970.

7. Nyland, T. W., England, D. R., and Anderson, R. C., "Frequency Response of Short Nozzle Probes," Instruments and Control Systems, August 1973, pp. 27-29.

8. Doebelin, Ernest O. Measurement Systems: Application and Design, McGraw-Hill, Inc., 1966, Section 6.

AFOSR INTERIM SCIENTIFIC REPORT

AFOSR-TR-

SOLID PROPELLANT ADMITTANCE MEASUREMENTS BY THE DRIVEN TUBE METHOD

Prepared for

Air Force Office of Scientific Research
Aerospace Sciences Directorate
Arlington, Virginia

by

B. T. Zinn
M. Salikuddin
B. R. Daniel
W. A. Bell

School of Aerospace Engineering
Georgia Institute of Technology
Atlanta, Georgia 30332

Approved for public release; distribution unlimited

Grant No. AFOSR-73-2571 October 1977

Conditions of Reproduction

Reproduction, translation, publication, use and disposal in whole or in part by or for the United States Government is permitted.

UNCLASSIFIED

SECURITY CLASSIFICATION OF THIS PAGE *(When Data Entered)*

REPORT DOCUMENTATION PAGE		READ INSTRUCTIONS BEFORE COMPLETING FORM
1. REPORT NUMBER	2. GOVT ACCESSION NO.	3. RECIPIENT'S CATALOG NUMBER
4. TITLE *(and Subtitle)* SOLID PROPELLANT ADMITTANCE MEASUREMENTS BY THE DRIVEN TUBE METHOD		5. TYPE OF REPORT & PERIOD COVERED INTERIM OCTOBER 1976-OCTOBER 1977 6. PERFORMING ORG. REPORT NUMBER
7. AUTHOR*(s)* B. T. ZINN M. SALIKUDDIN B. R. DANIEL W. A. BELL		8. CONTRACT OR GRANT NUMBER*(s)* AFOSR - 73- 2571
9. PERFORMING ORGANIZATION NAME AND ADDRESS GEORGIA INSTITUTE OF TECHNOLOGY SCHOOL OF AEROSPACE ENGINEERING ATLANTA, GEORGIA 30332		10. PROGRAM ELEMENT, PROJECT, TASK AREA & WORK UNIT NUMBERS 681308 9711-01 61102F
11. CONTROLLING OFFICE NAME AND ADDRESS AIR FORCE OFFICE OF SCIENTIFIC RESEARCH 1400 WILSON BOULEVARD ARLINGTON, VIRGINIA 22209		12. REPORT DATE OCTOBER 1977 13. NUMBER OF PAGES
14. MONITORING AGENCY NAME & ADDRESS*(if different from Controlling Office)*		15. SECURITY CLASS. *(of this report)* UNCLASSIFIED 15a. DECLASSIFICATION/DOWNGRADING SCHEDULE

16. DISTRIBUTION STATEMENT *(of this Report)*

APPROVED FOR PUBLIC RELEASE
DISTRIBUTION UNLIMITED

17. DISTRIBUTION STATEMENT *(of the abstract entered in Block 20, if different from Report)*

18. SUPPLEMENTARY NOTES

19. KEY WORDS *(Continue on reverse side if necessary and identify by block number)*

COMBUSTION INSTABILITY
SOLID PROPELLANT RESPONSE FUNCTIONS
SOLID PROPELLANT ROCKETS
IMPEDANCE TUBE MEASUREMENTS

20. ABSTRACT *(Continue on reverse side if necessary and identify by block number)*

The progress made during the fourth year of an investigation for the measurement of the response of a burning solid propellant to flow disturbances is presented. In this study a modification of the impedance tube technique is used to measure the response over a wide frequency range. Further refinements in the data reduction computer program are discussed. Anomalous behavior for high pressure (300 psig) tests which shows that the propellant sample periodically drives and damps acoustic oscillations during a burn was resolved. Techniques for improving the accuracy of the measured data and the quality of the burn

DD FORM 1 JAN 73 1473 EDITION OF 1 NOV 65 IS OBSOLETE

SECURITY CLASSIFICATION OF THIS PAGE *(When Data Entered)*

have been developed. Testing will resume during the next year.

TABLE OF CONTENTS

ABSTRACT

The progress made during the fourth year of an investigation for the measurement of the response of a burning solid propellant to flow disturbances is presented. In this study a modification of the impedance tube technique is used to measure the response over a wide frequency range. Further refinements in the data reduction computer program are discussed. Anomalous behavior for high pressure (300 psig) tests which shows that the propellant sample periodically drives and damps acoustic oscillations during a burn was resolved. Techniques for improving the accuracy of the measured data and the quality of the burn have been developed. Testing will resume during the next year.

INTRODUCTION

This report summarizes the objectives, research performed and results obtained under Air Force Grant No. AFOSR-73-2571. This grant was initiated on July 1, 1973 and it has been concerned with the "Determination of the Acoustic Responses of Solid Propellants by the Impedance Tube Method." This research is presently continuing under Air Force Contract F49620-78-C-0003.

Combustion instability has been recognized as one of the most serious problems encountered in the development of solid-propellant rockets. Combustion instability is the result of an interaction between the combustion process and disturbances within the rocket motor; an interaction which often leads to the amplification of these disturbances into finite amplitude oscillations. The appearance of combustion instability frequently produces dramatic and even catastrophic changes in the motor's performance. Combustion instability may also result in mechanical failure of engine components, extremely high heat transfer rates to the combustor boundaries and interference with the control and guidance systems. Any one of these effects can result in engine or mission failure.

To determine the susceptibility of a given propulsion system to combustion instability, it is necessary to determine the energy balance that exists between the various gains and losses of wave energy present within the combustor. Wave energy loss mechanisms tend to attenuate the amplitude of a disturbance in the combustor and thus exert a stabilizing influence upon the engine. Examples of wave energy loss mechanisms are convective energy losses caused by the mean flow, energy dissipation associated with viscosity and heat transfer, energy dissipation due to wave interaction with particulate matter, and energy losses resulting from the interaction of the disturbance with various mechanical components of the engine such as

the exhaust nozzle. On the other hand, wave energy gains tend to amplify engine disturbances and thus exert a destabilizing influence upon the combustor. The primary source of wave energy gain is the unsteady combustion process. If the energy gains are greater than the wave energy losses in the motor, an initial disturbance will amplify and lead to undesirable self-sustained oscillations inside the combustor. To evaluate the stability of a solid-propellant rocket motor, it is necessary to quantitatively describe the various gain and loss mechanisms that are present in the system.

The wave energy gain in a solid rocket may be determined from either a theoretical or an experimental investigation of the interaction between a burning solid propellant and an oscillating gas phase. This interaction can be described mathematically by specifying either the response factor or the admittance of the burning solid propellant surface. The admittance represents the boundary condition which must be satisfied at the burning propellant boundary in solid rocket stability analyses. The admittance is defined as the complex ratio of the gas velocity perturbation normal to the surface and the local pressure perturbation. The nondimensional form Y_b of the admittance of a burning propellant is often expressed in the following form:

$$Y_b = \frac{\gamma \bar{P}}{\bar{c}_b} \cdot \frac{u'}{P'} \qquad (1)$$

γ, P, u and c respectively describe the ratio of specific heats, pressure, flow velocity and sound velocity; primed quantities describe flow perturbations and superposed bars describe steady state quantities. The earlier mentioned propellant response factor R_b is defined as the complex ratio of the propellant burning rate perturbation to the pressure perturbation,

evaluated at the burning surface. The nondimensional form of the response factor is:

$$R_b = \frac{\bar{P}}{\bar{r}} \cdot \frac{r'}{P'} = \frac{\bar{P}}{\bar{m}} \cdot \frac{m'}{P'} \tag{2}$$

where r and m respectively describe the propellant regression rate and the gas flow rate at the propellant surface.

The relationship between the propellant response factor and its admittance is often of interest. The mass flux m at the burning surface is given by

$$m = \rho u = \rho_s r \tag{3}$$

It follows from Eq. (3) that

$$\frac{m'}{\bar{m}} = \frac{\rho'}{\bar{\rho}} + \frac{u'}{\bar{u}} \tag{4}$$

and using Eqs. (1), (2) and (4) one can easily show that:

$$R_b = \frac{Y_b}{\gamma \bar{M}_b} + \frac{\rho'/\bar{\rho}}{P'/\bar{P}} \tag{5}$$

If the oscillations are isentropic, then

$$\frac{\rho'}{\bar{\rho}} = \frac{1}{\gamma} \frac{P'}{\bar{P}} \tag{6}$$

and Eq. (5) reduces to the following expression:

$$R_b = \frac{1}{\gamma \bar{M}_b} \left[Y_b + \bar{M}_b \right] \tag{7}$$

The above quantities will be used later in this report in the presentation of some of the data measured under this program.

Since instability is often caused by small differences between wave energy gains and losses, it is imperative that the contributions from all processes affecting the stability of rocket engines be known as accurately as possible. Hence, it is of utmost importance that experimental techniques capable of accurate determination of the responses of burning solid propellants be available. The development of such an experimental technique was one of the main objectives of this research which has been concerned with the adaptation of the impedance tube method in the determination of the responses of burning solid propellants. The impedance tube technique has its origin in acoustics where it has been successfully utilized to measure the responses of sound absorbing materials under no flow conditions.[1] This technique was later modified to determine the responses of choked rocket nozzles[2] and acoustic liners[3] under cold flow conditions. It has been chosen as a potential means for the measurement of the admittances of burning solid propellants because (1) it offers the possibility for accounting for the influence of aluminum particles in both the combustion zone and gaseous phase; (2) the possibility of carefully controlling the frequency and growth rate of the oscillation; and, (3) contrary to T-burner type experiments, the same setup may be used to study the response of a given solid propellant over a whole frequency range and fewer tests are potentially needed than with any of the T-burner type experiments. A more detailed description of the impedance tube experiment is provided in the following section.

Considerable modifications to the classical impedance tube technique were necessary for use in the measurement of the admittances of burning solid propellants. In contrast with earlier applications[1,2,3] of this technique, the present application involves admittance measurements under

high pressure and temperature conditions . To achieve this objective, a new experimental facility capable of operation under high pressure and temperature was designed and fabricated; a new impedance tube theory accounting for the presence of a temperature gradient in the impedance tube was developed, a new experimental procedure was implemented; a new data reduction procedure utilizing a nonlinear reduction technique was employed; an analog-to-digital data acquisition system was developed; and numerous tests involving a variety of solid propellants have been conducted over a wide range of operating conditions. The work performed under this grant has described in detail in earlier interim reports[4,5,6] JANNAF publications[7,8] and an AIAA publication[9]. Additional publications based upon this work are currently in the planning stage. In what follows brief descriptions of what has been accomplished to date and future directions of this work are provided. This section is followed by a section describing the impedance tube technique, the theoretical aspects of the research, the experimental setup, the data reduction procedure, results obtained to date, and the current status of the program.

The Impedance Tube Technique

In the past the impedance tube has been used to measure the admittances of various sound absorbing materials. In such studies, the experimental setup (see Figure 1) consists of a tube with an acoustic driver at one end and the sample whose admittance is to be measured at the other end. During an experiment, the driver generates an incident wave P_i of a given frequency ω that propagates along the tube until it impinges upon the tested sample. Because of the interaction between the incident wave and the sample material, the incident wave reflects off the tested sample with modified amplitude and phase. The reflected wave P_r then combines with the incident wave to form a

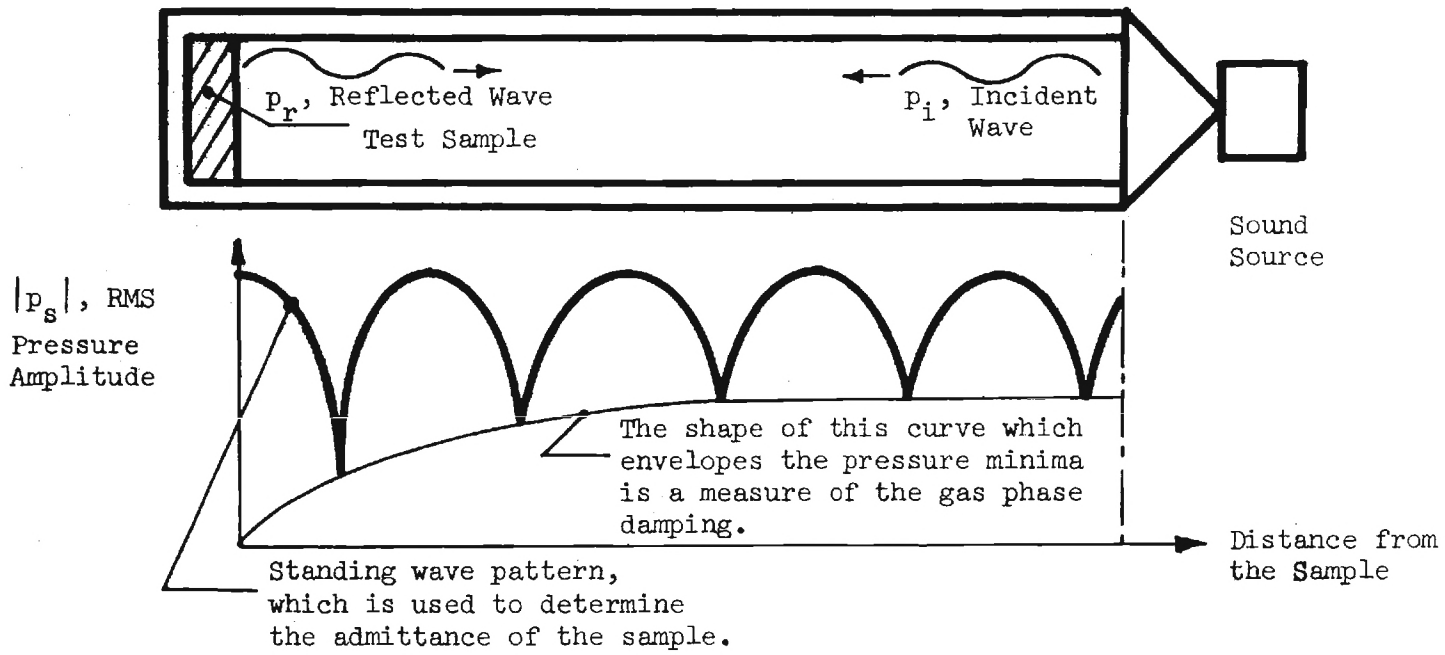

Figure 1. An Impedance Tube and a Typical Standing Wave Pattern

standing wave pattern in the tube whose structure depends, among other things, upon the admittance of the tested sample. It can be shown,[2],[10] that the sample admittance Y depends upon two parameters, α and β, which respectively describe the changes in amplitude and phase between the incident and reflected waves at the sample surface, that is

$$Y = \frac{u'}{P'} = f(\alpha,\beta,\omega,\ldots) \tag{8}$$

where f is a known functional form. The admittance Y can be determined once the parameters α and β are known. It can also be shown[2],[10] that the structure of the amplitude $|P(x)|$ of the standing wave in the tube can be described by an expression having the following functional form:

$$|P(x)| = g(\alpha,\beta,\gamma,\lambda,x\ldots) \tag{9}$$

where γ is a measure of attenuation of the waves due to acoustic energy losses in the gas phase, λ is the wave length of the oscillation and x describes the axial location in the tube. In impedance tube experiments a microphone is traversed along the tube to measure $|P(x)|$. Once this data is available, it can be used together with the above equation to determine the unknowns α, β and γ. The quantities α and β are then used to determine Y. This technique has recently been successfully applied to measure the admittances of choked nozzles in the presence of a mean flow[2],[3]. This data provides a measure of the attenuation provided[11] by choked nozzles during axial and three-dimensional instabilities.

To be applicable in solid propellant admittance measurements, the classical impedance tube setup and its associated theory need to be modified to account for the presence of a mean flow and a steady state temperature in the impedance tube during the experiment. These requirements con-

siderably complicate the execution of the required experiment and the associated data reduction scheme, as will be discussed in the following sections.

THEORETICAL INVESTIGATIONS

The theoretical efforts conducted under this program fall into the following two categories:

(1) Development of an analytical procedure for the utilization of measured acoustic pressure (amplitude and phase) data in the determination of the response factor and admittance of a burning solid propellant and

(2) Investigation of the wave behavior in the impedance tube under the range of conditions expected in the proposed solid propellant admittance measurements.

The first category above basically represents a modification of the classical impedance tube theory. This modification required the development of an analytical procedure capable of utilizing acoustic pressure data measured at discrete locations along the impedance tube, and accounting for a steady state temperature gradient and possibly gas phase acoustic energy dissipation, in the determination of the response factor and admittance at the burning solid propellant surface. It is basically an inverse problem; that is, the boundary condition at the burning solid propellant surface that results in the measured acoustic wave structure.

Before proceeding with a discussion of the developed data reduction procedure it is necessary to discuss some of the constraints imposed by the presence of high temperatue combustion products in the tube and the relatively short "burn time" of the tested solid propellant sample. These effects restrict the data acquisition time to a period of one or two seconds, which is too

short a period for traversing a microphone probe along the impedance tube. Thus, in the present study the traversing microphone used in the classical impedance tube setup is replaced by ten microphones which increase the acoustic pressures at preselected fixed locations along the impedance tube throughout the duration of the test. These data are used in the determination of the acoustic wave structure and the admittance at selected time intervals during the test. The method of measurement offers the possibility of determining the unknown solid propellant admittance as a function of time.

The procedures utilized in the development of the data reduction procedures are described in detail in Refs. 4 through 8. Briefly, the initial program efforts concentrated on the derivation of the conservation equations describing the behavior of the waves in the tube while accounting for the presence of a steady state temperature gradient and gas phase acoustic losses. Next, a numerical solution technique for the derived equations and a procedure for determining the steady state temperature distribution were developed. Assuming periodic time dependence for the dependent variables (e.g., $p' \alpha e^{i\omega t}$), the time dependence was "separated" out from the system of one dimensional wave equations and the latter was reduced to a system of coupled ordinary differential equation in the axial variable x. The latter could be solved numerically once the x distribution of the steady state variables and the initial conditions at a given location, say x_0 , were known. However, the determination of these initial conditions is the objective of the proposed experiment and their determination is the focus of the proposed data reduction procedure, as is discussed below.

It can be shown[4] that the complete steady state flow behavior can be determined once the x distribution of one of the dependent variables, say the temperature $\bar{T}(x)$, is known. Considerable effort has been expended under

this program on the development of an accurate and efficient method for the determination of $\bar{T}(x)$. The determination of $\bar{T}(x)$ by either direct thermocouple measurements or through wave length measurements were discarded, after some study, due to their inaccuracies and associated experimental difficulties. After investigating this problem for awhile it had been concluded that the appropriate distribution of $\bar{T}(x)$ should be determined by using the nonlinear regression technique, as will be described shortly. In this case the developed data reduction scheme determines, in addition to the unknown admittance, the temperature distribution $\bar{T}(x)$ that provides the optimum fit between the measured acoustic pressure data and the solution of the impedance tube wave equations. Description of the above mentioned efforts can be found in Refs. 4 through 8.

The solutions of the impedance tube wave equations can be expressed in the following functional form

$$p' = f(x,\omega, \bar{T}(\Lambda), u_o', \rho_o', p_o') \tag{10}$$

where x,ω,Λ respectively represent axial variable, frequency and a steady state heat transfer parameter and the subscripted variables describe a set of initial conditions. Incidentally, the steady state temperature distribution is determined once Λ is known[4,6].

The admittance and response factor at the burning propellant surface are determined in this program by determining the set of initial conditions u_o', p_o' and ρ_o', at some location in the impedance tube, and heat transfer parameter Λ that provides the best fit between the measured acoustic pressures and the solution of the wave equations for the impedance tube. Once this set of optimum initial conditions is found at some location in the tube the

corresponding set of dependent variables at the propellant surface can be readily found by integrating the tube wave equations from the chosen initial point x_o to the propellant surface. The calculated set of values for p',ρ' and u' and the corresponding steady state solutions can then be substituted into Eqns. (1) and (5) to determine the propellant admittance and response factors.

A nonlinear regression (NLR) has been utilized to determine the desired unknowns. In this case the optimum set of p_o', ρ_o', u_o' and Λ are found by determining the set of values that minimizes the following positive quantity

$$E = \sum_{i=1}^{N} \left\{ |P_T(x_i,\omega,\bar{T}(\Lambda),\ P_o',\ \rho_o',u_o')| - |P_E(x_i)| \right\}^2$$

$$+ \sum_{i=1}^{N} \left\{ \varphi_T(x_i,\omega,\bar{T}(\Lambda),\ P_o',\rho_o',u_o') - \varphi_E(x_i) \right\}^2 \qquad (11)$$

where the quantities N, $|P|$ and φ represent the number of experimental measurements, the i^{th} measurement location, the pressure amplitude and the pressure phase, while the subscripts T and E respectively describe theoretically and experimentally determined quantities. Carrying out the above minimization procedure requires the use of such concepts as "transmission matrices" and the development of iterative solution schemes for a system of nonlinear algebraic equations. The details of development of these solution techniques and description of their applications in the determination of the admittances of burning solid propellants can be found in Ref. 6.

Since its development under this program,the above-mentioned data reduction program has been applied successfully in a NASA sponsored program that was concerned with the determination of the admittances of coaxial gaseous injectors utilizing acetylene-air and methane-air as the fuel-oxydizer combinations. Descriptions of these investigations can be found in Refs. 12 and 13.

The second aspect of the theoretical studies conducted under this program was concerned with the investigation of the dependence of the impedance tube wave structure upon the various parameters (i.e., see Eq. (10)) that appear in the impedance tube wave equations. This investigation has been undertaken in order to develop an understanding that could be used in the interpretation of observed experimental trends. To accomplish this objective, various parameters that appear in the wave equations were varied systematically and the corresponding acoustic wave structure was determined by numerically solving the developed system of impedance tube wave equations. Parameters varied in this study included the magnitude of the real and imaginary parts of the admittance at the propellant surface, the gas phase losses and the heat transfer parameter Λ. The resulting variations in the computed acoustic wave structure were analyzed and compared with observed experimental trends. These comparisons provided considerable insight into the acoustic behavior of the developed impedance tube. More detailed descriptions of these experimental investigations can be found in Refs. 4 and 5.

The wave equations considered to date in the above-mentioned investigations included the effects of steady state temperature gradients and gas phase damping. Another phenomenon that could possibly affect the

impedance tube wave structure is the oscillatory heat transfer to the impedance tube walls. The effect of this phenomenon upon the measured impedance tube wave structure may have to be investigated in the future to determine whether this phenomenon needs to be included in the data reduction procedure.

In summary, the theoretical efforts conducted under this program to date have extended the theoretical foundation of the classical impedance tube technique to account for the presence of mean flow and a temperature gradient in the tube. The developed theory was then used in the development of data reduction procedure which acoustic pressure measurements taken at discrete locations along the impedance tube can be used to determine the admittance at the propellant surface. This is in contrast with the classical impedance tube technique where a traversing microphone is used to determine the wave structure in the impedance tube. Finally, an investigation of the dependence of the wave equations solutions upon the various parameters which appear in these equations provided considerable assistance in the interpretation of the experimental data.

EXPERIMENTAL EFFORTS

A. Developed Experimental Setups

The experimental efforts conducted under this program were divided into two phases with the initial phase being concerned with propellant admittance measurements under atmospheric pressure conditions and the second phase being concerned with propellant admittance determination under high pressure conditions. The atmospheric pressure studies were undertaken in order to minimize the difficulties associated with the initial development of the experimental technique. The atmospheric pressure experimental apparatus is shown schematically in Fig. 2 and its detailed description can be found in Ref. 4. Also included in Ref. 4 are plots of typical measured acoustic pressure data and steady state temperature distributions.

As solid propellant rockets normally operate under high pressure conditions, it becomes necessary to obtain propellant admittance data under high pressure conditions. Consequently the second phase of this program was concerned with the development of an experimental facility that could be utilized for propellant admittance measurement in the range 0-500 psig. A schematic of the high pressure facility is shown in Fig. 3. The impedance tube* with the propellant sample-holder, the pressure transducer, and the acoustic driver are all contained within the 0 to 500 psig pressurization tank which is equipped with high pressure hinged ports to allow easy access for propellant sample changes, burner tube removal, and maintenance.

Air supply for tank pressurization and the flow requirements of the

---

* In the present study the impedance tube has often been referred to as the driven tube burner.

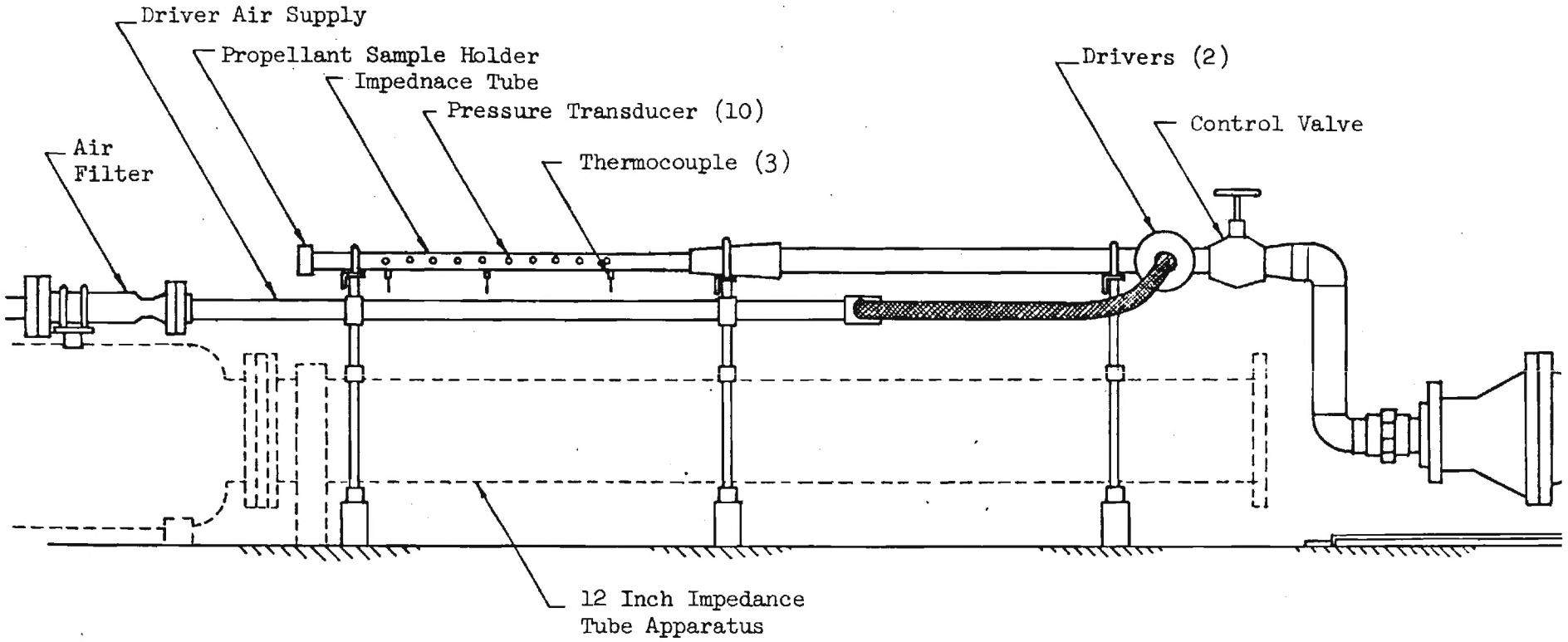

Figure 2. Sketch of the General Arrangement of the Unpressurized Driven Burner Experiment

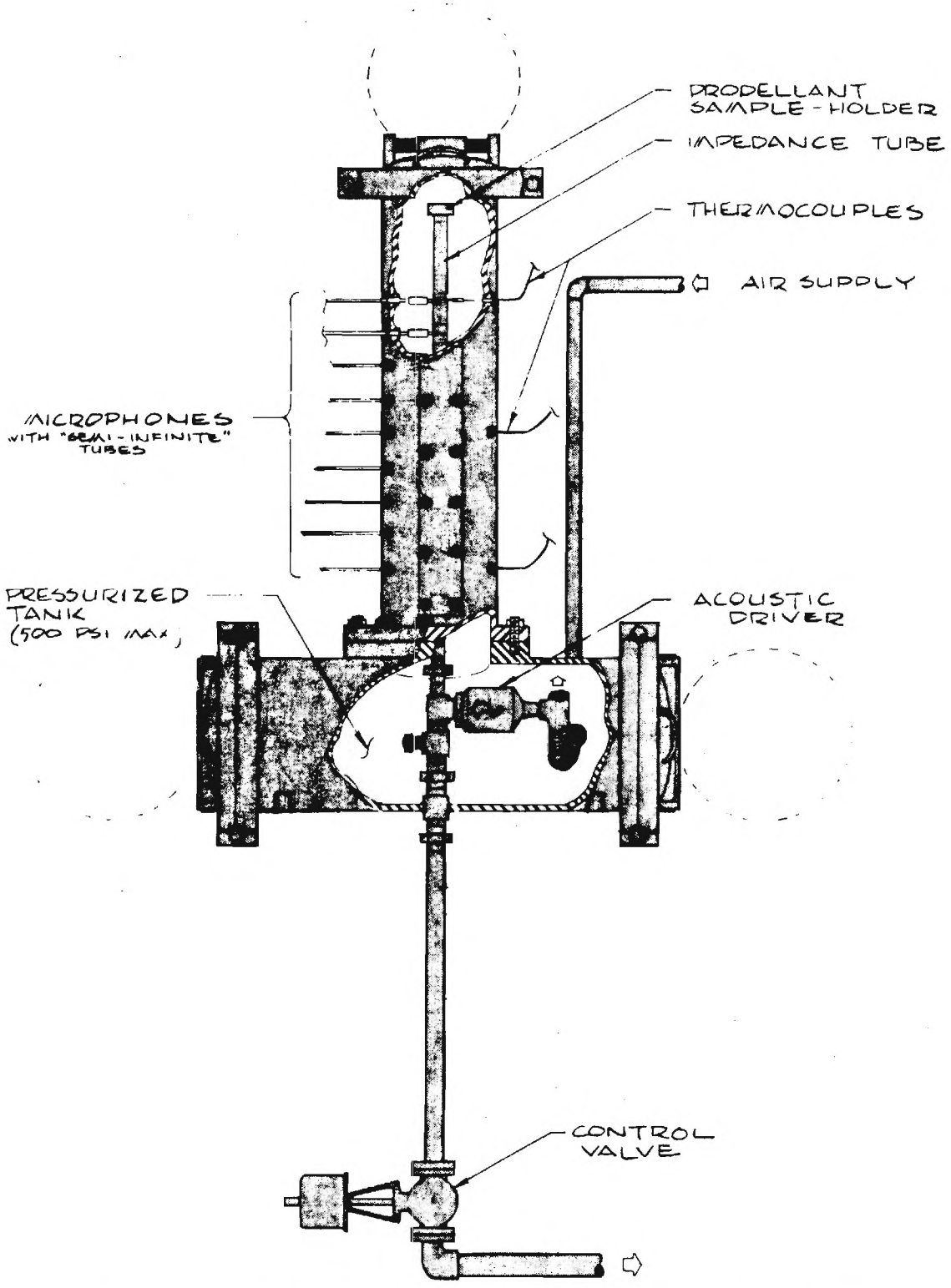

Figure 3. Schematic Diagram of Pressurized Driven Burner Facility

electropneumatic driver is provided by a 3000 psig, 500 cu.ft. blow down facility. The tank pressure and driver airflow are maintained by a pressure control valve in the exhaust line of the system as shown in the schematic of the flow system in Fig. 4.

The components of the high pressure driven burner tube facility and the principles of its operation are basically unchanged from the low pressure facility previously in operation. The impedance tube contained in the high pressure tank was fabricated from a stainless steel pipe with a two inch inside diameter. Provisions for a propellant sample holder are included on one end and an acoustic driver capable of developing 4,000 watts of acoustic power is close-coupled to the tube on the other end. Provisions for instrumentation (pressure and/or temperature measurements) have been included along six feet of the tube wall. The instrumentation locations are one-quarter inch apart measured from the face of the propellant sample. During a test, the propellant sample is ignited by a nichrome wire glued to the sample surface in an "S" shape. To assure a rapid and uniform ignition of the propellant, the surface of the sample is coated with a thin pyrotechnic mixture comprised of 72.4% potassium perchlorate, 14.8% titanium, 6.9% Boron powder, and 6.0% polyisobutylene binder dissolved in toluene. For ignition the nichrome wire is heated by a 40 volt, 15 ampere power supply. Measuring the standing wave pattern in the driven burner tube with a burning solid propellant sample imposes stringent requirements on the instrumentation. The pressure and high temperature pose the problem of protecting the highly sensitive transducer diaphragms from the hot gases in the tube. Various methods for the protection of the transducers have been investigated. The semi-infinite tube technique utilized in the atmospheric pressure studies[4,5] has proven unsatisfactory for high pressure operation because of a low frequency

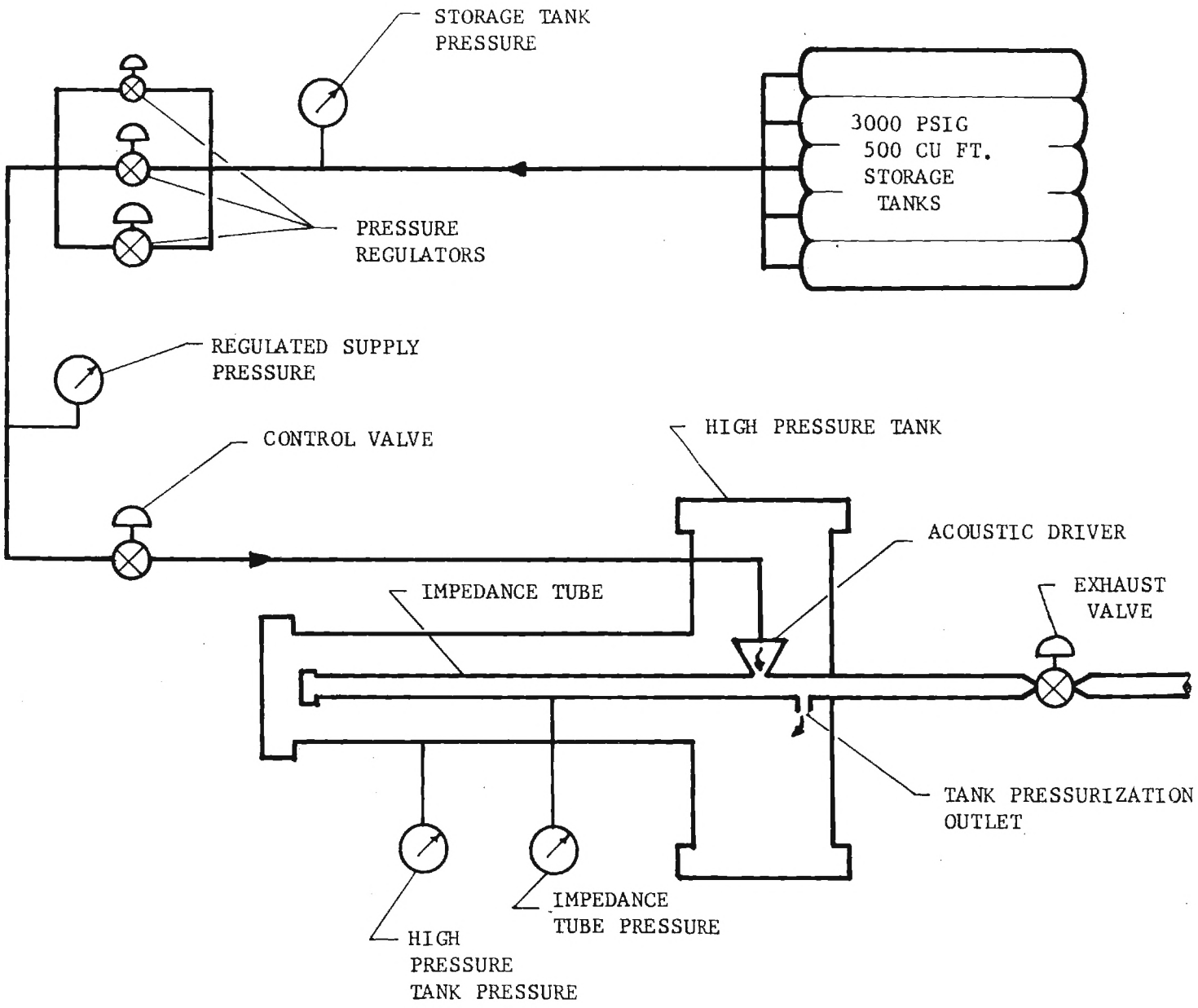

Figure 4. Schematic of Facility Flow System

resonance in the infinite tube at high pressures. Instead a short pressure transducer adaptor has been utilized in the high pressure investigation.[6] Further protection for the transducer is provided by a thin coating of clear silicone grease applied to the transducer diaphragm. Extensive calibration and testing of this short transducer adapter has been conducted and the results indicate that in the frequency range of interest for this experiment, (i.e., 300 Hz to 1100 Hz), the adapter provides highly satisfactory pressure amplitude and phase measurement characteristics.

The acoustic driver used in the high pressure driven burner tube is a Ling ETP-94 B electropneumatic driver capable of developing 4,000 watts of acoustic power which provides a sound pressure level of 170 decibels in the burner tubes. The driver is close-coupled to the tube wall at the downstream end of the burner tube. The frequency and waveform output of the acoustic driver is controlled by a Spectral Dynamics Oscillator, Model SD104A-5. For this investigation, the waveforms of the pressure oscillations are sinusoidal and the frequency of the oscillations are constant during a given test.

Small modifications to the developed experimental setup have been introduced in the course of this study. These modifications included changing the nature of the termination at the exhaust end of the tube and the utilization of both short (i.e., 4 feet) and long (i.e., 10 feet) impedance tubes. The nature of the exhaust termination was modified in order to assess the effect of the acoustic properties of the exhaust end upon the impedance tube acoustic wave structure and the four feet impedance tube was utilized in order to assure that both the acoustic driver and the pressure transducers are "located" within the hot combustion products shortly after ignition. When this condition is not satisfied, the measurement of the hot-cold

gas interface toward the acoustic driver results in periodic resonances in the impedance tube and amplitude variations of the standing acoustic wave within the impedance tube.

B. Test Procedures.

The data acquisition system and the equipment to establish and monitor test conditions are located in a laboratory area adjacent to the room housing the high pressure driven tube experiment. Test conditions are established by slowly pressurizing the high pressure tank housing and the burner tube to the desired operating pressure. The pressurization tank pressure and driver airflow requirements are maintained by the tank pressurization control valve in the exhaust line. With tank pressure stabilized and a standing waveform of a desired frequency established a test run is initiated. The data acquisition period of a test run includes four phases; a brief pre-ignition test period with the acoustic drivers on and test conditions established in the burner tube, ignition of the propellant sample, the propellant "quasi-steady" burning period and the propellant extinguishment phase. The data acquisition period is normally about two and one-half seconds. A more detailed discussion of the data acquisition and data reduction procedures are presented in the following section.

C. Minicomputer-Based Data Acquisition System

A minicomputer-based data acquisition system has been incorporated in the program to obtain improved pressure and temperature data. This system processes the data in three stages. First, during a test the analog signals from the transducer and thermocouple channels are sampled, digitized, and stored at a controlled rate. Next, the stored readings are processed by the computer. The transducer data are digitally filtered and pressure amplitude

and phase data are obtained at the frequency of interest. Likewise, thermocouple signals are converted to temperatures. Finally, the pressure and temperature data are printed out and plotted. These values are then used in the data reduction scheme described in Section II to obtain the admittance values. A more detailed description of this data acquisition system is presented in Ref. 6.

As reported in Ref. 6, the results obtained using this data acquisition system indicated that the propellant was alternately driving and damping during a burn. To check this anomaly, the signals from the pressure transducers and thermocouples were also recorded on a 14-channel Ampex tape recorder. These data were then played back at reduced speed and plotted to provide a time history of the sound pressure levels, phase relationship, and temperature of the hot gases inside the tube. These plots were then compared with the corresponding plots obtained from the computer - based data acquisition facility. The results of this comparison are presented in the following section.

EXPERIMENTAL RESULTS

Because of stringent requirements on the accuracy of the pressure amplitude and phase measurements, the major thrust of the work during this reporting period has been directed toward improving the quality of these data.

As explained in the preceeding sections, the response of a burning solid propellant in a driven tube can be determined from pressure amplitude, phase, and temperature measurements taken along the standing wave in the tube. The ratio of the minimum to maximum pressure amplitudes of the standing wave is a measure of the amount of amplification or attenuation of an acoustic oscillation by the burning solid propellant. This ratio decreases with decreasing admittance or propellant response. Since the propellants which are under investigation in this study have nondimensional admittance values on the order of 10^{-2}, the difference between the maximum and minimum amplitude during an experiment is typically 40 decibels or more. To obtain reliable results for this range of amplitudes, the data acquisition and reduction instrumentation must have a large dynamic range. By measuring the phase differences between successive points along the tube, it is possible to determine whether the sample is amplifying or attenuating the incident wave from the driver and by how much. However, the phase differences between successive points along the standing wave for nondimensional admittance values on the order of 10^{-2} is small (less than two degrees) except near the pressure minima where the amplitude is low and the noise to signal ratio of the transducers high. Thus, great care must be exercised to ensure data reliability.

In Figs. 5 and 6 data are presented for a test conducted at 742 Hz with an A-13 propellant with a closed-ended exhaust configuration.[6] Figure 5 is a plot of the pressure amplitudes in decibels (re 2×10^{-4} microbars) versus record number for three pressure channels located at different axial stations along the tube. Each record represents a short time interval during which data was recorded by the analog-to-digital converter. Consecutive records correspond to consecutive time instances with about 30 milliseconds between records; therefore the abscissa represents time.

The total duration of a typical experiment can be divided into four distinct periods: (1) the preignition period during which the Ling acoustic drivers are the only source of wave excitation (e.g. records 1 to 14 in Figs); (2) the propellant ignition phase (records 15 to 20); (3) the quasi-steady burning phase during which the pressure data are used to determine the burning solid propellant admittance values (records 21 to 40); and (4) the burnout phase (records 41 to 80). During the ignition and burnout phases, the temperature in the tube changes rapidly with time which produces large variations in the wavelength - and thus the amplitude distribution of the standing wave. Hence the observed large amplitude variations during these two phases is to be expected. What is not expected at a given location is the large fluctuations in amplitude of over ten decibels during the quasi-steady burning period when the temperature in the tube has nearly reached steady state. Also, as shown in Fig. 6, the phase differences between the transducer signal and the Ling driver changes rapidly during this period. As reported in Ref. 6, this phase data indicate that the solid propellant combustion process is randomly driving and damping the oscillations.

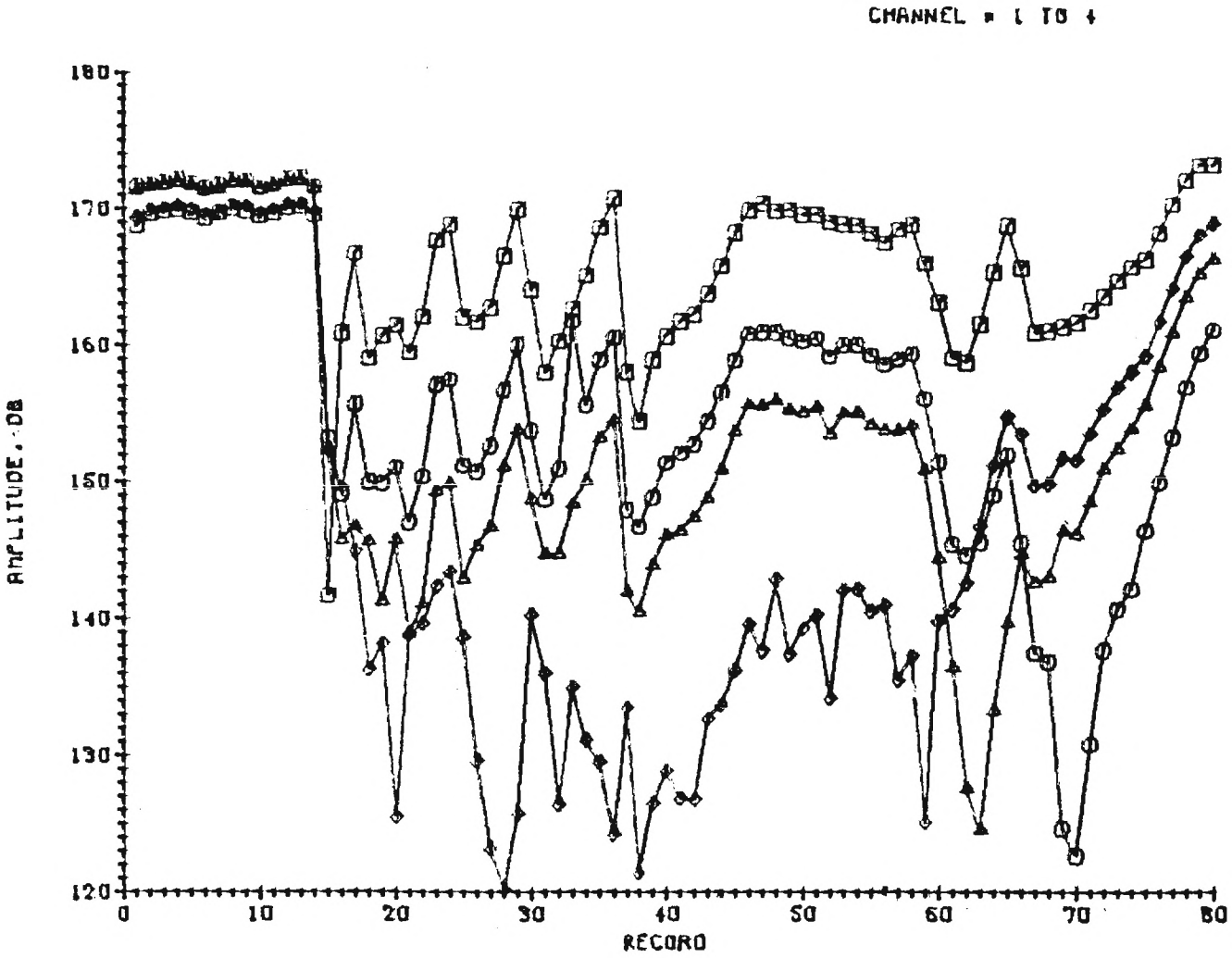

Figure 5. E-16-633-590.A-19.742HZ..300PSID.CLOSED END.

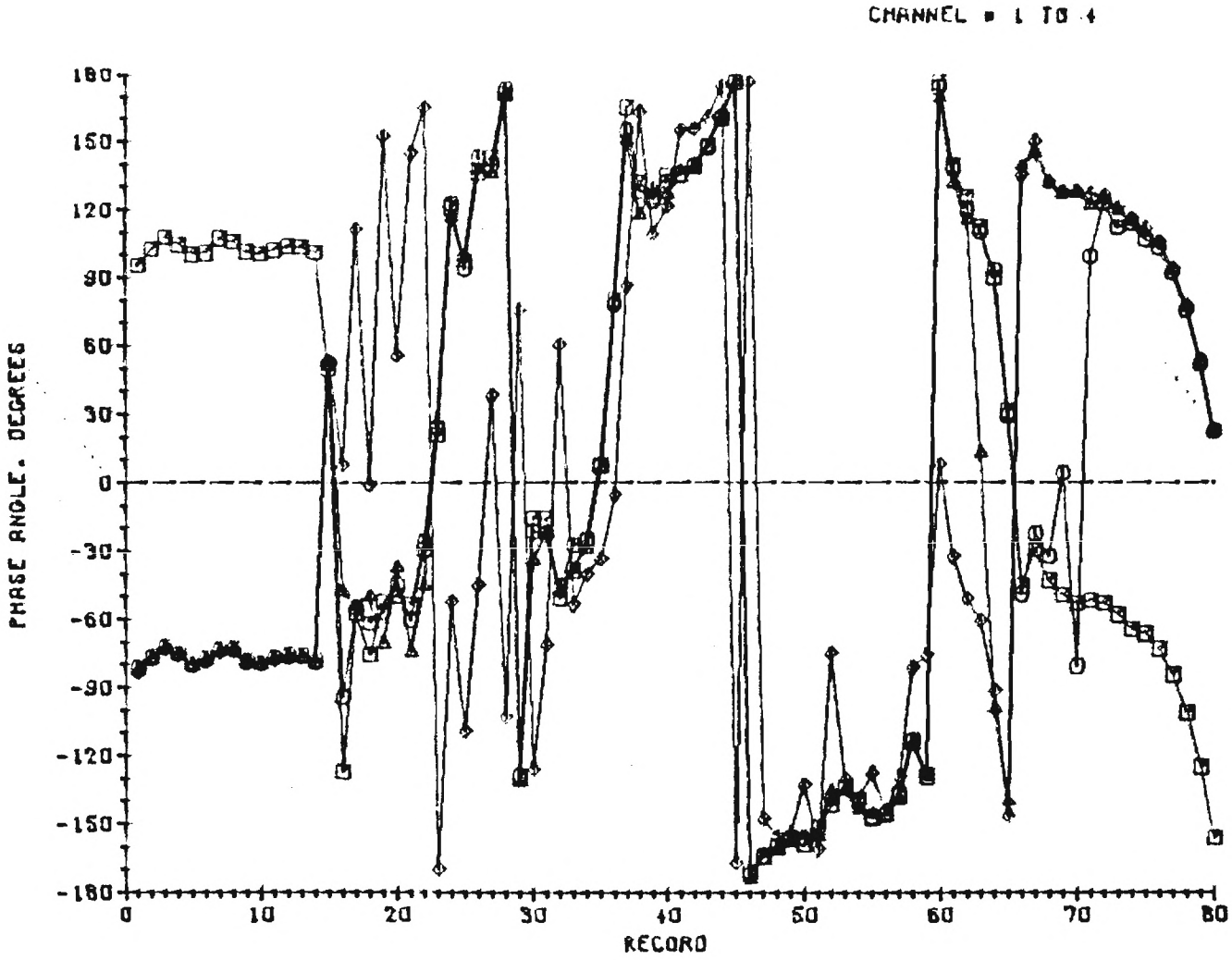

Figure 6. E-16-633-580,A-13.742HZ.,300P810,CLOSED END.

This anomalous behavior of the amplitudes and phases has been investigated intensively during the past year. The fluctuations can lead to significant errors in the pressure data. The digital filtering performed by the minicomputer-based data acquisition system assumes that the amplitude of the signal either remains constant or varies randomly during a sampling interval. If the signal amplitude either increases or decreases monotonically during the interval, errors in both the filtered amplitude and phase will occur. To ensure data accuracy during the quasi-steady burn period, methods for eliminating these fluctuations have been investigated.

Over the report period, 82 tests have been conducted to study the effect of (1) low and high power output of the acoustic drivers, (2) propellant composition, (3)exhaust end configuration, and (4) burner tube length on the amplitude variations during the burn. In addition, methods of improving transducer accuracy and ensuring uniform and instantaneous ignition have been investigated.

In the first series of tests, the effect of the acoustic power output - and thus the amplitude of the standing wave at the propellant face - on the combustion response was investigated for propellant B (Propellant B was provided for testing by the Thiokol Corporation; its composition is not known), a highly unstable propellant when used in T-burners. It was found that the propellant exhibited qualitatively the same behavior for both low and high power outputs. The large fluctuations in amplitude at a given location, the random driving and damping behavior as exhibited by the phase were present regardless of the magnitude of the peak amplitude of the standing wave.

The propellants in almost all tests conducted to date at 300 psig exhibited apparent driving at some times and damping at others.* The most unstable propellants - A-15 and propellant B- appear to exhibit the largest variation from driving to damping whereas the most stable propellant T-13 seems to show the least.

Further tests were conducted with a constant tube length and various exhaust end configurations as reported in Ref. 6. Although the amplitude variations can be decreased somewhat by changing the termination at the exhaust end, the random driving - damping behavior exhibited by the phase data is evident and it increases with increasing frequency. One test at a low frequency (280 Hz), however, did not exhibit this behavior and driving of the acoustic oscillations by the combustion process was indicated throughout the burn. This run gave the most consistent results in that the propellant exhibited constant properties over the burn period.

Because of the frequency dependence of the variation in the pressure amplitude during the burn, the following explanation of this behavior was put forth. The tube length in all runs was seven feet. Prior to ignition a series of pressure amplitude maxima and minima one-half wavelength apart exist between the sample and the acoustic driver. The positioning of the driver with respect to a maximum or minimum determines the overall amplitude of the standing wave. Changing this position changes the peak amplitude of the standing wave from a maximum at resonance to a minimum at off-resonant conditions. When the propellant sample is ignited, the temperature in the tube increases, which increases the wavelength. At the higher fre-

---

*It is quite possible that when gas phase acoustic losses in the driven tube are taken into consideration, the apparent damping may actually turn out to be a driving condition.

quencies several maxima and minima may pass by the driver after ignition which produces the large amplitude variations during a burn and as shown in Fig. 5. By decreasing the length between the acoustic driver and the tested propellant sample, the number of successive maxima and minima in between is reduced and thus less variation in the amplitude during a test should result.

Tests run with short tubes confirm this explanation. Amplitude and phase data are presented in Figs. 7 and 8 respectively for an A-13 propellant at 600 Hz with the acoustic driver 39 inches from the propellant face. In Figs. 5 and 6 the distance is 96 inches. After the ignition period (records 13 to 16) the amplitude slowly varies until relatively constant levels are reached from record 40 to 80. The burnout occurs after the time period over which these data were taken. The corresponding phase data exhibit the same behavior - varying slowly from record 17 to 40 and then remaining relatively constant with reference to the driver signal. However, the random driving - damping behavior previously experienced in the phase data is still present though at a reduced level.

A series of tests were conducted to investigate the observed random nature of the phase data. During these tests the digital data were compared with the correspondent analog data recorded on a tape recorder and played back at reduced speed. It was found from this comparison that the computerized data acquisition system was the source of the driving - damping behavior. When filtering the data, it is necessary to take samples over sufficiently long time periods to average out any noise or random amplitude fluctuations that are present in the signal so that only the sinusoidal signal remains. However, because of the short duration of the burn, the time over which the signal is filtered is insufficient to adequately

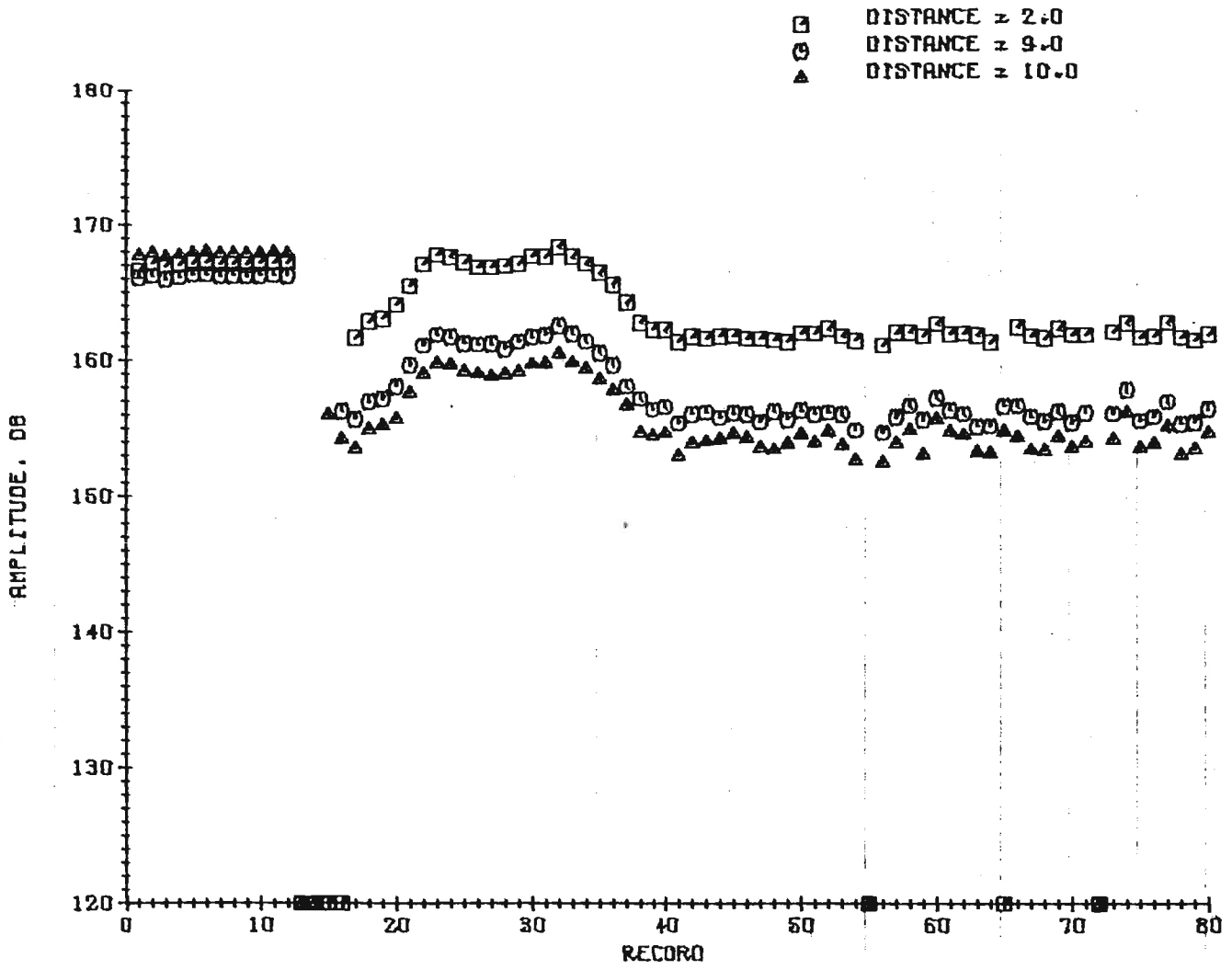

Figure 7. E16-633-714, A-13, 600HZ, DRIVER @ 39"

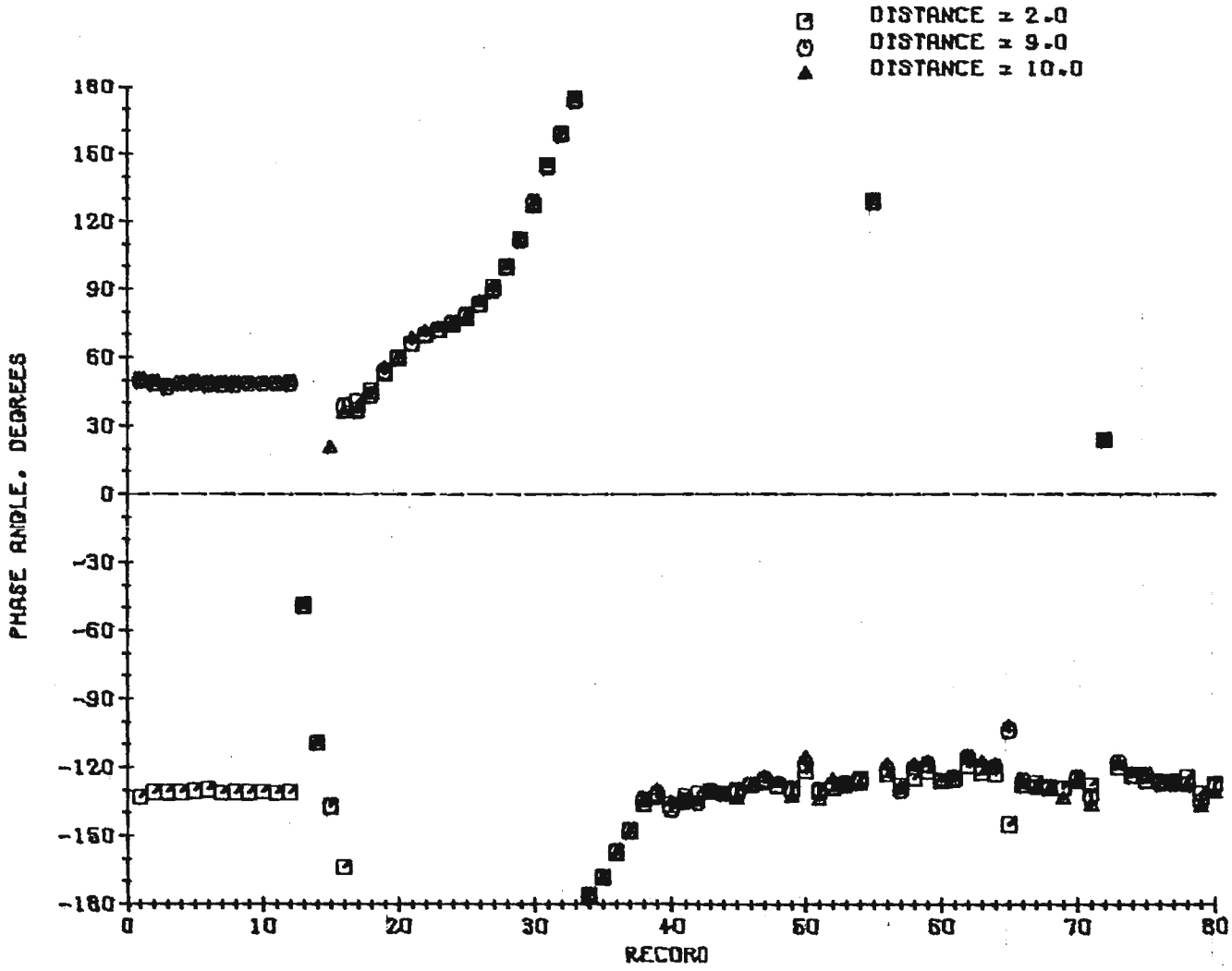

Figure 8. E16-633-714, A-13, 600HZ, DRIVER = 39°

average out the noise or any random fluctuations in amplitude. Therefore, small errors in phase can result. As mentioned earlier in this section, for the low admittances characteristic of burning solid propellants, small phase differences along the standing wave are to be expected. Therefore, the phase errors can lead to erroneous conclusions as to the propellants driving or damping behavior. In a related study[7,8] of the response of liquid rocket injector configurations, this data acquisition system gives excellent results. This is due to the fact that the injector tests are of sufficient duration to ensure accurate digital filtering.

Because of the difficulties in filtering the transducer data during the short burn times associated with the propellant tests, the data are first recorded on a 14-channel Ampex tape recorder. The signals are then played back at reduced speed which, in effect, lengthens the test period. The signals are then filtered using a long sampling interval to obtain reliable pressure amplitude and phase data.

In addition to the aforementioned tests, additional tests were conducted to determine the ignition and burnout characteristics of the propellant sample and tests to determine the admittance at the "driven" end of the tube. Twenty tests were conducted to determine the ignition and burnout characteristics of a typical propellant to assure uniform burning over the propellant face. Two methods of ignition were investigated. The first consisted of imbedding a nichrome wire in the igniter paste in an "S" shape. This method has been the standard technique used in this study. The second method, commonly used in T-burners, was to spread the igniter paste over the sample. In the center of the sample, the nichrome wire was imbedded in a spot of paste dabbed onto the surface. At atmospheric pressure the "S" configuration ignited the sample almost instantaneously in a uniform

manner over the propellant face. The sample appeared to burn evenly and the flame front remained uniform throughout the burn. In the test with the "spot" ignition, the electric match ignites the propellant almost explosively but the flame does not spread uniformly across the sample face. This igniter did not ignite the propellant as rapidly as the "S" configuration. Also, the burnout was not uniform and on many occasions the electric match ignited one side of the propellant before the other which caused uneven burning. Even under the best conditions, the ignition occurred at the match and the propellant center ignited before the remainer of the surface causing a concave burning surface which produced uneven burnout. As a result of these tests, the "S" ignition technique will continue to be used.

Current research efforts are directed at improving and maintaining the accuracy of the measured data. Extensive checkouts of the tape recorder system are being conducted, and testing will resume upon completion. The classical impedance tube technique has been successfully modified for high temperature and pressures with mean flow present in the tube. The proper operation of the method has been demonstrated in a related study of liquid rocket injectors; and,once the accuracy of the measured data in the research described in this report is improved, the technique should yield reliable results.

REFERENCES

1. Scott, R. A., "An Apparatus for the Accurate Measurements of the Acoustic Impedance of Sound Absorbing Materials," Proceedings of the Physical Society, Vol. 58, 1946, pp. 253-264.

2. Zinn, B. T., Bell, W. A., and Daniel, B. R., "Experimental Determination of Three-Dimensional Liquid Rocket Nozzle Admittances," AIAA Journal, Vol. 11, March 1973, pp. 267-272.

3. Zinn, B. T., Daniel, B. R., Janardan, B. A., and Smith, A. J., Jr., "Damping of Axial Instabilities by Minuteman II, Stage III, Minuteman III, Stage III, Exhaust Nozzles," Air Force Rocket Propulsion Laboratory Final Report, AFRPL-TR-73-69, September 1973.

4. Zinn, B. T., Daniel, B. R., Bell, W. A., and Salikuddin, M., "Solid Propellant Admittance Measurements by the Driven Tube Method," AFOSR Interim Scientific Report, AFOSR-TR-75-19, August 1974.

5. Zinn, B. T., Salikuddin, M., Daniel, B. R., and Bell, W. A., "Solid Propellant Admittance Measurements by the Driven Tube Method," AFOSR Interim Scientific Report, AFOSR-TR-75-1531, August, 1975.

6. Zinn, B. T., Salikuddin, M., Daniel, B. R., and Bell, W. A., "Solid Propellant Admittance Measurements by the Driven Tube Method," AFOSR Interim Scientific Report, August 1976.

7. Zinn, B. T., Daniel, B. R., Salikuddin, M., and Bell, W. A., "Determination of the Response of Solid Propellants by the Impedance Tube Method," Proceedings of the 12th JANNAF Meeting, CPIA Publication 273, Vol. II, December 1975, pp. 33ff.

8. Zinn, B. T., Salikuddin, M., Daniel, B. R. and Bell, W. A., "Measurements of the Response Factors of Burning Solid Propellants by the Driven Tube Method," Proceedings of the 13th JANNAF Combustion Meeting, CPIA Publication No. 281, Vol. II, December 1976, pp. 113ff.

9. Zinn, B. T., Daniel, B. R., Bell, W. A., and Salikuddin, M., "Determination of the Responses of Burning Solid Propellants by the Impedance Tube Method," AIAA Paper No. 75-227, January 1975.

10. Morse, P. M., and Ingard, K. V., Theoretical Acoustics, McGraw-Hill, Inc., New York, N. Y., 1968, pp. 467ff.

11. Brown, R. S., and Erickson, J. E., "Measuring Combustion Response by a Forced Oscillation Method," AIAA Paper No. 72-1054, December 1972.

12. Zinn, B. T., Janardan, B. A., and Daniel, B. R., "Experimental Determination of Rocket Injector Response Factors Under Reactive Conditions," Proceedings of the 13th JANNAF Combustion Meeting, CPIA Publication No. 281, Vol. III, December 1976. pp. 119-123.

13. Janardan, B. A., Daniel, B. R., Bell, W. A., and Zinn, B. T., "Measurements of Reactive Gaseous Rocket Injector Response Factors," Paper presented at the Spring Meeting of the Combustion Institute, Central Section, Lewis Research Center, March 28-30, 1977.